Publication No. 02-030-073

RECLAMATION OF PHOSPHATIC CLAY WASTE PONDS BY CAPPING

Volume 6: Consolidation Properties of Phosphatic Clays from Automated Slurry Consolidometer and Centrifugal Model Tests

Prepared by
University of Florida,
Department of Civil Engineering

under a grant sponsored by the
Florida Institute of Phosphate Research
Bartow, Florida

February, 1989

FLORIDA INSTITUTE OF PHOSPHATE RESEARCH

The Florida Institute of Phosphate Research was created in 1978 by the Florida Legislature (Chapter 878.101, Florida Statutes) and empowered to conduct research supportive to the responsible development of the state's phosphate resources. The Institute has targeted areas of research responsibility. These are: reclamation alternatives in mining and processing, including wetlands reclamation, phosphogypsum storage areas and phosphatic clay containment areas; methods for more efficient, economical and environmentally balanced phosphate recovery and processing; disposal and utilization of phosphatic clay; and environmental effects involving the health and welfare of the people, including those effects related to radiation and water consumption.

FIPR is located in Polk County, in the heart of the central Florida phosphate district. The Institute seeks to serve as an information center on phosphate-related topics and welcomes information requests made in person, by mail, or by telephone.

Research Staff

Executive Director
Richard F. McFarlin

Research Directors

G. Michael Lloyd Jr.	-Chemical Processing
Gordon D. Nifong	-Environmental Services
David J. Robertson	-Reclamation
Hassan El-Shall	-Beneficiation
Robert S. Akins	-Mining

Florida Institute of Phosphate Research
1855 West Main Street
Bartow, Florida 33830
(863) 534-7160

Reclamation of Phosphatic Clay Waste Ponds by 'Capping'

Volume 6a: Consolidation Properties of Phosphatic Clays from Automated Slurry Consolidometer and Centrifugal Model Tests

Research Project: FIPR 82-02-030
UF Project: 4910450406312

Prepared by

Department of Civil Engineering
University of Florida
Gainesville, Florida 32611

IMC Bartow, Florida
AGRICO, Mulberry, Florida
MOBIL, Nichols, Florida

Principal Investigators

F. C. Townsend
R. E. Martinez
D. Bloomquist
M. C. McVay

Prepared For

Florida Institute of Phosphate Research
1855 West Main Street
Bartow, Florida 33830

FIPR Project Manager: Dr. Henry L. Barwood

December 1987

DISCLAIMER

The contents of this report are reproduced herein as received from the contractor.

The opinions,findings and conclusions expressed herein are not necessarily those of the Florida Institute of Phosphate Research, nor does mention of company names or products constitute endorsement by the Florida Institute of Phosphate Research.

TABLE OF CONTENTS

ACKNOWLEDGMENTS

The sponsorship of the Florida Institute for Phosphate Research was instrumental in the development of this research and is acknowledged here. The support of Mr. Randy Bushey and the Florida Department of Natural Resources is also recognized.

This report representsthe PhD dissertation of Mr. Ramon E. Martinez.

CONSOLIDATION PROPERTIES OF PHOSPHATIC CLAYS
FROM AUTOMATED SLURRY CONSOLIDOMETER
AND CENTRIFUGAL MODEL TESTS

Abstract

As a by-product of phosphate mining and other industrial processes, a very dilute fine-grained slurry is produced, which consolidates over long periods of time in large retention ponds. Numerical prediction of the magnitude and time rate of settlement of these slurries requires a knowledge of the effective stress-void ratio and the permeability-void relationships of the material. The purpose of this research was to develop equipment and techniques for determining these relationships by (1) performing automated slurry consolidation experiments and (2) centrifugal model tests.

An automated slurry consolidometer, which is fully controlled by a computer-data acquisition system that monitors load, pore pressure, total stress, and deformation, was developed. The load is applied by a stepping motor. Results from the tests conducted show the effectiveness of the apparatus. The Constant Rate of Deformation test was found to have several advantages over the Controlled Hydraulic Gradient test and is recommended for future applications; the results from both tests were consistent. A "pseudo-preconsolidation" effect, attributed to the initial remolded condition of the specimen, was observed in

both constitutive relationships. Thus, the curves are not unique but depend upon the initial solids content. However, different curves approach what seems to be a "virgin zone." The compressibility relationship also was found to be dependent upon the rate of deformation.

The technique using centrifugal modelling is based on the measurement of pore pressure and void ratio profiles with time, and the use of a material representation of the specimen. The compressibility relationship obtained was in good agreement with the results of CRD tests performed at a slow rate of deformation. The permeability relationship plotted parallel to the CRD curves, however, permeability values were approximately a half order of magnitude higher. Further research is required to explain this difference.

The constitutive relationships obtained in the study were used to predict the behavior of hypothetical ponds modelled in the centrifuge. A good agreement between centrifugal and numerical models was found.

LIST OF TABLES

LIST OF FIGURES

CHAPTER I
INTRODUCTION

Problem Statement

The production of phosphate fertilizers from Florida's mines involves the excavation of approximately 300 million cubic yards of material (overburden and matrix containing the phosphate) annually. This is roughly equal to the entire volume excavated during the construction of the Panama Canal (Carrier; 1987). During the phosphate beneficiation process, large amounts of water are used to wash the matrix in order to separatethe phosphate from the sand and clay forming that layer. As a by-product of the process, a very dilute fine-grained slurry is produced with very low solids contents (weight of solids ÷ total weight). Florida's phosphate mines produce more than 50 million tons of such waste clays annually (Carrier et al., 1983).

Disposal of these waste clays is accomplished by storing them in large containment areas or ponds,and allowing them to settle/consolidate over long periods of time. During the initial sedimentation phase, the slurry reaches a solids content on the order of 10-15% within a few weeks-or months, depending on several physio-chemical properties of the material (Bromwell,1984; Bromwell and Carrier, 1979; Scott et al., 1985). Subsequently, a very slow process of

self-weight consolidation begins, which can require several decades to achieve a final average solids content of approximately 20-25%. Because of this time delay, research efforts have been concentrated on the consolidation behavior rather than the sedimentation phase of these slurries.

The design of the disposal areas, as well as the estimate of time required for reclamation thereof, presents a challenging problem to geotechnical engineers, who must estimate the magnitude and time rate of settlement of the slurry, as well as the final pond conditions. It has been well established that conventional linear consolidation theory is inappropriate for these materials (Bromwell, 1984; Cargill, 1983; Croce et al., 1984; McVay et al., 1986). This is primarily the result of the significant changes in permeability and compressibility that occur as these slurries consolidate to very large strains (Bromwell and Carrier, 1979). Accordingly, large-strain nonlinear consolidation theory has been used to model the self-weight consolidation process of these soft, very compressible soil deposits (see e.g. McVay et al., 1986), and several computer codes have been written to predict their behavior applying this theory (Cargill, 1982; Somogyi, 1979, Yong et al., 1983; Zuloaga, 1986).

The use of large-strain consolidation theory requires a clear definition of two constitutive relationships of the slurry, namely, the effective. stress-void ratio relation and the permeability-void ratio relation. Unfortunately, our

capability of measuring accurately these soil properties has not advanced as fast as our ability to represent the physical process by a mathematical model. The results of the numerical predictions are very susceptible to these input material properties, primarily the permeability. relationship (Hernandez, 1985; McVay et al., 1986). Comparison of centrifugal and numerical predictions has found good agreement on the magnitude of settlement. However, good predictions of the rate of settlement require improvement in laboratory input data, primarily the permeability relationship (Carrier et al.; 1983; Townsend et al., 1987).

Traditional consolidation tests are not suitable for the study of the consolidation properties of highly compressible clays, mainly because they rely on curve fitting methods and small strain theory to characterize the consolidation process. Although several attempts to develop large deformation consolidation tests are reported in the literature, the Slurry Consolidation Test-has emerged as one of the most popular (Ardaman and Assoc., 1984; Bromwell and Carrier, 1979; Carrier and Bromwell, 1980; Scott et al., 1985). Unfortunately, the test, which is essentially a large-scale version of the standard oedometer, suffers from some drawbacks, among them its extremely long duration of several months.

Alternative tests are being developed. These include settling column tests, constant rate of deformation consolidation tests, and others. Chapter II will discuss the

details of these tests. To date, however, there is no standard approach that satisfactorily measures the compressibility and permeability of very soft soils and soil-like materials.

Purpose and Scope of the Study

The purpose of this research is to develop a technique to determine accurately the compressibility and permeability relationships of phosphatic clays and other slurries. To achieve this objective, two approaches are followed. The first one involves testing in a newly developed automated slurry consolidometer, while the second involves centrifuge testing. The automated slurry consolidometer should be capable of (1) accommodating a relatively large volume of slurry, (2) producing large strains in the specimen, (3) allowing different loading conditions, (4) monitoring and/or controlling load, deformation, pore pressures, and other parameters, and (5) testing a wide range of solids content.

A major concern in the development of this consolidometer was to avoid the use of any assumptions concerning the theoretical behavior of the slurry in analyzing the data. Instead, the adopted test method measures directly many of the required parameters and computes others from well accepted soil mechanics principles, such as the effective stress principle and Darcy's law. This approach to the problem is different from those attempted by others, as will be discussed in Chapter II (literature review).

Chapter III describes in detail the test equipment and procedure while Chapter IV presents the proposed method of analysis of the test data. Chapter V presents the results of several tests conducted on a Florida phosphatic clay.

The second approach used to obtain constitutive relationships of the material is centrifugal testing. This involves measuring pore pressure and solids content profiles in a centrifuge model with time. The use of updated Lagrangian coordinates for a number of points along the specimen, in conjunction with the previously described data, allows the determination of the compressibility and permeability of the slurry. Chapter VI describes the test procedure, instrumentation, and method of data reduction. Chapter VII presents the results of several centrifuge tests on the same clay used in the slurry consolidation tests. A comparison of the results of both approaches is also presented in this chapter.

One of the main applications of centrifuge testing is to validate the results of computer predictions (McVay et al., 1986; Scully et al., 1984). In Chapter VIII the constitutive relationships obtained in this research are used to predict the behavior of a hypothetical pond. These predictions are compared with the results of centrifugal modelling. Finally, Chapter IX presents the conclusions and suggestions for future research.

CHAPTER II
BACKGROUND AND LITERATURE REVIEW

Introduction

The main reasons for performing a consolidation analysis are (1) to determine the final height of the deposit (theoretically at $t = \infty$) and (2) to evaluate the time rate of settlement. Other information, such as pore pressure or void ratio distributions at any time, can also be obtained from the analysis. Of course, such an analysis requires the determination of several consolidation properties of the soil. In traditional consolidation; analysis, the first of the two objectives is accomplished by knowing the preconsolidation pressure and the compression index. The second objective requires the determination of the coefficient of consolidation.

Along with the development of his classical one-dimensional consolidation theory, Terzaghi (1927) proposed the first consolidation test, known today with minor modifications as the step loading test and standardized as ASTM D 2435-80. Since its first introduction, several procedures, have been proposed to analyze the data in order to solve for the material properties; this is usually accomplished by a curve fitting procedure. The test has several drawbacks, among them that it is time consuming and the

results are highly influenced by the load increment ratio (Znidarcic, 1982). To overcome some of the limitations of the step loading test, other testing techniques have been proposed. Among the most popular are the Constant Rate of Deformation test (Crawford, 1964; Hamilton and Crawford, 1959) and the Controlled Hydraulic Gradient test (Lowe et al., 1969). The analysis procedure for these tests relies on small strain theory to obtain the material properties. Znidarcic et al. (1984) present a very good description of these and other consolidation tests, with emphasis on their different methods of analysis. They conclude that these tests are limited to problems where linear or constant material properties are good approximations of the real soil behavior.

Consequently, conventional consolidation tests are not suitable for very soft soils or slurries, which will undergo large strains and exhibit highly nonlinear behavior. In large strain theory the soil is characterized by two constitutive relationships, namely, the effective stress-void ratio relation and the permeability-void ratio relation, and not by single parameters such as the coefficient of consolidation or the compression index.

Slurry Consolidation Laboratory Tests

Accordingly, there is a definite need to develop testing techniques appropriate to study the consolidation properties of soft soils and sediments. Lee (1979)

describes a number of early efforts (1964-1976) to develop large deformation consolidation tests. He developed a fairly complicated step loading oedometer, which monitored the load, pore pressures, and deformation of a 4-inch diameter and 6-inch high specimen. Interpretation of his test data was based on a linearized form of the finite strain consolidation theory, using a curve fitting construction analogous to the square root of time method in the conventional oedometer. The test provided the stress-strain relationship (compressibility) and a coefficient of consolidation, which is assumed to be constant for a given load increment. Permeability values could be obtained from this

Lee introduced, in a special test, the use of a flow restrictor in order to reduce the pore pressure gradient across the specimen and approximate this to a uniform condition. This allowed him to make direct computations of the permeability. The test program conducted by Lee was on specimens with initial void ratios in the order of 6. Although some of the characteristics of Lee's apparatus are valuable, the overall approach. is probably not appropriate for testing dilute slurries with initial void ratios of 15 or more.

A very popular test, most probably due to its relative simplicity, developed specifically for testing very dilute fine-grained sediments is the Slurry Consolidation Test (Ardaman and Assoc., 1984; Bromwell and Carrier, 1979;

Carrier and Bromwell, 1980; Keshian et al., 1977; Roma, 1976; Scott et al., 1985; Wissa et al., 1983). The test is essentially a large-scale version of the standard oedometer, using a much larger volume of soil to allow the measurement of large strains. The specimen diameter is usually in the order of 10-20 cm and its initial height is 30 to 45 cm. Slurry consolidation tests are usually conducted on specimens with initial solids content near the end of sedimentation. The specimen is first allowed to consolidate under its own weight, recording the height of the specimen periodically. The average void ratio at any time is computed from this height and the initial conditions.

Subsequent to self-weight consolidation, the specimen is incrementally loaded and allowed to consolidate fully under each load. Typical loading stresses begin as low as 0.001 kg/cm^2 and increase, using a load increment ratio of 2, to values usually less than 1 kg/cm^2 (Ardaman and Assoc., 1984; Bromwell and Carrier; 19.79). At the end of each load increment, average values of void ratio and effective stress are computed, leading to the compressibility relationship, A typical test will last several months.

To determine the permeability relationship several approaches can be used. First, a constant head permeability test can be conducted at the end of each load increment. However, in doing this, care must taken to minimize seepage-induced consolidation, which is commonly accomplished by applying very small gradients (Ardaman and Assoc., 1984;

Wissa et al., 1983), or by reducing the applied load to counterbalance the tendency of the effective stress to increase (Scott et al., 1985).

In a different approach, the coefficient of permeability, k, at the end of each load increment is computed from the coefficient of consolidation at 90% consolidation, obtained from a square root of time method similar to the conventional oedometer; this is given by (Carrier and Bromwell, 1980)

$$k = \frac{c_v \, a_v \, \gamma_w}{1 + e_f} \qquad (2.1)$$

with

$$c_v = \frac{T \, h_f^2}{t_{90}} \qquad (2.2)$$

where e_f = final void ratio

a_v = coefficient of compressibility = $de/d\grave{U}'$

h_f = final height of specimen

t_{90} = elapsed time to 90% consolidation

T = factor similar to the standard time factor, which depends on the void ratio; typically 0.85 to 1.2.

Such an approach is based on a modified form of Terzaghi's theory, obtained from finite strain computer simulations of the slurry consolidation test (Carrier et al., 1983; Carrier and Keshian, 1979). In some instances (e.g. Ardaman and Assoc., 1984; Keshian et al., 1977; Wissa et al., 1983), Terzaghi's classical theory is used directly to backcalculate the permeability.

In a third approach, used during the self-weight phase of the test the permeability is obtained from the

self-imposed hydraulic gradient (Bromwell and Carrier, 1979). Of course, this approach requires very accurate measurements of pore pressure, which is not a standard part of the test; for example, for a 45-cm height specimen of a typical phosphatic clay, with initial solids content of 16%, the initial maximum excess pore is only about 0.07 psi.

In summary, the slurry consolidation test is a relatively simple procedure to obtain the constitutive relationships of diluted soils. However, it suffers from two major drawbacks, specifically, its extremely long duration of up to 6 to 7 months (Carrier et al., 1983) and the shortcoming of partially relying on small strain theory to interpret the test results.

Settling Column Tests

Several variations of self-weight settling column tests have been used to study the settlement behavior of slurries. Relatively small specimens have been used to study the end of sedimentation conditions of very dilute sediments (Ardaman and Assoc., 1984), to define the compressibility relation of the material at low effective stresses (Cargill, 1983; Scully et al., 1984; Wissa et al., 1983) and the highest possible void ratio of the material as a soil, i.e. the fluid limit, (Scully et al., 1984), and in some cases, even the permeability relationship (Poindexter, 1987). In these tests, the compressibility relationship is readily obtained from water content measurements with depth at the

end of the consolidation process. Determination of the permeability, on the other hand, requires curve fitting methods using a linearized version of the finite strain consolidation theory.

Larger settling tests with specimen heights of up to 10 meters (Been and Sills, 1981; Lin and Lo, 1984; Scott et al., 1985) are perhaps the best approach to study the sedimentation/consolidation behavior of sediments. If properly monitored, such tests can provide all the needed characteristics of the slurry. Proper monitoring of the test includes measurements of pore pressure and density profiles with time. The approach, however, has major limitations. Specifically, those tests on small and very dilute samples only cover a small range of effective stress, while the tests with large specimens would take so long that they become impractical for any purpose other than research.

CRD Slurry Consolidation Tests

Perhaps, one of the most promising tests to study the consolidation properties of slurries and very soft soils is the constant rate of deformation (CRD) consolidation test. The test is applicable over a wide range of initial void ratios (e_i = 10-20) (Scully et al., 1984). Very large strains can be achieved (up to 80%) and, compared to other tests, it can be performed in a relatively short period of time (in the order of one week) (Schiffman and Ko, 1981). The test allows automatic and continuous monitoring and with

the right approach it can provide both, the compressibility and permeability relationships, over a wide range of void ratios.

To interpret the results of CRD tests, two different philosophies can be followed. In one case, one could choose to measure experimentally only those variables needed to solve the inversion problem, i.e. obtain the material characteristics from the governing equation, usually after some simplifications, knowing the solution observed experimentally; this would be the equivalent of the curve fitting methods in conventional tests. For example, in the conventional approach only the specimen height is monitored in the test. By curve fitting techniques and the solution of the governing equation, the coefficient of consolidation and other properties, including compressibility and permeability, are computed.

Alternatively, one could try to measure directly as many parameters as possible and avoid the use of the governing equation, reducing the number of assumptions concerning the theoretical behavior of the material. For example, measuring the pore pressure distribution in a conventional oedometer could lead to the compressibility curve by only using the effective stress principle. With the rapid development in the areas of electronics and instrumentation the use and acceptance of this last approach will definitely grow.

The University of Colorado's CRD test (Schiffman and Ko, 1981; Scully et al., 1984; Znidarcic, 1982) can be classified in the first one of these categories. The test uses a single-drained 2-inch specimen. The analysis procedure neglects the self-weight of the material and assumes the function g(e) to be piecewise linear in order to simplify the governing equation (Znidarcic, 1982; Znidarcic et al., 1986); this is given by

$$g(e) = - \frac{k}{\gamma_w (1+e)} \frac{d\sigma'}{de} \qquad (2.3)$$

where γ_w is the unit weight of water, e is the void ratio, and the other terms have been previously defined.

The test only measures the total stress and pore pressure at both ends of the specimen, as well as its deformation. An iterative procedure using the solution of the linearized differential equation, in terms of the void ratio, yields the void ratio-effective stress relationship, The permeability-void ratio relation can then be computed from the definition of g(e). However, Znidarcic (1982) found that this approach produced a 15%-30% error in the computed values of g(e), and therefore the permeability; this was for a case where the compressibility relationship was accurate within 2%.

In an alternative method suggested to overcome the above problem, the solution of the linearized governing equation is used as before to obtain the compressibility relationship. From the theoretical distribution of excess pore pressure, the hydraulic gradient, i, at the drained

boundary can be determined. With this value the coefficient of permeability is readily obtained from

$$k = \frac{v}{i} \qquad (2.4)$$

where v is the apparent relative velocity at the boundary, equal to the imposed test velocity; in this form, k is not directly affected by errors in the calculated values of g(e).

Due to the limitations of using consolidation tests to obtain the permeability, Znidarcic (1982) stressed the importance of a direct measurement using the flow pump test. In this technique a known rate of flow is forced, by the movement of a piston, through the sample and the generated gradient is measured. This induced gradient must be small (less than 2) in order to minimize seepage-induced consolidation (Scully et al., 1984).

The flow pump test is used in conjunction with a step loading test to generate the permeability-void ratio relationship. This technique, however, is more appropriate in the case of very stiff and permeable samples (Znidarcic, 1982), where no significant excess pore pressures would be developed. It has been used for slurries at relatively low void ratios ($e < 8$) (Scully et al., 1984), and soft samples of kaolinite ($e < 2.8$) (Croce et al., 1984).

Znidarcic (1982) has also proposed the use of a simplified analysis procedure to obtain the permeability from a CRD test. If the void ratio and therefore the coefficient of permeability are assumed uniform within the

specimen, then the pore pressure distribution is found to be parabolic. This is justified in those cases where the test produces very small but measurable pore pressures at the undrained boundary. From here the hydraulic gradient and permeability are easily computed.

An important parameter in any CRD consolidation test is the rate of deformation. This will determine the amount of excess pore pressure that builds up in the specimen. Most analysis procedures assume that the void ratio within the sample is uniform. However, even when the weight of the material is negligible, the pore pressure and the effective stress are not uniform, due to the boundary conditions. Thus, the assumption of uniform void ratio could never be met. Nevertheless, it is desirable to keep the hydraulic gradient small in order to minimize the error introduced by the assumption. This can be achieved by running the test at the lowest possible velocity. In the case of the small strain controlled rate of strain consolidation theory (ASTM D 4186), an estimate strain rate of 0.0001 %/minute is suggested for soils with high liquid limits of 120%-140%; the liquid limit of a typical phosphatic clay is even higher. The test procedure specifies that the strain rate should be selected such that the generated excess pore pressure be between 3% and 20% of the applied vertical stress at any time during the test. Unfortunately, there are no equivalent recommendations for the case of large deformation consolidation tests. It has been suggested that an

acceptable deformation rate should produce a maximum excess pore pressure of up to 30%-50% of the applied stress (Znidarcic, 1982).

A variation of the CRD consolidation test was developed at the U.S. Army Engineer Waterways Experiment Station (WES) for testing soft, fine-grained materials (Cargill, 1986) and to replace the use of the standard oedometer as the tool to obtain the compressibility and permeability relationship of dredged materials (Cargill, 1983). In this test, denoted large strain, controlled rate of strain (LSCRS) test, a 6-inch in diameter specimen of slurry is loaded under a controlled, but variable, strain rate; the specimen height can be up to 12 inches. The main reason for selecting a controlled and not a constant rate of strain was to minimize testing time to, typically, 12-16 hours (Poindexter, 1987).

The WES test monitors the pore pressure at 12 ports along the specimen using 3 pressure transducers and a system of lines and valves, with the associated problems of system compliance and dearing. The effective stress at each end of the specimen as well as its deformation are also measured with time.

Analysis of the LSCRS data requires the use of the results obtained from the small self-weight consolidation test (Poindexter, 1987) in order to generate the compressibility and permeability relationships. In the approach, the first void ratio distribution in the specimen is computed from the measured effective stress, using the

value of the compression index, C_c, obtained from the self-weight test; at point i the void ratio is given by

$$e_i = e_{ref} - C_c \log(\sigma'_i/\sigma_{ref}) \qquad (2.5)$$

where e_{ref} = reference void ratio on the previously determined e-σ' curve

σ_{ref} = value of effective stress at e_{ref}

σ' = effective stress for which e_i is being calculated

Between any two points where the void ratio is being computed, the volume of solids, l_i, is given by

$$l_i = h_i/(1 + e_i) \qquad (2.6)$$

where h_i = actual thickness of the increment

e_i = average void ratio of the increment

Since the total volume of solids is constant throughout the test, the calculated void ratio distribution is adjusted to satisfy this condition. After this adjustment is done, the compressibility curve is extended further by using the average values of effective stress and void ratio of points next to the moving end as the next reference point. The process is repeated using the new measured data at increasing loads.

Determination of the coefficient of permeability at the moving boundary of LSCRS test is obtained from Darcy's law using an expression equivalent to equation 2.4. In addition, the approach obtains the permeability at interior points from an estimate of the apparent fluid velocity,

obtained from the equation of fluid continuity (Poindexter, 1987).

Many deficiencies have been found in the LSCRS test. Because of the rapid rate of deformation, consolidation does not occur uniformly throughout the specimen and a filter cake of material forms at the drained boundary. Additionally, the analysis of the test data requires a trial and error procedure which depends on the results of a self-weight test to provide a starting point. Last, but not least, the test equipment is extremely complicated and requires frequent manual adjustment and monitoring. WES is currently working on the development of a new test device and procedure (Poindexter, 1987) to replace the LSCRS test; it will be a constant rate of strain apparatus and the test is expected to last from 5 to 10 days. Automatic controlling and monitoring, through a computer/data acquisition system, will be incorporated in the test.

Conventional consolidation tests, such as the step loading test or the CRSC test are very frequently used to complement the results of large-deformation consolidometers (Ardaman and Assoc., 1984; Cargill, 1983; Poindexter, 1987; Wissa et al., 1983). In some cases, conventional testing methods and analysis procedures have been used exclusively (Cargill, 1983). These tests are usually conducted on preconsolidated specimens to facilitate handling and trimming. Such tests will provide information on the behavior

of the material at relatively low void ratios (e < 7) (Ardaman and Assoc., 1984).

Centrifugal Modelling

Centrifugal modelling has been used quite extensively to predict the consolidation behavior of slurries under different disposal schemes (Beriswell, 1987; Bloomquist and Townsend, 1984; McClimans, 1984; Mikasa and Takada, 1984; Townsend et al., 1987). Several attempts have been made to determined the soil's constitutive relationships from centrifuge testing (Croce et al., 1984; McClimans, 1984; Townsend and Bloomquist, 1983) with relatively good results obtained in the case of effective stress-void ratio relation. Perhaps, one of the most valuable applications of centrifugal modelling is to validate computer predictions (Hernandez, 1985; McVay et al., 1986; Scully et al., 1984)

The main advantages of centrifugal modelling in the study of the consolidation behavior of slurries are (1) the duplication in the model of the stress level existing in the prototype and (2) the significant reduction in the time required to achieve a given degree of consolidation in the model. This is given by

$$t_m = t_p/n^x \qquad (2.8)$$

where t_m = elapsed time in the model

t_P = elapsed time in the prototype

n = acceleration level in number of g's

x = time scaling exponent

A major problem with centrifugal modelling is the determination of the time scaling exponent, x. Theoretically, this exponent is 1.0 for sedimentation and 2.0 for consolidation. In Appendix A a proof is presented where the governing equation of the finite strain self-weight consolidation theory holds in the model if and only if $x = 2$. A different proof of this result, based on mechanical similarity, is given by Croce et al. (1984).

However, experimental results based on modelling of models and reported by several researchers indicate somewhat contradictory conclusions. An exponent of 2.0 has been confirmed for the centrifugal modelling of the consolidation of soft kaolinite clay with a relatively low initial void. ratio of 2.86 (Croce et al., 1984). Scully et al. (1984) found that the time scale exponent varied from 1.90 to 2.3 for a slurry with initial void ratio of 15; they concluded that the exponent could be assumed to be 2.0 and that sedimentation probably did not occur in the tests.

By contrast, the results of Bloomquist and Townsend (1984) show that starting with an initial void ratio of 16, the scaling factor progresses from 1.6 to 2.0. They attributed these values to the existence of two zones in the slurry, hindered settlement and consolidation. As these zones approach, consolidation predominates and the theoretical exponent of 2.0 is achieved; this occurred at an average solids content of 20.9% ($e \simeq 10.3$), practically at the end of the test.

Constitutive Properties

One of the basic assumptions of any of the formulations of large strain consolidation theory is that the soil's constitutive relationships are of the general form (e.g. Cargill, 1982)

$$\sigma' = \sigma'(e) \tag{2.7a}$$

$$k = k(e) \tag{2.7b}$$

and that they are unique for a given material. Equation 2.7a determines how much consolidation will take place, while equation 2.7b describes how fast this will happen.

Roma (1976) reported that the best compressibility relationship for phosphatic clays was a power curve of the form

$$e = A \cdot (\sigma')^{B} \tag{2.8}$$

Likewise, the permeability relationship was expressed by the function

$$k = C \cdot (e)^{D} \tag{2.9}$$

Traditionally, it has been accepted that phosphatic clays can be characterized by these relationships (Ardaman and Assoc., 1984; Carrier and Bromwell, 1980; Somogyi, 1979), and very little effort, if any, has been dedicated to corroborate the validity of such relationships. This may be attributed, in part, to the convenience presented by the simplicity of the expressions and, just maybe, to the bad habit or tradition of geotechnical engineers to stay with the "status-quo."

The parameters A,B,C,D obtained by several studies for Kingsford phosphatic clay are presented in Table 2-1.

Table 2-1. Kingsford Clay Parameters

Source	A	B	C	D
Ardaman and Assoc. (1984)	26.81	-0.269	7.74E-7	3.56
Somogyi et al. (1984)	23.00	-0.237	1.03E-6	4.19
Carrier et al. (1983)	24.36	-0.290	1.34E-6	3.41
McClimans (1984)	19.11	-0.187	7.59E-14	11.12
Townsend/Bloomquist (1983)	22.30	-0.230	2.03E-9	7.15

These parameters are for σ' in psf and k in ft/day. Ardaman and Assoc.'s parameters are based on slurry consolidation tests and conventional CRSC and incremental loading tests. Somogyi et al. parameters were obtained from laboratory slurry consolidation tests and CRSC tests, as well as field data.

The parameters attributed to Carrier et al. (1983) were obtained from the constitutive relationships proposed by them in terms of the Atterberg limits of the clay, as preliminary design properties. These relationships, for a specific gravity of the solids of 2.7, are given by

$$e = (0.48PI)(\sigma')^{-0.29} \qquad (2.10a)$$

$$k = (2.57PI)^{-4.29}(e)^{4.29}/(1+e) \qquad (2.10b)$$

where PI is the plasticity index in percentage, σ' is in kPa, and k is in m/sec. Using a plasticity index of 156% reported for this clay (Ardaman and Assoc., 1984; McClimans,

1984), a number of data points with void ratios between 5 and 15 were generated. A log-log linear regression, with very high correlation coefficients, led to the parameters given in Table 2-l after the necessary units conversion. Finally, McClimans' and Townsend and Bloomquist's parameters were obtained by back-calculations from selected centrifugal tests.

Table 2-l shows a tremendous discrepancy in the parameters defining the constitutive relationships, mainly in those corresponding to the permeability-void ratio relation. This can be the result of improper testing techniques, the, relationships not being unique, or both.

The use of the power functions in computer predictions introduces an important inconsistency. Under quiescent conditions, for example, the slurry is deposited at a known and usually constant solids content. According to equation 2.8, the material must have an initial effective stress throughout its depth. This implies two things; first, the initial excess pore pressure will be less than the buoyant stress and, second, the points at the surface will have an effective stress which does not exist. The computer programs overcome this inconsistency by imposing on the pond a dummy surcharge equal to the initial effective stress (Somogyi, 1979; Zuloaga, 1986).

The results of several studies suggest that the constitutive relationships of slurried soils not only are not power curves, but also are not unique. Specifically,

variations in the compressibility relations have been observed in different soils, especially at low effective stresses (Been and Sills, 1981; Cargill, 1983; Imai, 1981; Mikasa and Takada, 1984; Scully et al., 1984; Umehara and Zen, 1982; Znidarcic et al., 1986). These variations have been attributed by some to the effect of the initial void ratio.

Scully et al. (1984) reported the existence of a "preconsolidation" effect in the compressibility curves obtained from CRD tests; they concluded that this effect was most probably the result of the initial void ratio. Similar results on the permeability-void ratio relation have not been specifically reported. However, the curves presented by several researchers suggest the existence of a zone similar to the apparent preconsolidation effect observed in compressibility curves (Scully et al., 1984; Znidarcic, 1986).

Another important aspect that may be conclusive to better understand the consolidation behavior of slurries is their initial conditions when they are first deposited. Scott et al. (1985) found in their large settling column tests that, when the material was first placed in the cylinders, the pore pressures were equal to the total stresses over the full height. A similar response was observed in samples with initial solids content of 10% and 31%. In the case of the denser specimen, a uniform decrease in pore pressure was observed in 30 days, when no

significant consolidation had taken place; this was attributed to the appearance of an effective stress by thixotropy. Thus, these results indicate that the slurry has no effective stress when deposited, regardless of its initial solids content. If this is the case, the compressibility relationship can not be unique, at least initially.

CHAPTER III
AUTOMATED SLURRY CONSOLIDOMETER-- EQUIPMENT AND TEST PROCEDURE

Introduction

This chapter describes the test equipment and procedure of a new automated slurry consolidation test, developed specifically to obtain the compressibility and permeability relationships of slurries and very soft soils. Figure 3.1 shows a schematic arrangement of the equipment, which consists of the following components:

1) test chamber,
2) stepping motor,
3) data acquisition/control system.

The following sectionsdescribe in detail each one of these components. At the end of the chapter, the test procedure is presented.

The Test Chamber

The specimen of slurry is contained in an acrylic cylinder with a diameterof 0.2 meters (8 inches) and 0.35 meters (14 inches) height. Figure 3.2 is a schematic of the test chamber. The initial height of the specimen can be varied between 0.10 and 0.20 meters (4-8 inches).

A double-plate piston is used to apply the load on the specimen; the two plates, 3.75 inches apart, help prevent

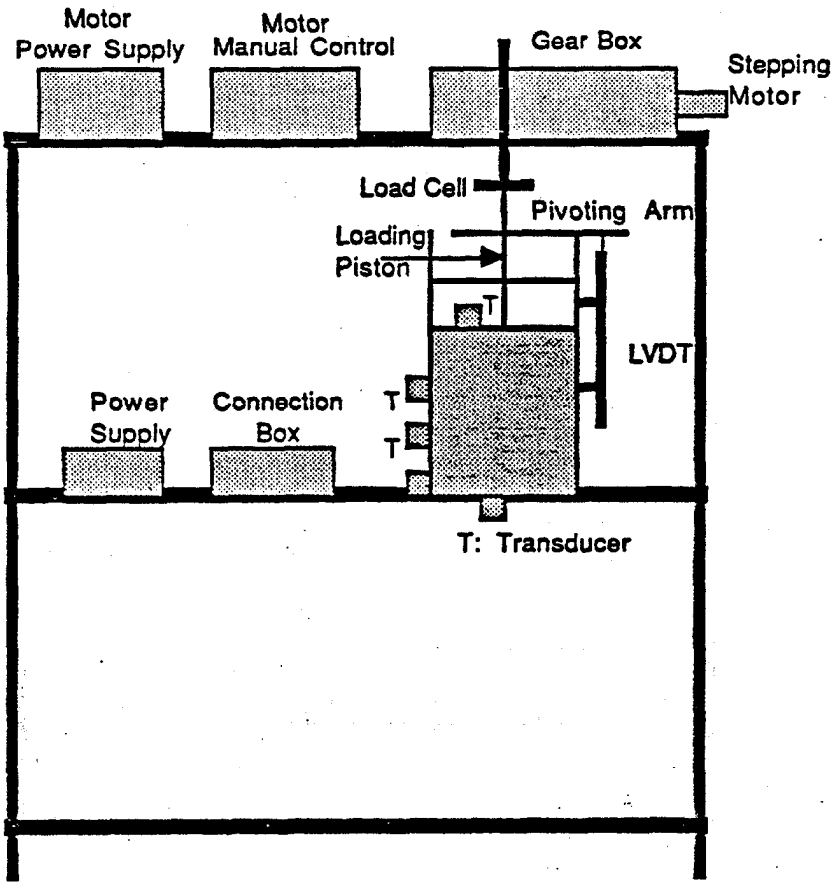

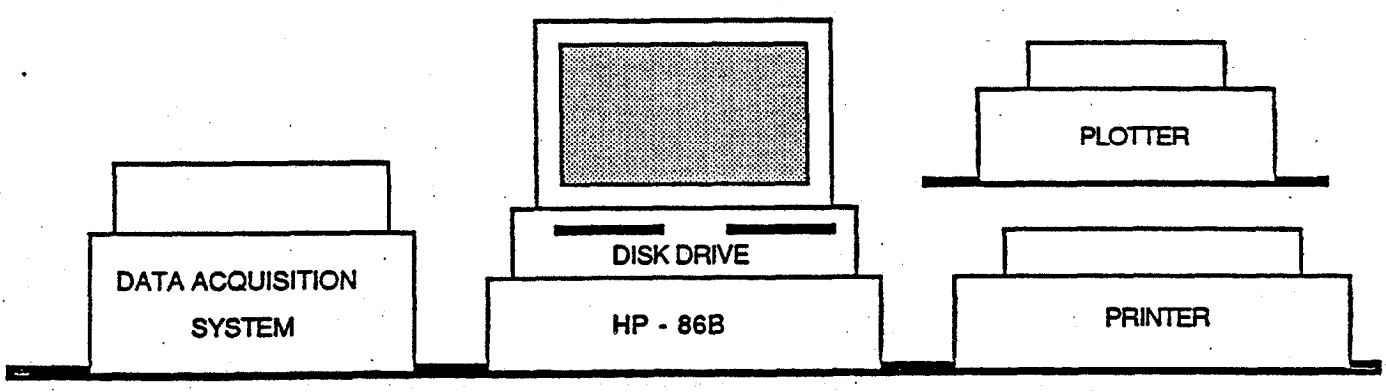

Figure 3.1 - Schematic of Automated Slurry Consolidometer

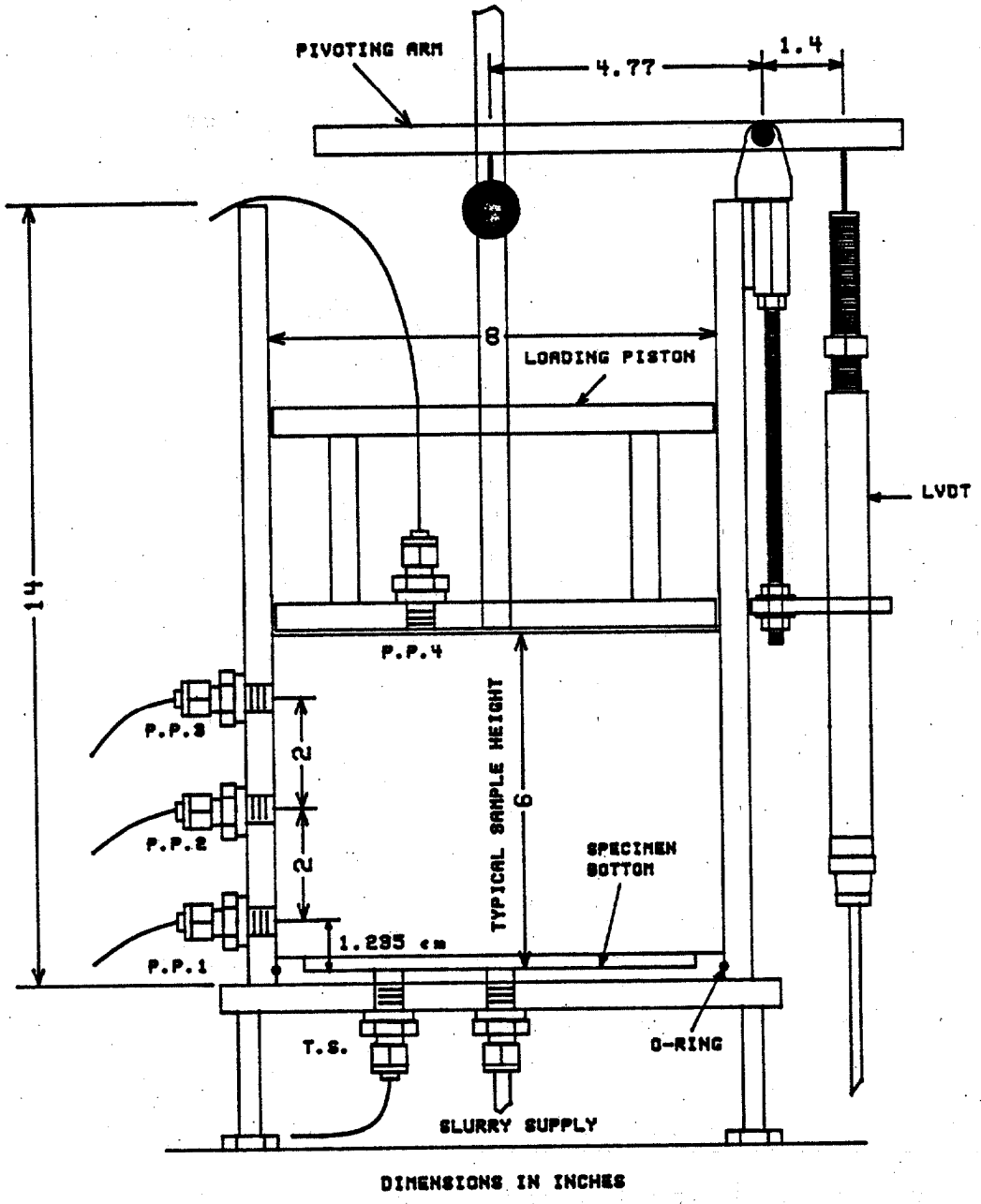

Figure 3.2 - Schematic of Slurry Consolidometer Chamber

tilting of the piston. At the bottom of the piston, a porous plastic plate allows top drainage of the specimen. A filter cloth, wrapped around the bottom plate, closes the small, nonuniform gap between the piston and the walls of the cylinder, while allowing water to drain freely. Originally, this gap was filled with a rubber O-ring around the bottom plate; however later, it was found that the filter cloth served the function better and reduced the piston friction.

Located directly on top of the piston rod, a load cell measures the load acting on the specimen at any time. Two load cells, 200-lb and l000-lb range, both manufactured by Transducers, Inc. have been used in this research.

Along the side of the acrylic cylinder, two 1-bar (1 bar = 100 kPa = 14.5 psi) and one 20-psi miniature pressure transducers are used to monitor the excess pore pressure in the specimen. Transducer No. 1 is located 1.235 centimeters from the bottom of the chamber. Transducers No. 2 and No. 3 are placed 5 centimeters above the previous one. An additional 350-mbar (5 psi) transducer (No. 4), located on the moving piston, is used to. detect any excess pore pressure building up at the supposedly free-drainage boundary. The transducers were mounted inside an O-ring sealed brass fitting, which threads directly onto the wall of the chamber. Locating the transducers directly in contact with the specimen eliminates the problems of tubing, valves, and system dearing.

All the pressure transducers used in the test are model PDCR 81, manufactured by Druck Incorporated, of England. They consist of a single crystal silicon diaphragm with a fully active strain gauge bridge diffused into the surface. These transducers are gage transducers, thus eliminating the potential problem of variations in atmospheric pressure, with a combined nonlinearity and hysteresis of ±0.2% of the best straight line. To resist the effective stress of the soil, i.e. only measure pore pressure, a porous filter plate or stone is placed in front of the diaphragm. The standard porous stone is made of ceramic with a filter size of l-3 microns; a 9-12 microns sintered bronze stone is also available. Figure 3.3 shows a photograph of the PDCR 81 and a sketch indicating its dimensions.

At the bottom of the specimen another pressure transducer (3-bar range), without the porous stone, is used to measure the total vertical stress at this point. This measurement, coupled with the load cell readings, makes it. possible to determine the magnitude of the side friction along the specimen.

A major objective during the design phase of the equipment was to make it fully automatic. This presented an obstacle when trying to define the best way to measure the specimen deformation, which was anticipated to be up to 4-6 inches. The problem was solved using a Direct Current Linear Variable Differential Transformer (LVDT) and the pivoting arm arrangement shown in Figure 3.2. The LVDT,

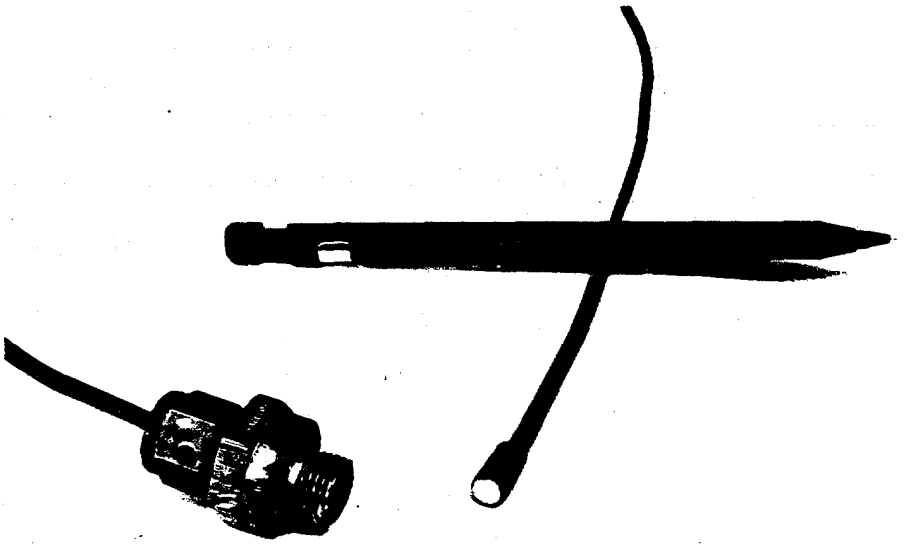

(a)

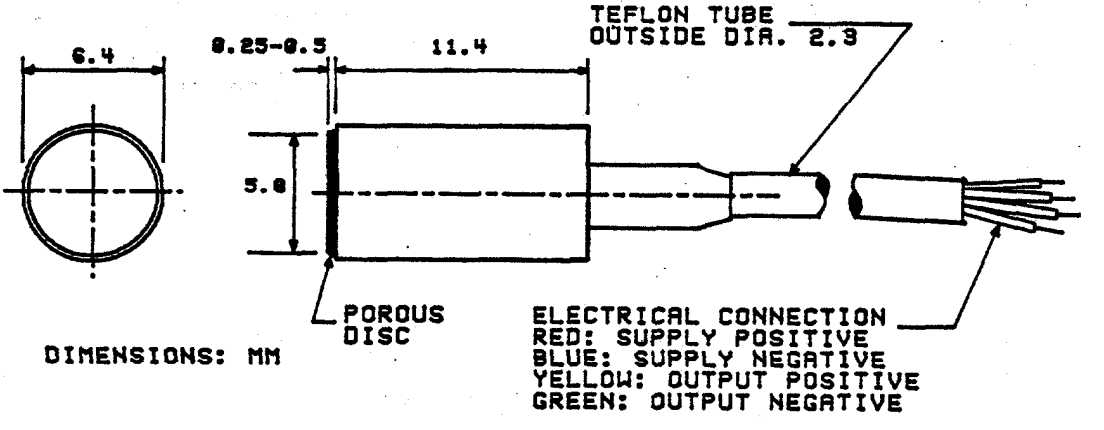

(b)

Figure 3.3 - Pore Pressure Transducer PDCR81. a) Photograph; b) Sketch Showing Dimensions

model GCD-121-1000 and manufactured by Schaevitz, has a nominal range of ±l inch and linearity of ±0.25% at full range.

The horizontal distances from the pivoting point of the arm to the center of the specimen and to the LVDT tip were accurately measured as 121.2 mm and 35.6 mm, respectively, which resulted in an arm ratio of 1:3.40. This arrangement allows measuring specimendeformations over 6 inches. The factory calibration of the LVDT was converted using the arm ratio to yield directly the deformation of the specimen. Appendix B evaluates the converted calibration of the LVDT and proves that computations of the deformation are independent of the initial inclination of the arm.

Figure 3.4 is a photograph of the test chamber showing the pressure transducers, the loading piston, the LVDT, and the pivoting arm. Table 3.1 summarizes the information on the different devices. The recommended excitation for these transducers is 5 VDC, but this was increased to 10 VDC, the maximum allowed, to improve the transducer sensitivity. Although the 200-lb load cell was used in most of the tests, the information on the 1000-lb load cell is also included since this was used in some tests where the load was expected to be large.

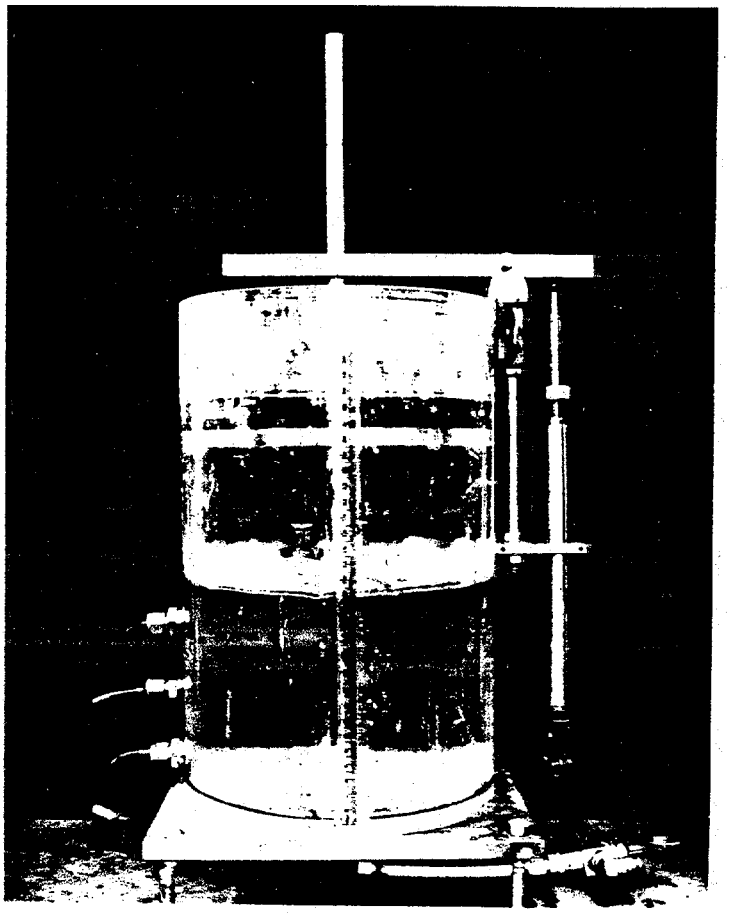

Figure 3.4 - Photograph of Slurry Consolidometer Chamber.

Table 3-1. Slurry Consolidometer Transducer Information

DEVICE	MODEL	SERIAL No.	RANGE	EXCITATION	CALIBRATION
TOTAL STRESS	PDCR 81	3021	3 bars	10 VDC	3.568 mV/psi
PWP #1	PDCR 81	2998	1 bar	10 VDC	6.370 mV/psi
PWP #2	PDCR 81	2955	1 bar	10 VDC	7.418 mV/psi
PWP #3	PDCR 81	3092	20 psi	10 VDC	6.900 mV/psi
PWP #4	PDCR 81	3241	5 psi	10 VDC	12.80 mV/psi
LOAD CELL	T182-200-10P1	73169	200 lb	10 VDC	0.099805 mV/lb
	T182-1K-10P1	49650	1000 lb	10 VDC	0.019943 mV/lb
LVDT	GCD-121-1000	3220	2 in	+/- 15 VDC	0.117 V/mm

The Stepping Motor

The load applied to the specimen is produced by a computer-controlled stepping motor and a variable speed transmission arrangement, located as shown in Figure 3.1. The stepping motor is a key element of the apparatus; its versatility is crucial in allowing different types of loading conditions.

The stepping motor is manufactured by Bodine Electric Company, model 2105, type 34T3FEHD. It operates under 2.4 VDC and 5.5 amps/phase. The motor has a minimum holding torque of 450 oz-in and a SLEW (dynamic) torque of 400 oz-in, producing 200 steps per revolution or 1.8 degree per step.

The motor is driven by a THD-1830E Modular Translator, model No. 2902, also made by Bodine. The translator uses and external 24 VDC power supply. The photograph of Figure 3.5 shows the front panel of the translator (left), and the stepper motor (right), while Figure 3.6 presents a schematic diagram of the back of the instrument with the cover removed, showing the connections to the stepping motor. For this configuration, the following resistances are required

Suppression Resistor: R_1 = 13 ohms @ 18W

Series Resistors (2): R_2 = 3.6 ohms @ 175W

Logic Resistor: R_3 = 15 ohms @ 2W

All control line connections to the stepping motor control card are made through a 15 pin. "D" connector, located on the side of the translator. For manual (front panel) control of

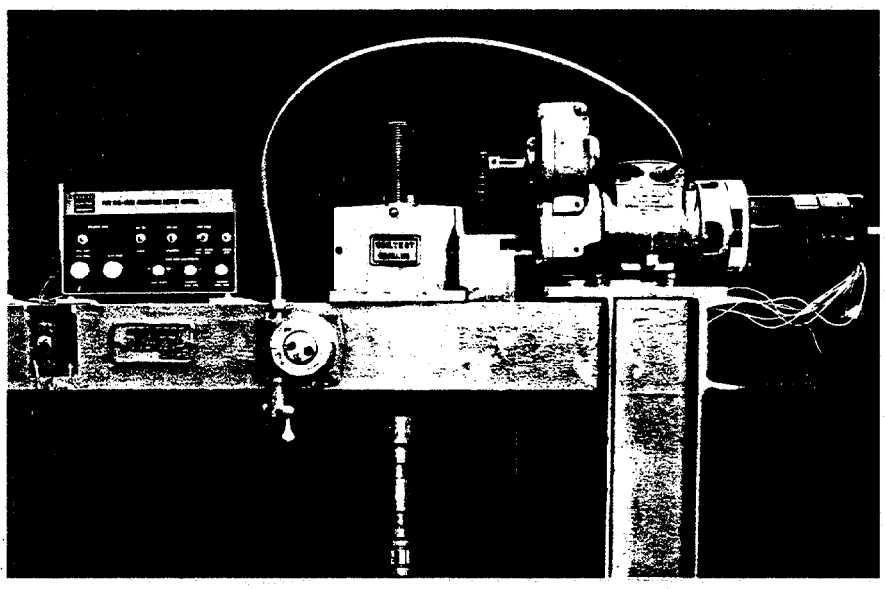

Figure 3.5 - Motor Translator, Gear Box, and Stepper Motor

OVERALL SYSTEM SCHEMATIC

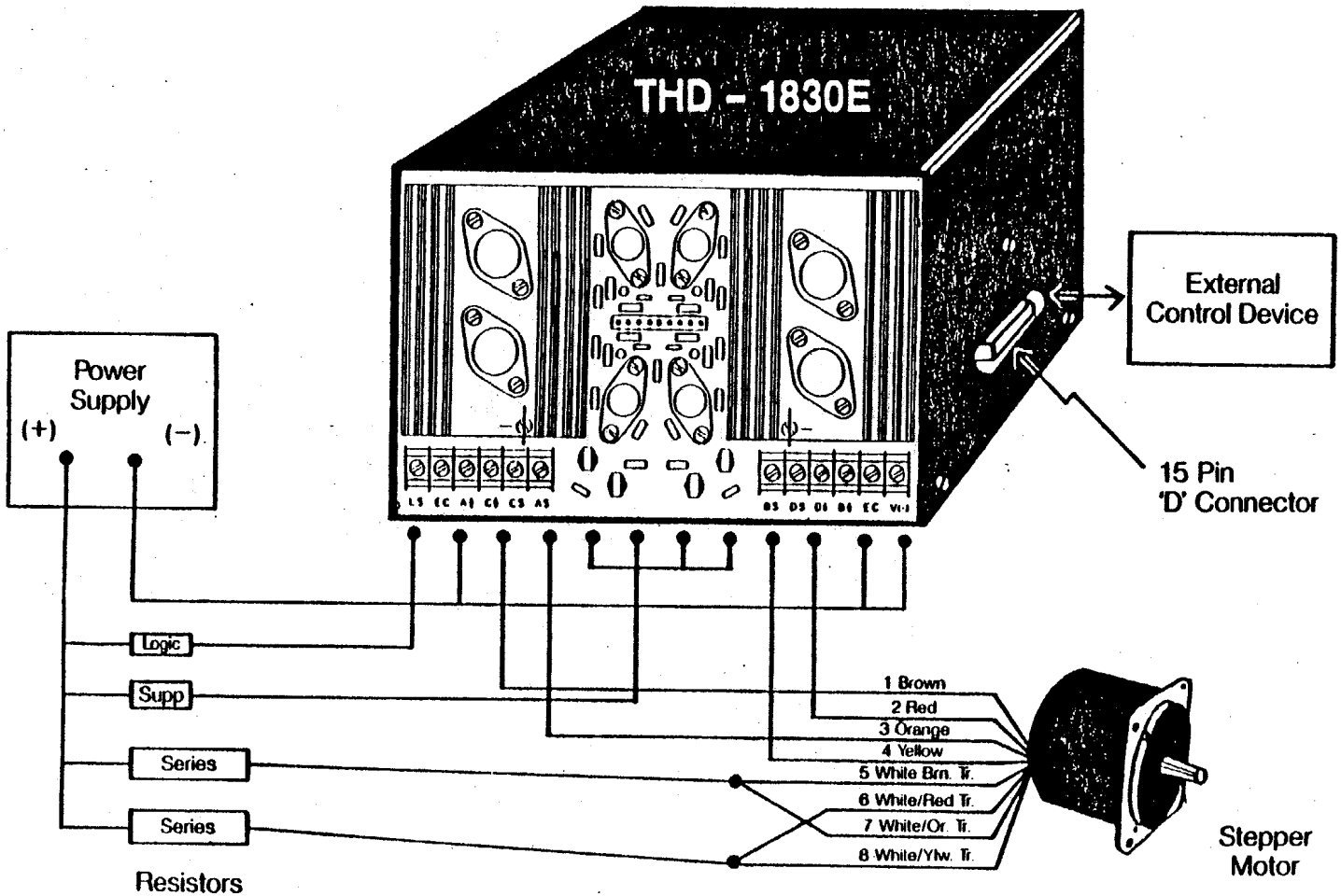

Figure 3.6 - Schematic of Motor Translator Connections

the motor, pins 6 and 13 of the connecter are jumped. A switch that allows this jumping was installed next to the translator. In this way the control of the motor can be easily switched between manual and computer. Manual operation of the motor is very important during setting up and dismantling of the test.

The variable speed transmission (gear box), made by Graham, converts the motor rotation into vertical movement of a threaded rod, which acts directly on the loading piston (Figure 3.5). Even if the motor is running at full speed, the gear box allowsminute movement of the loading piston. During the testing program, the speed control of the gear box was set at its maximum, producing a vertical displacement in the order of, 3E-05 mm/step. Figure 3.5 also shows the load cell at the bottoms of the threaded rod.

Figure 3.7 shows a photograph of the entire test assembly. The equipment was mounted on a steel frame.

The Computer and Data Acquisition/Control System

Figure 3.8 shows a photograph of the computer system used to control and monitor the test. The computer is a Hewlett Packard, model 86B, with 512 KB of memory and a build-in BASIC Interpreter.

The data acquisition/control system has two components: an HP-3497A and an HP-6940B, both manufactured by Hewlett Packard. The HP-3497A, a state-of-the-art data acquisition and control unit, is used to monitor the pressure

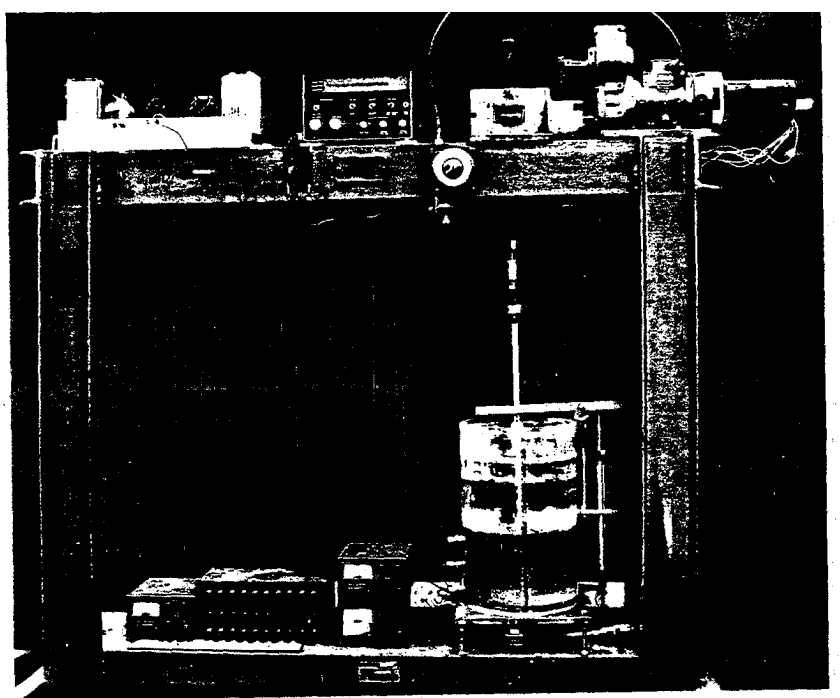

Figure 3.7 - Entire Slurry Consolidometer Assembly

transducers, load cell, and LVDT outputs. The unit can be remotely operated from the computer or through the front panel display and keyboard.

The 3497A Digital Voltmeter (DVM) installed in the unit is a 5½ digit, 1 microvolt sensitive voltmeter. Its assembly is fully guarded and uses an integrating A/D conversion technique, which yields excellent noise rejection. Its high sensitivity, together with autoranging and noise rejection features, makes it ideal for measuring the low level outputs of thermocouples, strain gauges and other transducers. The DVM includes a programmable current source for high accuracy resistance measurements when used simultaneously with the voltmeter.

The 3497A DVM assembly is very flexible and can be configured to meet almost any measurement configuration. It may be programmed to obtain a maximum of 50 readings per second in 5½ digit mode or 300 readings per second in 3½ digit mode. The 3497A DVM may be programmed to delay before taking a reading to eliminate any problem with settling times. Similarly, the DVM assembly can be programmed to take a number of readings per trigger with a programmable delay between readings. This feature, combined with internal storage of sixty 5½ digit readings, permits easy stand-alone data logging.

Installed in the 3497A, there is a 20 channel analog signal reed relay multiplexer assembly. This assembly is used to multiplex signals to the 3497A DVM. Each channel

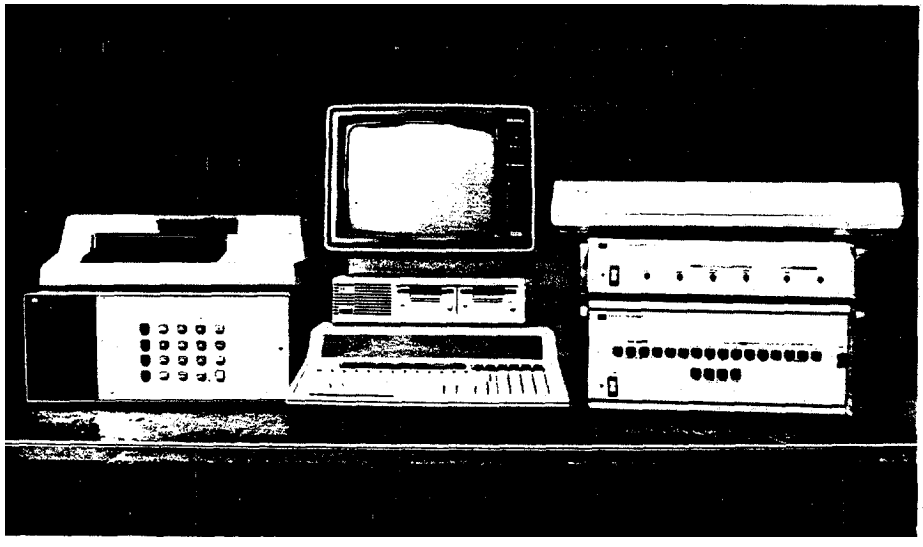

Figure 3.8 - Computer and Data Acquisition/Control System

consists of three, low thermal offset dry reed relays, one relay each for Hi, Lo and Guard. The low thermal offset voltage characteristics of this multiplexer makes it ideal for precise low level measurements of transducers. The relays may be closed in a random sequence or increment between programmable limits.

The other component of the data acquisition/control system, the HP-6940B Multiprogrammer, provides flexible and convenient Input/Output expansion and conversion capability for computers. This versatility has made the Multiprogrammer an important part of many different types of automatic systems, including production testing, monitoring and control (e.g. Litton, 1986). In the current application, however, the 6940B, interfaced to the computer through the HP-59500A Multiprogrammer Interface, is used exclusively to control the stepping motor.

A stepping motor control card, model 69335A, was installed in the Multiprogrammer. The card is programmed by a 16-bit word originating at the computer to generate from 1 to 2047 square wave pulses at either of two output terminals of the card. When these outputs are connected to the clockwise and counterclockwise input terminals of the stepping motor translator, the output pulses are converted to clockwise or counterclockwise steps of the associated motor. As the card is supplied from the factory, the output is a waveform of positive symmetrical square-wave pulses with a nominal frequency of 100 Hz. If this frequency is

not suitable, it can be changed to any value between 10 Hz and 2 kHz by changing the value of one resistor and one capacitor in the card. The output frequency can also be made programmable by connecting to the card an external programmable resistor.

During early stages of the research, the Multiprogrammer was also used to monitor all the devices by means of Relay Output/Readback and High Speed A/D Voltage Converter cards, as used by Litton (1986). Electrical noise rejection in the low level outputs of the pressure transducers and load cell-was attempted by means of analog low pass filters (Malmstadt et al., 1981). Several preliminary tests were performed using this hardware configuration, whereby each transducer output was obtained as the average of 10-20 individual readings, to further reduce any noise. It was found, however, that the level of noise in the response was still unacceptable. Therefore, it was decided to undertake a detailed investigation of the transducers response using different size capacitors. In addition, the use of digital filters (Kassab, 1984) was incorporated, and the HP-3497A was tried for the first time, as an alternative to the Multiprogrammer. Appendix C describes the study undertaken. It was concluded, as a result of the study, that the HP-3497A would be used to monitor all transducers. In the case of the LVDT, the output is not affected so much by noise. However, it was decided to change it to the HP-3497A also

and to leave the HP-6940B exclusively to control the stepping motor.

The Controlling Program

The program that controls the test, called SLURRYl, was written in BASIC for the HP-86B. It is a user-friendly program and presently allows two types of test: a Constant Rate of Deformation test (CRD) and a Controlled Hydraulic Gradient test (CHG). However, other types of loading conditions can be very easily incorporated in the program, such as constant rate of loading, step loading, etc.

In the CRD test, the program sends a signal to the stepper motor every half-second to turn forward a given number of steps, corresponding to the desired rate of deformation. A calibration between number of steps and vertical displacement of the piston was made for the gear box speed set at its maximum value; the value obtained was 30,000 steps/mm. Based on this value, the two deformation rates used in the testing program correspond to the motor speeds given in Table 3-2.

Table 3-2. Deformation Rates in CRD Tests

Deformation Rate (mm/min)	Steps/min
0.008	240
0.02	600

In the CHG test,the excess pore pressures at the bottom and top of the specimen,as well as the specimen deformation, are continuously monitored. The average hydraulic gradient acrossthe specimen is computed from this information. If the gradient differs from the desired value by more than a defined percentage, the motor is activated forward or backward accordingly to keep the gradient within the desired range. The required number of steps at any moment is estimated from the previous value of number of steps per unit change in gradient. The experience with the tests performed in this study shows the effectiveness of this approach.

SLURRY1 is organized in a main program and several subroutines. The main program reads the input information and contains the two routines that control the CRD and CHG tests, as described previously. Eight subroutines interact with the main program to perform the operations described below.

Subroutine CALIBRATIONS reads the calibration factors for all the devices from a file on disk; it allows changing or adding new devices to the file, after displaying the current configuration on the monitor. Subroutine INITIALI-ZATION takes the initial readings of the transducers and LVDT; it also prints the general test information and headings of the results table.

Subroutine STEPPING activates the motor as requested by either the CRD or CHG routines. Subroutine RUNTIME

evaluates the elapsed time of the test at any moment. Subroutines READLOWVOLT and READHIGHVOLT read consecutively all the devices.

Subroutine CONVERTDATA uses the readings of the transducers and LVDT, and their calibrations, to compute all the pressures, load, and specimen deformation; these parameters are stored on disk for future data reduction. Subroutine TESTEND decides whether any of the conditions to finish the test has been reached. Appendix D presents a flowchart of the main routine of SLURRYl, and a listing of the full program.

Test Procedure

The test, being controlled by the computer, runs by itself without any human assistance. However, setting up the apparatus requires 2 to 3 hours and is somewhat complicated. This section describes details of the test procedure.

In broad terms, the test procedure consists of the following steps: (a) specimen preparation, (b) deairing and calibration of the pressure transducers, (c) filling the chamber with slurry and adjusting the load cell and LVDT, (d) initiating computer control, (e) reading devices periodically, (f) coring specimen at the end of the test, and (g) reducing data.

The specimen is prepared in a 5 gallon plastic bucket just before the beginning of the test. The slurry is

strongly stirred with an egg beater attached to an electrical drill, to provide a uniform solids content. To reach the desired value of solids content, quick determinations of this value were made using an Ohaus Moisture Determination Balance. This turned out to be a very handy tool. If needed,water or thicker slurry was added to the mix to achieve the desired solids content. Due to the lack of available supernatant water in sufficient amount, tap water was used in most of the tests. Two samples were always used to perform a regular water content determination, from which the initial solids content was determined. It was found that the solids contents obtained with the Moisture Determination Balance were always within ±0.5% of the oven-determined values.

An important part of the test preparation procedure is the vacuum system shown schematically in Figure 3.9. This is used to fill the test chamber with deaired water to produce full saturation of the porous stones and to take the zero readings of the pore pressure transducers (under hydrostatic conditions). The operation of the vacuum system is controlled by a series of four 3-way valves, used as described in the following paragraph.

Water is sucked into the chamber by turning the vacuum pump on with all four valves in the 'a' position. The water can be drained out of the chamber by gravity. However, the process is accelerated by pulling the water with vacuum with valves 1 and 3 in the position 'b', and valves 2 and 4 in

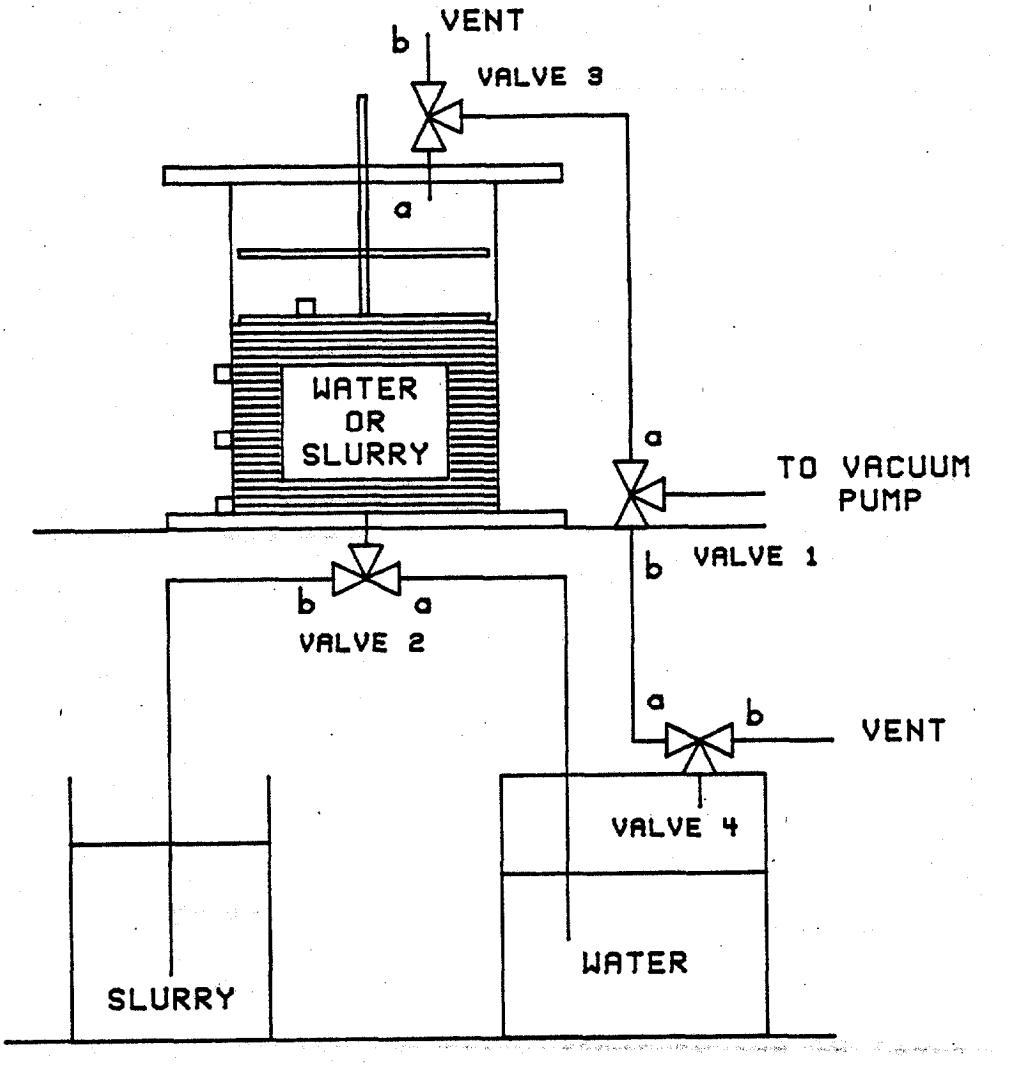

Figure 3.9 - Vacuum System

Table 3-3. Valve Positions in Vacuum System

Operation	Valve 1	Valve 2	Valve 3	Valve 4
Fill with water	a	a	a	a
Drain water	b	a	b	a
Fill with slurry	a	b	a	a,b

the position 'a'; toward the end of this process, however, care must be exercised to prevent the entrance of air into the water container. To avoid this, the vacuum pump is turned off and valve 4 is vented (position 'b') when most of the water has been drained; the remaining will drain by gravity. The vacuum system is also used to fill the chamber with slurry prepared in a container at the desired solids content. To do this, valves 1 and 3 must be set to the position 'a', while valve 2 is on the 'b' position. Table 3-3 summarizes the valve positions required for each operation.

The following is a list of the steps followed in the test procedure:

1. Assemble the vacuum system, set the piston to the sample height, and pull deaired water into the chamber.
2. Turn on the transducers power supply and HP-3497A; check the supply voltage of 10 Volts by reading it from the front panel of the HP-3497A. Allow a warming up time of 10-15 minutes.
3. Apply full vacuum to the chamber to deair the porous stones; check how fast the transducers respond by turning the vacuum on and off several times.
4. Check the calibration of all five transducers by raising (or lowering) the height of water by 10 cm and taking the corresponding voltage readings using the front panel of the HP-3497A; the computed change in height of water must be 10 ± 1 cm.

5. Set the height of water to the height to be used in the test.

6. Run the program SLURRY1 and enter the required data (sample height, initial solids content, etc.); the program will take the zero readings of the pore pressure transducers at this point.

7. When prompted by the program, drain the water and pull the slurry into the chamber using the vacuum system; check that the piston is at the right height. The program has paused at this moment.

8. Take the vacuum attachment off and set the motor control switch to "manual".

9. Set up the load cell by operating it manually, the LVDT, and the pivoting arm.

10. Add water over the piston to reach the-desired height (usually 11 cm. over the slurry height), as used for the zero readings; this is done to guarantee that the piston is always submerged.

11. Change the motor control to "computer" and check that the LVDT power supply is on.

12. After everything has been verified press the "CONT" key to resume the computer control of the test.

13. SLURRY1 prints heading of the output printout and the test starts.

From this moment the control and monitoring of the test is completely taken by the computer. Readings of the different devices are taken periodically as specified by the

user. The time of reading, pressures, load, and specimen deformation are stored on a disk file specified by the user, for future data reduction. The test stops automatically when the maximum time specified is reached. Termination of the test also occurs when any of several abnormal conditions occurs, such as exceeding a pressure transducer or the load cell.

Once the testis completed and the chamber attachments have been removed, the supernatant water is removed and the specimen iscored using a device similar to that used by Beriswill (1987) in his centrifuge bucket. The cored material was sectioned into three pieces to determine the solids content near the top, at the middle, and near the bottom of the specimen. Due to the difficulties in obtaining a good sample, no attempt was made to determine the solids content-depth relationship. An average final solids content was determined from these three values.

The allowed deviation in the transducers response, recommended in step 4 of the test procedure, is the result of observations about the transducers sensitivity during the testing program. Table 3-4 shows the results of one pre-test verification of the calibration/sensitivity of all five pressure transducers.

With water in the test chamber, a set of readings, R_1, was taken using the front panel of the HP-3497A. The height of water was then increased by exactly 10 cm, and new readings were taken, R_2. With these values and the factory

Table 3-4. Verification of Transducer Calibration

Transducer No.	R_1 (mV)	R_2 (mV)	Calibration (mV/psi)	Δp (psi)	Δh (cm)
T.S.	-1.586	-2.115	3.568	0.1483	10.43
1	-17.610	-18.568	6.370	0.1504	10.58
2	-22.856	-24.002	7.418	0.1545	10.87
3	9.363	8.364	6.900	0.1448	10.18
4	8.698	6.970	12.800	0.1350	9.50

calibration factors, the change in hydrostatic pressure, Δp, was computed. Assuming the unit weight of water as 62.4 pcf, the change in the height of water, Δh, was computed.

Four of the five transducers gave heights above 10 cm, with a maximum deviation of 0.87 cm for transducer No. 2. Surprisingly, in this test the total stress transducer (3-bar range) did not produce the maximum deviation, and pore pressure transducer No. 4 (5-psi range) did not produce the minimum. In the case of the total stress transducer, where similar results were observed in other tests, the low deviation was attributed, at least partially, to the beneficial effect of not having the porous disc. The relatively large deviation of pore pressure transducer No. 4 is probably the result of the random nature of the variation. In another test, for example, the same transducer gave a deviation of only 0.024 cm when the height of water was increased by 10 cm.

These observations led to the conclusion of allowing a deviation of ± 1 cm, when checking the calibration of the transducers prior to the test. One centimeter of water

(0.014 psi) is taken as the approximate sensitivity of these pressure transducers.

CHAPTER IV
AUTOMATED SLURRY CONSOLIDOMETER-- DATA REDUCTION

Introduction

A main objective during the development of this new test was to make direct measurements of as many variables as possible, in order to minimize the use of theoretical principles or assumptions. The formulation of the two constitutive relationships required in finite strain consolidation theory involves three variables, namely, void ratio, effective stress, and coefficient of permeability. Direct measurement of these parameters is not feasible. Instead, they will be evaluated from well accepted soil mechanics principles, such as Darcy's law and the effective stress principle, using the measured values of load, excess pore pressures, specimen, deformation, and others.

The following sections describe the proposed method of data analysis to obtain the constitutive relationships of the slurry. In the analysis, the specimen is treated as an element of soil with uniform conditions, although it is recognized that the void ratio and other parameters change with depth mostly due to the boundary conditions. This assumption was necessary due to the lack of a proper method to measure this variation. Thus, the specimen will be characterized by average values of void ratio, effective

stress, and coefficient of permeability. If certain conditions of the test are controlled, the errors introduced by this assumption can be minimized as will be discussed later in this chapter.

Determination of Void Ratio

A direct evaluation of the void ratio in a sample of soil is not usually possible since volumes are not easily measured. Instead, the void ratio is most commonly obtained from unit weights and the use of phase diagram relationships. In the slurry consolidometer, however, an average value of void ratio can be readily obtained from the specimen height and the initial conditions.

Figure 4.1 shows the phase diagrams of the specimen initially and at any later time, t. Two assumptions are made at this point, namely, that the slurry is fully saturated and that the volume of solids in the specimen, V_s, does not change throughout the test. Both of these assumptions can be made with confidence.

From Figure 4.1a, the total volume of specimen at the beginning of the test can be expressed as

$$A \cdot h_i = (1 + e_i) \cdot V_s \qquad (4.1)$$

where A is the cross section of the specimen, h_i is the initial height, and e_i is the initial void ratio.

At time t (Figure 4.1b), the height of the specimen has been reduced to h, due to the compression of volume of voids ΔV. The volume of the specimen is now

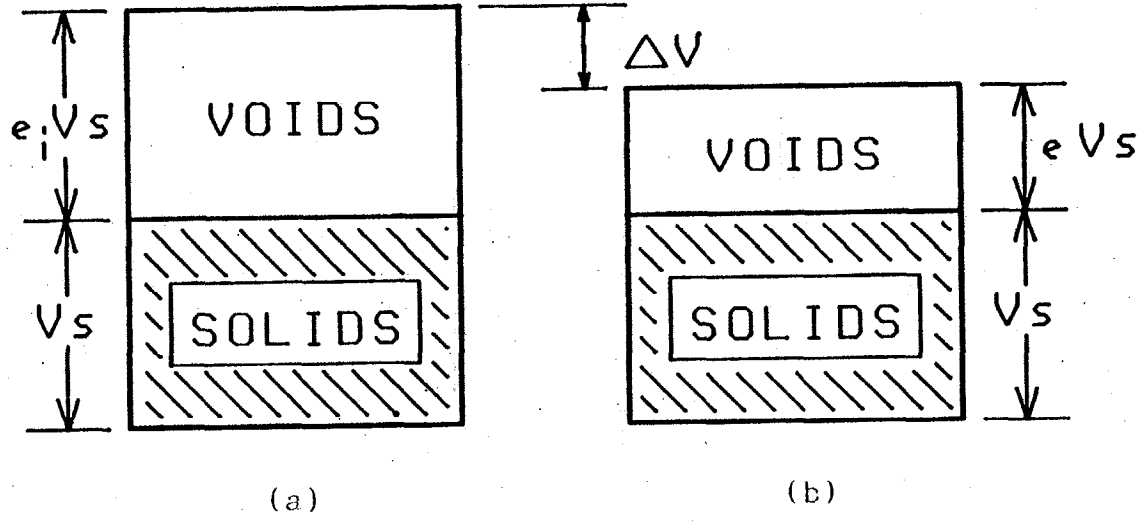

Figure 4.1 - Phase Diagrams. a) Initial Conditions; b) Conditions at time t

$$A \cdot h = (1 + e) \cdot V_s \qquad (4.2)$$

where e is the new void ratio.

Dividing equation 4.2 by equation 4.1 and solving for the void ratio leads to

$$e = (h/h_i) \cdot (1+e_i) - 1 \qquad (4.3)$$

considering that both A and V_s are constant.

The phosphate industry uses the term solids content, S, to describe the consistency of the slurry. This is defined as

$$S(\%) = (W_s/W_t) \cdot 100 \qquad (4.4)$$

where W_s is the weight of solids, and W_t is the total weight. It can be easily shown that this is related to the water content by the relation

$$S(\%) = 100/(1 + w) \qquad (4.5)$$

where w is the water content in decimal form.

From phase diagrams, it is easily proved that

$$S_r \cdot e = G_s \cdot w \qquad (4.6)$$

where S_r is the degree of saturation, and G_s is the specific gravity of the solids.

Combining equations 4.5 and 4.6, for a degree of saturation of l00%, leads to a useful relationship between the void ratio and the corresponding solids content of the slurry. This is

$$S(\%) = 100 \cdot G_s/(G_s + e) \qquad (4.7)$$

Determination of Effective Stress

The evaluation of an average value of effective stress involves a large number of variables, including the applied load, specimen weight, four excess pore pressures, and sample and piston friction. First, the effective stress at the location of each transducer is expressed as

$$\sigma' = \sigma_m + \sigma_w - u_h - u_e \qquad (4.8)$$

where

- σ' is the effective stress
- σ_m is the total stress component due to the applied load
- σ_w is the total stress component due to the specimen weight
- u_h is the hydrostatic pore pressure and
- u_e is the excess pore pressure recorded in the transducer.

The buoyant stress is defined as

$$\sigma_b = \sigma_w - u_h = \gamma_b \cdot z \qquad (4.9)$$

where z is the depth of the transducer and γ_b is the buoyant unit weight, to be computed from the average void ratio as

$$\gamma_b = \gamma_w \cdot (G_s - 1)/(1 + e) \qquad (4.10)$$

Substituting equation (4.9) into equation (4.8) we obtain

$$\sigma' = \sigma_m + \sigma_b - u_e \qquad (4.11)$$

The total stress σ_m is to be computed from the load cell reading, but it must include two important effects, namely, piston and sample friction. In order to account for the first one of these effects in the CRD test, dummy tests were run with the piston in water, while recording the load cell readings. The values obtained for two different deformation rates are reported in next chapter. The

estimated piston friction is subtracted from the load cell readings in the actual test to obtain a corrected load value, P. In the case of the CHG test, due to the nature of the test, the behavior of piston friction is expected to be more erratic and unpredictable, and no attempt was made to estimate its value.

The reading of the 3-bar PDCR 81 pressure transducer installed at the bottom of the chamber, σ_{tb}, is used to estimate the side friction along the specimen. The zero reading of this total stress transducer is taken after the specimen is placed in the chamber. Therefore, if there were no friction, this transducer would record the stress induced by the piston load. However, this is not the case. In a very simplistic approach, the difference between σ_{tb} and the piston pressure, σ_{tt}, obtained from the corrected load cell reading is distributed linearly with depth to evaluate the total stress induced by the motor load σ_m. This is

$$\sigma_m = \sigma_{tt} - (\sigma_{tt} - \sigma_{tb}) \cdot (z/h) \qquad (4.12)$$

where z is the depth of the transducer under consideration.

Once the effective stress has been computed at the depth of every transducer, the average effective stress is obtained from the area of the σ'-z curve as

$$\bar{\sigma}' = (\text{Area under } \sigma'\text{-z})/h \qquad (4.13)$$

Figure 4.2 shows schematically the variation of σ' with depth, indicating the distances between transducers in the test chamber. The effective stress exactly at the bottom of

the specimen is assumed equal to σ'_1. For this case the average effective stress simplifies to

$$\bar{\sigma}' = [1.235\sigma'_1+2.5(\sigma'_1+2\sigma'_2+\sigma'_3)+\tfrac{1}{2}(h-11.235)(\sigma'_3+\sigma'_4)]/h \quad (4.14)$$

where σ'_j represents the effective stress at the jth transducer, and h must be in centimeters.

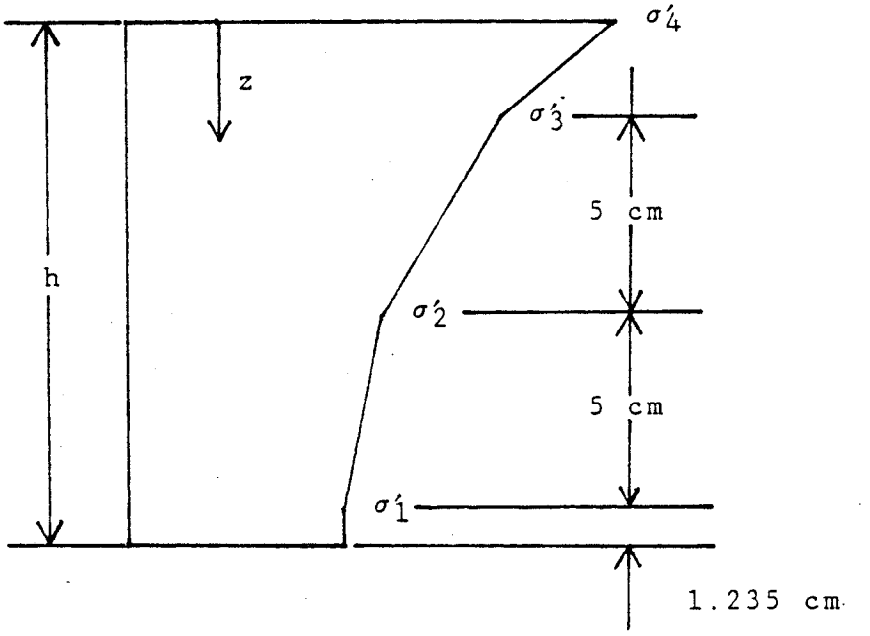

Figure 4.2 - Variation of Effective Stress with Depth

Obviously, if the specimen has deformed such that the piston passes beyond the location of transducer No. 3, or even No. 2, equation 4.14 must be modified accordingly not to include those transducers readings. The corresponding equations are given below.

For transducers 1 and 2 in the specimen (h < 11.235 cm.),

$$\bar{\sigma}' = [1.235\sigma'_1 + 2.5(\sigma'_1+\sigma'_2) + \tfrac{1}{2}(h-6.235)(\sigma'_2+\sigma'_4)]/h \quad (4.15)$$

For only transducer 1 in the specimen (h < 6.235 cm),

$$\bar{\sigma}' = [1.235\sigma'_1 + \tfrac{1}{2}(h - 1.235)(\sigma'_1 + \sigma'_4)]/h \qquad (4.16)$$

It must be emphasized that these equations are valid only for the dimensions of this particular chamber, as given in Chapter III.

In this approach it is important that the distribution of effective stress with depth be close to uniform, to conform to the assumption of specimen uniformity. This can be obtained by having a relatively small hydraulic gradient across the specimen. In the CHG test this can be easily achieved since the gradient is controlled. In the CRD test, however, the hydraulic gradient is not controlled. Thus, to overcome this limitation the rate of deformation can be slowed sufficiently to produce acceptable pore pressure ratios.

Determination of Permeability

The coefficient of permeability, k, is obtained from Darcy-Gersevanov's law (McVay et al,, 1986):

$$n(V_f - V_s) = -ki \qquad (4.17)$$

where n is the soil porosity,

V_f is the fluid velocity,

V_S is the solids velocity, and

i is the hydraulic gradient.

A second equation, however, is needed in order to solve for the coefficient of permeability. McVay et al. (1986) expressed the mass conservation of the fluid phase as

$$\frac{\delta q}{\delta \in} + \frac{\delta n}{\delta t} = 0 \qquad (4.18)$$

and the volume conservation of the solids as

$$\frac{\delta [1-n]}{\delta t} + \frac{\delta [(1-n)V_s]}{\delta \in} = 0 \qquad (4.19)$$

where $q = n \cdot V_f$ is the exit fluid velocity, and

$\in$ is the spatial coordinate.

Replacing equation 4.18 into equation 4.19 leads to

$$\frac{\delta q}{\delta \in} + \frac{\delta [(1-n)V_s]}{\delta \in} = 0 \qquad (4.20)$$

Being a function of only one independent variable, equation 4.20 can be directly integrated to give

$$q + (1-n)V_s = \text{constant} \qquad (4.21)$$

and replacing the expression for q, we obtain

$$nV_f + (1-n)V_s = \text{constant} \qquad (4.22)$$

Since at the bottom boundary $V_f = V_s = 0$, equation 4.22 further reduces to

$$nV_f + (1-n)V_s = 0 \qquad (4.23)$$

This equation representsthe condition of continuity of the two-phase system at any given time t, and was first proposed by Been and Sills (1981). Combining equations 4.17 and 4.23 to eliminate the fluid velocity leads to

$$V_s = k \cdot i \qquad (4.24)$$

the relationship from which the coefficient of permeability will be evaluated. By substituting equation 4.24 into either equation 4.17 or 4.23, an expression for the fluid velocity, is obtained. This is

$$V_f = -\frac{(1-n)}{n} \cdot ki = -\frac{ki}{e} \qquad (4.25)$$

which can be expressed in terms of the solids velocity by using equation 4.24 as

$$V_f = -V_s/e \tag{4.26}$$

Equations 4.24 through 4.26 allow an interesting comparison between small and large deformation consolidation processes. First, equation 4.24 shows that, for a given hydraulic gradient, the higher the coefficient of permeability, the higher the velocity of solids. Let us consider, for example, a slurry consolidation under its own weight from an initial void ratio of 15 ($S \approx 15\%$). At the end of the consolidation process,the slurry will probably have deformed about half of its initial height, reaching a void ratio around 6 or 7. Experimental data to be presented in Chapter V will reveal that such a slurry has an initial permeability in the order of 10^{-4} cm/sec.

If the same clay existed in a natural state with a void ratio of only 1 or 2, it would probably have a, permeability in the order of 10^{-8} cm/sec;this is 10,000 times smaller than that of the slurry with initial void ratio of 15. The consolidation of such a material would be considered a small strain process. Thus, assuming the same hydraulic gradient, the solids velosity of the second material (small strain) would be 10,000 times smaller than that of the former (large strain). This simple example may help to justify the assumption of a rigid skeleton i.e. zero solids velocity, made in small strain consolidation theory.

Additionally, the fluid velocity expressions also provide, some information that may help to understand the difference between small and large strain consolidation theories. It can be observed from equation 4.26 that the fluid velocity is e times smaller than the solids velocity. This means that V_f is relatively smaller in the case of a slurry with a very large void ratio. In a natural clay stratum, where the void ratio is commonly less than 1, the fluid velocity would actually be larger than the solids velocity.

Returning to the determination of the coefficient of permeability, to obtain its average value, one must use the average hydraulic gradient across the specimen and the average solids velocity. The average hydraulic gradient is obtained from the weighted average slope of excess pore pressure distribution. The distance between transducers is used as the weighing factor. The resulting average hydraulic gradient is

$$\bar{i} = (u_1 - u_4)/h/\gamma_\omega \qquad (4.27)$$

which only dependson the excess pore pressure at the boundaries. The evaluation of the average solids velocity, on the other hand, presents a problem. Specifically, between any two readings, taken at times t and $t+\Delta t$, the mean velocity of the piston represents the solids velocity at the top of the specimen. This is

$$V_{piston} = \Delta h/\Delta t \qquad (4.28)$$

It is also known that the solids velocity at the bottom of the specimen is zero. However, the actual distribution

of V_s along the specimen is not known. Since it is not believed that the error introduced will be significant, the average solids velocity is taken as the average of the solids velocity at the two boundaries, i.e.

$$\bar{V}_s = V_{piston}/2 \tag{4.29}$$

Using equations 4.24 and 4.27 through 4.29, the average coefficient of permeability is easily obtained from

$$\bar{k} = \bar{V}_s/\bar{i} = V_{piston}/(2\bar{i}) \tag{4.30}$$

To carry out the data reduction using the approach described above, a BASIC program, SLURRY2, was developed to run in the HP-86B. The program, that reads directly the data stored by SLURRYl, computes the average values of void ratio, effective stress, and coefficient of permeability at every time that a set of readings was taken. These values, together with the corresponding time, specimen height, gradient, and other parameters, are printed out as they are computed.

For the case of the phosphatic clays of Florida, it has been suggested that the two constitutive relationships can be described as power curves of the form (e.g. Ardaman and Assoc., 1984):

$$e = A(\sigma')^B \tag{4.31}$$

$$k = Ce^D \tag{4.32}$$

Using a log-log linear regression, SLURRY2 computes the parameters A, B, C, and D and the corresponding coefficients of correlation. The program can also plot the two curves (experimental data) using different units and arithmetic or

log axes, according to the user's choice. A listing of SLURRY2 is included in Appendix E.

CHAPTER V
AUTOMATED SLURRY CONSOLIDOMETER-- TEST RESULTS

Testing Program

The material selected for this study was Kingsford clay, a waste product of the mining operations by IMC Corporation in Polk County, Florida. This slurry has been studied extensively (Ardaman and Assoc., 1984; Bloomquist, 1982; McClimans, 1984), and it is typical of the very plastic clays found in Florida's phosphate mines (Wissa et al., 1982). Kingsford clay consists mostly of montmorillonite and has the following index properties (Ardaman and Assoc., 1984; McClimans, 1984):

LL = 230% PI = 156% G_s = 2.71 Activity = 2.2

The testing program developed during this part of the study consisted of four Constant Rate of Deformation tests and four Controlled Hydraulic Gradient tests. The former were intended to investigate the effect of the initial solids content and the deformation rate upon the compressibility and permeability relationships. In the CHG tests the influence of the hydraulic gradient on the results was to be studied. The effect of the initial specimen height, about 15 cm. for all the tests, was not investigated. Table 5-1 presents the testing conditions of both groups of tests.

Table 5-1. Conditions of Eight Tests Conducted

Test	hi (cm)	Si (%)	Rate (mm/min)	Gradient
CRD				
CRD-1	14.7	15.3	0.02	-
CRD-2	14.9	10.2	0.02	-
CRD-3	15.0	16.2	0.008	-
CRD-4	15.0	10.7	0.008	-
CHG				
CHG-1	15.0	15.6	-	2.0
CHG-2	15.0	16.4	-	4.0
CHG-3	15.0	16.3	-	10.0
CHG-4	15.0	16.0	-	20.0

CRD Tests Results

Of the four CRD tests, two of them were conducted on dilute slurries with solids content between 10% and 11% (CRD-2 and CRD-4), while the other two tests were conducted on denser specimens with solids contents in the order of 15% to l6% (CRD-1 and CRD-3). In each group, one test was run at a slow rate of deformation of 0.008 mm/min (CRD-3 and CRD-4), while the other was run at a faster rate of 0.02 mm/min (CRD-1 and CRD-2).

Tests CRD-1 and CRD-2 were performed with an early version of the test chamber whose differences from the present design are worth mentioning. Originally the pressure transducers were mounted in a pipe-threaded brass fitting, which had to be tighten in order to seal properly. This fitting soon began to crack the acrylic and therefore it was replaced with the O-ring sealed fitting currently used. In the original chamber,, transducer No. 1 was located at 0.6 cm from the bottom of the chamber, and not 1.235 cm as in the present chamber.

During the development of the equipment several pistons were tried in the chamber to produce a snug fitting with the minimum possible friction. In the case of test CRD-1 the piston used was fairly loose and a filter cloth was wrapped around the bottom plate to prevent the escape of slurry, but allowing free drainage. This arrangement allowed the piston to fall freely in water. Therefore,no piston friction was included in the analysis of test CRD-1. Instead, the submerged weight of the piston was added to the applied motor load. The resulting additional pressure of 0.0109 psi is not significant for most of the test, but it does affect the initial portion of the compressibility curve.

The specimen of test CRD-1 started at a solids content of 15.3%. (e =14.97) and a height of 14.7 cm. The test was conducted at a rate of deformation of 0.02 mm/min for 62 hours (≈2.5 days). Readings were taken every 3.0 minutes (124 data points). The final specimen height was 7.19 cm and the computed average solids content was 28.5% (e = 6.81). Direct measurement of the solids content led to an average value of 28.7% with a variation of 4.7% across the specimen, which indicates a very good agreement. Figure 5.1 shows the compressibility and permeability plots for test CRD-1 as produced by the data reduction program. Both curves show a very well defined behavior.

For test CRD-2, the old chamber was still used but a much tighter piston was tried. At this point in time no attempt was made to estimate the magnitude of the piston

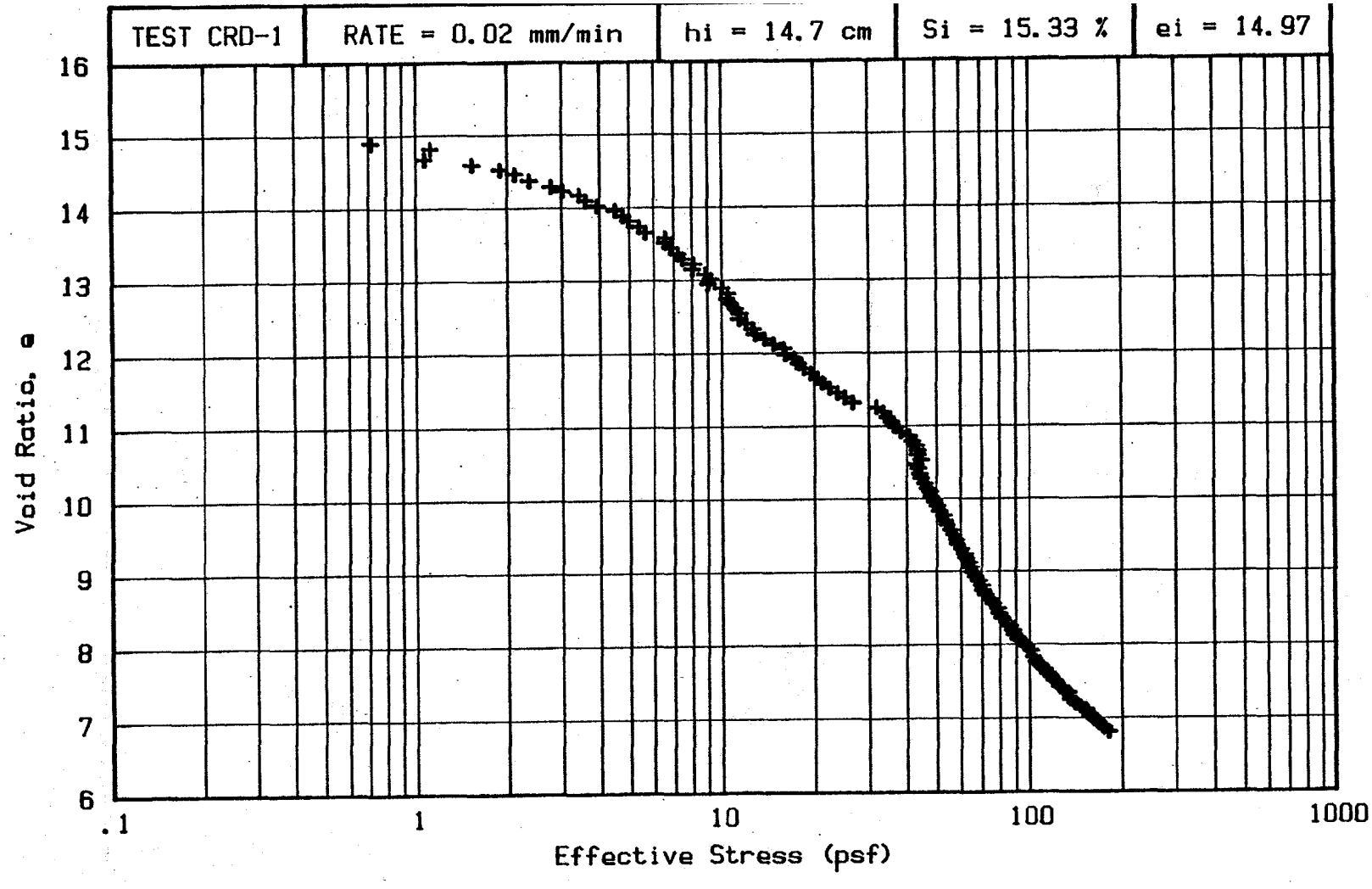

(a)

Figure 5.1 - Results of Test CRD-1. a) Compressibility Relationship; b) Permeability Relationship

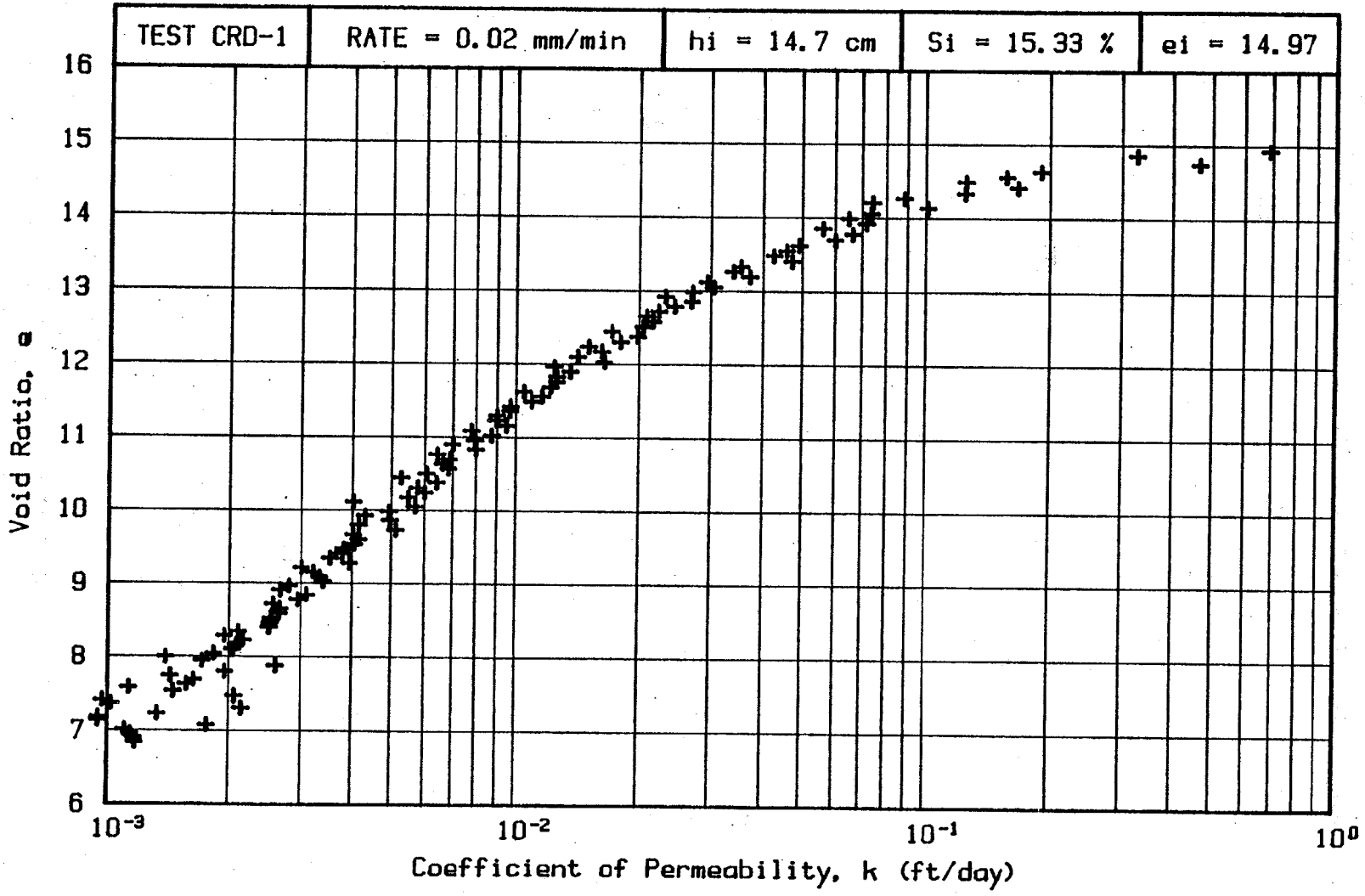

(b)

Figure 5.1--Continued

friction, but it was suspected to be large enough to affect the compressibility curve. The specimen in this test began at a solids content of 10.2% (e = 23.96) with a height of 14.9. The test was run at a deformation rate of 0.02 mm/min for 72 hours (3 days), with 30 minutes between readings. At the end of the test, the LVDT-based height of the specimen was 6.02 cm, but visual observation of the specimen indicated a value of around 5.7 cm. A similar discrepancy was also found in the solids content. The computed value was 22.97% (e = 9.09), while the measured average was 24.37% with a gradient of 6.98% across the specimen. If the observed specimen height of 5.7 cm were accepted as correct, then the computed solids content would be about 24%, which agrees very well with the measured value. This discrepancy is attributed to possible disadjustment of the pivoting arm-LVDT arrangement.

When the data of test CRD-2, with a dilute specimen, was first reduced, the average effective stress showed negative values up to asolids content of about 13.5%. The data reduction program was later modified to make zero any negative effective stress computed at the location of the pore pressure transducers. This result seems to indicate that below this solids content the slurry has no effective stresses, or these are two low to be detected with the equipment used. Once the program was modified to eliminate negative values, it was observed that the average effective stress increased above 0.01 psi (the estimated sensitivity

of the transducers) when the solids content was again about 13.4%. Figure 5.2 shows the compressibility and permeability curves of test CRD-2 as plotted by SLURRY2. The initial portion of the compressibility plot (Figure 5.2a) shows clear evidence of pseudo-static piston friction. Another interesting aspect of the plot is the step-like shape. This effect may be attributed to a discontinuity in the computed effective stress when the piston passes by transducer No. 3 (at h = 11.235 cm.), as a result of the analytical approach used. However, this irregular effect is not observed with the same magnitude in all the tests. The permeability plot, on the other hand, exhibits a well defined trend with almost no scatter.

The new chamber described in Chapter III was used for the rest of the tests. It was found that the O-Ring sealed piston did not fall freely in the chamber; a study was conducted to estimate the magnitude of the piston friction. With water in the chamber, dummy tests were conducted and the load cell readings recorded with time. Since transducer No. 4 did not record any build-up of pressure, it was assumed that the load cell reading was only reflecting the piston friction. For the deformation rate of 0.02 mm/min, the average friction obtained was 6.5 lbs,, while for the rate of 0.008 mm/min the average value was 8.6 lbs; in both cases the variation of the recorded load was very small.

The testing program carried out in this part of the research never attempted to study the statistical validity

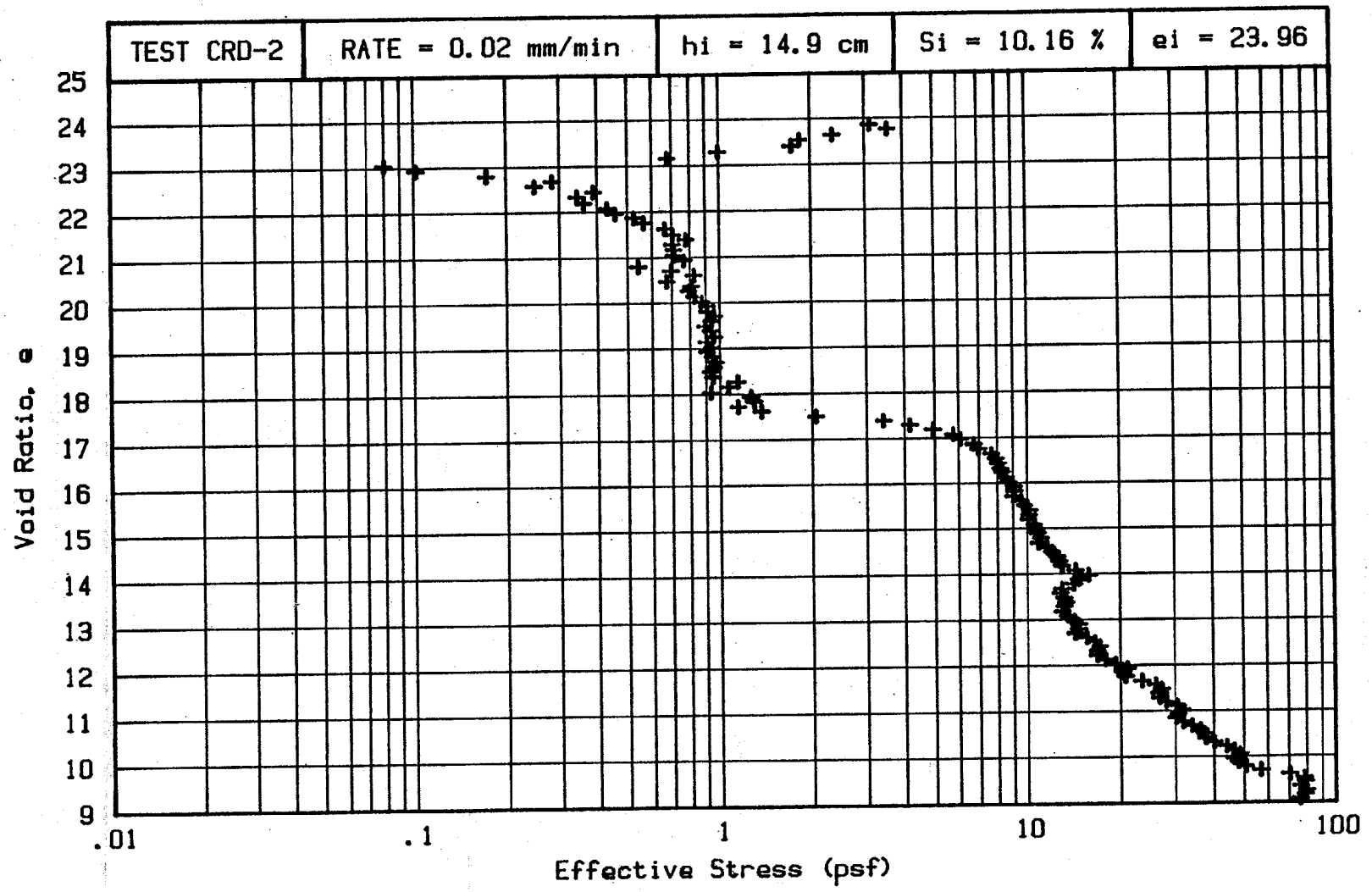

(a)

Figure 5.2 - Results of Test CRD-2. a) Compressibility Relationship; b) Permeability Relationship

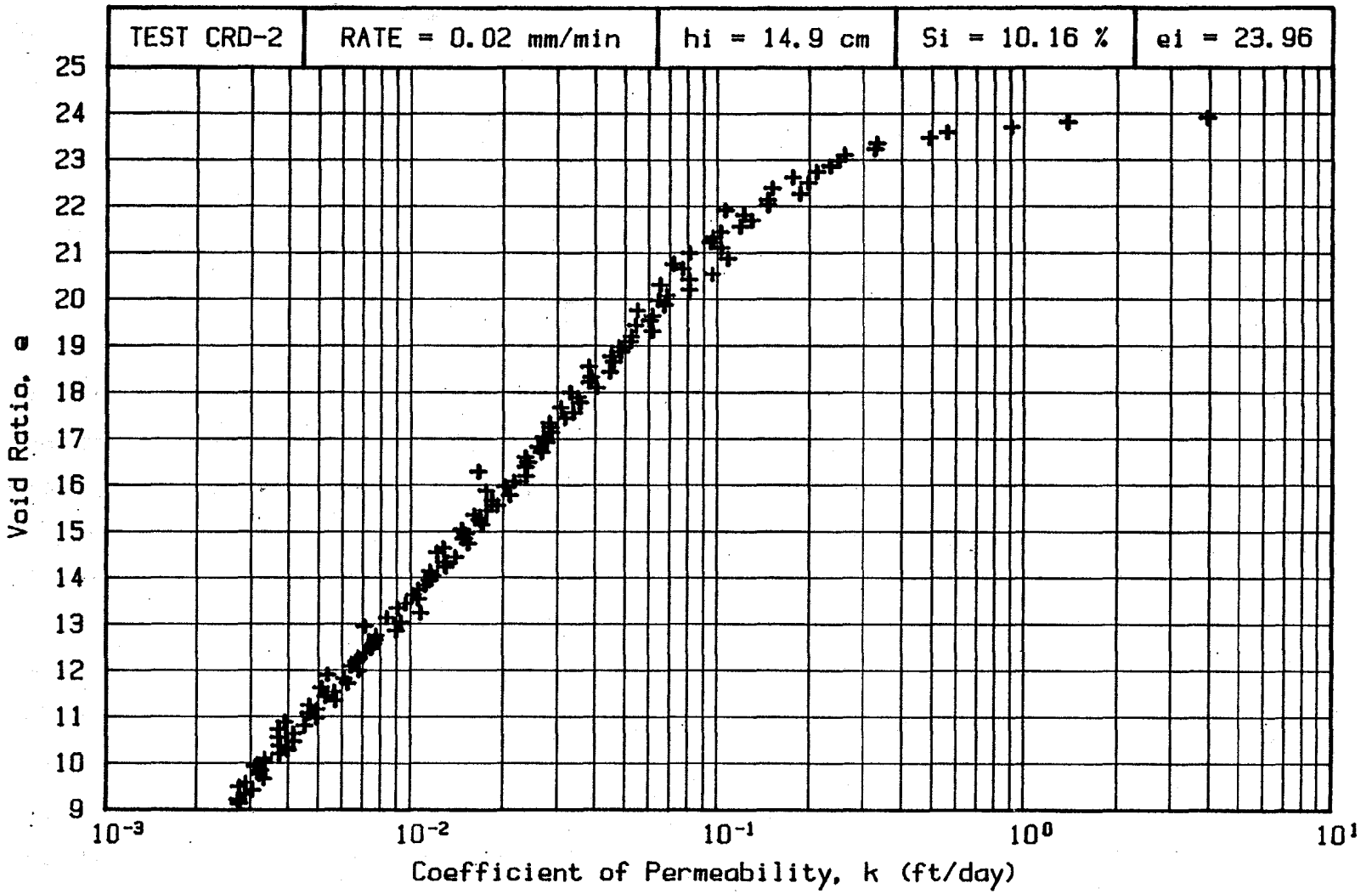

(b)

Figure 5.2--continued

of any particular observation. Nevertheless, it was interesting to investigate the duplicability of the tests results. With this in mind, an additional test was conducted with similar conditionsto those of test CRD-1. This test, the first one with the new chamber, was originally intended to be a different test, conducted for 7 days at the slower rate of deformation of 0.008 mm/min. After the test had been running for 6 hours, it was sadly discovered that somebody had turned the main breaker off and that the test had been aborted. To avoid wasting the specimen, it was decided to run a quicker test (3 days) which would approximately duplicate test CRD-1. The initial height of the aborted test was 14.7 cm and the initial solids content was 15.7%. Although the specimenhad deformed about 3 mm when the test stopped, no corrections were made on the initial values once the test was restarted. The results of both tests, CRD-1 and its duplicate, are shown in Figure 5.3. Considering the conditions under which the duplicate test was conducted and expected variations in the material itself, it can be said that the results are reproduced quite well.

The compressibility plot of the duplicate test shows an abrupt discontinuity in the effective stress. This could be explained with the same arguments given for test CRD-2.

The other two CRD tests were run at the slower rate of deformation (0.008 mm/min). Test CRD-3 was initiated at a solids content of 16.2% (e = 14.01) with a specimen height

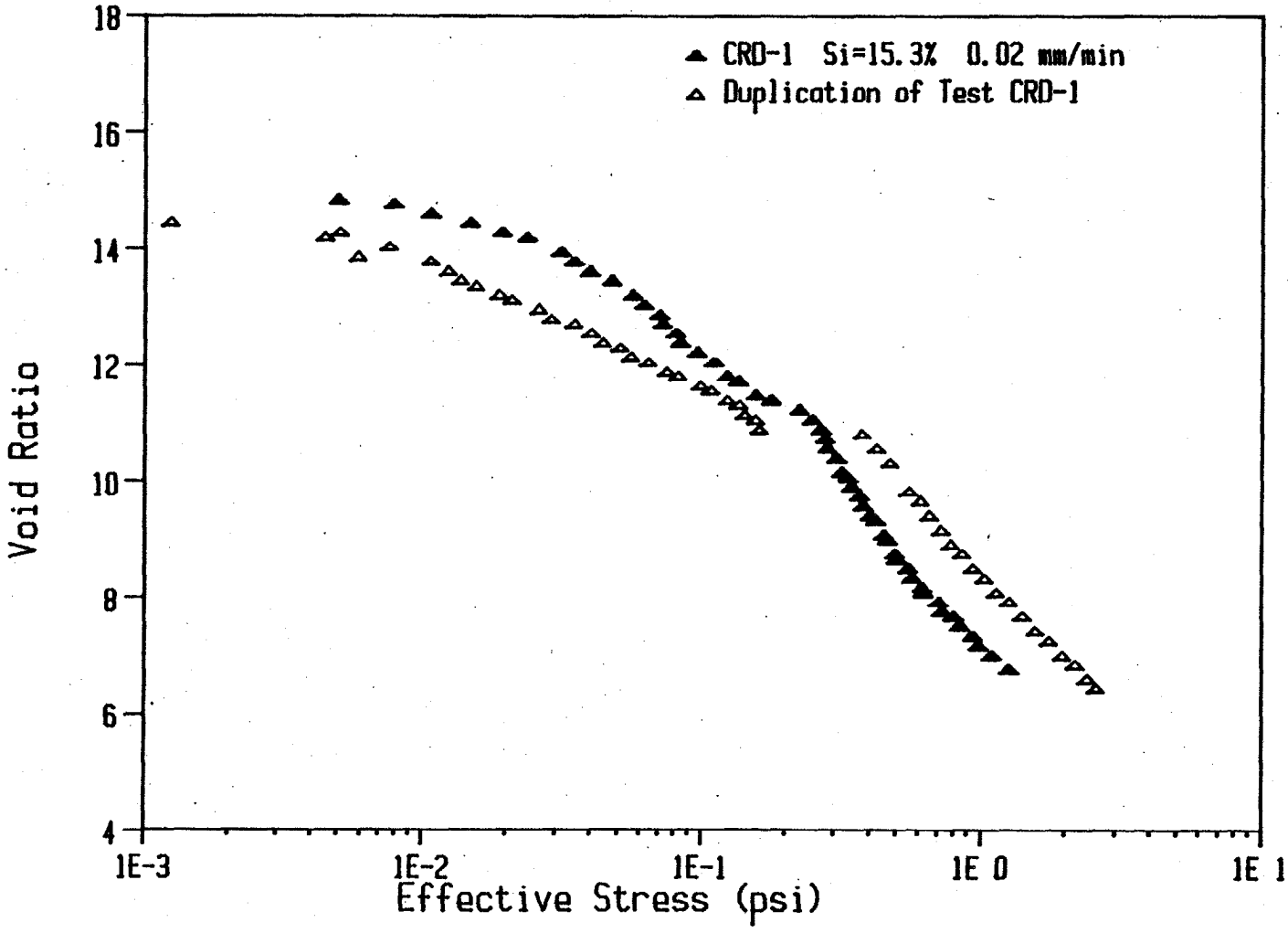

(a)

Figure 5.3 - Duplication of Test CRD-1. a) Compressibility Relationship; b) Permeability Relationship

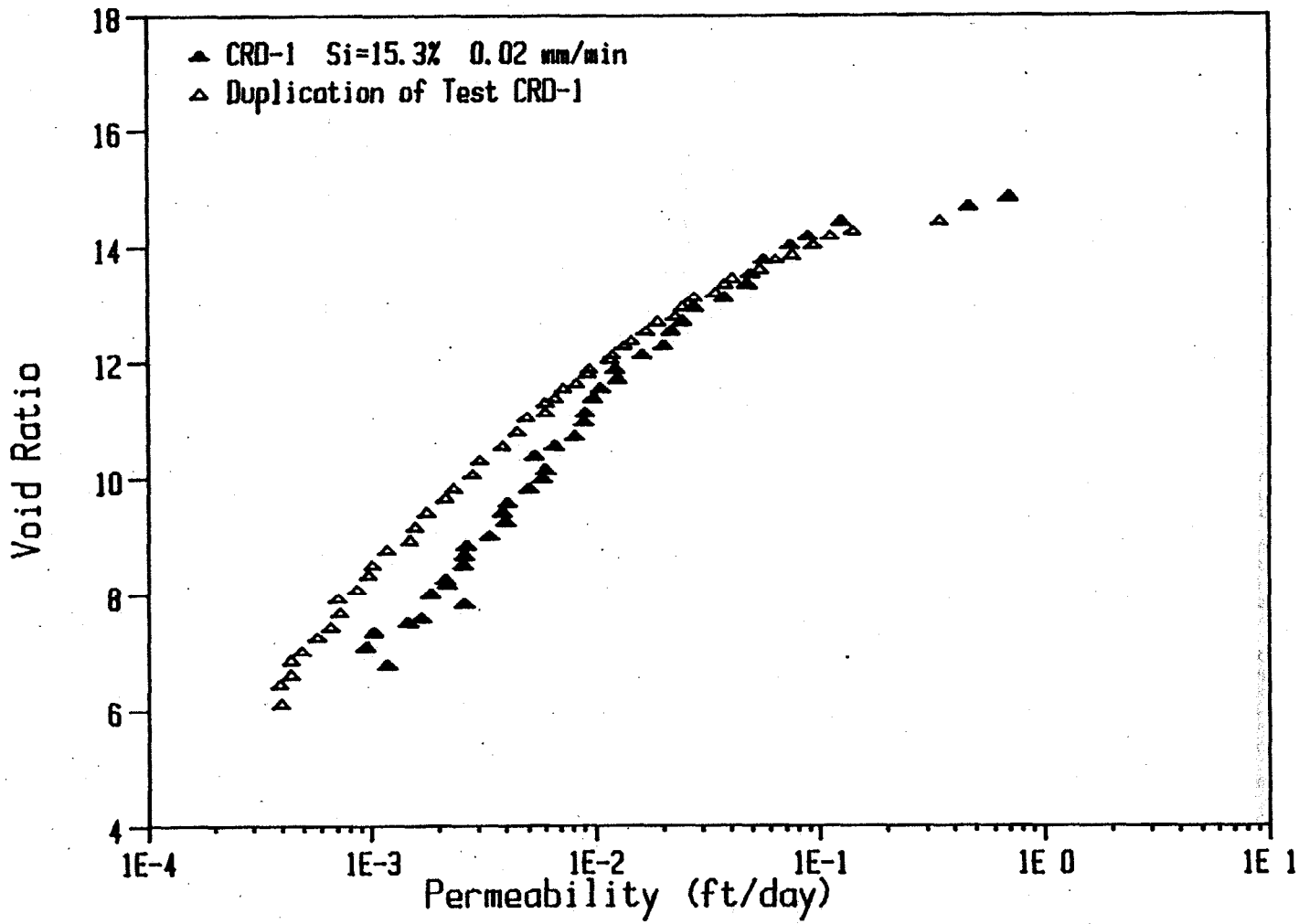

(b)

Figure 5.3--continued

of 15 cm. After running for 168 hrs (7 days), with 2 hours between readings, the final height was 7.32 cm (computed), while the observed value was 7.1 cm, indicating a very good agreement. As for the final solids content, the computed value was 29.99% (e = 6.33),while the measured average was 29.94 with a variation of only 2.66% across the specimen, again an excellent agreement. Figure 5.4 shows the compressibility and permeability curves obtained from test CRD-3. The fact that the time interval between readings was relatively large may have resulted in the loss of valuable information during early parts of the test.

Finally, test CRD-4 began at a solids content of 10.66% (e = 22.70) with the specimen height at 15 cm. This test was the longest one, running for 216 hr (9 days), and proving that the apparatus is capable of working for long periods of time without any problem. For approximately 1 day, the results of this test indicated inconsistent results, such as negative values of permeability. These results were attributed to the extremely low pore pressures being read; these points were discarded. At the end of the test the computed specimen height was 5.1 cm, while the observed value was 4.5, a quite significant difference. The computed final solids content was 27.75% (e = 7.06) and the measured value was 29.68%, with a variation across the specimen of only 1.56%. Figure 5.5 shows the compressibility and permeability plots obtained from test CRD-4. The compressibility plot shows significant scatter with initial

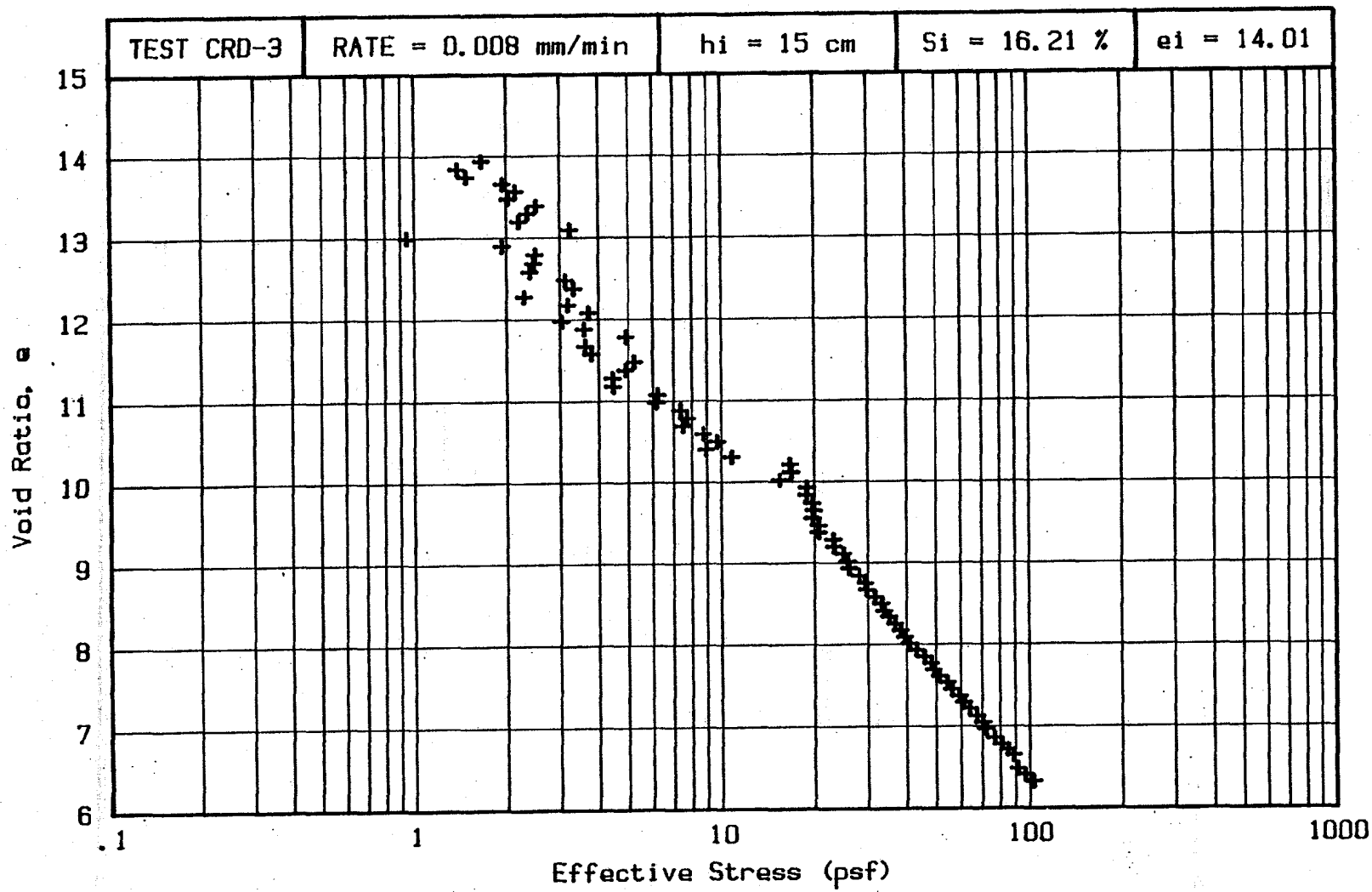

(a)

Figure 5.4 - Results of Test CRD-3. a) Compressibility Relationship; b) Permeability Relationship

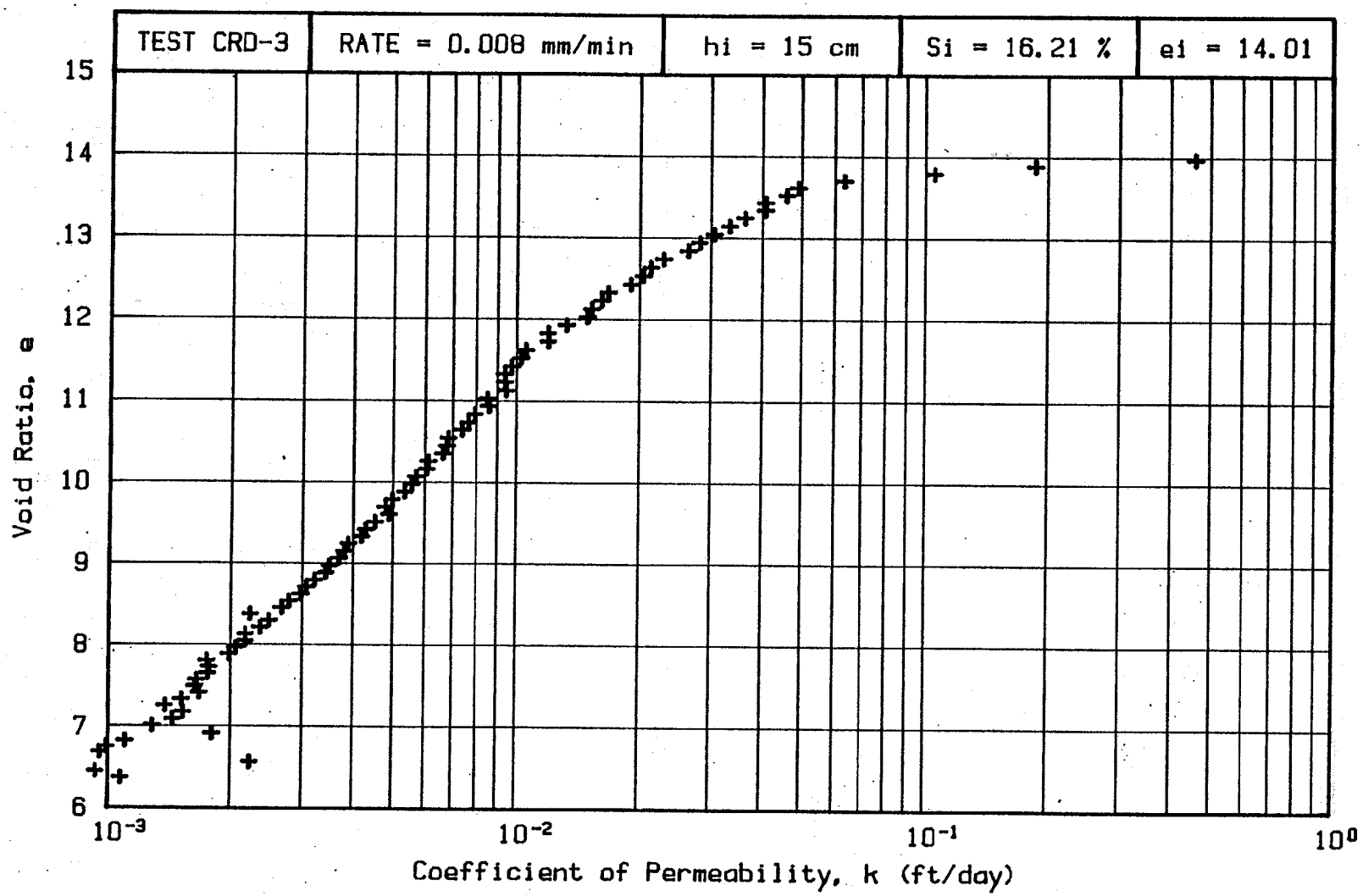

(b)

Figure 5.4--continued

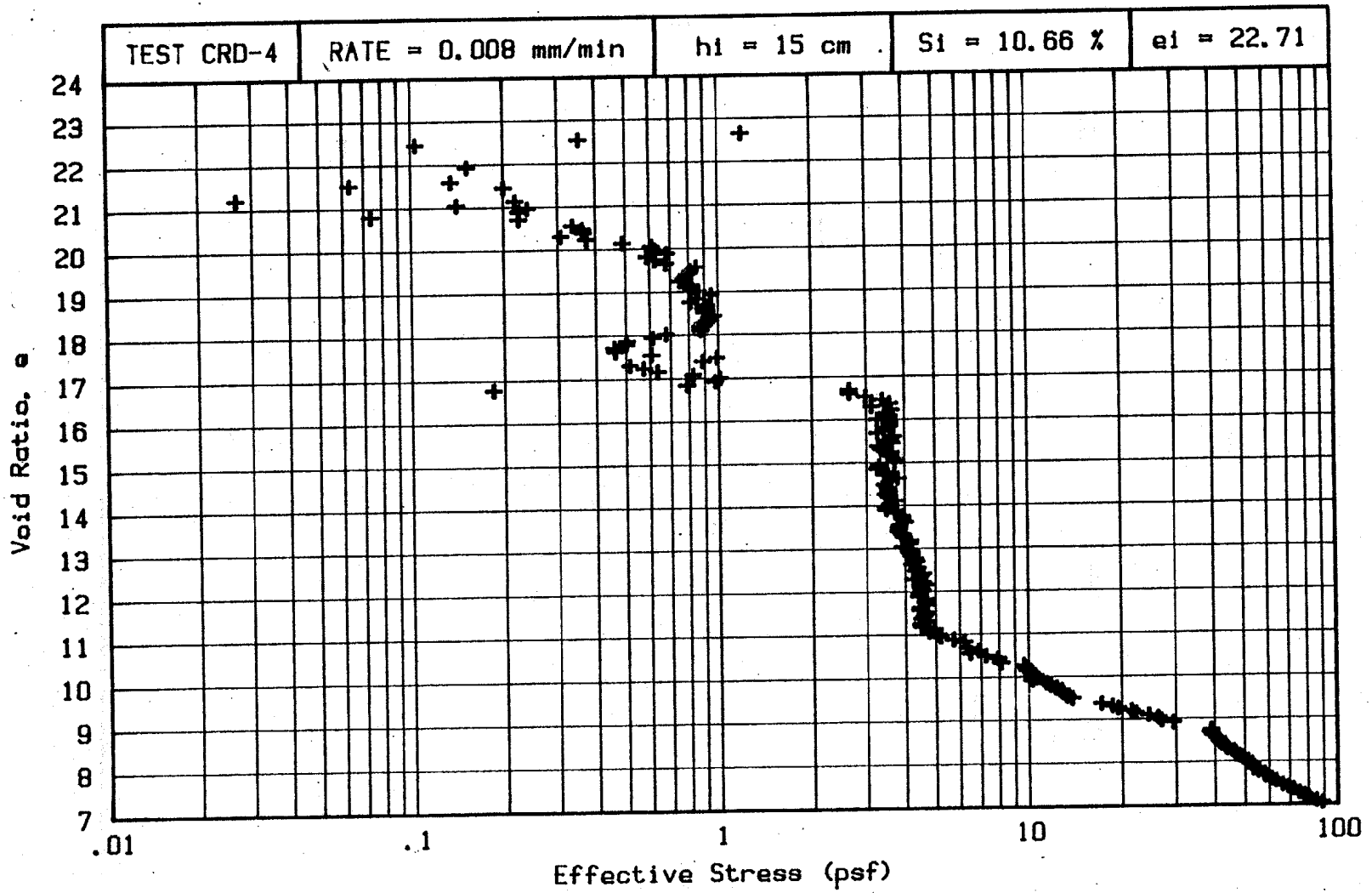

(a)

Figure 5.5 - Results of Test CRD-4. a) Compressibility Relationship; b) Permeability Relationship

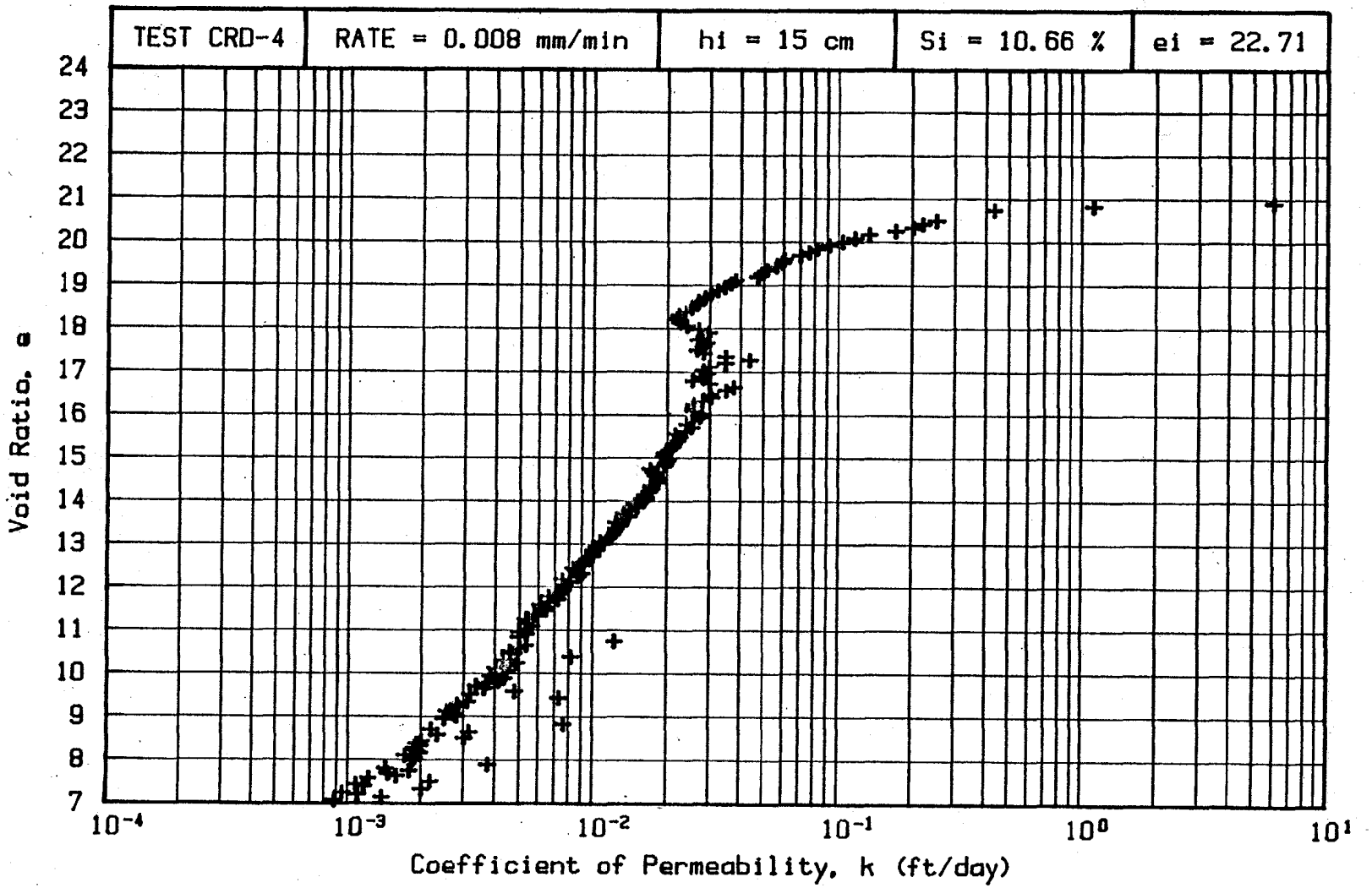

(b)

Figure 5.5--continued

evidence of piston friction and some irregular behavior around an effective stress of 1 psf, in a way similar to test CRD-2. Both of these tests started at the low solids content level, and this may be partially responsible for these results.

Table 5-2 summarizes the conditions of the specimens at the end of the four CRD tests, and shows the duration of each test.

Table 5-2. Summary of CRD Tests Results

Test	Duration (hrs)	Final Height (cm)		Final Solids Cont.(%)		
		Computed	Observed	Computed	Measured	Gradient
CRD-1	62	7.19	7.1	28.5	28.7	4.7
CRD-2	72	6.02	5.7	23.0	24.4	7.0
CRD-3	168	7.32	7.1	30.0	29.9	2.7
CRD-4	216	5.10	4.5	27.8	29.7	1.6

The results of these tests clearly show that the variation in solids content with depth is significantly smaller in those tests performed at the slower rate of deformation. This result is important considering the assumption of specimen uniformity made during the analysis of the data. This condition, however, can never be completely satisfied sincethe excess pore pressure dissipates faster at the top boundary. Thus, although the total stress in the specimen is close to uniform (assuming self-weight is smaller than the motor load), the excess pore pressure distribution is not. Figure 5.6 shows the distribution of

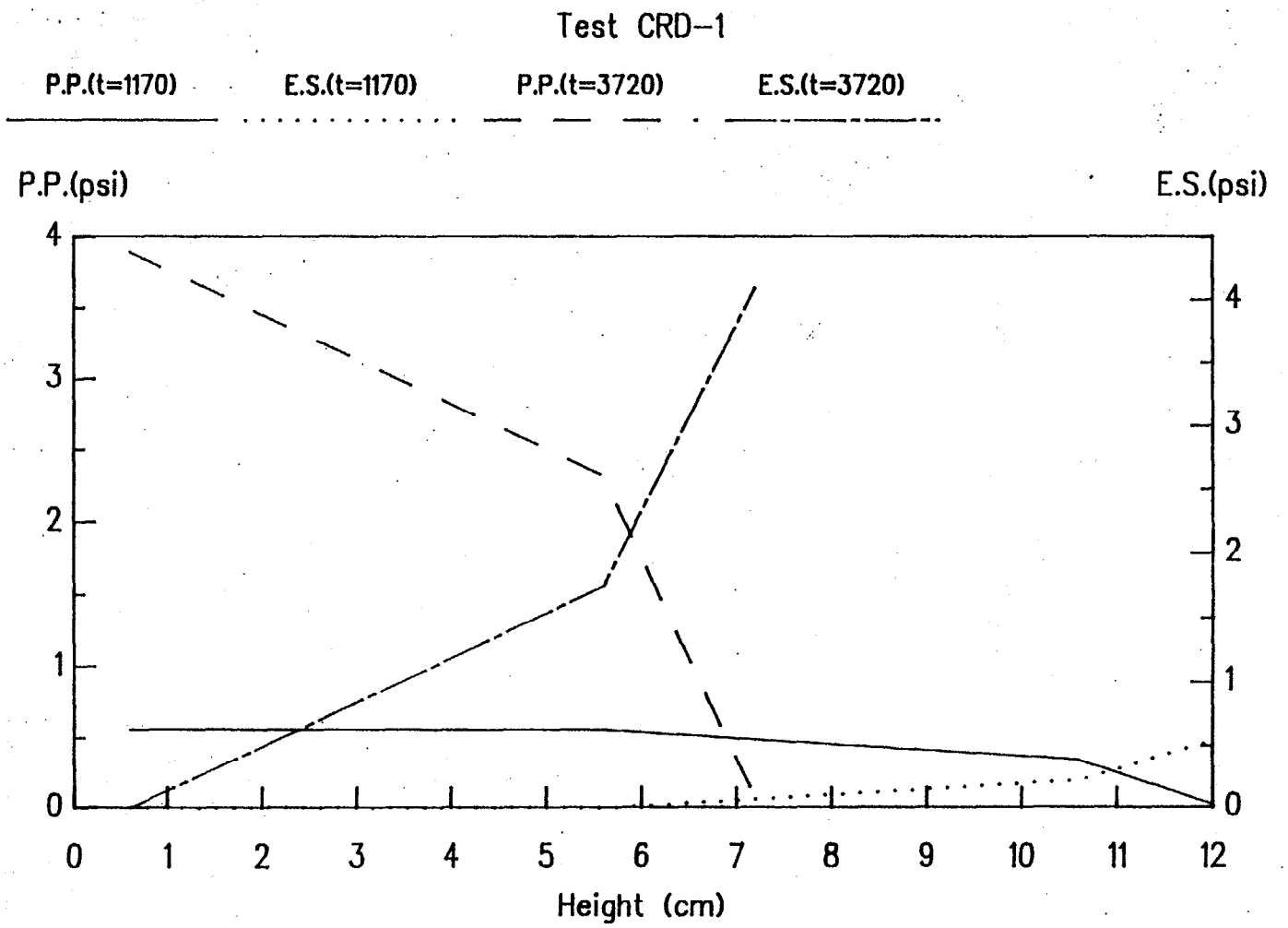

Figure 5.6 - Pore Pressure and Effective Stress Distributions with Depth for Test CRD-1

excess pore pressureand effective stress with depth at two different times in test CRD-1. The first one, for t = 19.5 hr, corresponds to an average solids content of 18.3% (e = 12.13), and an average effective stress of only 0.11 psi. The second time plotted isat the end of the test (t = 62 hr), corresponding to an average solids content of 28.5% (e = 6.81) and an average effective stress of 1.27 psi.

It is clear from Figure 5.6 that the effective stress and therefore the void ratio are far from being uniform with depth, especially toward the end of the test when the hydraulic gradient increases significantly. The pore pressure ratio, defined in this test as the ratio of the excess pore pressure in transducer No. 1 to the total stress at the bottom of the specimen, is commonly used in CRD tests to limit the magnitude of the excess pore pressure. For test CRD-1, for example, performed at the rate of 0.02 mm/min, the pore pressure ratio increased up to about 88% at the end of the test. Contrarily, for test CRD-4, performed at the slow deformation rate, the maximum pore pressure ratio was about 54%. Pore pressure ratios between 30% and 50% have been recommended by Znidarcic (1982).

The results of the four CRD tests are plotted together in Figure 5.7. The compressibility curves shown in Figure 5.7a demonstrate the effects of initial solids content and rate of deformation. First, all four tests show a "preconsolidation" effect, which depends on the initial solids content. Such an effect has been reported without any

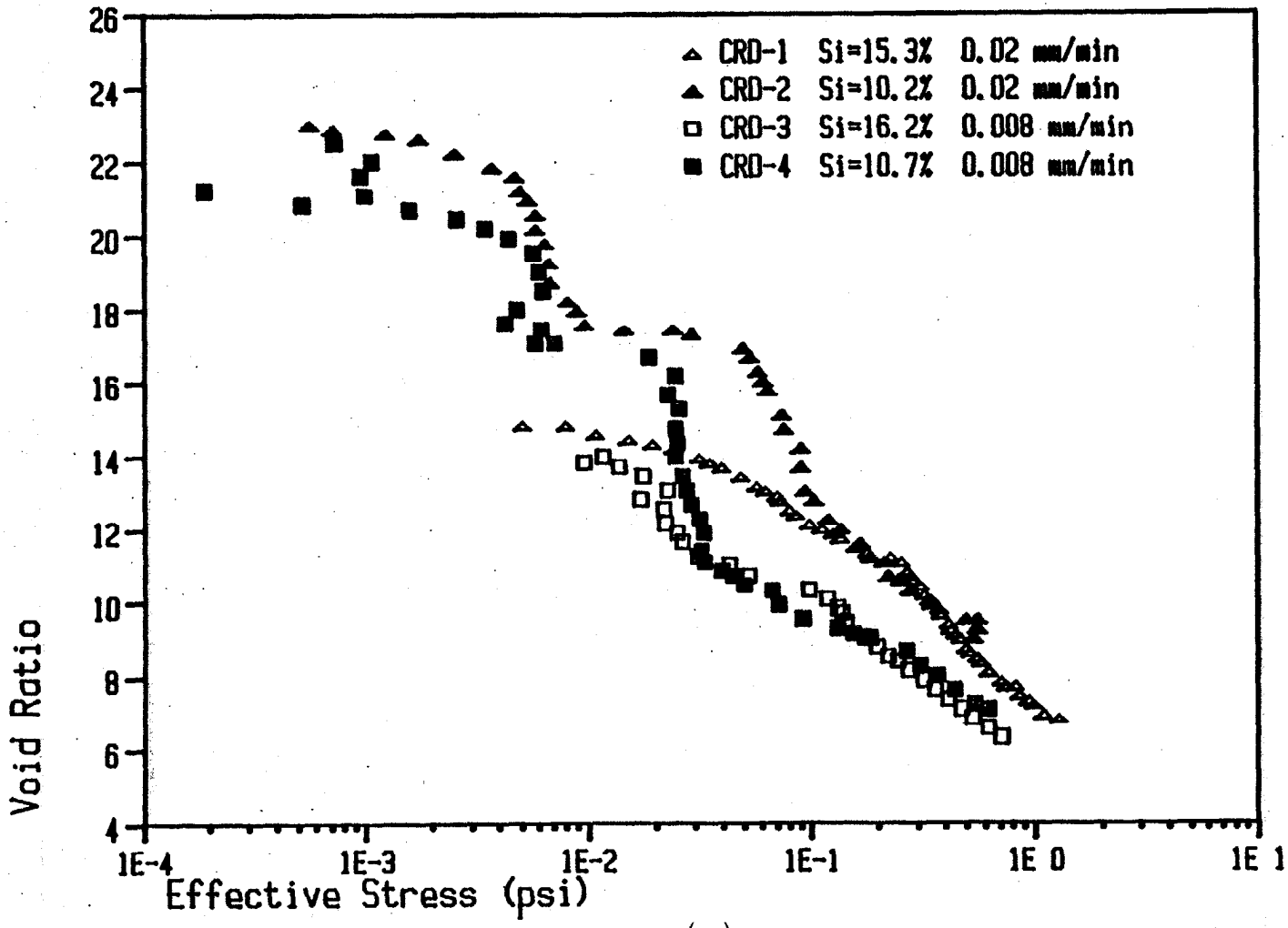

(a)

Figure 5.7 - Summary of CRD Tests. a) Compressibility Relationship; b) Permeability Relationship

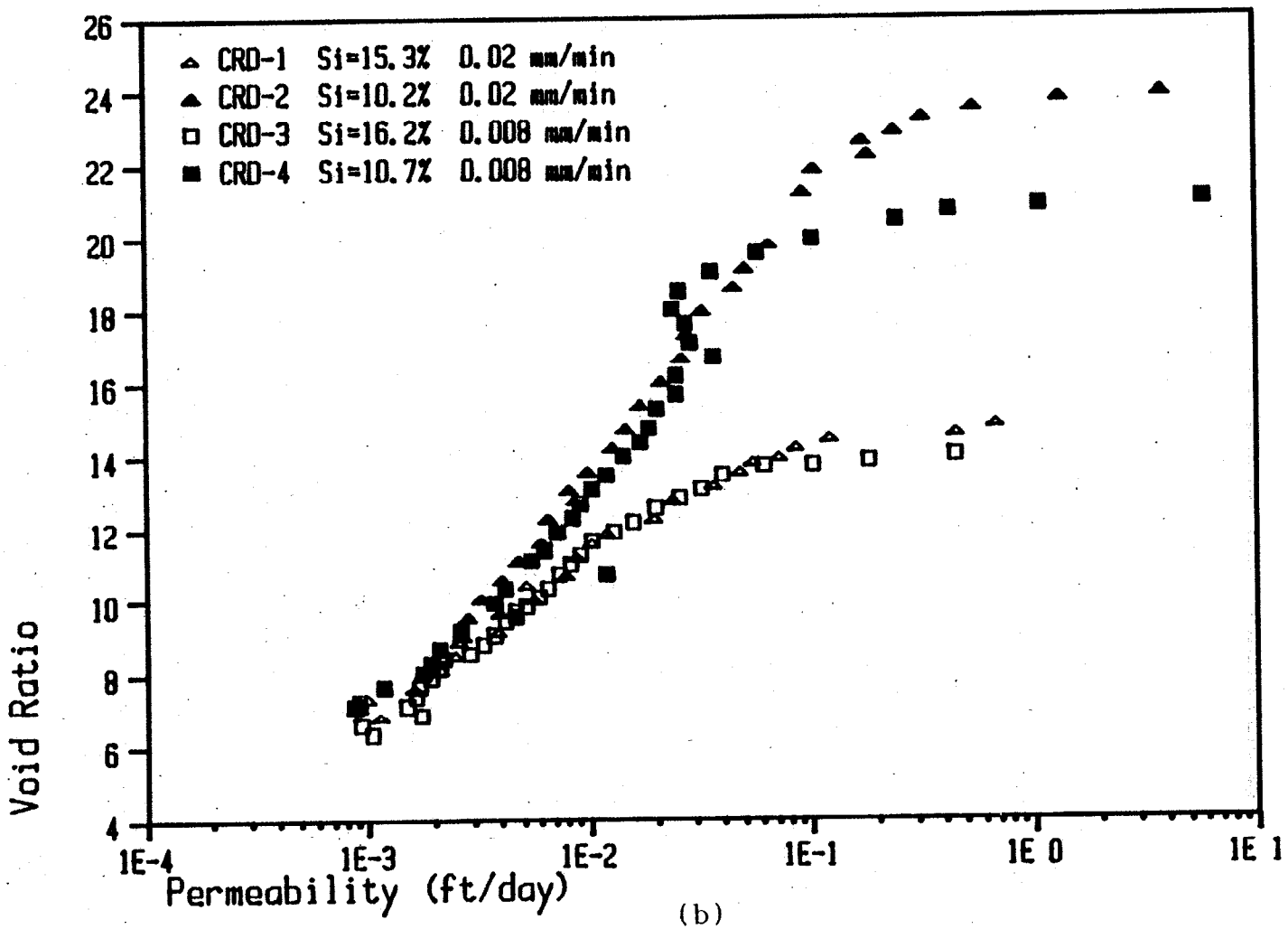

(b)

Figure 5.7--continued

explanation by Scully et al. (1984), and can also be observed in tests reported by Mikasa and Takada (1984).

It is believed that the preconsolidation effect is the result of testing a specimen that begins in a highly remolded state,due to specimen mixing and preparation. Under such conditions the effective stresses are practically zero at the beginning of the test, regardless of the initial solids content. As the specimen is initially stressed, the soil particles start interacting and regaining the structural arrangement that was lost during remolding, in some kind of thixotropic effect. Thus, the effective stresses increase relatively quickly early in the test, without significant reduction in void ratio, until the compression curve reaches a point where it breaks down to enter the virgin zone. It is believed that this behavior also occurs in the field since mining slurries are deposited in a very remolded condition. Poindexter (1987) justifies the use of remolded specimens of dredged material on the basis of the destruction of any insitu internal structure by the dredging process.

It is clearly noticeable in Figure 5.7a that the two lower solids content curves, CRD-2 and CRD-4, approach almost perfectly the virgin zone of the corresponding higher solids content curves, CRD-1 and CRD-3. Thus, the initial solids content affects the preconsolidation zone, but the virgin zone slopes areindependent of initial conditions. The rate of deformation appears to have a similar effect on

both the dilute and the dense specimens. In the virgin portion of the curves, the faster tests (CRD-1 and CRD-2) plot parallel and to the right of the slower tests (CRD-3 and CRD-4). Thus, the slope of the virgin curve is independent of deformation rate for the range of these test conditions.

It is conceivable that a minor part of the disagreement on the compressibility curves between the fast and slow tests may be attributed to equipment problems. For example, test CRD-1 was analyzed assuming no piston friction; on the contrary, the submerged weight of the piston (0.0109 psi) was added to the effective stress, based on observations that indicated that the piston moved freely inside the chamber. However, for subsequent tests this approach was changed when a new chamber and piston were introduced, and piston friction was incorporated. However, the magnitude of these effects has been analyzed and found to be small. Their influence will be more significant early in the test, when the effective stress are relatively small. For example, at the end. of test CRD-1, if piston friction is considered, the effective stress would only decrease by about 5%. However, the comparison shows that the effective stress in test CRD-3 at the same void ratio is almost 60% smaller than that of test CRD-1.

Thus, the effect of deformation rate on the compressibility relationship is believedto be a true soil response. In the case of small strain CRD tests, it is a well accepted

fact that decreasing the rate produces a decrease in the measured effective stress (Mesri and Choi, 1987). A comprehensive study by Leroueil et al. (1985) on five different natural Canadian clays clearly showed that, at a given strain, the higher the strain rate, the higher the effective stress. They proposed a rheological model in which the effective stress-void ratio relationship is not unique but incorporates the strain rate. Although similar results have not been reported for large deformation consolidation tests, there is no reason to eliminate the possibility of the same behavior on remolded slurries.

The permeability curves of the four CRD tests, presented in Figure 5.7b, show less scatter than those corresponding to the compressibility relationship. In this case the rate of deformation does not have any significant effect on either the dilute (S_i = 10-11%) or dense (S_i = 15-16%) specimen. Similar to the compressibility relationships, the permeability curves show an initial preconsolidation portion, changing at a point which is a function of the initial solids content. All curves clearly approach a well defined virgin zone. A possible explanation for this behavior could be found under the same arguments previously given to explain the preconsolidation effects observed in Figure 5.7a. Thus, the virgin slope of the e-k relationship is independent of initial solids content and deformation rate for this range of test conditions.

CHG Tests Results

The controlled gradient tests were performed under different hydraulic gradients, but with initial solids contents of 15% to 16%, similar to those of the constant rate of deformation tests CRD-1 and CRD-3 (see Table 5-1). In all the tests the specimen height was 15 cm. The magnitude of the pistonfriction is undetermined in the CHG tests.

The first test, CHG-1, was set for a low gradient of 2, allowing a variation of ±5%. The initial solids content was 15.6% (e = 14.64). The test lasted for 192 hours (8 days), taking readings every 2 hours for a total of 97 data points, including the first time the desired gradient was reached at about 15 minutes. The final height of the specimen was computed from the LVDT reading as 9.23 cm, matching almost exactly the observed value. The final solids content computed was 23.9%, while the measured average value was 24.4% with a variation across the specimen of only 2%. With the low gradient used in this test, the recorded values of pressuresand load were extremely small, producing signifi-cant scatter in the results. The maximum average effective stress in this test was less than 0.2 psi. Figure 5.8 shows the compressibility and permeability plots of test CHG-1.

The existence of an unpredictable piston friction was a major disadvantage of the CHG tests. In trying to reduce its magnitude, the O-Ring around the bottom plate was replaced by a filter cloth, and the friction estimated for

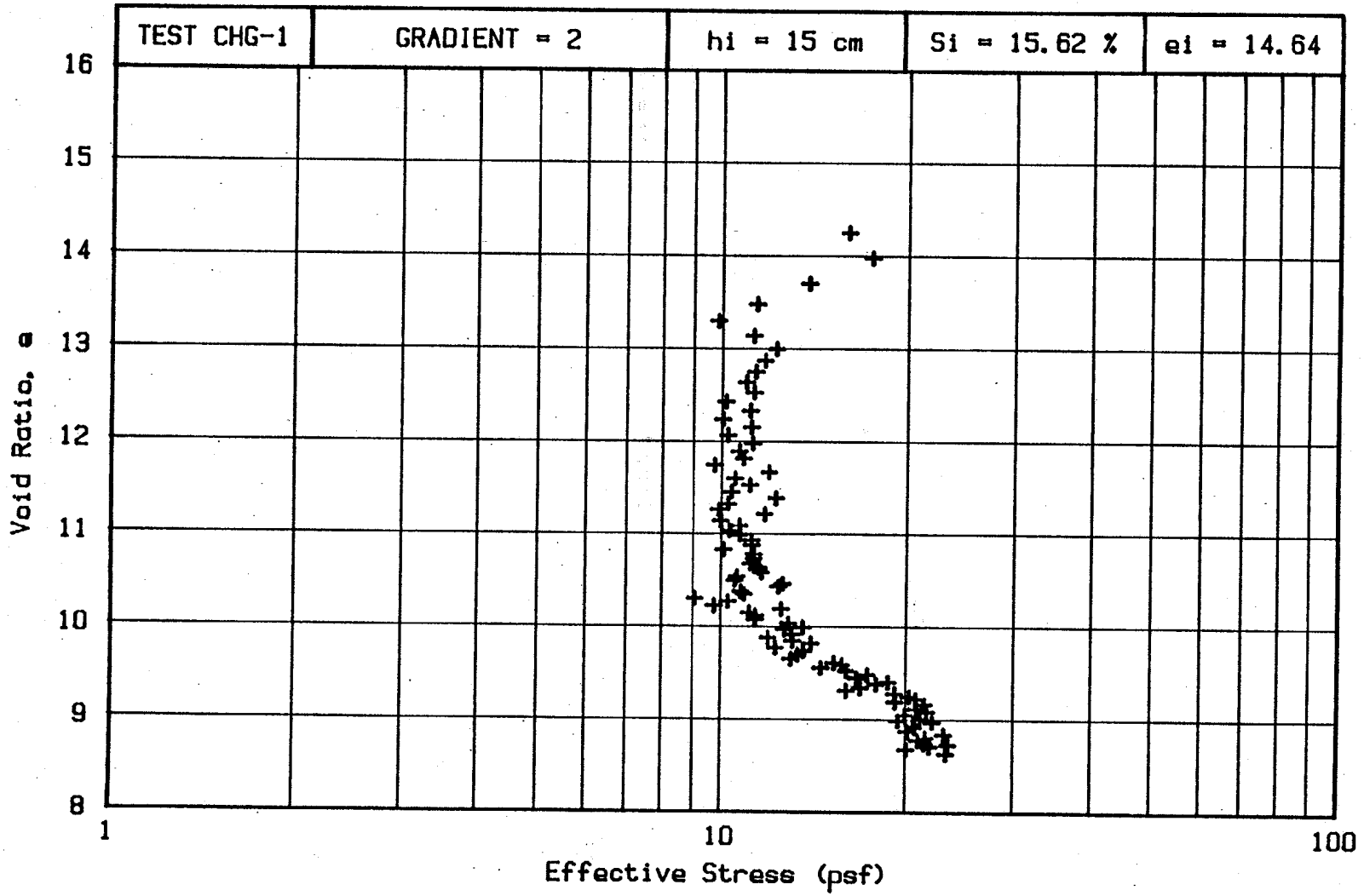

(a)

Figure 5.8 - Results of Test CHG-1. a) Compressibility Relationship; b) Permeability Relationship

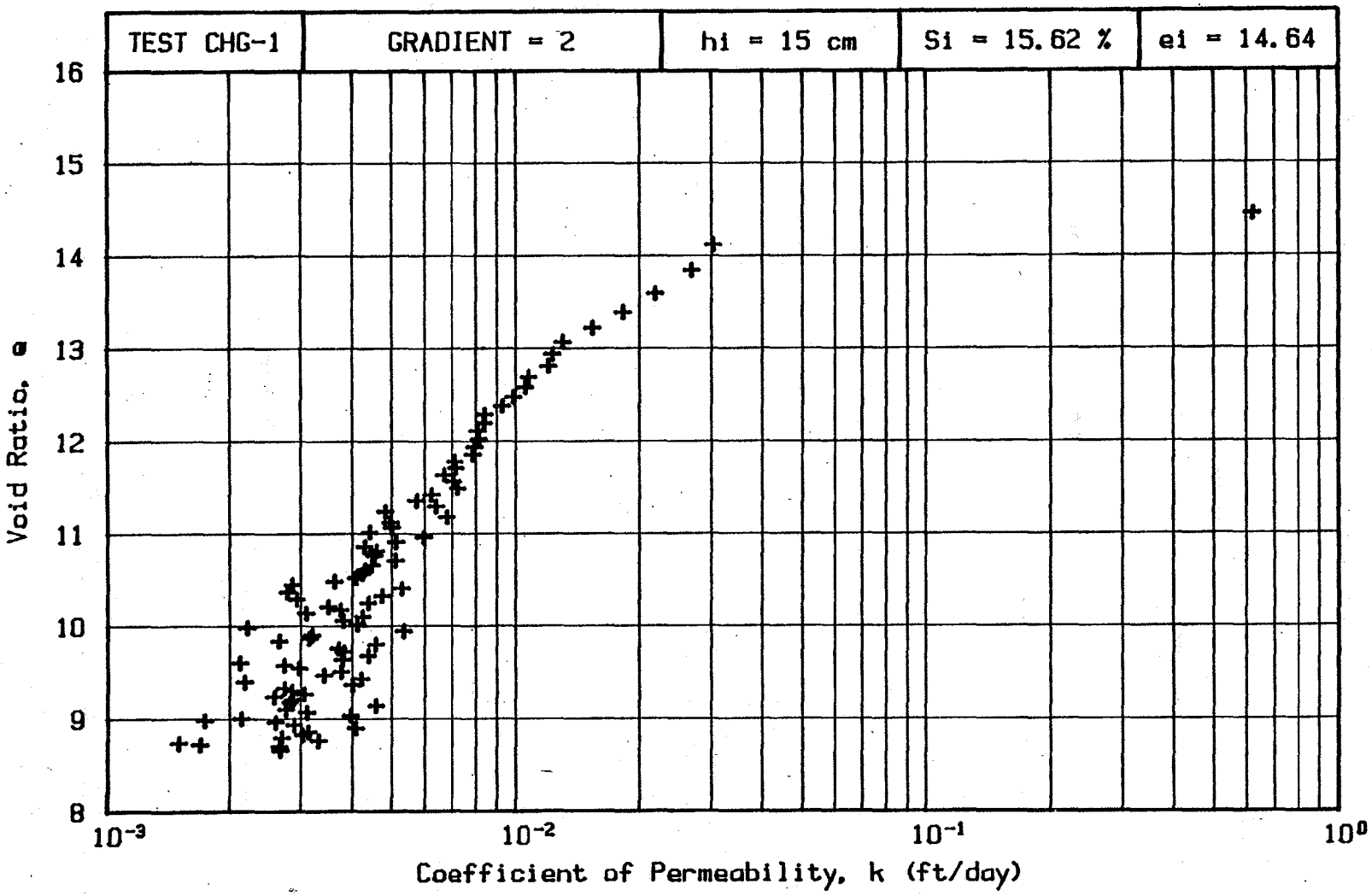

(b)

Figure 5.8--continued

constant rates of deformation. It was found that for a rate of 0.02 mm/min the average friction was 1.25 lb compared to 6.5 lb with the O-Ring. For a deformation rate of 0.008 mm/min the friction was 2.06 lb versus 8.6 lb when the O-Ring was used. These results led to the decision of using the filter cloth for the rest of the CHG tests, and simply neglecting the effect of the piston friction.

In the case of test CHG-2, the gradient was 4 ± 5%, with an initial solids content of 16.4% (e = 13.77). The test duration was 168 hours (7 days). Readings were taken every hour fora total of 169 data points. At the end of the test the computed specimen height was 8.33 cm, while the observed value was 8.3 cm. The final solids content was computed as 27.3% (e = 7.20), and the average measured value was 28.1% with a variation of 2.2% across the specimen. Figure 5.9 shows the compressibility and permeability curves of test CHG-2. The higher gradient used produces values of pressures and load which are read more accurately by the devices, which in turn produces better defined curves.

The specimen of test CHG-3 had an initial solids content of 16.3% (e = 13.86) and ended at a height of 6.55 cm with an average solids content of 33.0% (e = 5.49) (computed values), after 168 hours (7 days) of testing. Direct measurements of solids content at the end of the test produced an average value of 3.5% with a variation of only 0.44% across the specimen,with an observed final height of 6.2 cm. The gradient set for this test was of 10 ± 5%.

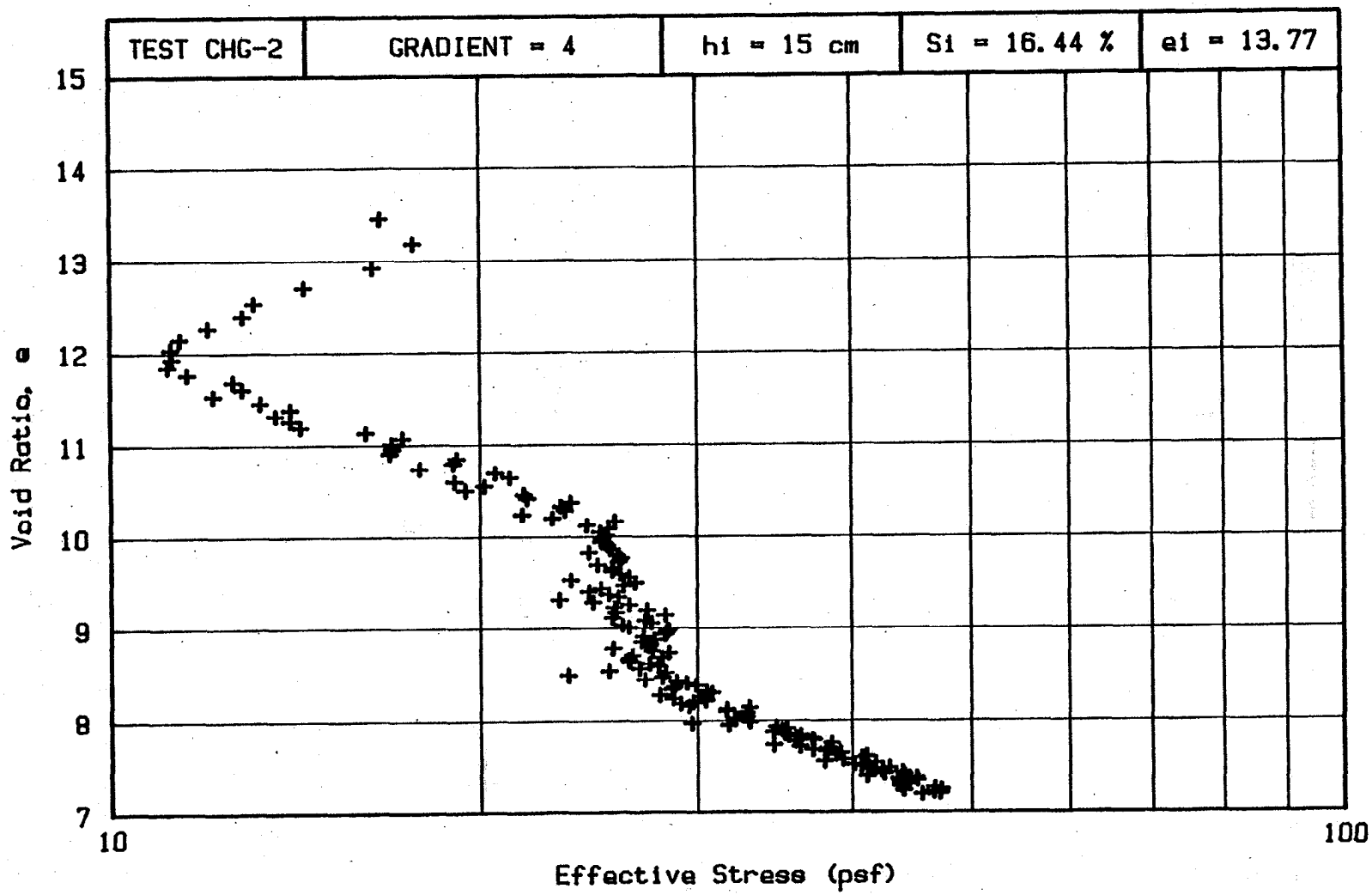

(a)

Figure 5.9 - Results of Test CHG-2. a) Compressibility Relationship; b) Permeability Relationship

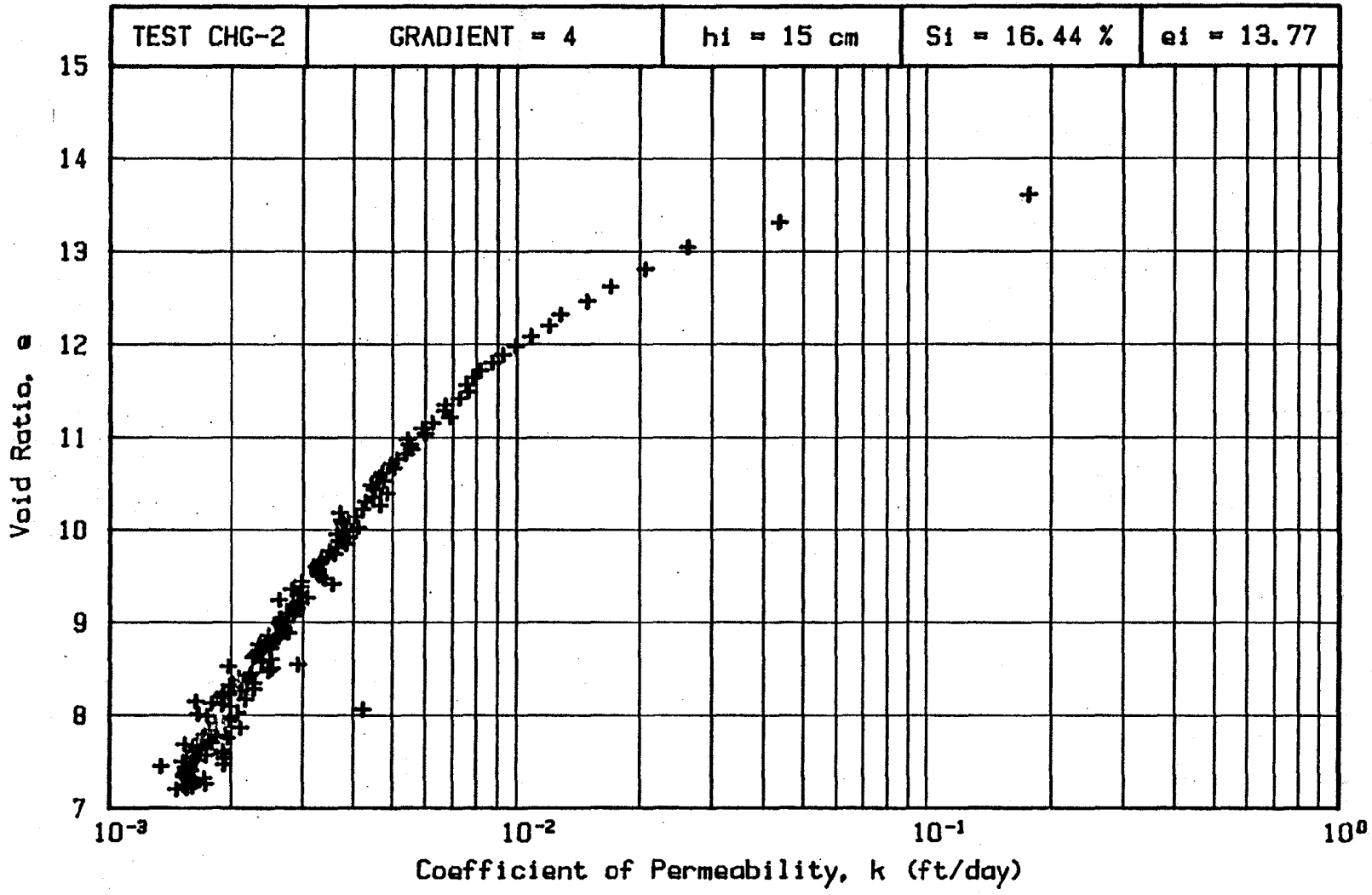

(b)

Figure 5.9--continued

Readings for test CHG-3 were taken every hour, producing a total of 169 data points. Figure 5.10 shows the plots produced by SLURRY2 as the data is reduced. Again, the higher gradient produces less scatter in the results.

The last test, CHG-4, was run at the highest hydraulic gradient, 20 ± 2.5%, for 120 hours (5 days). The initial solids content was 16%. Readings weretaken again every hour,producing 121 data points. At the end of the test the computed height was 6.22 cm, corresponding to a solids content of 33.8%. The observed final height was 6.0 cm and the measured average solids content was 35.9% with a variation of 1.18% across the specimen. Figure 5.11 shows the plots obtained from test CHG-4. The final conditions for the specimens of the four CHG tests are summarized in Table 5-3.

Table 5-3. Summary of CHG Tests Results

Test	Duration (hrs)	Final Height (cm)		Final Solids Cont.(%)		
		Computed	Observed	Computed	Measured	Gradient
CHG-1	192	7.23	7.2	23.9	24.4	2.0
CHG-2	168	8.33	8.3	27.4	28.1	2.2
CHG-3	168	6.55	6.2	33.0	35.0	0.4
CHG-4	120	6.22	6.0	33.8	35.9	1.2

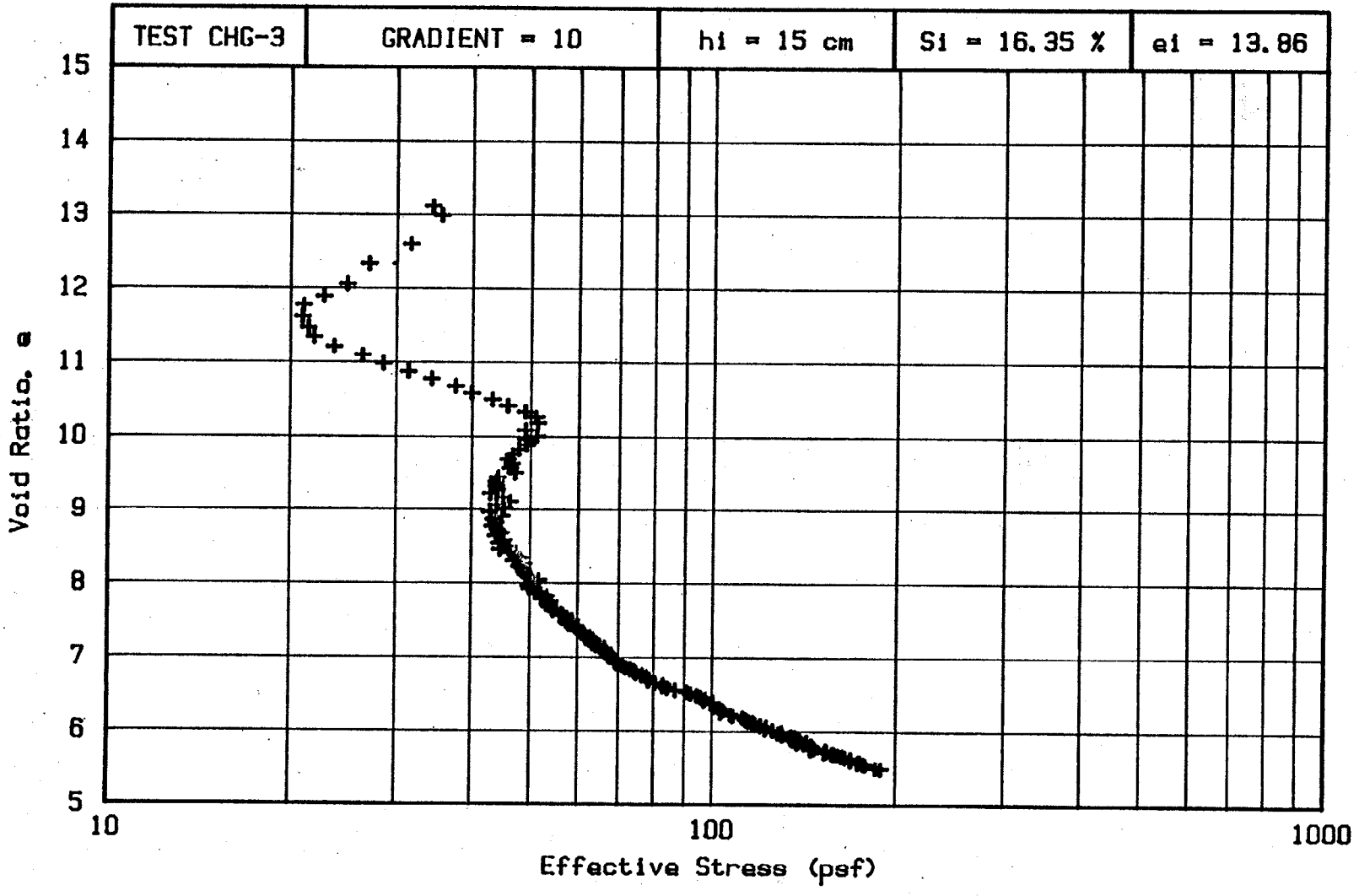

(a)

Figure 5.10 - Results of Test CHG-3. a) Compressibility Relationship; b) Permeability Relationship

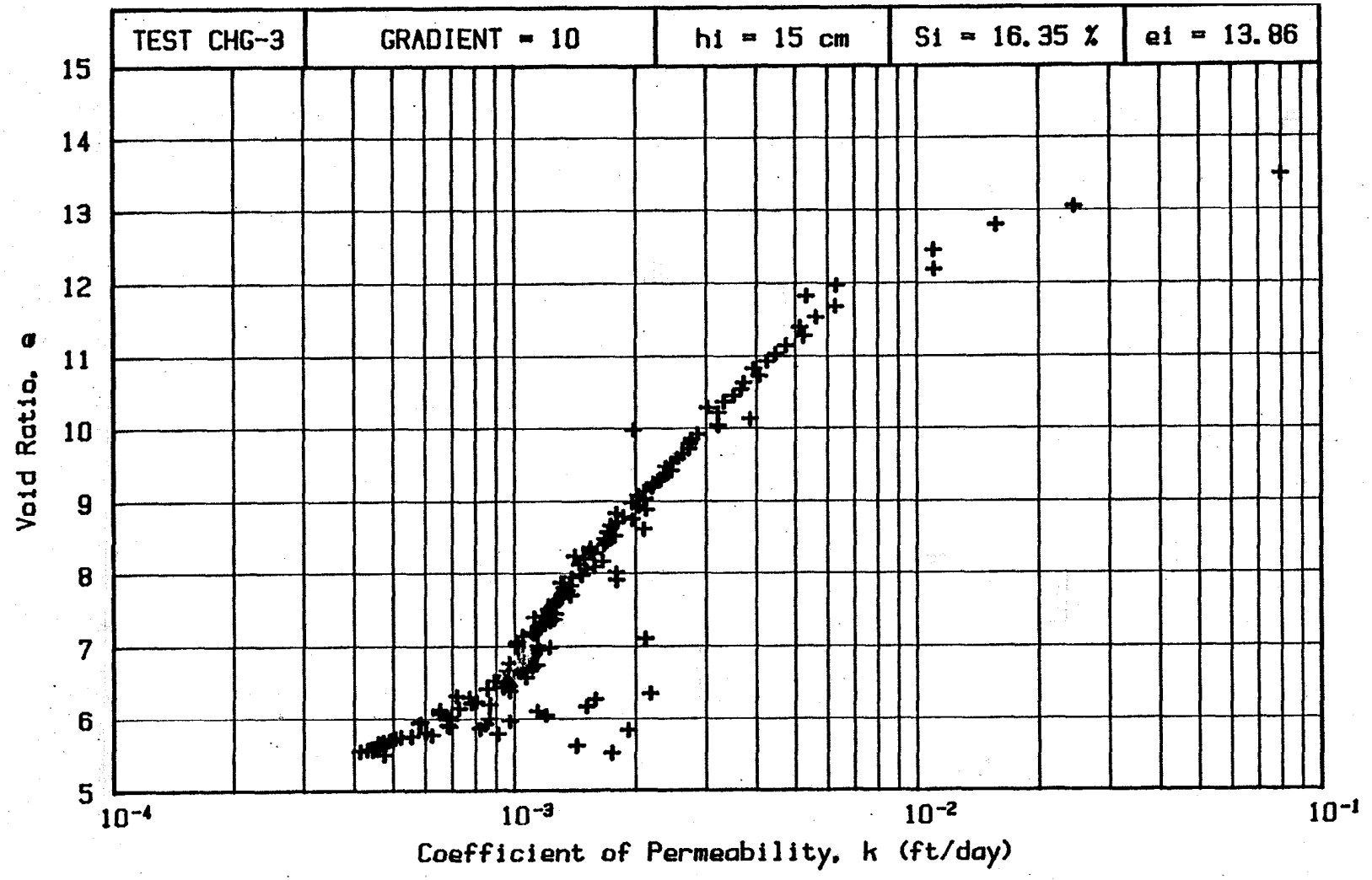

(b)

Figure 5.10--continued

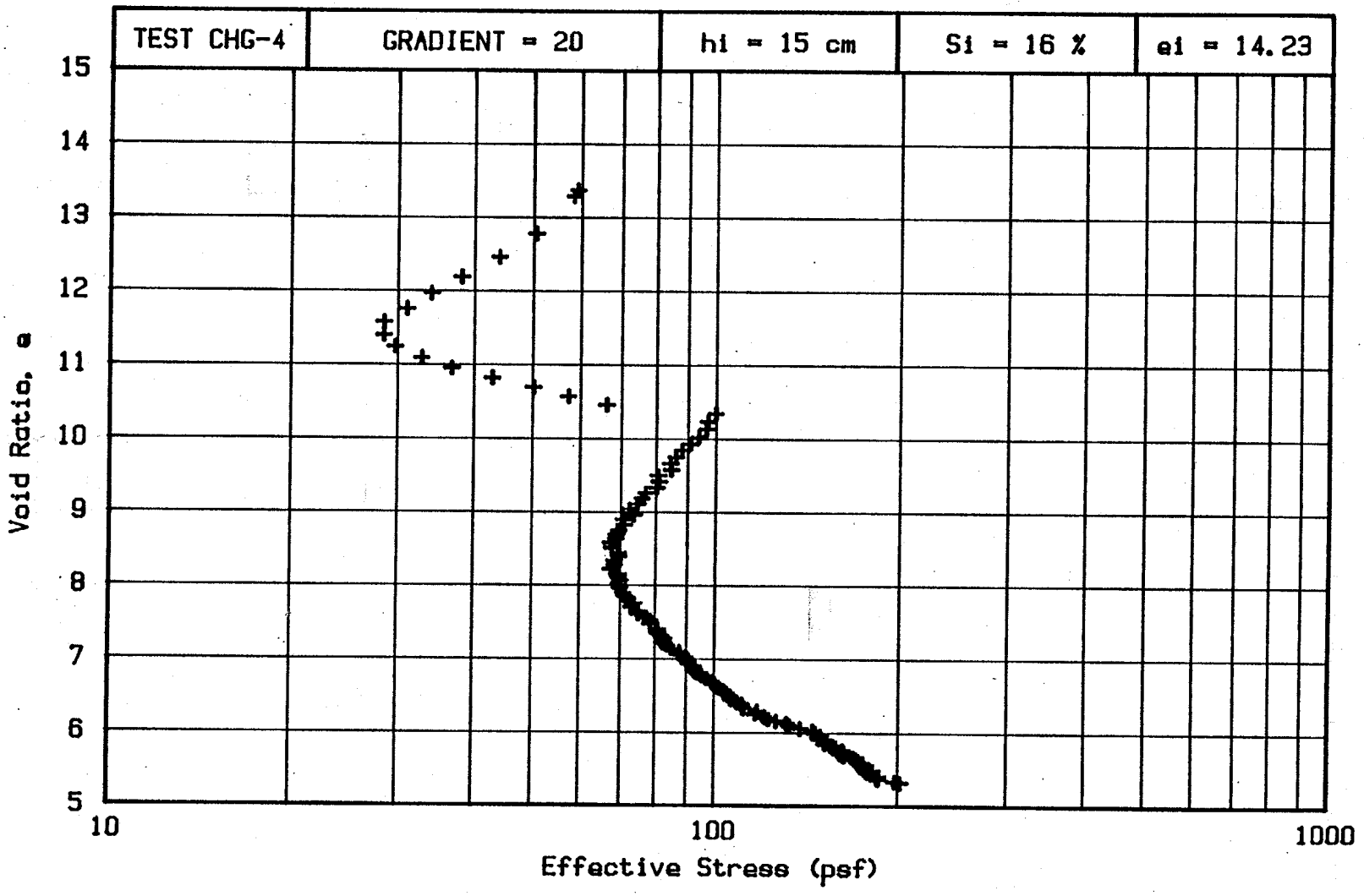

(a)

Figure 5.11 - Results of Test CHG-4. a) Compressibility Relationship; b) Permeability Relationship

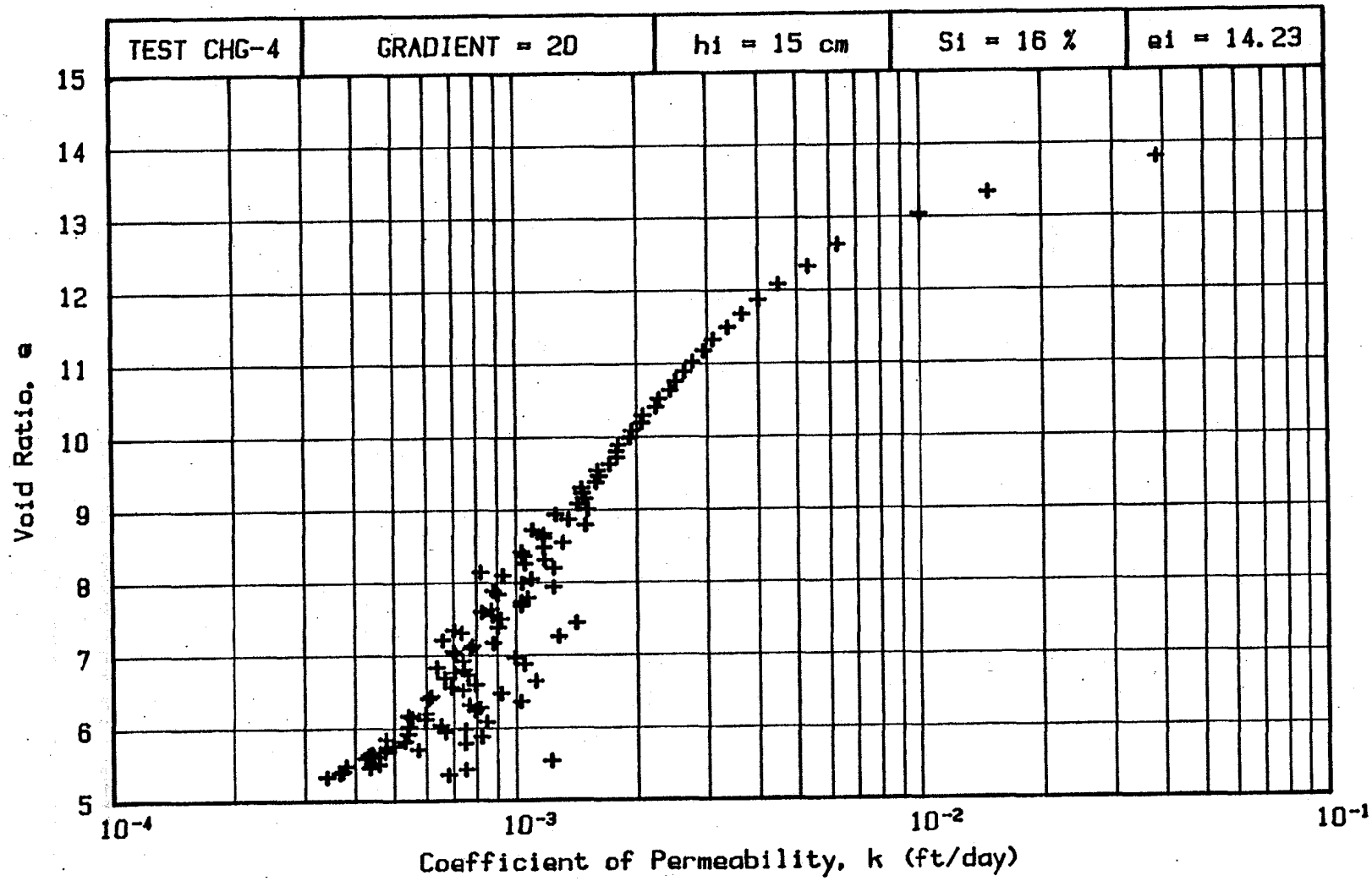

(b)

Figure 5.11--continued

Figure 5.12 shows the pore pressure and effective stress distributions at two different times for one of the CHG tests. The first time is when the desired gradient of 4 ± 5% is first reached at about 23 minutes. At this time the solids content is 16.8% (e = 13.45) and the average effective stress, occurring mostly on the top fourth of the specimen, is only about 0.12 psi. The second set of curves is practically at the end of the test (167 hours), when the average solids content is 27.3% (e = 7.21) and the average effective stress is 0.33 psi, which is still relatively low. These plots show that even at relatively low gradients, the variation of effective stress with depth is significant.

The results of the four CHG tests are presented together in Figure 5.13. The compressibility curves of Figure 5.13a show a very interesting behavior. First, the preconsolidation effect is not observed in these curves, due in part to the fact that the specimen is loaded very fast initially, without any reading taken until the desired gradient is reached. In all the cases, the effective stress initially jumped to a relatively high value, and immediately started decreasing, contrary to all expectations. After some time the effective stress began to increase again, as the specimen continued to deform. It is interesting to observe how parallel these initial portions of curves 2, 3 and 4 are. In the case of test CHG-1, with the lower gradient, the curve shows a lot more scatter but a similar trend is observed. Although not clearly understood, this

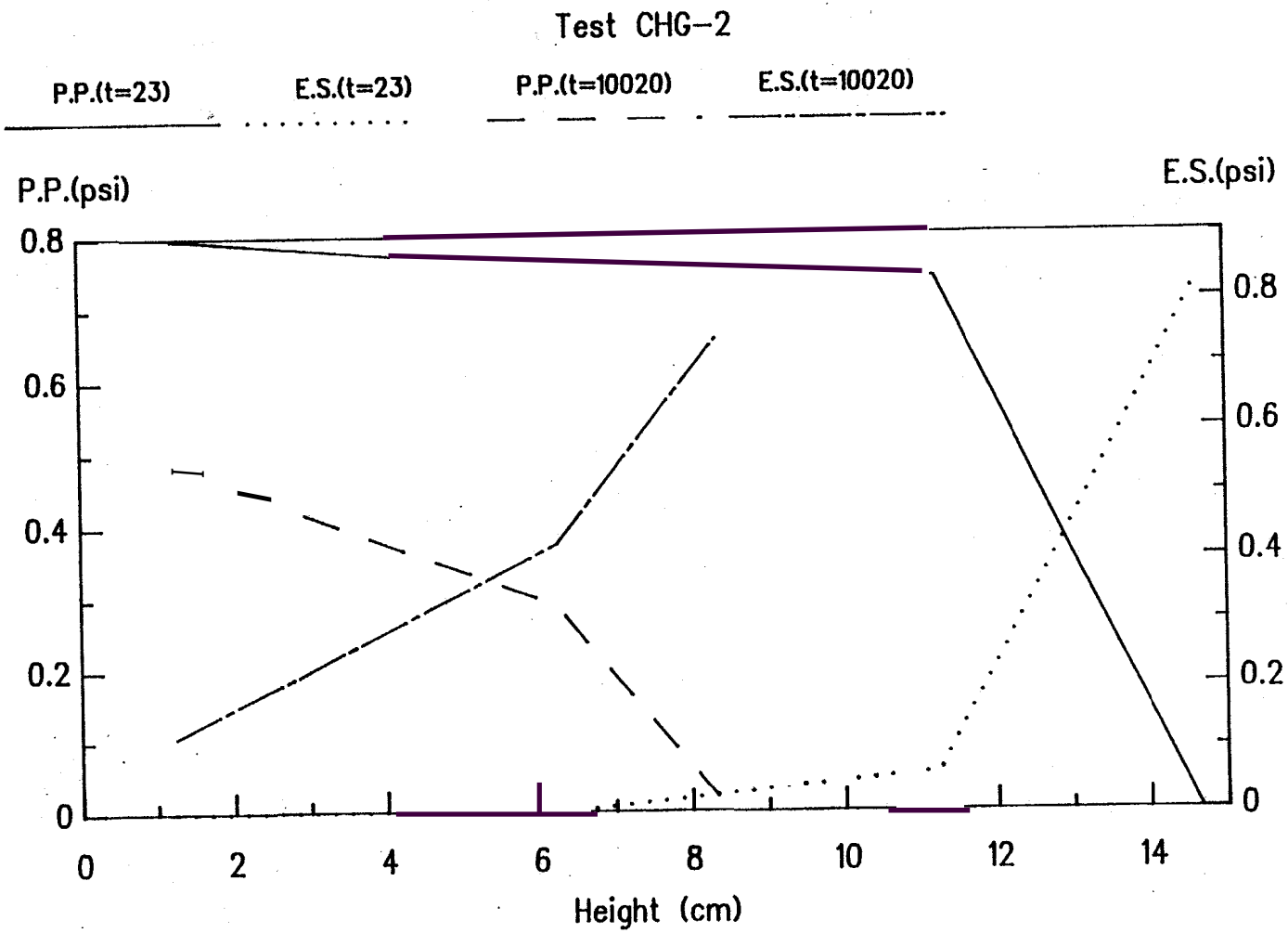

Figure 5.12 - Pore Pressure and Effective Stress Distributions with Depth for Test CHG-2

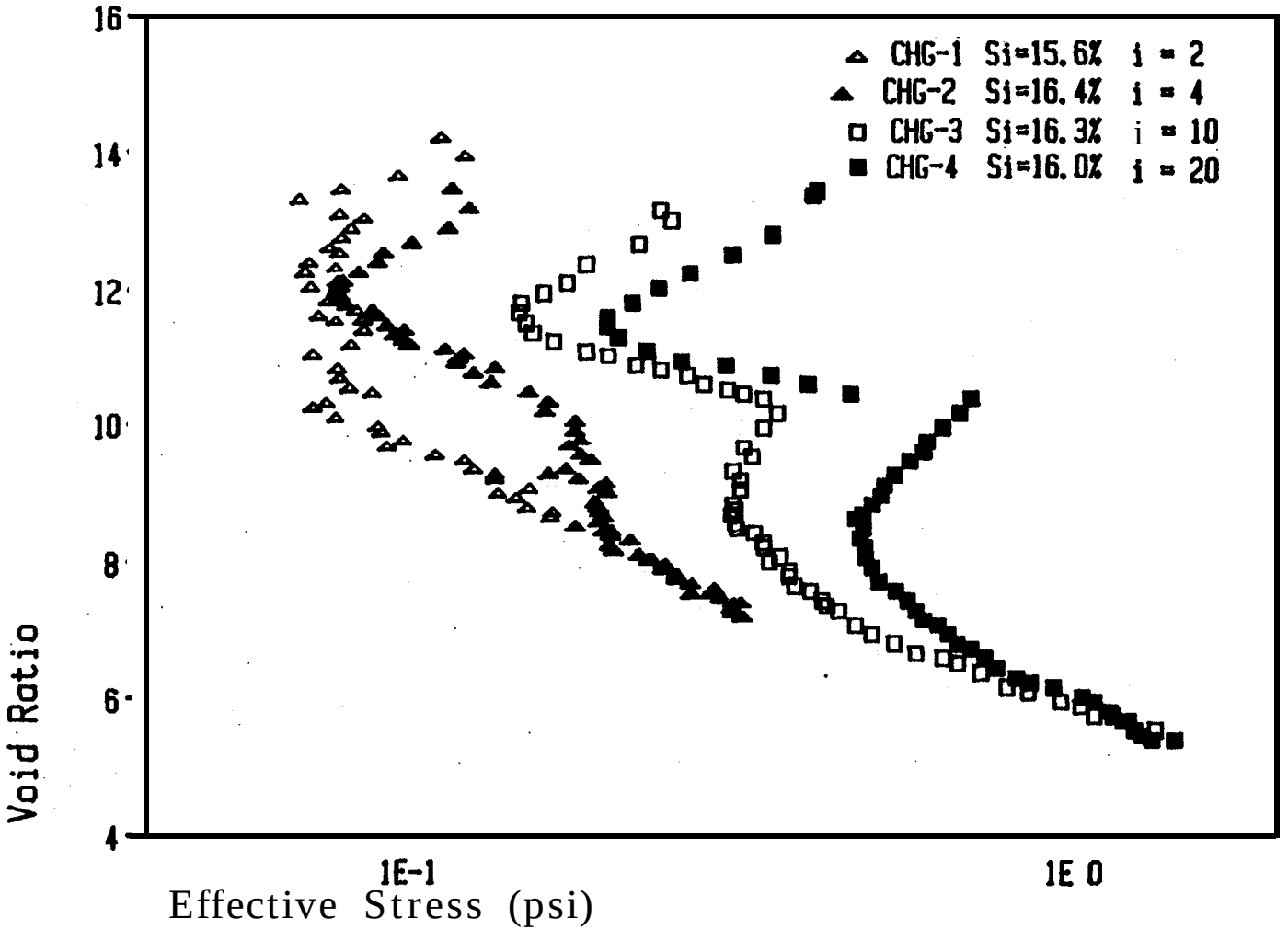

(a)

Figure 5.13 – Summary of CHG Tests. a) Compressibility Relationship; b) Permeability Relationship

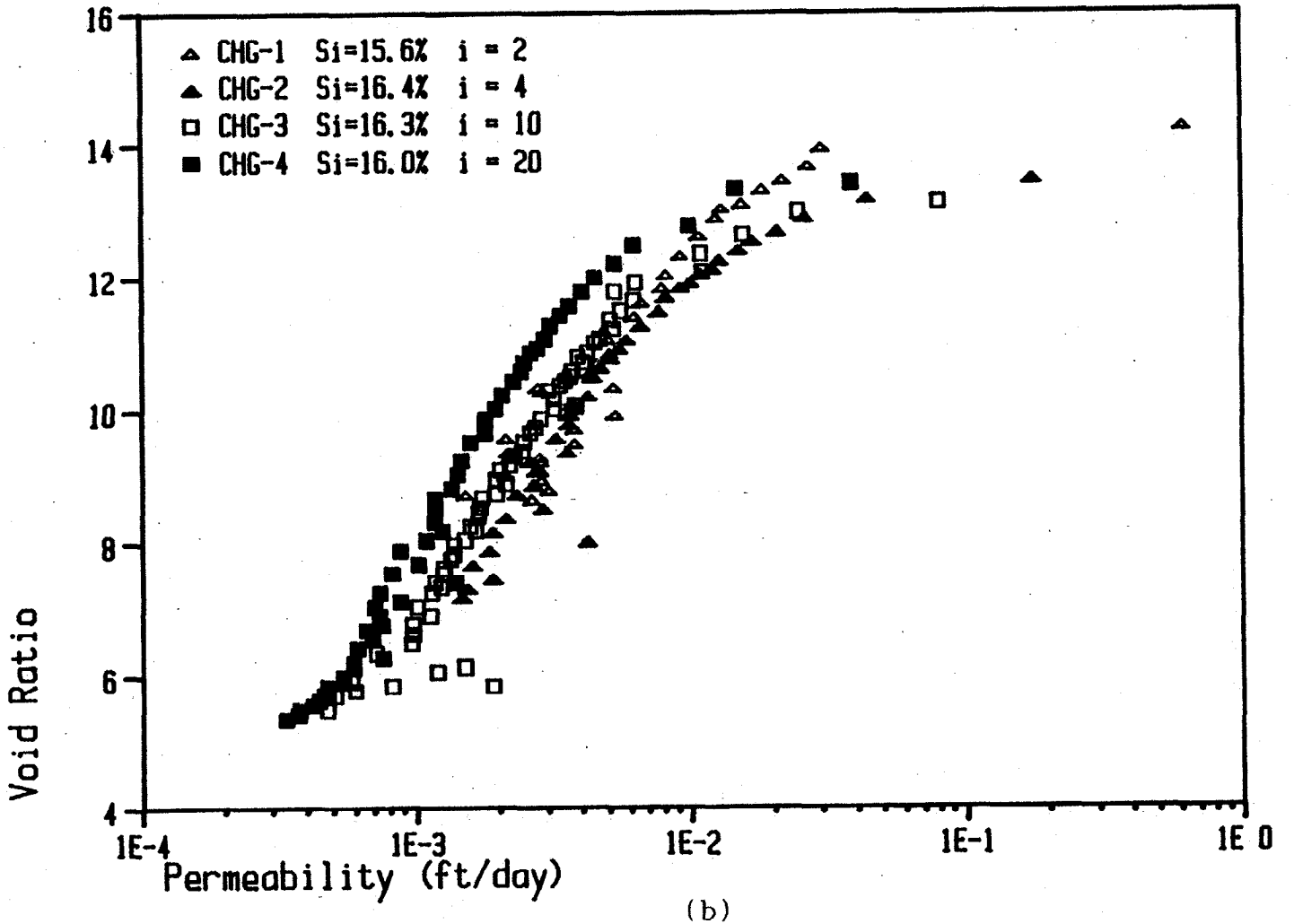

(b)

Figure 5.13--continued

strange behavior of the initial portion of the compressibility curves is attributed to the drastic decrease in rate of deformation in the controlled gradient tests; for example, the mean deformation rate in test CHG-3 dropped from a very high initial value of 0.15 mm/min to about 0.02 mm/min in just six hours. This result seems to corroborate the conclusion obtained in the previous section concerning the effect of deformation rate upon the compressibility.

Figure 5.13a also showshow all four compressibility plots convergeto a unique curve. This virgin zone of the plot is independent of the hydraulic gradient or the irregular behavior observed in the early portion of the curves.

The permeability results of the four CHG tests are presented in Figure 5.13b. The data points fall in a relatively small band. Thus the permeability relationship obtained from these tests can be said to be independent of the hydraulic gradient for the range of values considered in the tests.

Testing Influences

In a CRD test,maintaining the deformation rate constant forces the hydraulic gradient to increase with time. Conversely, in a CHG test, keeping the hydraulic gradient constant makes the deformation rate decrease from very high valuesinitially to extremely low values near the end of the test. This effect is shown in Figure 5.14, where plots of the rateof deformation and hydraulic gradient with time are shown for one test of each type. First, it is clearly observed that neither the rate of deformation in a CRD test, nor the hydraulic gradient in a CHG, is completely constant, due to equipment characteristics in the first case and allowed variation in the second.

For the CRD test, the hydraulic gradient remains very small (less than 2) for the first 2000 minutes of testing. After this point, it increases. very rapidly. In the case of CHG test, the deformation rate is initially very high but decreases very quickly to a value around 0.02 mm/min in 300-400 minutes. This deacceleration effect is reduced from that point on.

A comparison of the various constitutive curves clearly shows that there is a more irregular behavior in the compressibility plots obtained from CHG tests (Figure 5.7a vs. Figure 5.13a). This is attributed, at least partially, to piston friction which probably behaves in a more erratic and unpredictable way in the controlled gradient tests, due to the way the specimen is loaded; its real magnitude is

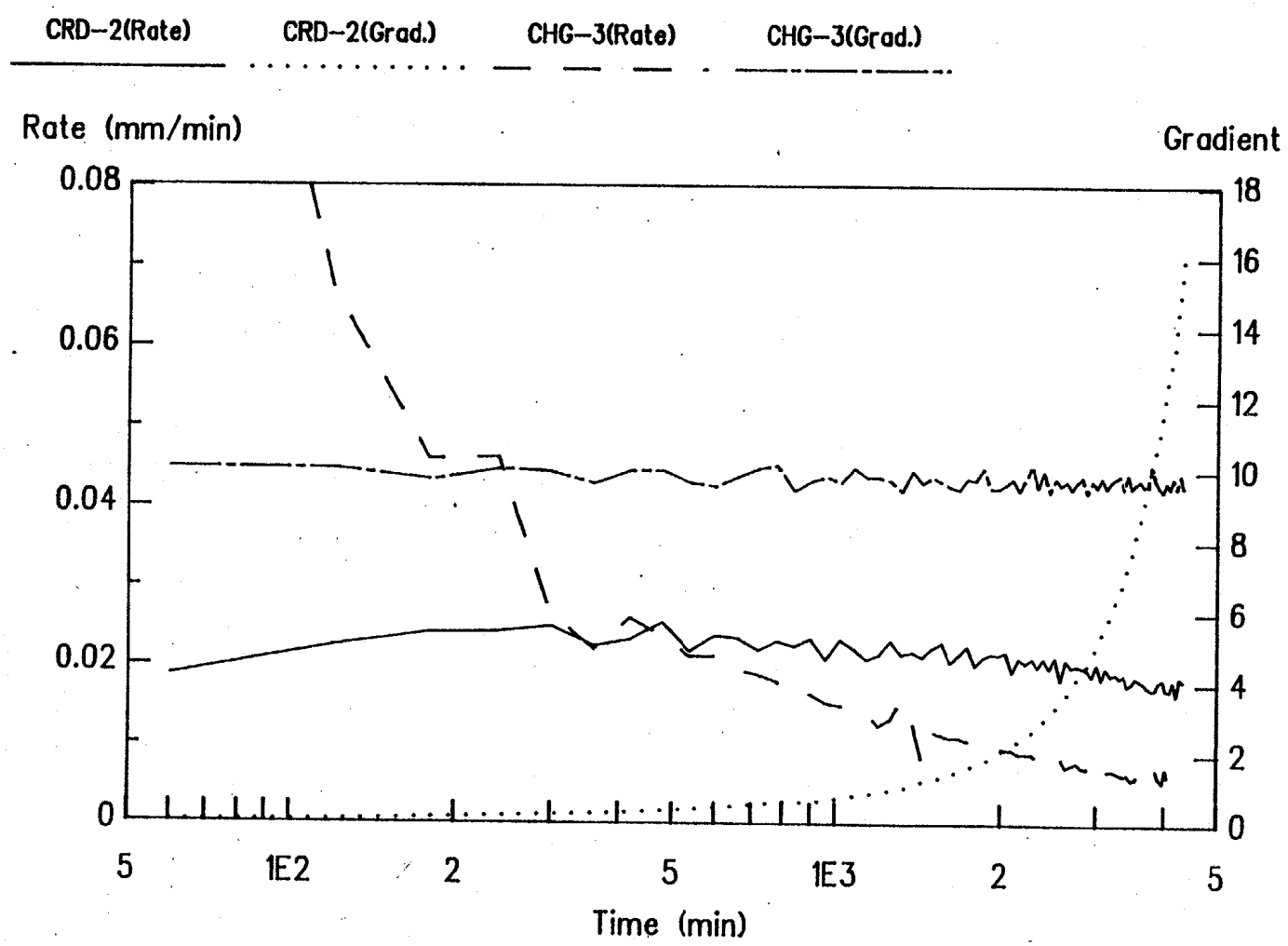

Figure 5.14 - Deformation Rate and Hydraulic Gradient with Time for Tests CRD-2 and CHG-3

completely unknown. For the CRD tests, on the other hand, the piston friction was estimated from tests using only water, indicating an almost constant value for a given rate of deformation.

A comparison of the resultsof two CRD tests (1 and 3) with two CHG tests (2 and 3) is shown in Figure 5.15. All four tests had an initial solids content around 15% to 16%.

The permeability results of the CRD and CHG tests are in good agreement, regardless of hydraulic gradient or deformation rate. Conversely, in the case of the compressibility, at effective stresses of 0.2-0.4 psi (S = 23-25%) the CHG curves approach the virgin portion of the curve obtained from the test with low rate of deformation (CRD-3).

In all the tests performed to this date, it has been observed that the permeability plot always shows a better defined trend with less scatter. This is reasonable, considering that the average values of void ratio and coefficient of permeability are calculated from few parameters, namely the specimen height and the pore pressures at the bottom and top of the specimen (which are measured with the two most accurate transducers). The calculated average effective stress, on the other hand, not only depends upon four pore pressure measurements plus that from the load cell, but also depends on specimen friction estimated from the total stress transducer reading (not very accurate) and piston friction, which is completely unknown for the GHG tests and only approximated for the CRD tests. With more

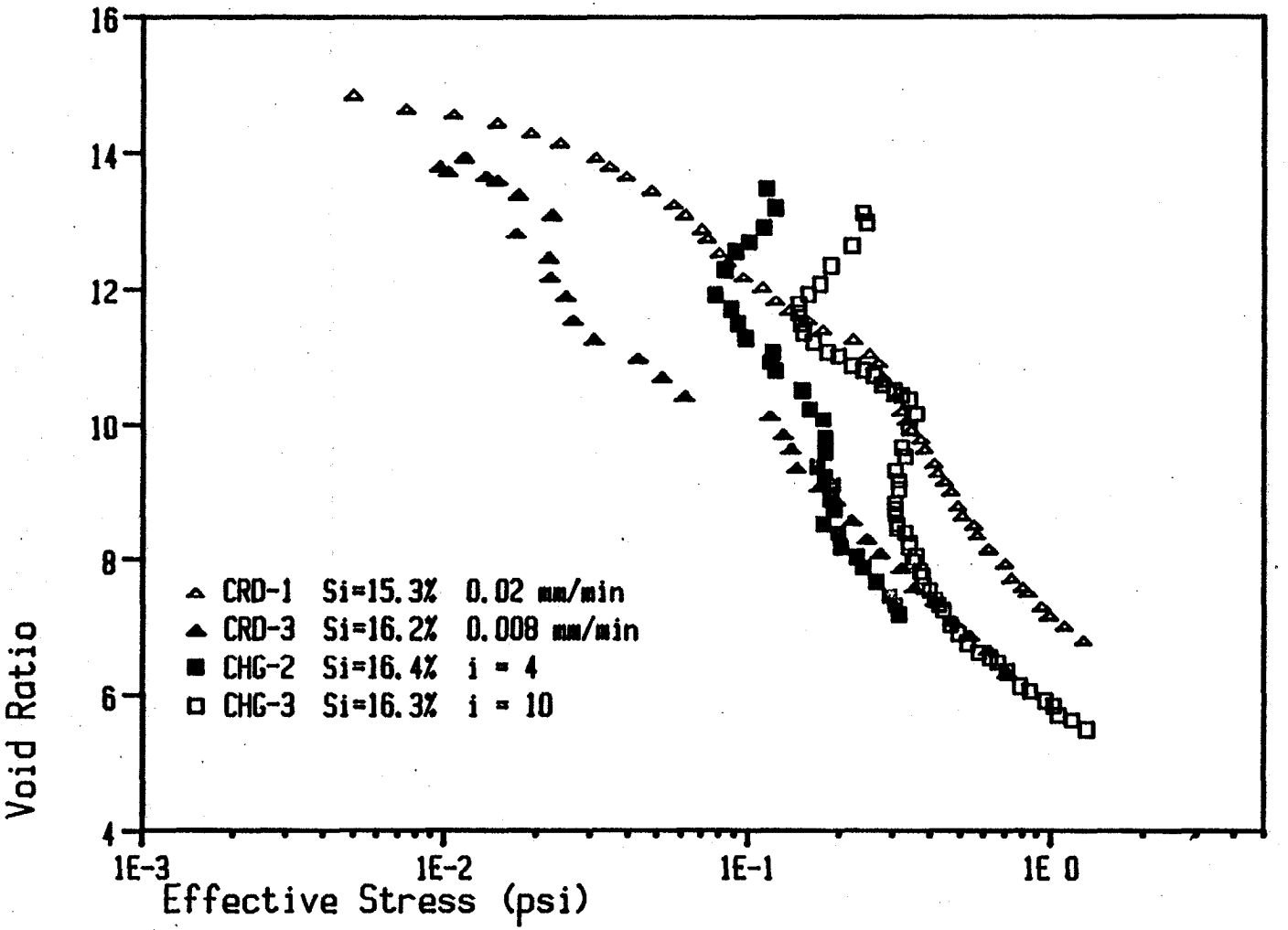

(a)

Figure 5.15 - Comparison of CRD and CHG Test Results. a) Compressibility Relationship; b) Permeability Relationship

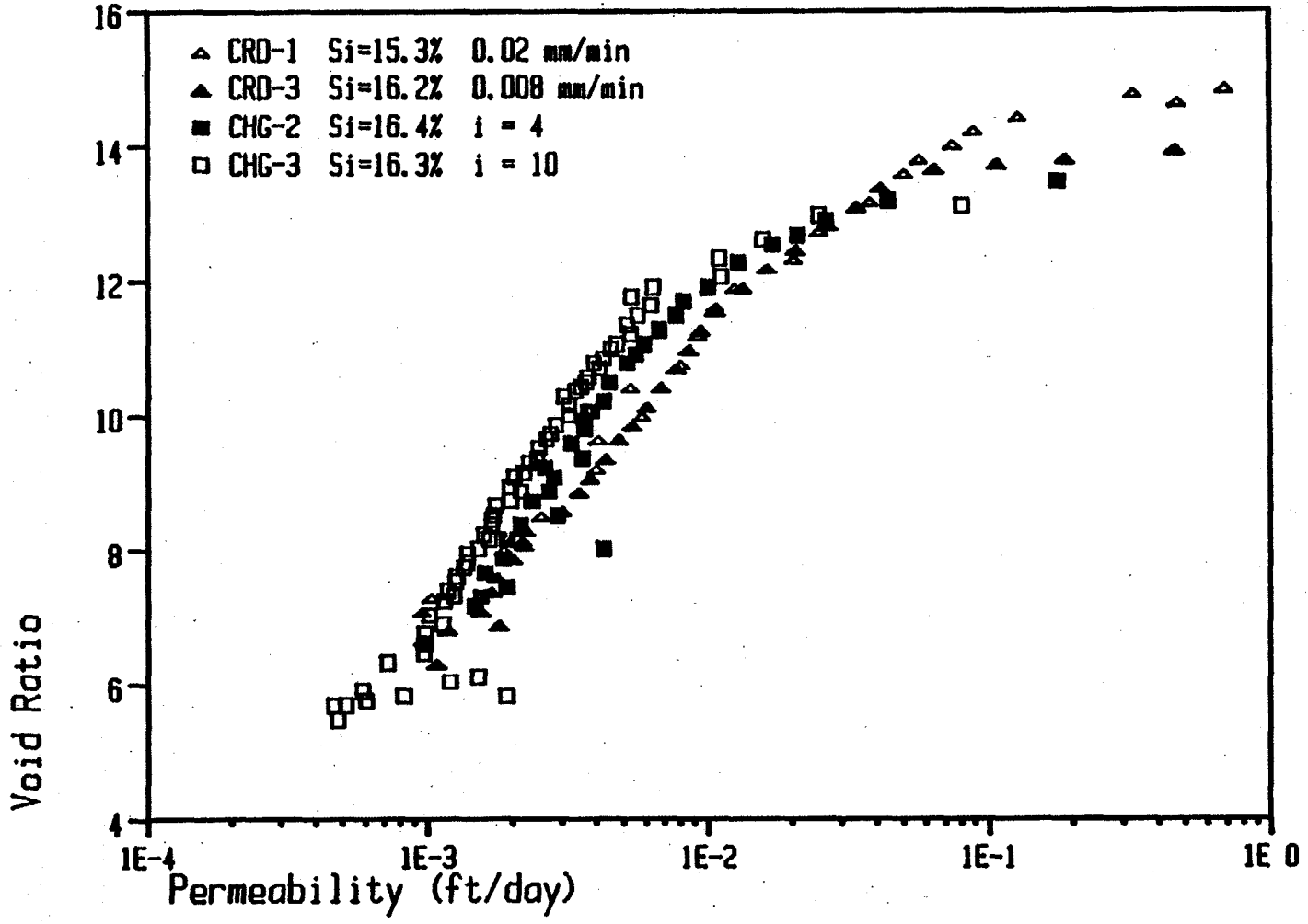

(b)

Figure 5.15--continued

variables containing more measurement error, it could be anticipated that the compressibility plots would show more scatter. In addition, the compressibility relationship depends more on the assumption of specimen uniformity since the approach computes an average value of effective stress from a distribution that may be highly variable due to the boundary conditions.

A key element in the computation of the coefficient of permeability is Darcy's law. Therefore, it is very important to evaluate its validity in the slurry consolidometer. Darcy's law is accepted as valid when the fluid flow is laminar. The criterion to evaluate this condition is based on Reynolds number. For the case of flow through porous media, a Reynolds number has been defined as (Bear, 1979)

$$R_e = q \cdot d/v \qquad (5.1)$$

where q, the specific discharge, is defined as the volume of fluid passing through a unit area of soil in a unit time; d, a representative length of the porous matrix, is taken as the diameter such that 10% of the soil by weight is smaller (D_{10}); and v is the kinematic viscosity of the fluid.

Goforth (1986) found that, for sands, Darcy's law was valid for Reynolds numbers below 0.2. A critical value of Reynolds number in the slurry consolidometer tests is probably obtained in a fast CRD test, near the end of the test when the void ratio is minimum. The specific discharge, q, will be assumed to the average relative velocity of the fluid with respect to the solids particles, since

both phases are moving. For example, for test CRD-1 with a rate of deformation of 0.02 mm/min, the average solids velocity is 0.01 mm/min (1.67E-04 mm/sec). Near the end of the test, when the void ratio reaches a value of 7, the absolute value of the average fluid velocity is computed from equation 4.16 as

$$V_f = (1.67E\text{-}04)/7 = 2.38E\text{-}05 \text{ mm/sec} \quad (5.2)$$

Thus, the specific discharge is simply

$$q = 2.38E\text{-}05 + 1.67E\text{-}04 = 1.91E\text{-}04 \text{ mm/sec} \quad (5.3)$$

Using a value of D_{10} of 0.002 mm and a kinematic viscosity for water at 75^o of 1 mm^2 /sec (Streeter and Wylie, 1975), the Reynolds number is computed by substituting Equation 5.3 into Equation 5.1 as

$$R_e = (1.91E\text{-}04 \text{ mm/sec})(0.002 \text{ mm})/(1 \text{ mm}^2/\text{sec}) = 3.8E\text{-}07 \quad (5.4)$$

This very low value of Reynolds number indicates that Darcy's law is valid in the tests, even for the fast deformation rate. This result may very well explain the agreement obtained in the permeability among the different tests, regardless of the rate of deformation or hydraulic gradient.

The results of the tests reported here suggest that power functions like equations 4.31 and 4.32 may not be the best mathematical representation of either the compressibility or permeability relationship. Although the virgin zone of the experimental curves could be represented fairly, well by this type of function, the introduction of the

initial preconsolidation zone changes the entire picture. The immediate result of this is that the permeability and compressibility relationships would not be unique but would depend on the initial solids content, as demonstrated by the plots of Figure 5.7. In addition, computer codes that allow the input of data points instead of the traditional A, B, C and D power curve parameters to characterize the soil would be more appropriate.

Finally, because of the abnormal behavior of the CHG compressibility curves and other disadvantages of the test, this testing method is not recommended for practical applications or even for future study. The CRD test, on the other hand, offers a number of advantages, such as the possibility of anticipating the testing time required to achieve a desired final condition. The results of the CRD tests reported in this research are more reasonable. For the sake of comparison, the constitutive curves obtained from test CRD-1 are plotted in Figure 5.16, together with the power curves fit to the experimental data and other functions proposed for Kingsford clay (Table 2-l). The power curve parameters obtained for test CRD-1, which include the points in the preconsolidation zone, are

A = 18.03 B = -0.165

C = 3.619E-09 D = 6.27

with a correlation coefficient around 0.95 for both curves. Although the power curves do not show the preconsolidation effect observed in the CRD test, Figure 5.16 shows that

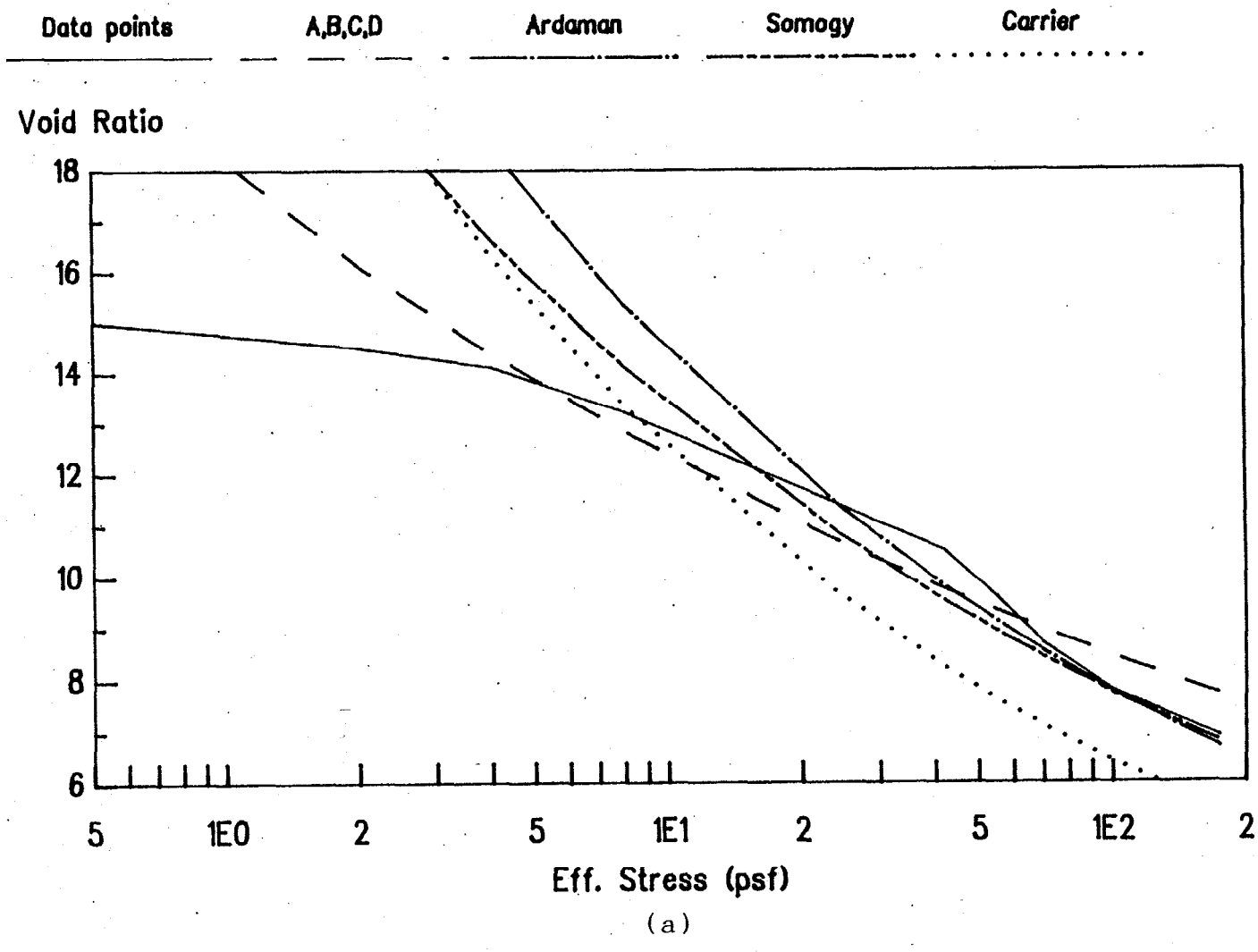

(a)

Figure 5.16 - Constitutive Relationships Proposed for Kingsford Clay.
a) Compressibility; b) Permeability

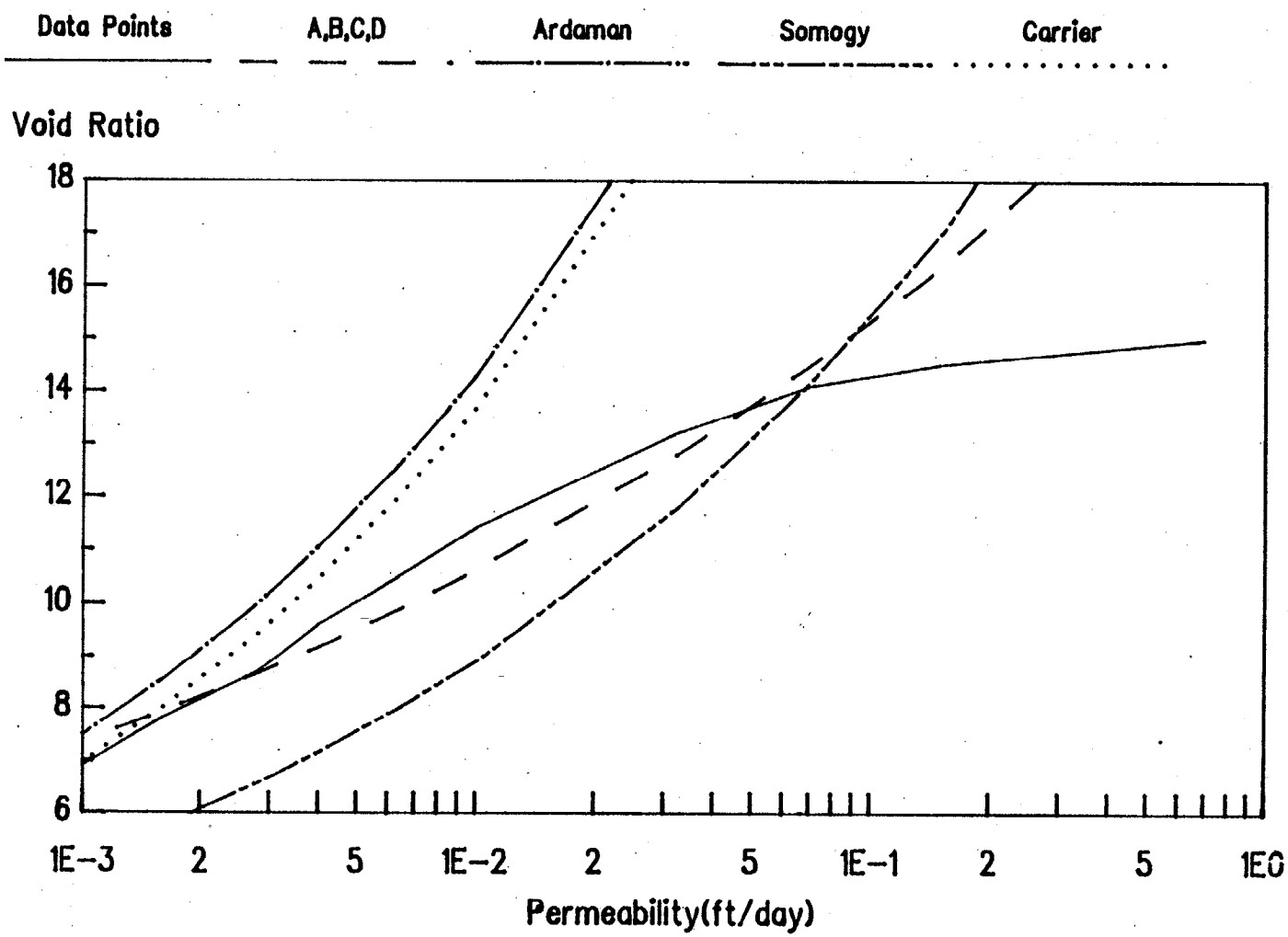

(b)

Figure 5.16--continued

the overall behavior of the results of the CRD tests falls within the range of the other curves.

CHAPTER VI
CENTRIFUGE TESTING--EQUIPMENT, PROCEDURE, AND DATA REDUCTION

Introduction

Centrifuge testing has been used quite extensively to model the sedimentation/consolidation process of slurries, including the analysis of different disposal techniques (Beriswill, 1987; Bloomquist, 1982; McClimans, 1984; Townsend and Bloomquist, 1983), and to a lesser extend to validate the results of numerical predictions (Hernandez, 1985; McVay et al. 1986; Scully et al., 1984).

Few attempts have been made, however, to obtain the constitutive relationships of the slurry from centrifuge testing. The compressibility relationships obtained by McClimans (1984) and Townsend and Bloomquist (1983) agree relatively well with the results of other tests (see Table 2-1). Their approach is based on the measurement of solids content with depth after selfweight consolidation, when all excess pore pressure has been dissipated. This measurement allows determining the void ratio and the effective stress with depth in the specimen. However, the number and quality of the points obtained with this approach are largely dependent upon the quality of the coring process. On the other hand, the back calculations and curve fitting methods

suggested in these studies to obtain the permeability relationships yielded parameters which disagree significantly with the results of other tests.

Takada and Mikasa (1985) have also used centrifuge tests for the determination of consolidation parameters. Similar to the studies previously cited, the compressibility curve is obtained from the water content profile at the end of the test. The coefficient of permeability is obtained from the initial settlement rate of selfweight consolidation. They derived the following expression for k, valid only at the surface of the layer and for the early stage of selfweight consolidation under single drainage.

$$k = \frac{s}{n} \frac{\gamma_w}{\gamma'_o} \qquad (6.1)$$

where s is the initial settlement rate,

n is the acceleration level in g's

γ_w is the unit weight of water, and

γ'_o is the initial buoyant unit weight.

In this approach, one test at a given initial void ratio will represent one point of the permeability plot; thus, a large number of tests with different initial conditions are needed. Another disadvantage of the approach is the difficulty in estimating the initial settlement rate.

This chapter describes a new technique developed specifically to obtain the compressibility and permeability relationships of soils from centrifuge testing. The approach is based on measurements of excess pore pressure and solids content with depth and time during the test.

These allow computing the void ratio, effective stress, and coefficient of permeability using a material representation of the sample: Perhaps, the main advantage of the approach is that the curves are obtained from a model with stress conditions similar to those existing in the slurry pond, The following sections of this chapter describe the test equipment, procedure and method of data reduction.

Test Equipment and Procedure

The geotechnical centrifuge at the University of Florida was used for the testing program carried out in this study. The l-m radius centrifuge can accelerate 25 Kg to 85 g's (2125 g-Kg) (Bloomquist and Townsend, 1984). In the standard test procedure, the waste clay is contained in a 14 cm diameter by 15.25 cm high cast-acrylic container. This container is housed in a swinging aluminum bucket, with a vertical window that allows visual observation of the model. A Polaroid camera in combination with a photo-electric pick-off and flash delay are used to monitor the model height during the test. Figure 6.1 shows a schematic drawing of the centrifuge and photographic equipment. More detailed descriptions of this equipment have been reported elsewhere (Beriswill, 1987; Beriswill et al., 1987; McClimans, 1984).

A specimen height of 12 centimeters was selected for this testing program. The distance from the center of rotation to the bottom of one of the four buckets (bucket A)

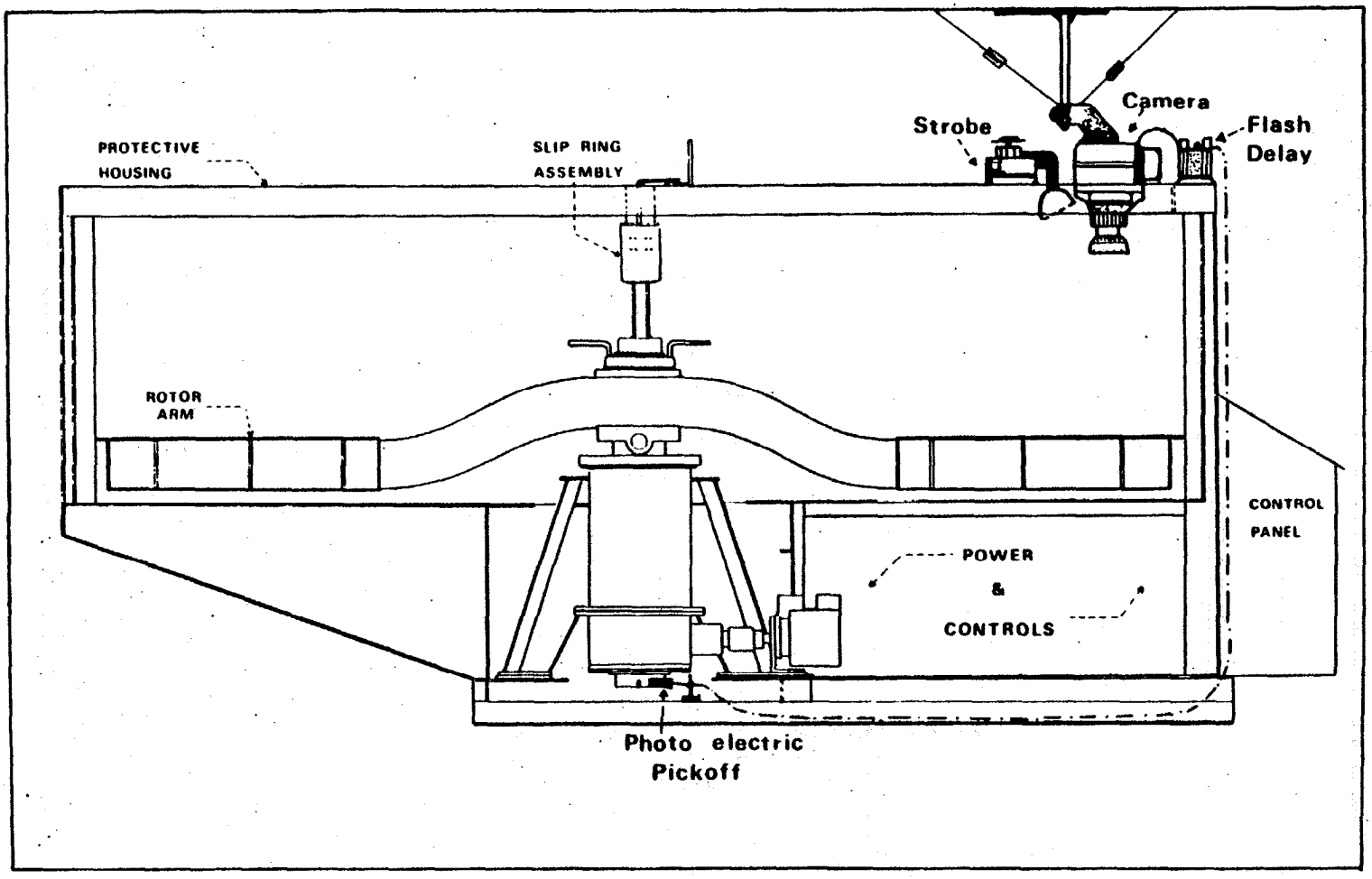

Figure 6.1 - Schematic of Centrifuge and Camera Set-up

was measured as 43.125 inches (109.54 cm), and the distances to the other buckets were adjusted to the same value. For a 12-cm specimen, the radius to the center of gravity is then 103.54 cm. Average acceleration levels of 60g and 80g are achieved in this specimen with angular velocities of 228 and 263 r.p.m., respectively. The radial acceleration gradient in each case is about ±5.6%, representing about ±3.5g in a 60g test and ±4.6g in 80g test.

Two new elements were added to the test in order to accomplish the objectives established. They are the measurements of excess pore pressureand solids content with depth and time.

To measure the excess pore pressure distribution, the acrylic bucket was modified by attaching three of the pressure transducers used in the automated slurry consolidometer described in Chapter III. Figure 6.2 shows a photograph of the modified bucket. Information on the three transducers selected is shown in Table 6-1. The transducers were located at 1, 5, and 9 centimeters from the bottom of the specimen. For the model height used in the tests, this arrangement was expected to produce a good pore pressure curve. The excitation of the transducers was 10 VDC, as used in the slurry consolidometer tests. Monitoring of the pressure transducers was done with the HP-3497A also described in Chapter III.

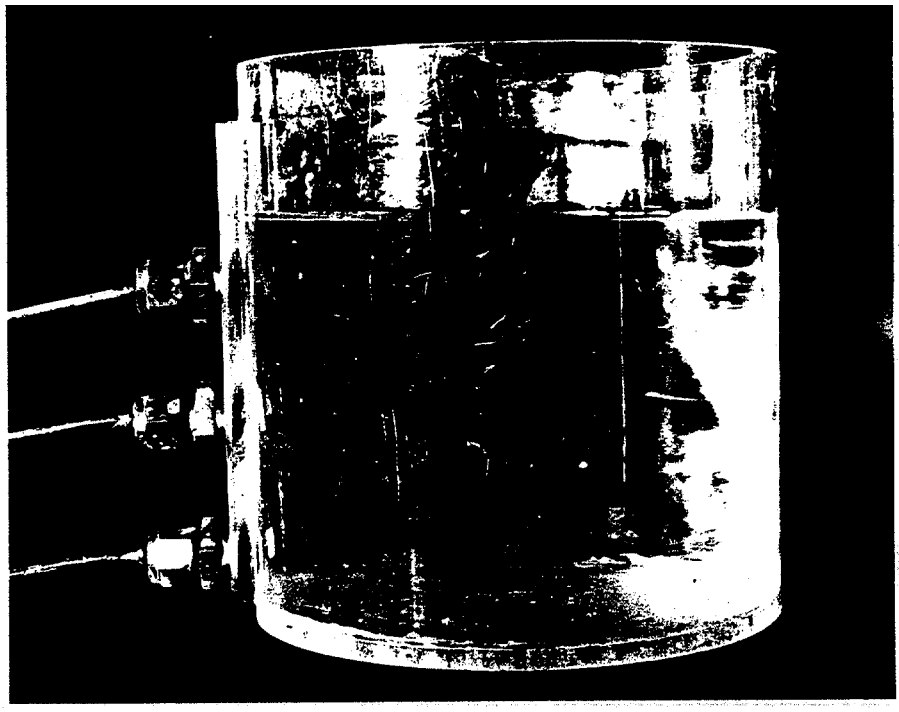

Figure 6.2 - Centrifuge Bucket

Table 6-1. Centrifuge Test Transducer Information

Transd. No.	Distance from bottom (cm)	Serial Number	Factory Calibration (mV/psi)	Zero-Reading in 12-cm Water (mV) 60g	80g
1	1.0	2998	6.370	41.913	61.729
2	5.0	2955	7.418	19.145	33.329
3	9.0	3241	12.800	35.308	44.253

An evaluation of the transducer calibration in the high acceleration level of the centrifuge was necessary. The results of this study are presented in Appendix F. It was found that the transducers performed well and that the factory calibration factors were valid in the centrifuge. These values were used in the analyses and are also included in Table 6-1.

The second requirement of the approach was the solids content distribution. Two unsuccessful attempts were made to measure it indirectly. One attempt tried to correlate electrical resistivity with solids content, while the other depended on measuring the total vertical stress at different points in the specimen and from there computing the density distribution; the density would readily lead to the void ratio distribution. After failure of these approaches, it was decided to measure the solids content directly. This approach required the design of a system of small sub-samples that could be removed from the centrifuge periodically. Each individual sub-sample is contained in a perforated 2-in PVC tube, as shown in Figure 6.3. The small holes 2-cm apart along the side of the tube are designed to

allow insertion of the modified 3-cc syringe shown also in Figure 6.3, and obtain a sample large enough to measure the, solids content by the standard procedure. These holes are sealed with rubber plugs during the test. Depending on the current height of the model, four to six solids content points can be obtained, from each sub-sample.

Three of these samples can be accommodated in a 14-cm acrylic bucket. Three of the four buckets in the centrifuge are used for this purpose, for a total of nine sub-samples. Each bucket is filled with water around the PVC samplers to reduce the possibility of slurry leakage. The fourth bucket is reserved for the master specimen used to monitor the specimen height and pore pressure distribution. Sub-samples can be obtained at any chosen time interval; a good sequence might be 1, 2, 4, 6, 8, 12, 24, 36, and 48 hours. Depending on the initial solids content the obtaining of a reasonably good solids content profile before 1 hour is very difficult, due to the diluteness of the material.

An obvious disadvantage of the direct measurement of the solids content distribution is that the centrifuge must be stopped to take the samples out. Of course, the time that the centrifuge is not spinning must be excluded from the total elapsed time of consolidation, with the starting and stopping time accounted for as explained below.

A BASIC program written for the HP-86B monitors the elapsed time of consolidation and reads the pressure transducers. A listing of the program is included in

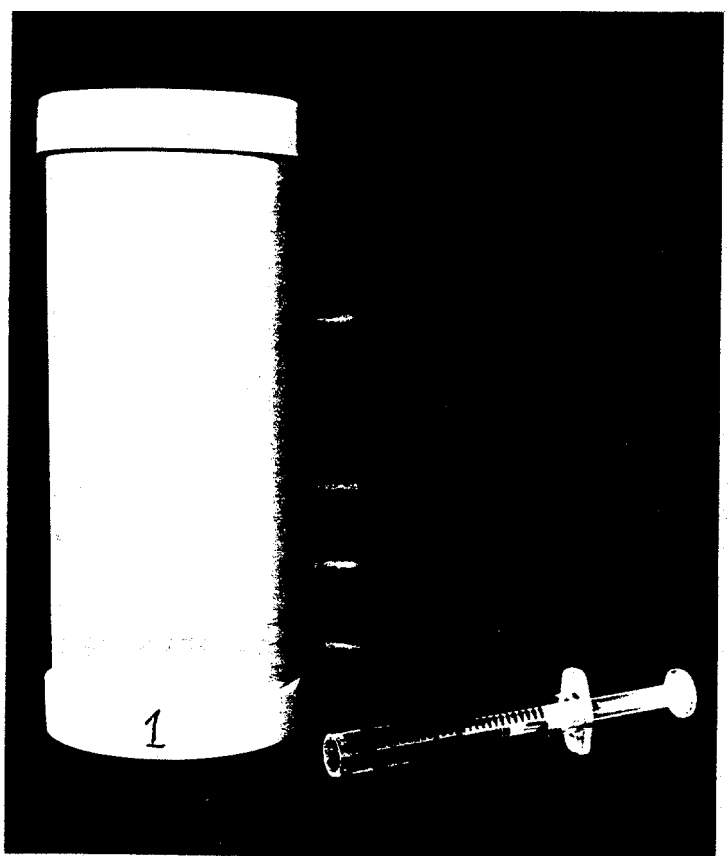

Figure 6.3 - Sampler for Solids Content Distribution

Appendix G. When the program is run, the user enters the general test information. Depending on the acceleration level entered, the program selects the appropriate zero readings for each one of the three transducers. These values were previously obtained from several runs using only water at the exact model height, and are give in Table 6-1. The corresponding calibration factors of the transducers are incorporated into the program. After printing the general test data and the headings for the excess pore pressure table, the program pauses to allow synchronization with the centrifuge.

When the centrifuge is started there is a start-up time before reaching the desired acceleration. Bloomquist et al. (1984) have shown that for consolidation, the elapsed time should begin to be measured at two-thirds of the start-up time. Considering that the start-up time is about two minutes, for simplicity the elapsed time of consolidation is recorded beginning one minute after starting the centrifuge.

With the program paused, the centrifuge is started at the same time the CONT key is pressed in the HP-86B. The program will then wait exactly one minute before setting the time counter equal to zero. To account for the stopping and re-starting time during the retrieval of each sample, it is further assumed that both stopping and start-up times are equal (Figure 6.4).

After the computer has taken the corresponding pore pressure readings, the user pauses the program and

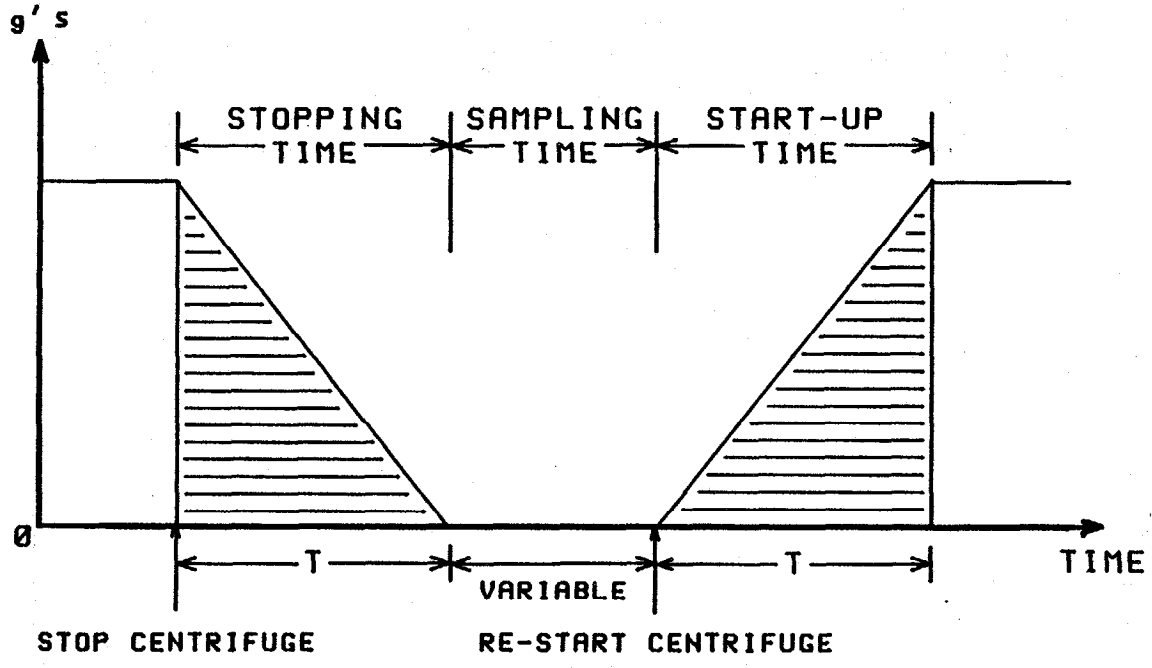

Figure 6.4 - Effect of Stopping and Re-starting Centrifuge

immediately stops the centrifuge. When spinning has fully ceased, the sample is removed and replaced with a dummy sampler with water to maintain proper balance of the centrifuge. Just before re-starting the centrifuge, the CONT key is pressed to continue the program. This approach assumes that not including the stopping time in the elapsed time is compensated by continuing the time count when the centrifuge is re-started, as shown in Figure 6.4.

The computer takesthe first readings of the transducers at 2, 4, 8, 15, 30, and 60 minutes, time when the first solids content sample is obtained. After that, a set of readings is taken every hour. These readings and the corresponding time are printed out in a table form. A disk file of these data is not kept since the data reduction is not done with the HP computer, but using a FORTRAN program written for a DOS-based PC, as described in the next section.

Method of Data Reduction

Analysis of the centrifuge data in order to obtain the constitutive relationships of the slurry is based on updated Lagrangian coordinates. The use of this coordinate system is necessary since the computations of permeability are based on the displacement of material points in the specimen. In general terms, the approach can be explained as follows. The model is divided into a number of equal thickness elements (10-20), and the reduced coordinates of their

boundaries, refered to here as material nodes, are calculated. When a new distribution of void ratio is obtained from each sample, the updated Lagrangian coordinate of each material node can be computed from its known (constant) reduced coordinate. By keeping track of the location of each material node in this way, and using the measured pore pressure distribution, it is possible to compute the effective stress and the coefficient of permeability at each point. This involves the use of the effective stress principle, the generalized Darcy's law, and the principle of continuity.

A key element in the approach to be followed is the relationship between convective and reduced or material coordinates (Cargill, 1982). The convective coordinate is the "real" distance from a reference point, say the bottom of the specimen, to the point under consideration. The material coordinate, on the other hand, is a measure of the volume of solids that exists up to that point. If x denotes the convective coordinate of a point in the sample, and z is the corresponding material coordinate, then they must be related by the following relation.

$$\frac{dx}{dz} = 1 + e \tag{6.1}$$

The material height of the specimen is readily obtained by integrating equation 6.1, considering that the initial void ratio is constant. This is,

$$z_t = \frac{h_i}{1 + e_i} \tag{6.2}$$

where h_i is the initial height, and ei is the initial void ratio. If the model is to be divided in N elements, then the material thickness of each element is simply

$$\Delta z = z_t/N \tag{6.3}$$

and the reduced coordinate of each one of the material nodes or boundaries between these elements is

$$z_i = (i - 1)\ \Delta z \tag{6.4}$$

for i = 1 to (N+1). Of course, the material coordinate of the first node (i = 1) is zero, and that of the node at the surface (i= N+1) is z_t. It is important to bear in mind that these material coordinates are time-independent, i.e. the material position of each node does not change throughout the consolidation process.

The buoyant stress at each material node is also time-independent. At node i this can be easily computed, assuming a constant acceleration field, as

$$\sigma_{bi} = n(G_s-1)(z_t-z_i)\gamma_w \tag{6.5}$$

where n is the acceleration of the centrifuge in g's, G_s is specific gravity of the solids, and γ_w is the unit weight of water.

At time t,a discrete distribution of void ratio with depth is obtained from a sample taken out of the centrifuge, as shown in Figure 6.5a. It is assumed that a straight line connects the points where the void ratio is known. In the diagram, the distance x_j represents the convective coordinate of the jth point and h is the current model height. The number of points where the solids content is known is

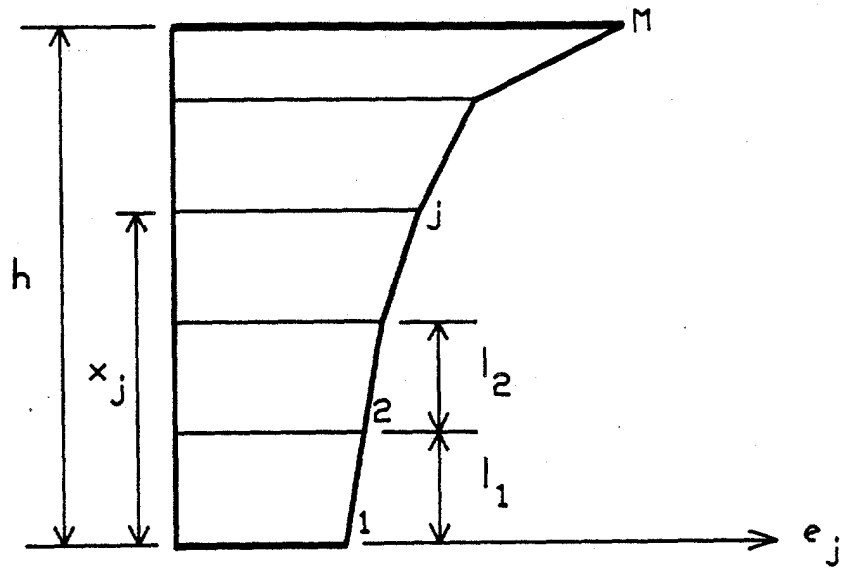

(a)

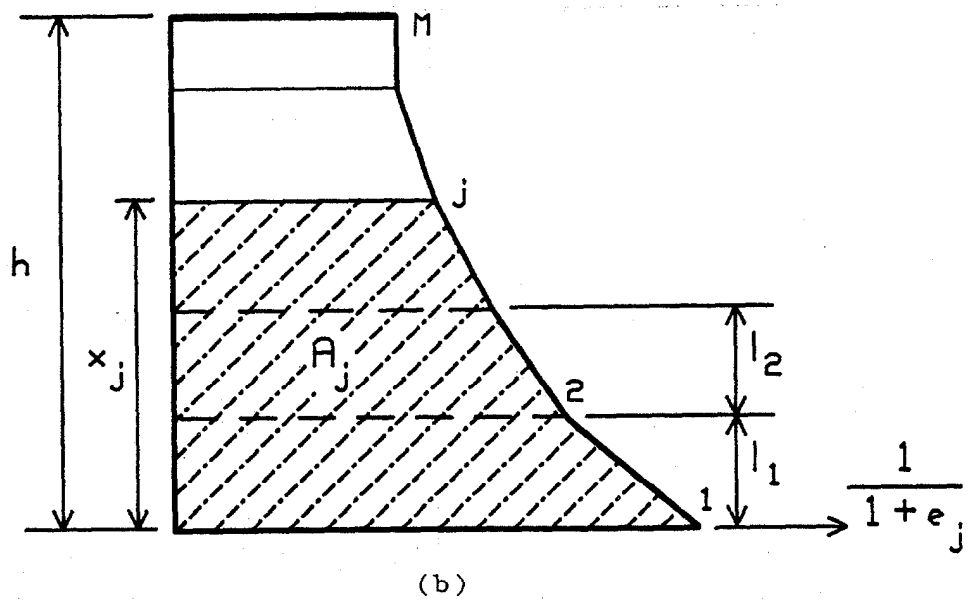

(b)

Figure 6.5 - Variation of Void Ratio with Depth. a) Void Ratio Distribution; b) $(1+e)^{-1}$ Distribution

denoted by M, and the distance between two consecutive points is l_j (equal to 2 cm., except for the top segment).

The material or reduced coordinate of point j can be obtained integration Equation 6.1 as,

$$z_j = \int_0^{x_j} \frac{dx}{1 + e(x)} \tag{6.6}$$

where e(x) indicates that the void ratio is a known function of the convective coordinate x.

The integral of Equation 6.6 is nothing more than the area under the curve of the inverse of (1 + e) versus x, schematized in Figure 6.5b. Assuming straight lines between points, the area up to point jis easily obtained from simple geometry as

$$A_j = A_{j-1} + \tfrac{1}{2}[(1+e_j)^{-1} + (1+e_{j-1})^{-1}] \cdot l_{j-1} \tag{6.7}$$

for j = 2 to M, with $A_1 = 0$. In particular, the total area, A_M, represents the material height of that particular sample, which must be equal to the value obtained with Equation 6.2 assuming that the samples are exactly equal and that no errors exist in the sampling process or integration scheme. The value of A_M computed for each sample will be an indication of the accuracy of the approach.

A second objective for computing this areas is to locate the current position (updated Lagrangian coordinate) of each one of the material nodes, and whose material coordinate was computed with Equation 6.4. The first step is to identify in which region the node under consideration falls, by comparing its reduced coordinate to the areas

A_j's. For instance, if $A_2 < z_i < A_3$, then node i falls in the second region, i.e. between nodes 2 and 3. In general, let us say that $A_j < z_i < A_{j+1}$, as shown in Figure 6.6.

The updated Lagrangian coordinate of node i is

$$h_i = v + \sum_{k=1}^{j-1} l_k \qquad (6.8)$$

Thus, the problem reduces to evaluating the distance v in the region where the node under consideration falls. To achieve this goal, its reduce coordinate is expressed as

$$z_i = A_j + \tfrac{1}{2}[(1+e_j)^{-1} + ee]\cdot v \qquad (6.9)$$

The distance ee is a function of v, and is obtained by interpolating between points j and j+1; this is

$$ee = (1+e_j)^{-1} - v[(1+e_j)^{-1}-(1+e_{j+1})^{-1}]/l_j \qquad (6.10)$$

After substituting Equation 6.10 into Equation 6.9, and simplifying, the following quadratic equation in v is obtained.

$$[(1+e_j)^{-1}-(1+e_{j+1})^{-1}]v^2 - 2(1+e_j)^{-1}(v) + 2(z_i-A_j) = 0 \qquad (6.11)$$

Of the two real roots of this equation, one will not satisfy the condition that $0 < v < l_j$, and it is discarded. The other root is used in Equation 6.8 to obtain the new convective coordinate of node i. Although physically the coordinate z_i should fall between two areas A_j and A_{j+1}, the possibility of not finding the right root, or even obtaining imaginary roots, still exists if the void ratio distribution is not correct.

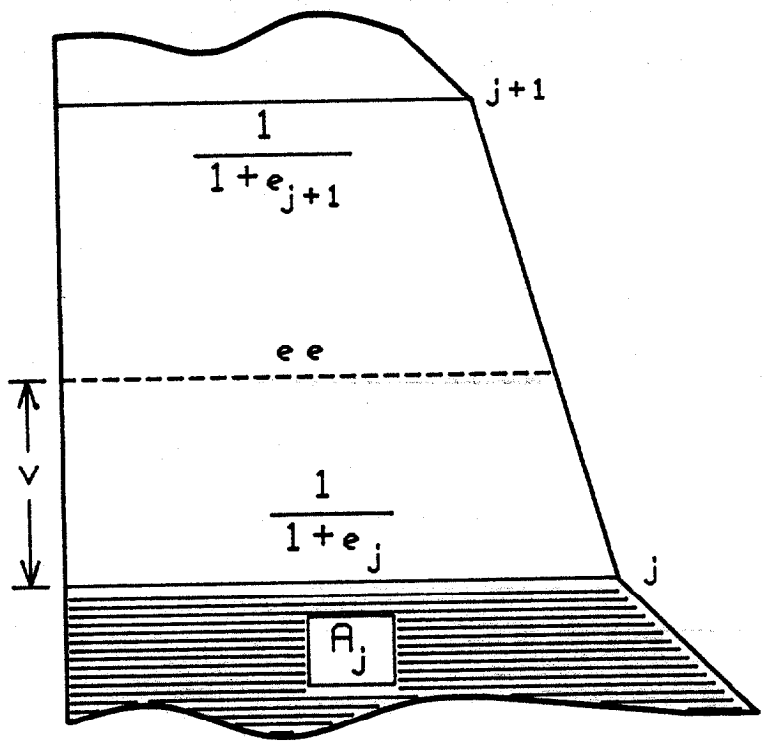

Figure 6.6 - Location of Material Node i

Once the distance v is determined, the void ratio at the node is obtained using Equation 6.10 and

$$e_i = 1/ee - 1 \qquad (6.12)$$

The procedure is repeated for each material node. Thus, at time t the new location of each node and its new void ratio would be known.

Next, the excess pore pressure and the hydraulic gradient at each node are obtained from the pore pressure distribution recorded at the time under consideration. An example of such a distribution is shown in Figure 6.7. For simplicity, a linear behavior is assumed between measured values of u.

Once the excess pore pressure at node i is determined, the corresponding effective stress is easily obtained using the effective stress principle. This is,

$$\sigma'_i = \sigma_{bi} - u_i \qquad (6.13)$$

with σ_{bi} computed from Equation 6.5. Thus, the void ratio and effective stress at each material node represent one point in the compressibility curve. With nine samples obtained at different times, the approach should yield a considerable number of points, including a wide range of effective stress. This apparent advantage may also lead to a problem, namely, the existence of a large scatter in the curve. Finally, it is worth mentioning that during the consolidation process several material nodes will reach the same void ratio levels in different times and, hopefully, at the same effective stresses.

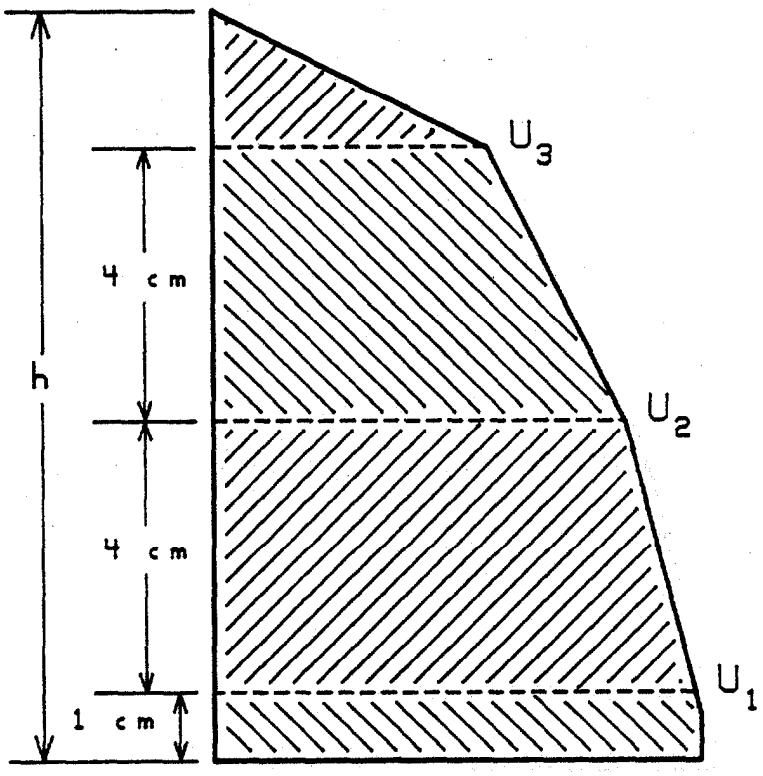

Figure 6.7 - Excess Pore Pressure Distribution

The next objective of the test is to determine the permeability relationship. For a sample taken from the centrifuge at time t, the void ratio at each material node has already been determined as previously explained. The determination of the coefficient of permeability is then based on equation 4.24, repeated here for convenience.

$$v_s = k \cdot i \tag{6.14}$$

The hydraulic gradient at time t has been already obtained for each node from the recorded pore pressure distribution. However, the instant solids velocity at that precise moment is not known. Nevertheless, an estimate of this can be obtained from the change in convective position of the nodes. For node i this is

$$v_{si} = \frac{h_i(t-\Delta t) - h_i(t)}{\Delta t} \tag{6.15}$$

where Δt is the time interval between samples taken, hi (t) is the convective coordinate of node at time t, and $h_i(t-\Delta t)$ is the value at time $t-\Delta t$. This mean solids velocity will approach the instant value if the time interval is small enough.

Thus the coefficient of permeability for node i, at time t, is obtained from Equations 6.14 and 6.15 as

$$k_i(t) = \frac{v_{si}(t)}{i_i} \tag{6.16}$$

A new set of pore pressure and void ratio readings obtained at time $t+\Delta t$ will allow determination of new values of the coefficient of permeability for each material node. As for the compressibility relationship, this approach would

yield a large number of data points, but considerable scatter. may exist in the results.

The determination of theconstitutive relationships by the numerical analysis described above requires a considerable number of repetitive calculations in time and space. Therefore, it was necessary to write a FORTRAN program to handle this data reduction. Appendix H presents a listing of this program.

CHAPTER VII
CENTRIFUGE TESTING RESULTS

Testing Program

A total of five centrifuge tests were performed to implement the numerical analysis presented in Chapter VI for determining the effective stress-void ratio-permeability relationships, or for other complementary analyses. The material used in the tests was the same as used in the slurry consolidometer testing program, namely Kingsford waste clay. The index properties of this material were given in Chapter V.

Table 7-l summarizes the conditions of the tests conducted. The specific purpose of each test is included in the table for ease of future reference, as well as a listing of the necessary data obtained in the test.

Table 7-1. Centrifuge Testing Program

Test No.	Acceleration (g's)	h_i (cm)	S_i (%)	Data Obtained	Purpose of the Test
CT-1	80	12.0	15.72	h,u,S	σ'-e-k
CT-2	60	12.0	16.05	h,u,S	Ú'-e-k, M/M
CT-3	80	9.0	16.02	h	M/M
CT-4	60	11.0	16.04	h,u	Surcharge
CT-5	80	11.0	15.95	h,u	Surcharge

The first two tests, CT-1 and CT-2, were the only two tests where the specimen height, pore pressure, and solids content were monitored, in order to obtain the constitutive relationships of the slurry according to the approach presented in Chapter VI. Tests CT-2 (60g) and CT-3 (80g) were used for a modelling of models (M/M); only the specimen height was monitored in test CT-3.

After observing an unexpected behavior in the pore pressure profiles of tests CT-1 and CT-2, and suspecting the possibility of radial drainage in the specimens, tests CT-4 and CT-5 were designed to apply a surcharge load. The main objective of these tests was to observe the behavior of the pore pressure distribution for comparison with the profiles observed in tests CT-1 and CT-2.

Determination of Constitutive Relationships

Two tests were conducted with measurements of pore pressure and solids content, thus making it possible to obtain the constitutive relationships of the material. The first test, CT-1, was performed at 80 g's, with a specimen initial height of 12 cm and initial solids content of 15.72%. Photographic monitoring of the specimen height was done following the standard UF procedure. The test duration was 38 hours, and the final model height was 5.95 cm.

To obtain the void ratio profiles, the sampling operation described in Chapter VI was performed at times of 1, 2, 4, 8, 12, 22, and 38 hours, for a total of 7 sub-samples.

These sub-samples provide a second measurement of the specimen height at the corresponding time. Figure 7.1 presents the height-log time relationship for test CT-1 obtained from both the photographs and the sub-samples. The agreement between the two methods is very good.

However, the main objective of the sampling operation is the determination of the solids content with depth. Six solids content points were obtained at times 1 and 2 hours, five points at times 4, 8 and 12 hours, and only four points at times 22 and 38 hours. These samples, obtained with the mini-piston sampler, weigh in the order of 5 grams including the tare. Once oven-dried, the specimens weigh only around 2 grams. Thus an accurate weight determination is critical. A 0.01 gram sensitivity electronic balance was used for this purpose.

Figure 7.2 presents the solids content profiles for test CT-1 obtained at various times. It is important to notice that for the first two or three profiles, the solids content is larger near the surface, then decreases substantially with depth, and finally increases at the bottom of the specimen. This behavior is not expected in a self-weight one-dimensional consolidation process, and leads to the first suspicions that something different is occurring. Toward the end of the test the solids content distribution behaved in a more expected way, specifically the solids content increases with depth.

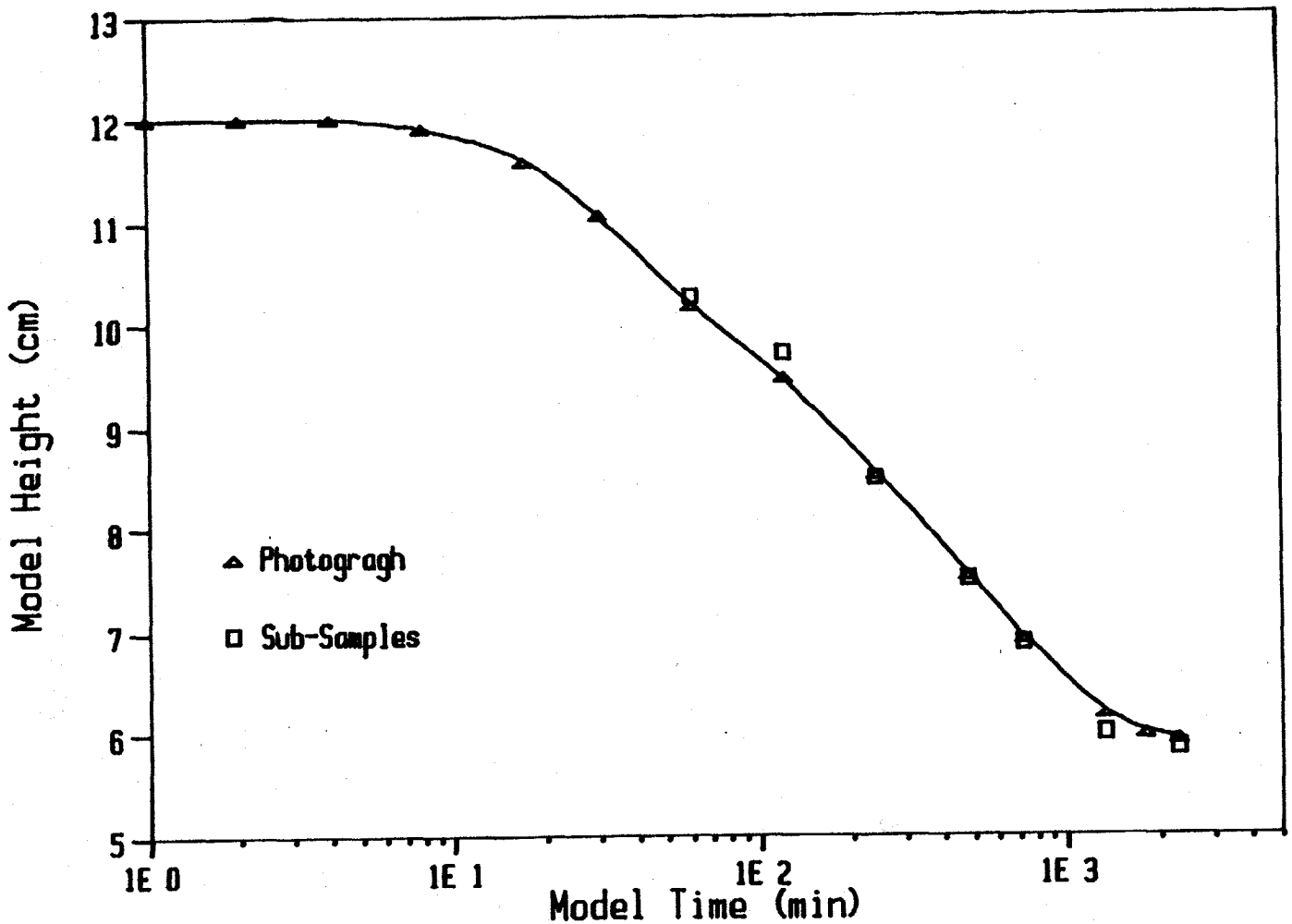

Figure 7.1 - Height-Time Relationship for Test CT-1

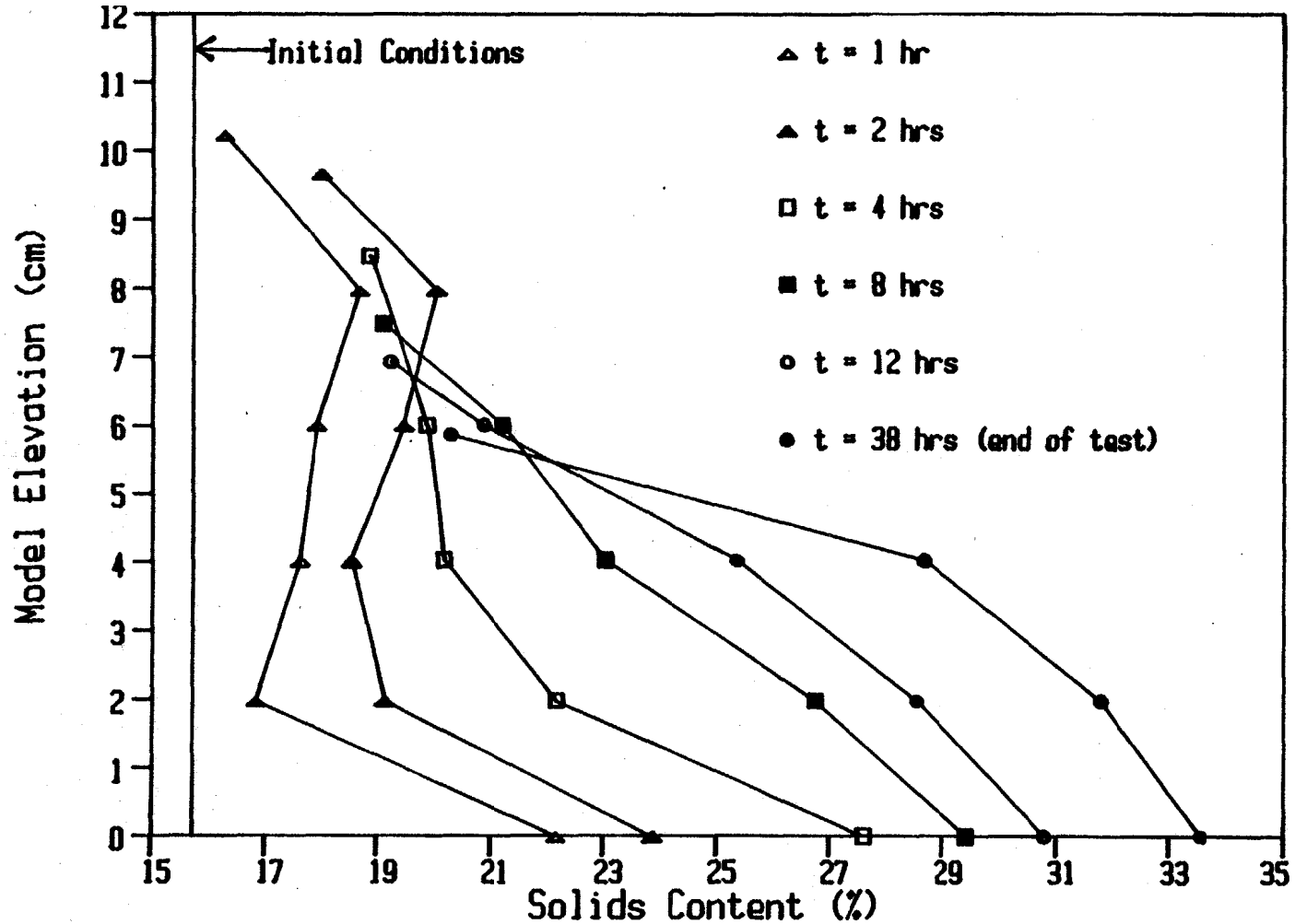

Figure 7.2 - Solids Content Profiles for Test CT-1

Monitoring of the excess pore pressure is accomplished through the computer/data acquisition system. For the first hour of the test, the monitoring program takes transducer readings at 2, 4, 8, 15, 30, and 60 minutes; afterwards, a set of readings is taken every hour.

An aspect of the test which affects the excess pore pressure evaluation is the evaporation of supernatant water. The zero readings of the pressure transducers were obtained with water in the container at the exact specimen height, thus representing hydrostatic pore pressure. As supernatant water evaporates during the test, the hydrostatic pore pressure decreases (however, the buoyant stress does not change). Since the excess pore pressures are computed every time from the same pre-recorded zero readings, there will be an error in them equal to the variation in hydrostatic pore pressure. This effect is depicted in Figure 7.3. An estimate of the correction for evaporation can be obtained from the readings of the top transducer (No. 3), once this is above the slurry-supernatant interface.

In the case of test CT-1, the time at which the specimen height reaches the top transducer (h = 9 cm.) is readily obtained from Figure 7.1 as 163 minutes. After this moment, transducer No.3 should theoretically read zero (hydrostatic) pressure. Instead, it reads increasingly higher negative values. At the end of the test, transducer No. 3 recorded a pressure of -1.875 psi. Examination of the specimen indicated that 1.6 cm of supernatant water had

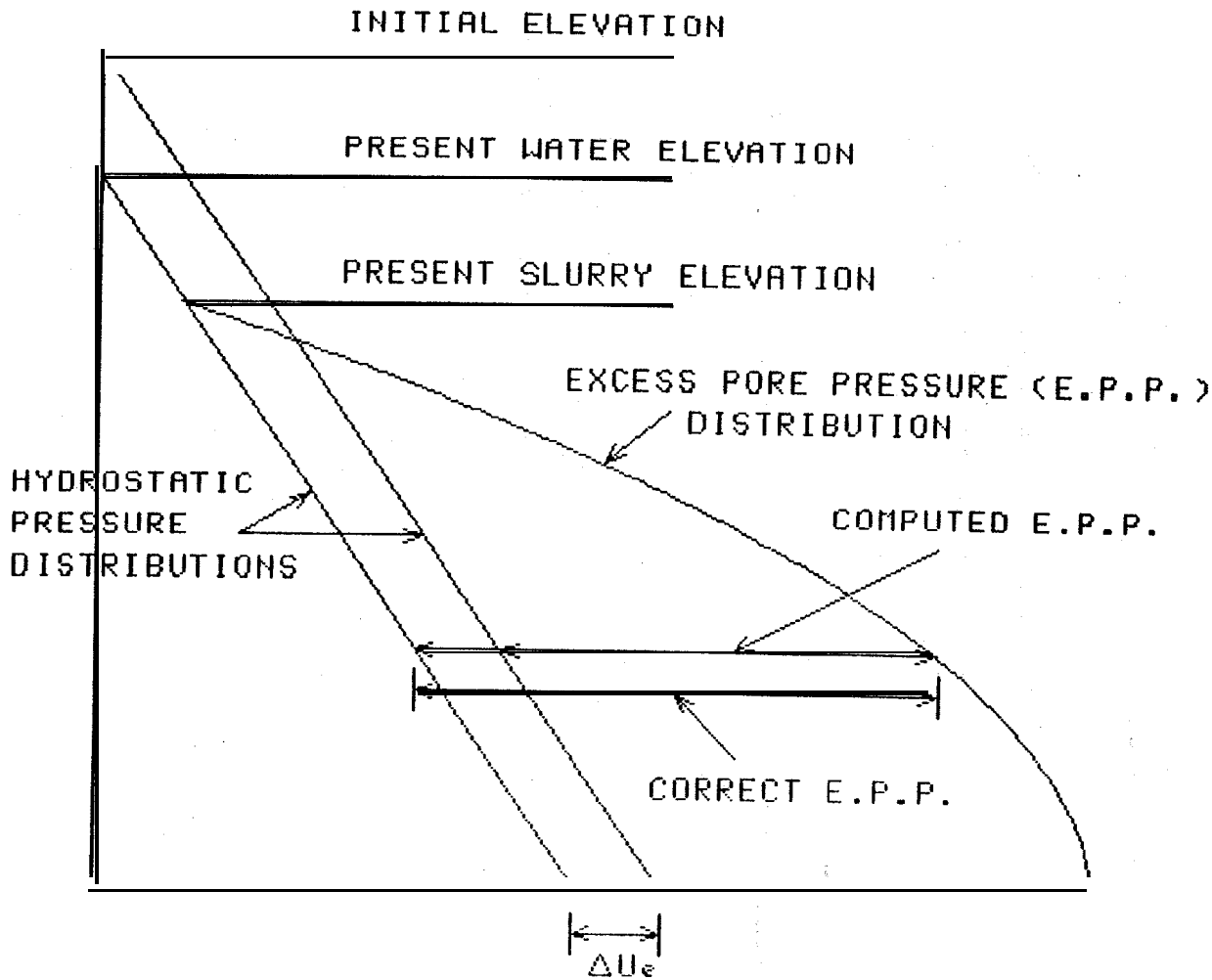

Figure 7.3 - Evaporation Effect on Excess Pore Pressure

evaporated during the test. At 80 g's, this loss of water represents a decrease in hydrostatic pressure of about 1.8 psi, which is in good agreement with the value recorded by the transducer.

The absolute value of the pressures recorded at transducer No. 3 from t = 180 minutes to the end of the test are plotted versus time in Figure 7.4. A linear correlation, indicating a constant rate of water evaporation, is clearly observed in the figure. A linear regression analysis led to the following expression for the correction for evaporation in test CT-l,

$$\Delta u_e = -0.0254 + (8.453E\text{-}04) \cdot t \qquad (7.1)$$

where t is the elapsed time of test in minutes. The zero-intercept of this equationis not zero as expected, but the error is considered minor. The correlation coefficient found in the analysis was 0.999.

Because of the very high correlation coefficient, i.e. good agreement between experimental readings and best fit line, it was decided to simply use the negative of the pressure recorded at transducer No. 3 as the correction for evaporation after t = 163 min. The correction was added to the excess pore pressures computed by the monitoring program to obtain the correct values. The corrected excess pore pressures at the location of the three transducers are plotted versus time in Figure 7.5. The curves show the expected pressure dissipation. Only the readings at 8 and 15 minutes seem to be off, with readings that are abnormally

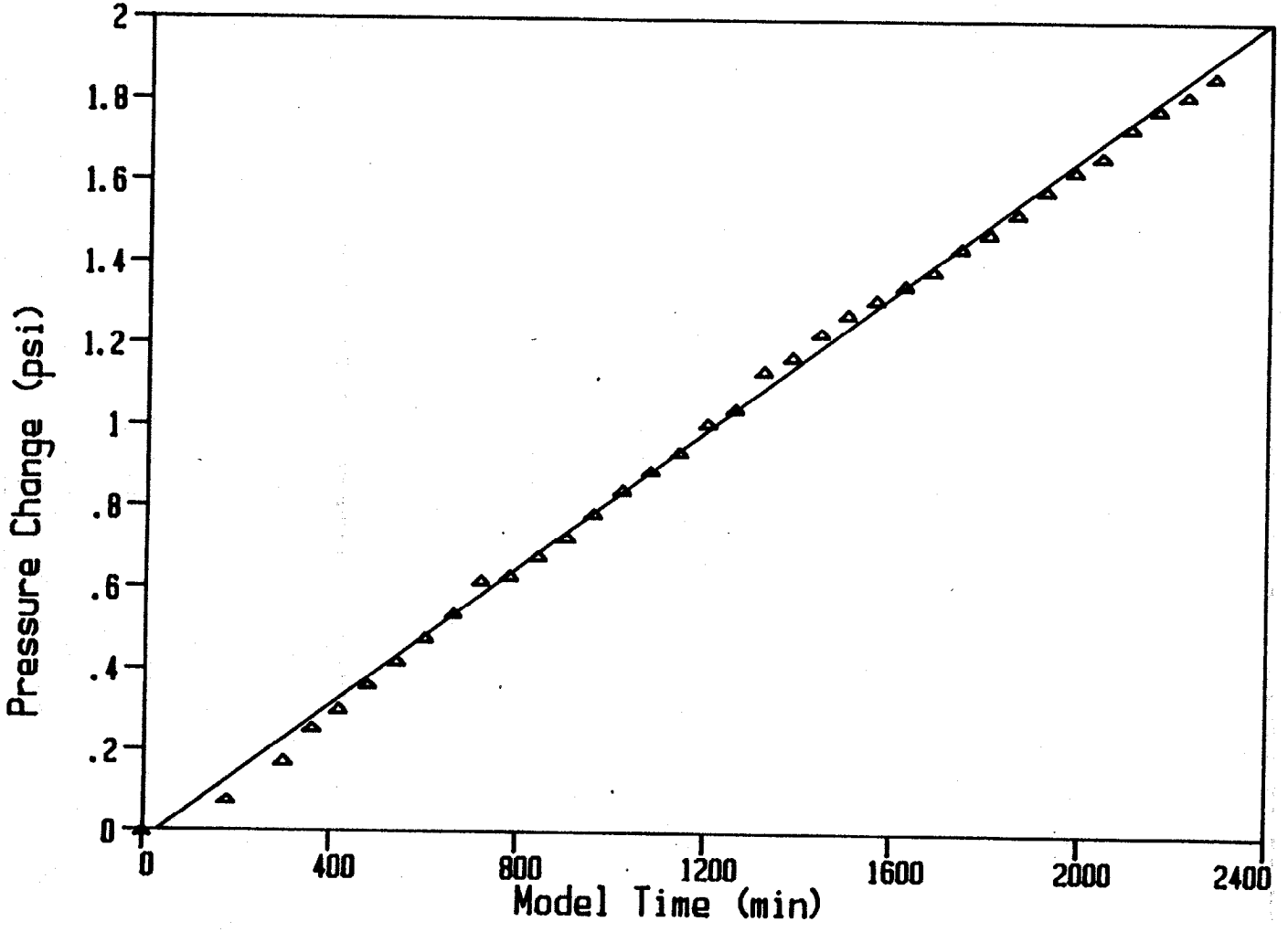

Figure 7.4 - Evaporation Correction for Test CT-1

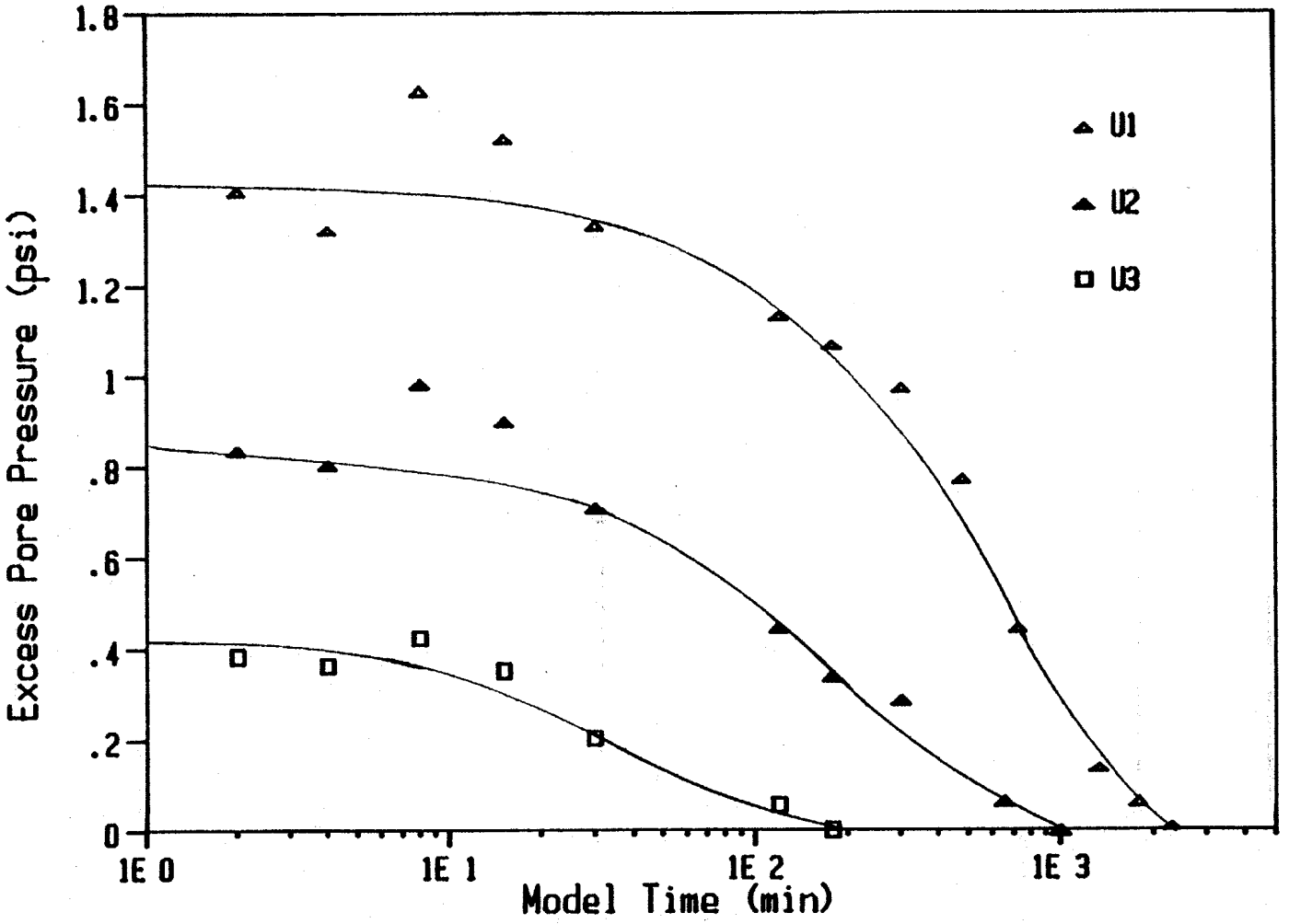

Figure 7.5 - Pore Pressure with Time for Test CT-1

high in all three transducers. An explanation for this result has not been found.

The excess pore pressure profiles at several times are plotted in Figure 7.6. The initial buoyant stress distribution is also shown in the figure. The excellent overlapping between this and the excess pore pressure curve for t = 2 minutes leads to a very definite and important conclusion, namely that the effective stresses are initially zero throughout the specimen. This result immediately implies that the power curve of equation 4.31 can not represent properly the compressibility of the slurry.

As time progresses, the excess pore pressure profiles exhibit a very peculiar and interesting behavior. The pressure at transducer No. 2 (elevation 5 cm.) dissipates at a rate so fast that the pore pressure profile soon shows a curvature oppose to that expected. An extreme example of this trend is observed at t = 12 hours, when the specimen height is about 7 cm. Nevertheless, transducer No. 2 registers zero pressure, thus implying that the top 2 centimeters of the specimen are under hydrostatic conditions.

At first instance, this pore pressure response seemed impossible to explain. To eliminate the possibility of erroneous transducer readings, other complementary tests were conducted, even switching transducer positions. These tests confirmed that the response of the transducers was reflecting a real process taking place in the specimen.

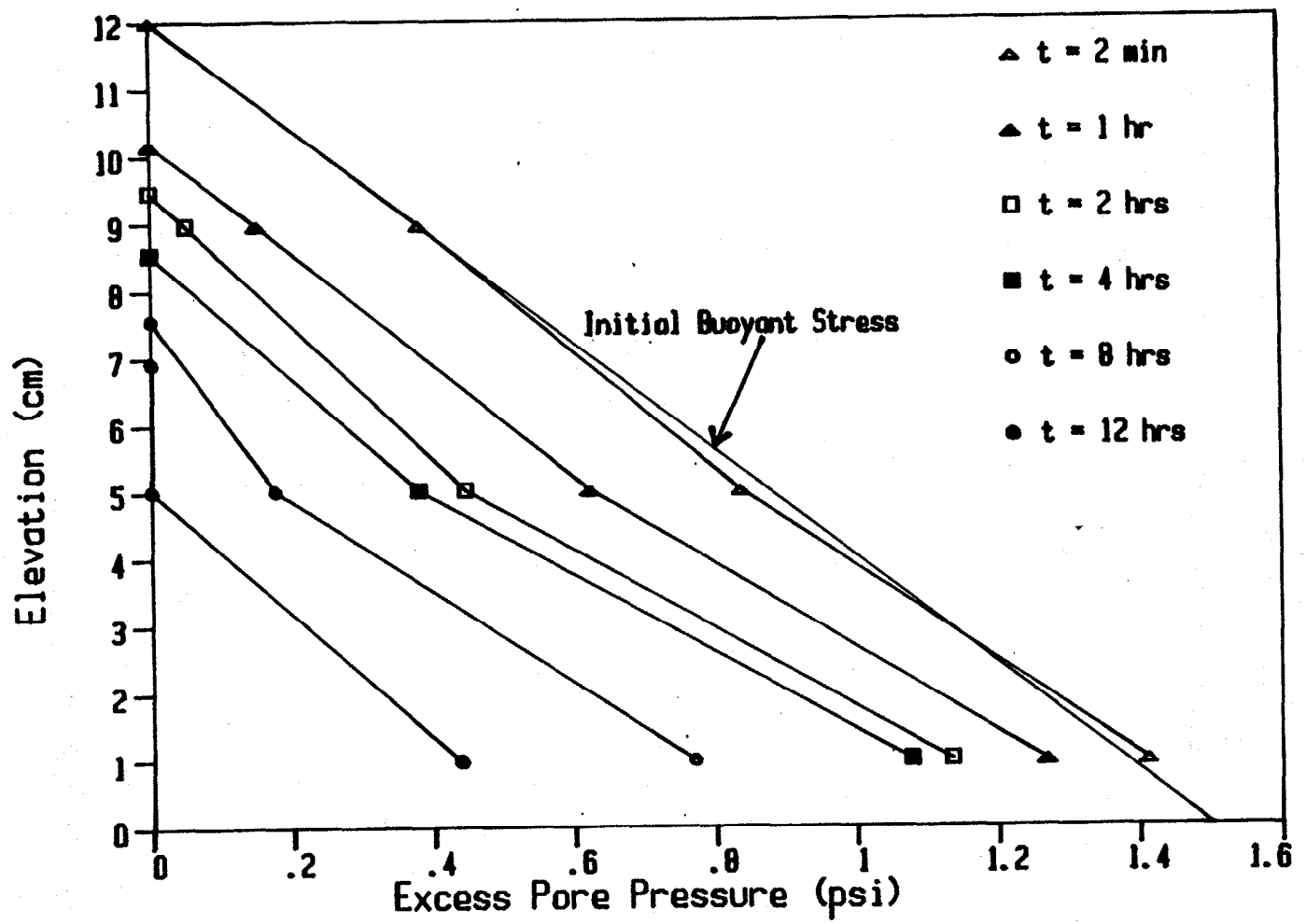

Figure 7.6 - Pore Pressure Profiles for Test CT-1

To explain this strange pore pressure behavior it is necessary to start by realizing that the transducers are recording the excess pore pressure along the walls of the acrylic container. As a result of the specimen deformation, the relative movement of the slurry with respect to the bucket walls apparently produces a shearing zone where the confining horizontal stress is small and the permeability is relatively higher; this effect, of course, diminishes with depth. Thus, it is believed that the initial excess pore pressures, generated by the buoyant weight of the slurry, dissipate faster along the bucket-slurry boundary than at the center of the specimen.

As a consequence. of the above statement, radial drainage will be taking place, at least in the upper part of the specimen, speeding up the process of consolidation. This conclusion is consistent with the results shown in Figure 7.2, where the solids content increased faster near the surface. Additionally, there is clear visual evidence that at the end of the test a gap exists between the bucket walls and the upper part of the specimen.

If the above reasoning is correct, then a major problem arises, namely that the process taking place in the centrifuge is not one-dimensional consolidation. Later in this chapter, additional evidence of the possibility of radial drainage will be presented, as well as the implications on modelling of models and the time scaling exponent.

Nevertheless, the data collected in the test will be used in the numerical approach to obtain the constitutive relations.

If the hypothesis of radial gradient is correct, it becomes imperative to determine the excess pore pressure distribution at the center of the specimen. Unfortunately, placing transducers at the axis of the model is not an easy task. Consequently, an approximation was made. It was assumed that the excess pore pressure profile along the axis of the specimen was parabolic, and that the value recorded at transducer No.1 (elevation 1 cm) represents also the value at the center of the specimen. This last assumption is justifiable by realizing that the conditions that may produce radial drainage near the surface of the specimen disappear near the bottom.

Knowing the values of the excess pore pressure at the elevation of 1 cm and at the top of the specimen, and the gradient at the bottom, an expression for the excess pore pressure at any elevation, y, is readily obtained as

$$u = - \frac{u_1}{(h^2-1)} y^2 + \frac{h^2}{(h^2-1)} u_1 \qquad (7.2)$$

where u_1 is the excess pore pressure at transducer No. 1, and h is the current height of the specimen in centimeters.

Figure 7.7 shows, as an example, the assumed parabolic distribution for t = 2 hours, along with the excess pore pressures recorded at the transducers at the same time. In order to idealize a pseudo-one-dimensional situation and have the opportunity of using the method proposed in Chapter

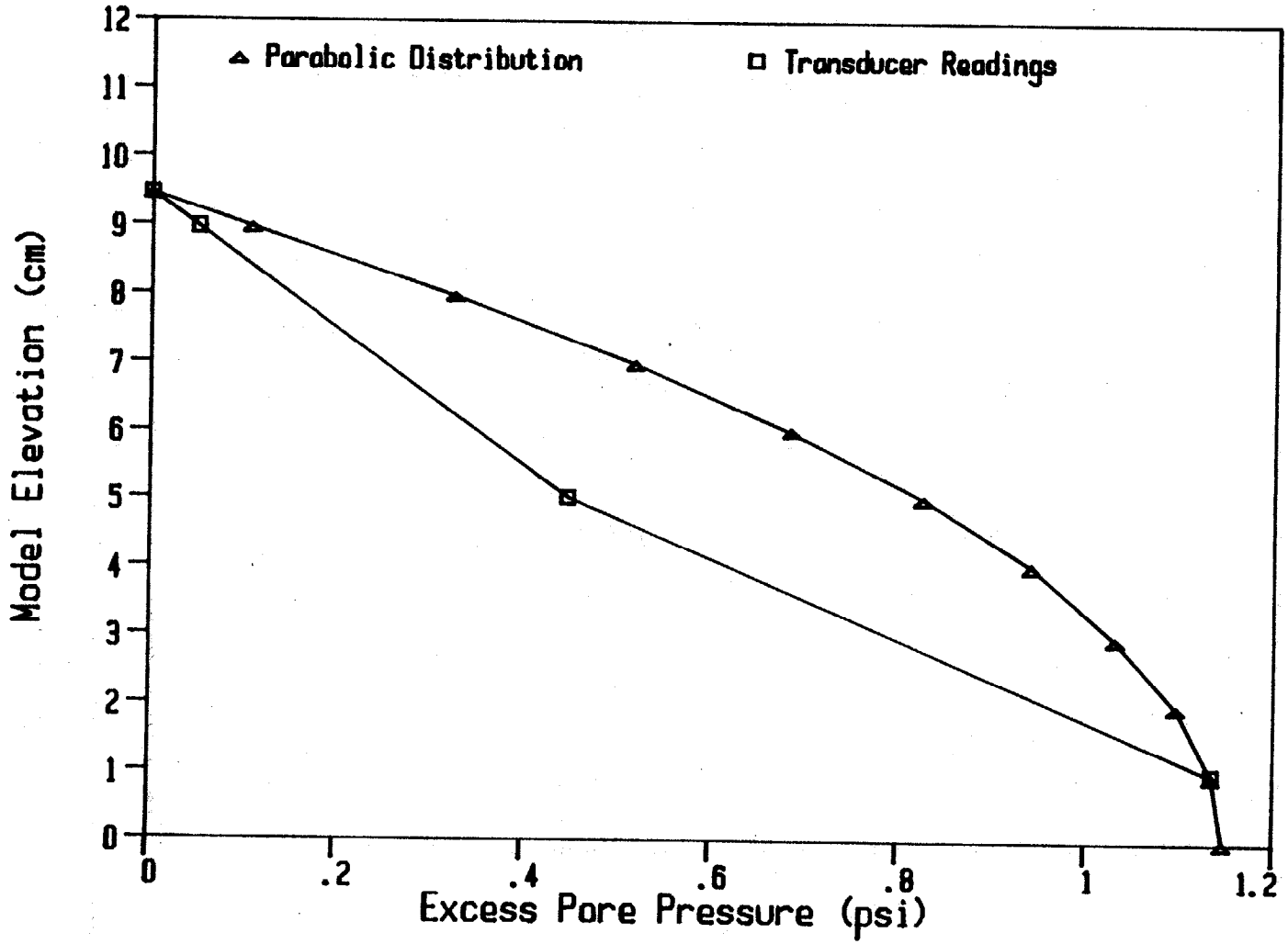

Figure 7.7 - Parabolic Excess Pore Pressure Distribution at t = 2 hours for Test CT-1

VI, a rather crude but quite logical approach was followed. The excess pore pressure and hydraulic gradient required in the analysis were obtained as the average of the values obtained with the recorded distribution at the boundary and the assumed distribution at the center of the specimen. The data reduction program listed in Appendix H was modified accordingly to incorporate this approach. It was expected that the approximation would, at least, provide a range wherein the actual constitutive relationships exist.

Following this approach, the computer program was run with the data collected in the test. In the analysis the specimen was divided into 10 layers. A printout of the output is included in Appendix H. The general test information, initial conditions, and the results of the analysis for the first time increment analyzed (1 hour) are reproduced in Table 7-2. Several points of the program output are worth highlighting.

The reduced height of the specimen computed from the initial height and void ratio is 0.772 cm. The solids content profiles obtained from the sub-samples allow computing a new value of this height, as explained in Chapter VI. Comparison of these values with the initial value provides an evaluation of the quality of the sampling process. For the first sub-sample, for instance, the reduced height of the specimen is computed as 0.768 cm, an agreement with the initial value of 0.772 cm that is excellent considering the difficulties associated with

Table 7-2. Partial Output of the Analysis of Test CT-1

*** Centrifuge Test CT-1 ***
Acceleration level = 80. g

Initial Height = 12.0 cm

Solids Content = 15.72% Void Ratio = 14.535

Number of Layers = 10

Reduced Height of the Specimen = 0.772 cm

Initial Conditions
Theoretical Gradient = 0.110

NODE	H(I)	Z(I)	BUOY.ST.	EXC.P.P.	EFF.STR.	GRADIENT
11	12.0000	0.7725	0.0000	0.0000	0.0000	0.1119
10	10.8000	0.6952	0.1502	0.1527	-0.0024	0.1119
9	9.6000	0.6180	0.3005	0.3054	-0.0049	0.1119
8	8.4000	0.5407	0.4507	0.4501	0.0006	0.1002
7	7.2000	0.4635	0.6009	0.5869	0.0140	0.1002
6	6.0000	0.3862	0.7512	0.7237	0.0275	0.1002
5	4.8000	0.3090	0.9014	0.8664	0.0350	0.1262
4	3.6000	0.2317	1.0516	1.0386	0.0130	0.1262
3	2.4000	0.1545	1.2019	1.2109	-0.0090	0.1262
2	1.2000	0.0772	1.3521	1.3831	-0.0310	0.1262
1	0.0000	0.0000	1.5024	1.5553	-0.0530	0.1262

New Time = 60.0 min New Height = 10.20 cm
New Reduced Height of the Specimen = 0.768 cm

U(I) = 1.266 0.624 0.152 psi
S(J) = 22.19 16.86 17.65 18.68 16.29 %

NODE	H	e	u	Eff.Str.	i	Vs	k (ft/day)
11	10.263	13.998	-0.012	0.012	0.167	0.4824E-03	0.1228E+00
10	9.152	12.830	0.191	-0.041	0.155	0.4578E-03	0.1218E+00
9	8.121	11.898	0.362	-0.061	0.140	0.4109E-03	0.1158E+00
8	7.123	12.050	0.514	-0.063	0.129	0.3546E-03	0.1097E+00
7	6.104	12.356	0.657	-0.056	0.118	0.3046E-03	0.9899E-01
6	5.065	12.506	0.790	-0.038	0.107	0.2596E-03	0.8895E-01
5	4.017	12.642	0.931	-0.029	0.114	0.2175E-03	0.6419E-01
4	2.949	13.013	1.062	-0.011	0.102	0.1808E-03	0.5605E-01
3	1.853	12.987	1.183	0.019	0.091	0.1518E-03	0.4963E-01
2	0.861	10.877	1.279	0.073	0.080	0.9413E-04	0.3237E-01
1	0.000	9.503	1.352	0.150	0.071	0.0000E+00	0.0000E+00

obtaining the solids content profile. For the other sub-samples, the reduced height of the specimen ranges between 0.776 and 0.792 cm.

Additionally, the measured solids content profile is verified by comparing the computed model height and the photographic value. For t = 60 minutes, for instance, the photograph reveals a model height of 10.20 cm, while the computed value is 10.26 cm, which represents an excellent agreement. In other cases, however, the discrepancy is somewhat larger.

Since the excess pore pressures are not known at t = 0, the values used by the program as an approximation to obtain the initial conditions correspond to those at t = 2 min. A phenomenon already addressed is observed in the Table 7-2 column of initial effective stress; all the values (negative or positive) are small enough to be considered zero for all practical purposes. These results corroborate the conclusion of zero initial effective stresses. Additionally, the theoretical initial gradient of 0.11, due to the buoyant weight, compares well with the values computed from the pore pressures recorded at 2 minutes.

For every time analyzed, the analysis provides a total of eleven points, with information on location of the point, its void ratio, excess pore pressure, effective stress, hydraulic gradient, solids velocity, and coefficient of permeability. At t = 60 minutes, the results shown in Table 7-2 indicate that the effective stresses in the specimen are

still negligible, except at the very bottom. As time progresses, the effective stress front moves upward as can be seen in the complete output printout of Appendix H.

Of the 11 points obtained for each time analyzed, the one at the surface always has zero effective stress (very small values are computed). However, its void ratio does not remain constantly equal to the initial value, but instead tends to decrease. It is admitted that this is the location with the largest possibility of error in the solids content measurement; however, its proximity to the supernatant water makes it very likely that the error would be an underestimation of solids content (overestimating the void ratio). This tendency of the void ratio at the surface to decrease, regardless of the zero effective stress condition, has been observed in other studies (Been and Sills, 1981; Lin and Lohnes, 1984), but has not been explained.

Figure 7.8 presents the compressibility and permeability plots obtained from the analysis of test CT-1. Obviously, the compressibility graph (Figure 7.8a) does not include the surface point and those points where the effective stress is either negative or less than 0.01 psi, the minimum accurately measured value. The plot shows considerable scatter at void ratios above 9. This is largely the result of error in the determination of low solids content values. It is clear from the figure how all the points corresponding to different times converge to a unique curve. Moreover, each set of points for a given time

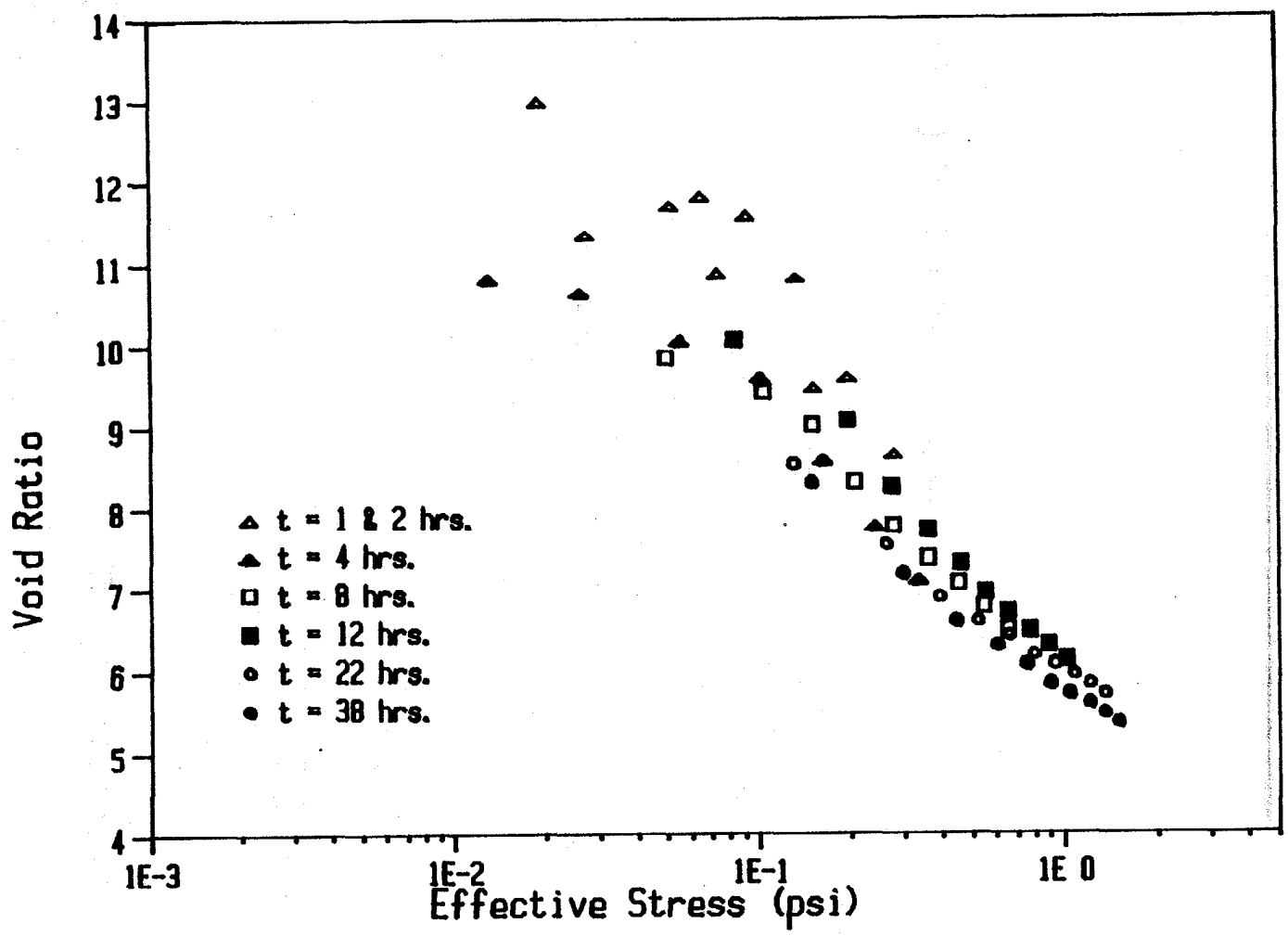

(a)

Figure 7.8 - Constitutive Relationships from Centrifuge Test CT-1.
a) Compressibility; b) Permeability

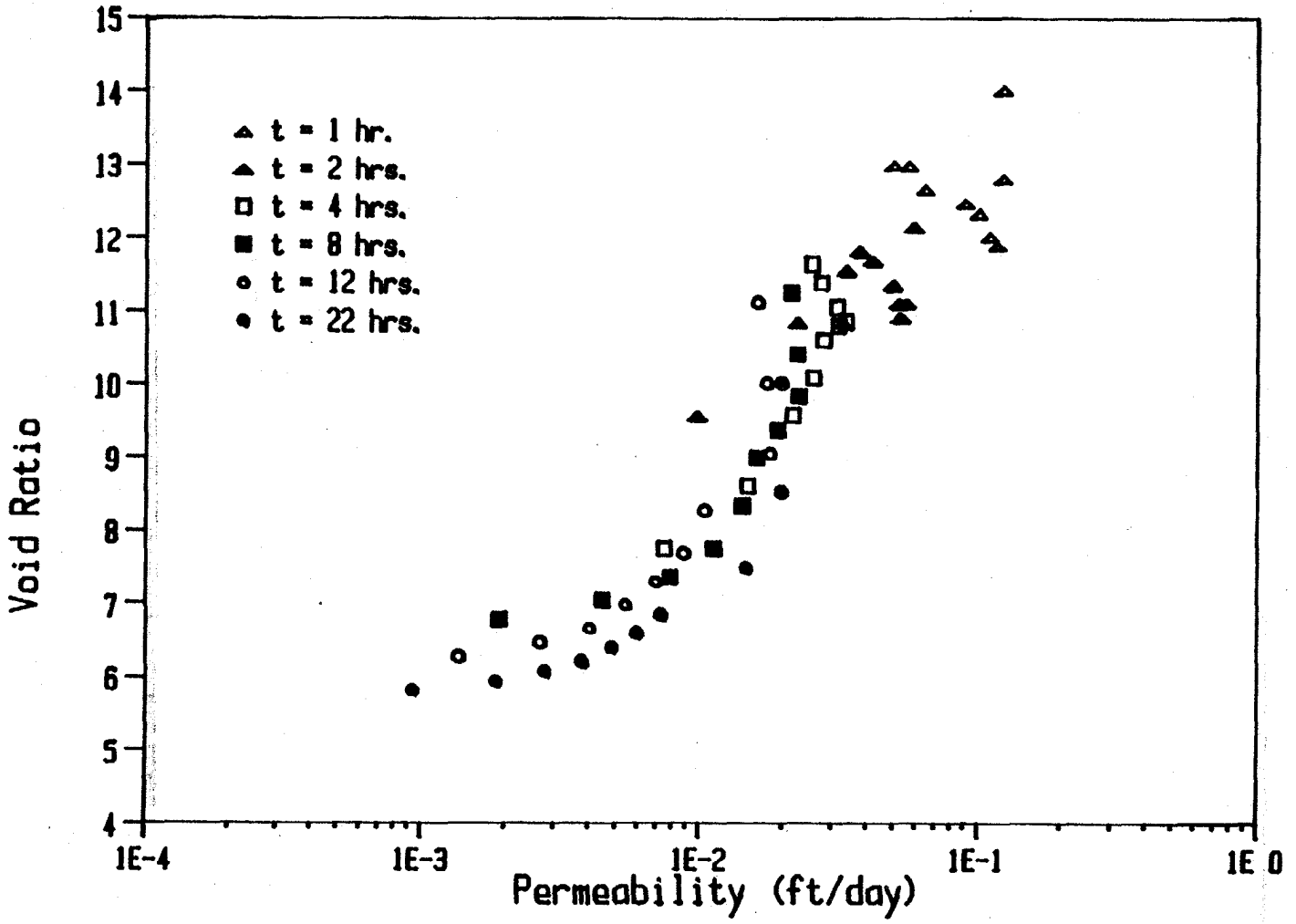

(b)

Figure 7.8--continued

clearly extends the curve produced by points from previous times.

Unfortunately, the plot of Figure 7.8a does not provide information on the first portion of the compressibility relationship (e > 12). In order to obtain this information, it would be necessary to obtain sub-samples earlier in the test and improve the sampling technique and accuracy of pore pressure measurement. Consequently, the preconsolidation effect observed in the results of CRD tests can not be corroborated with these test results.

In the case of the permeability graph (Figure 7.8b), the values calculated by the computer program correspond to the prototype coefficient of permeability, which is n (the centrifuge acceleration in g's) times smaller than the model permeability, as demonstrated in Appendix A. In the analysis, the bottom point of the specimen has zero solids velocity at any time, and therefore does not provide any permeability information. Similarly, all the points at the end of the test (t = 38 hours) are excluded from the permeability plot because the hydraulic gradient has been reduced to practically zero (0.001), and the computed coefficient of permeability is meaningless.

As in the case of the compressibility plot, the permeability graph of Figure 7.8b shows significant scatter. Nevertheless, the points define a definite trend. Although the preconsolidation effect is not fully observed, the curve seems to flatten at void ratios above 12.

The second centrifuge test, CT-2, was analyzed following the same procedure outlined for test CT-1. Test CT-2 was conducted under a normal centrifuge acceleration of 60 g's, versus 80 g's of test CT-1. The specimen initial height was also 12 cm, and the initial solids content was 16.05%. The test duration was 48 hours and the final model height was 6.0 cm.

Figure 7.9 shows the height-time curve obtained for test CT-2 from the photographs and from direct observation of the sub-samples obtained at times 1, 2, 4, 8, 12, 24, 35, and 48 hours. The agreement is good, but the sub-sample heights are slightly larger due to side effects.

The solids content profiles obtained from the sub-samples at various times are plotted in Figure 7.10. The first three profiles show solids content at the surface which are lower than the initial value; this absurd result is easily explained by the high degree of wetness left on the surface by the supernatant water. The initial solids content was used for this point in the numerical analysis.

The same behavior observed in test CT-1, where the solids content increases relatively faster near the surface, is also clear in test CT-2. Later in the test, the solids content profile behaves as expected, except that at the surface the solids content increases above the initial value. At the end of the test, two sub-samples were obtained for verification. The agreement between the solids content profiles of the two sub-samples was very good.

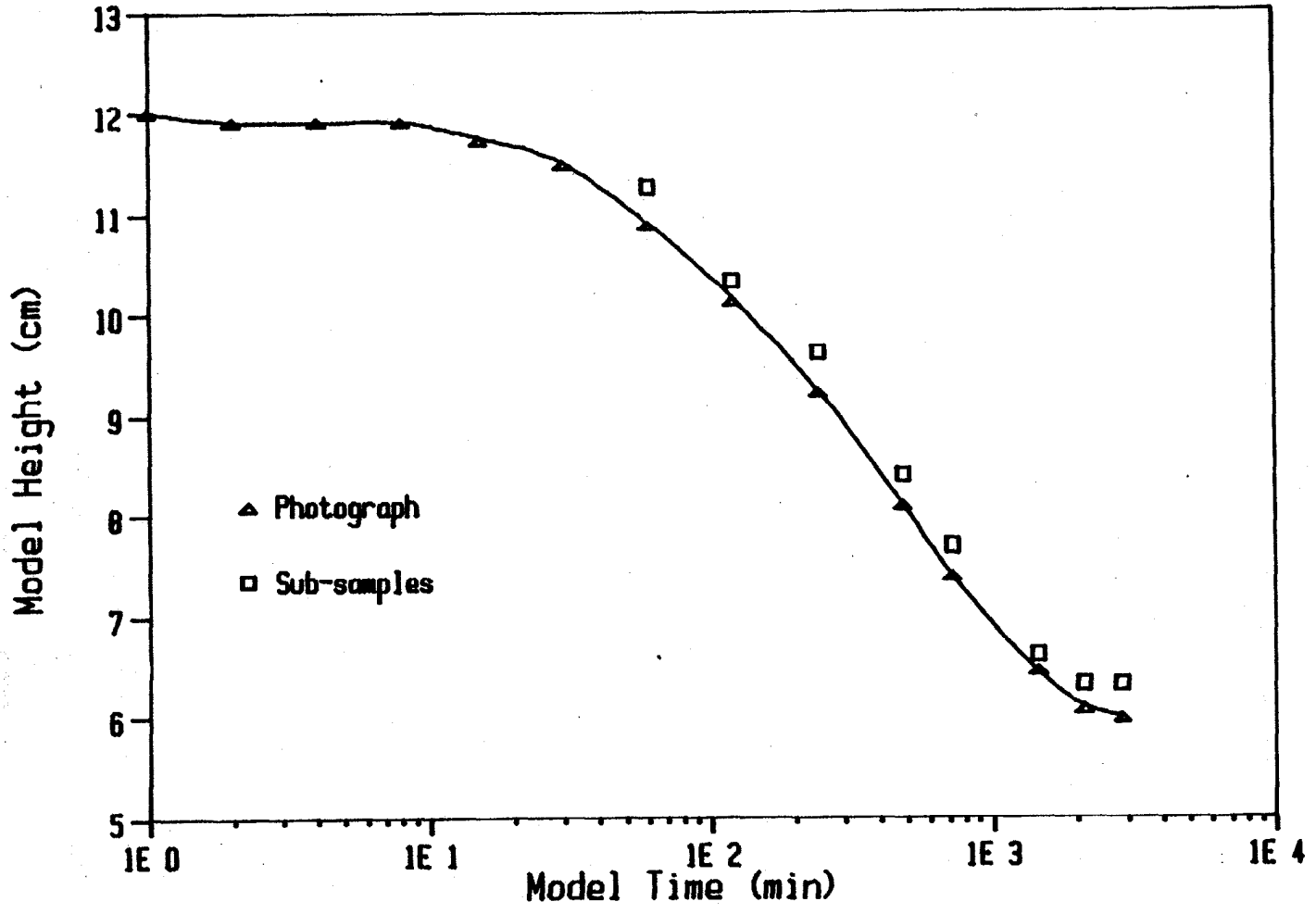

Figure 7.9 - Height-Time Relationship for Test CT-2

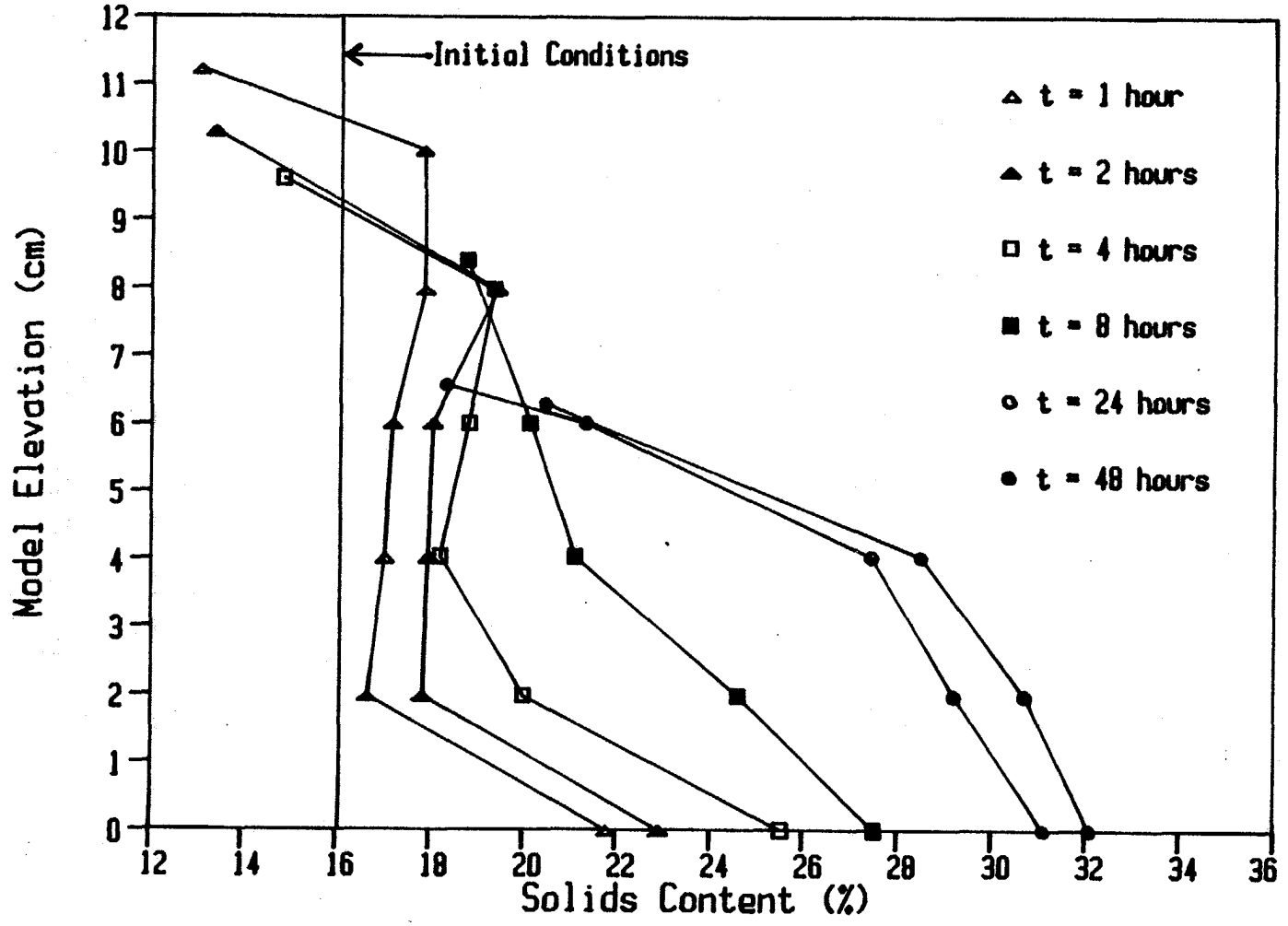

Figure 7.10 - Solids Content Profiles for Test CT-2

For the measurement of the excess pore pressure distribution, it was decided to re-evaluate the zero readings of the transducers in the 12 cm of water. A test conducted for this purpose prior to the actual test recorded values of 41.913, 19.145, and 35.308 mV for transducers No. 1, 2, and 3, respectively. These values compare well with those given in Table 6-1 for 60 g's, with a maximum difference of about 1%. The new values were used to compute the excess pore pressure.

The evaporation effect was analyzed as explained for test CT-1, and the correction pressure is plotted versus time in Figure 7.11. With a coefficient of correlation of 0.998, the equation of the best fit straight line is

$$\Delta u_e = - 0.04584 + (4.334E-04) \cdot t \qquad (7.3)$$

In this case, it was decided to use the equation obtained to compute the correction for evaporation at all times. After the correction is applied, the excess pore pressure at the transducers is plotted versus time in Figure 7.12. The curves show the expected pore pressure dissipation. Figure 7.13 presents the profiles of excess pore pressure at various times, along with the initial buoyant stress distribution. Comparison of the latter with the profile at t = 2 min. again demonstrates that the effective stresses are initially zero throughout the specimen.

The sequence of excess pore pressure profiles of Figure 7.13 behaves much like that resulting from test CT-1. A relatively faster dissipation of excess pore pressure takes

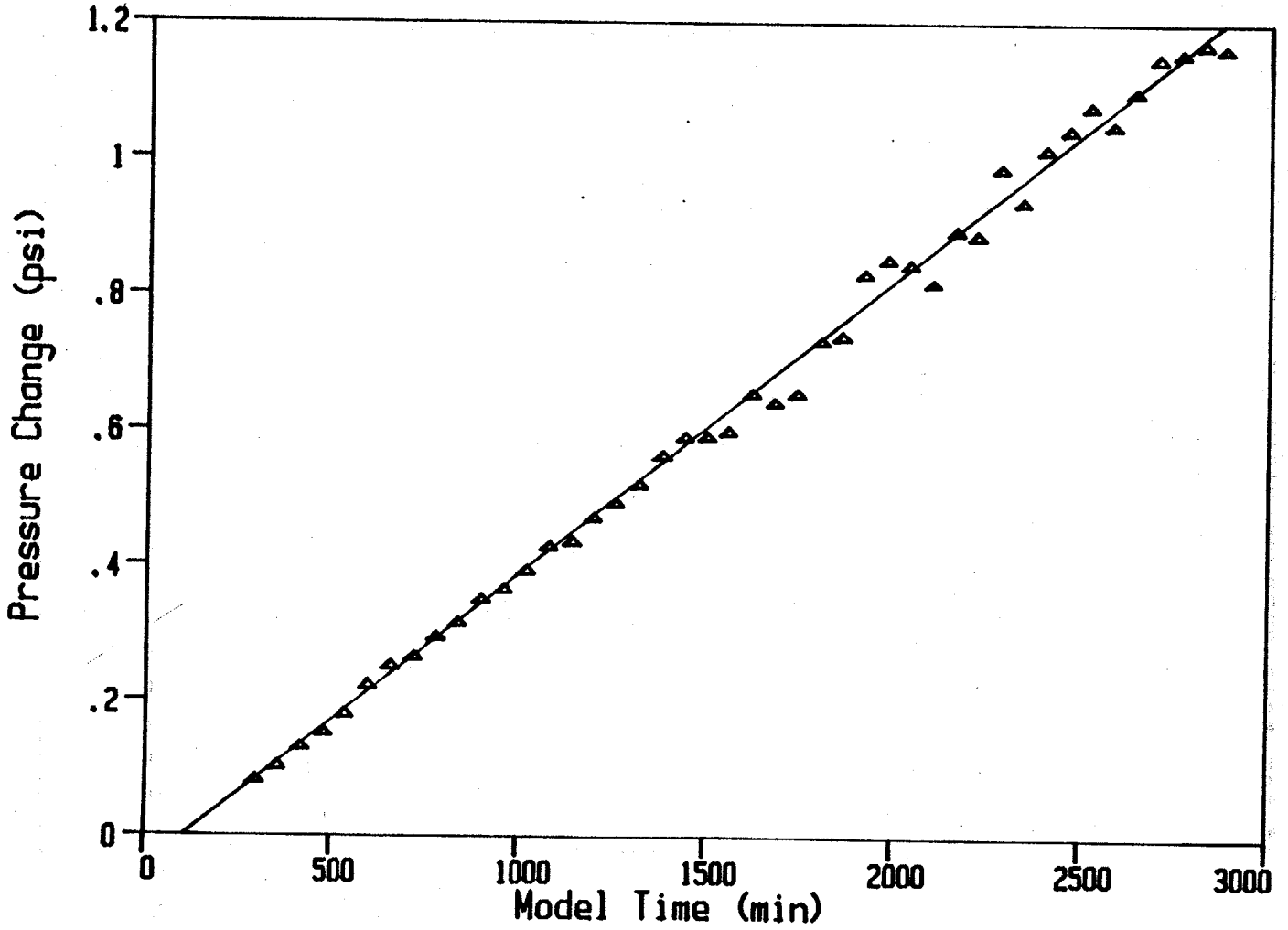

Figure 7.11 - Evaporation Correction for Test CT-2

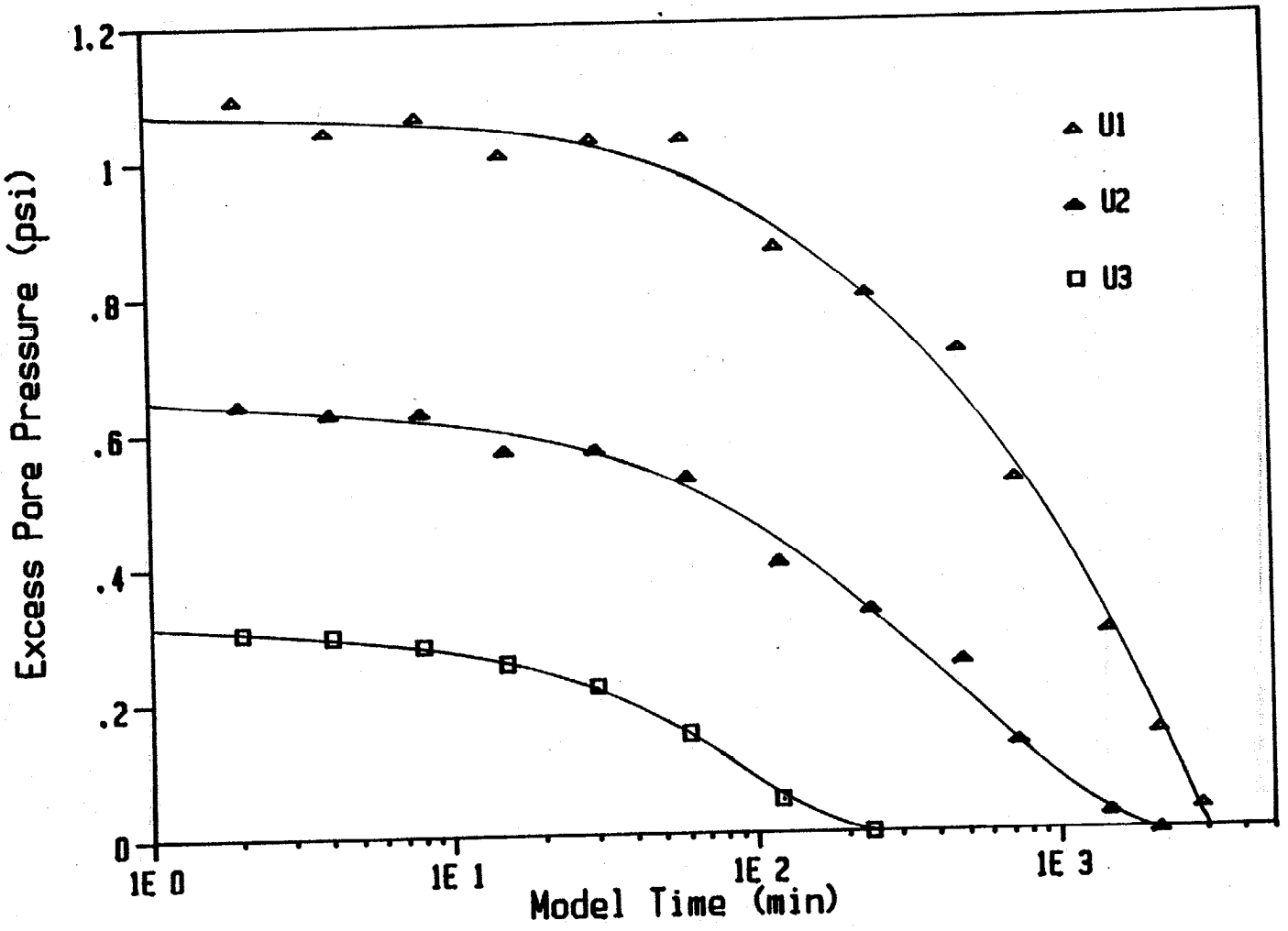

Figure 7.12 - Pore Pressure with Time for Test CT-2

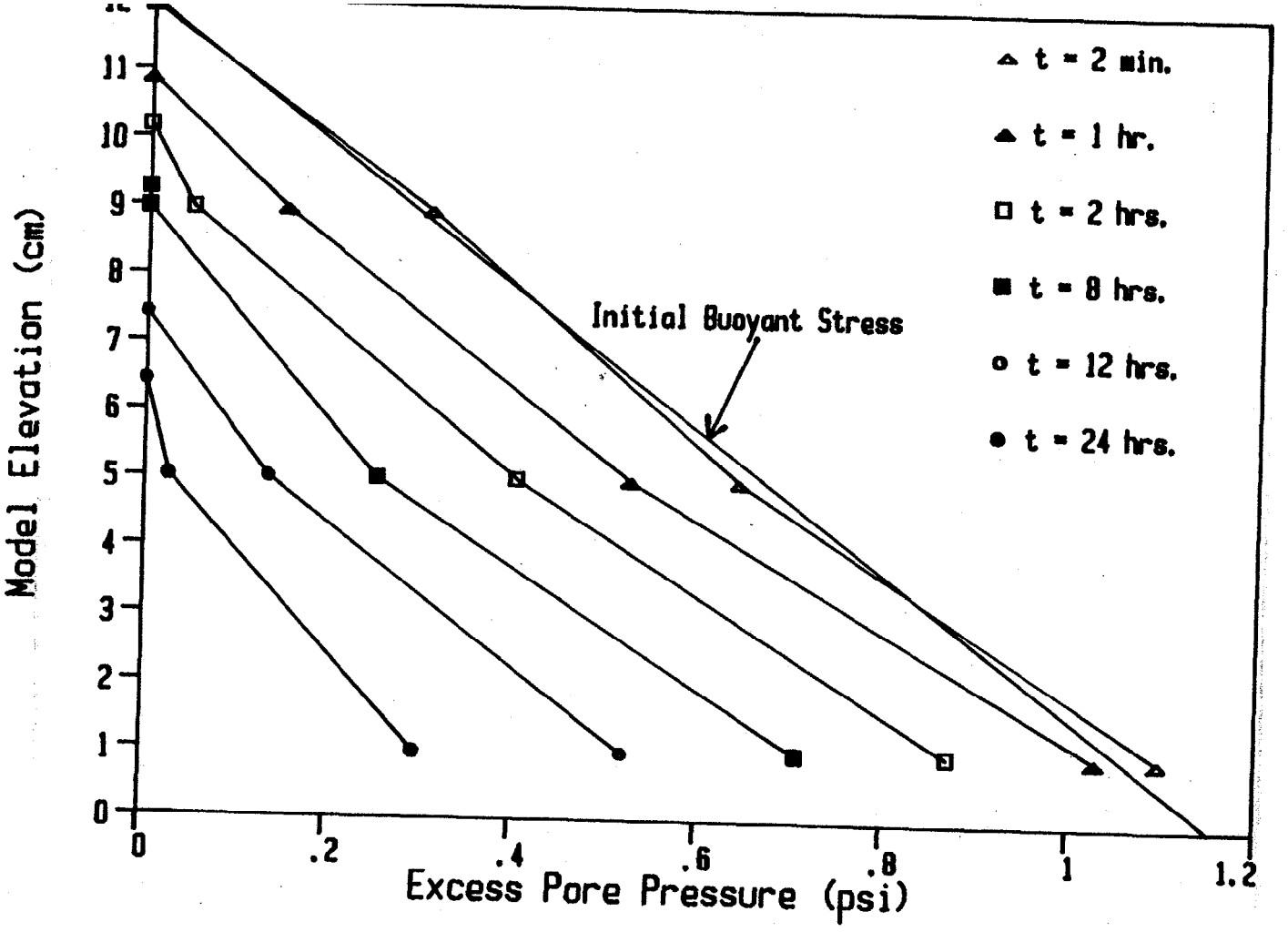

Figure 7.13 - Pore Pressure Profiles for Test CT-2

place near the surface, an effect that is consistent with the solids content profiles of Figure 7.10. Thus, again radial drainage seems to be occurring in the test.

Following the same approximation of using the average of the values at the boundary and at the center of the specimen to estimate the one-dimensional excess pore pressure and hydraulic gradient, the data reduction program analyzed the data of test CT-2. Ten layers were also used in the analysis. A complete printout of the results is included in Appendix H. The general test information, initial conditions, and the results of the analysis for t = 1 hour are reproduced in Table 7-3.

All the observations made about the results of test CT-1 are found to be valid for test CT-2 as well. The agreement between the initial reduced height of the specimen and those computed from the sub-samples is good. The effective stresses are initially zero and begin to increase at the bottom of the specimen; as time progresses, an effective stress front moves upward.

Figure 7.14 shows the compressibility and permeability plots obtained from the analysis of test CT-2. Figure 7.14a does not include those points with effective stress less than 0.0l psi or negative. In the case of the permeability plot, when the point at the surface results with an abnormally high void ratio (as a result of an erroneous solids content), the point was discarded. Also, the permeability values computed at the end of the test (t = 48 hours) were

Table 7-3. Partial Results of the Analysis of Test CT-2

*** Centrifuge Test CT-2 ***
Acceleration level = 60. g

Initial Height = 12.0 cm

Solids Content = 16.05% Void Ratio = 14.175

Number of Layers = 10

Reduced Height of the Specimen = 0.791 cm

Initial Conditions
Theoretical Gradient = 0.113

NODE	H(I)	Z(I)	BUOY.ST.	EXC.P.P.	EFF.STR.	GRADIENT
11	12.0000	0.7908	0.0000	0.0000	0.0000	0.1194
10	10.8000	0.7117	0.1153	0.1222	-0.0069	0.1194
9	9.6000	0.6326	0.2307	0.2445	-0.0138	0.1194
8	8.4000	0.5536	0.3460	0.3563	-0.0103	0.0991
7	7.2000	0.4745	0.4614	0.4577	0.0037	0.0991
6	6.0000	0.3954	0.5767	0.5592	0.0176	0.0991
5	4.8000	0.3163	0.6921	0.6664	0.0257	0.1329
4	3.6000	0.2372	0.8074	0.8024	0.0050	0.1329
3	2.4000	0.1582	0.9228	0.9385	-0.0157	0.1329
2	1.2000	0.0791	1.0381	1.0745	-0.0364	0.1329
1	0.0000	0.0000	1.1535	1.2106	-0.0571	0.1329

New Time = 60.0 min New Height = 10.90 cm
New Reduced Height of the Specimen = 0.800 cm

U(I) = 1.0295 0.5259 0.1512 psi
S(J) = 21.77 16.67 17.04 17.18 17.90 17.83 16.05 %

NODE	H	e	u	Eff.Str.	i	Vs	k (ft/day)
11	10.765	13.895	0.018	-0.018	0.157	0.3432E-03	0.1173E+00
10	9.662	12.479	0.160	-0.045	0.146	0.3161E-03	0.1127E+00
9	8.597	12.447	0.291	-0.060	0.143	0.2785E-03	0.1003E+00
8	7.532	12.573	0.416	-0.070	0.132	0.2410E-03	0.9851E-01
7	6.446	12.918	0.533	-0.071	0.121	0.2096E-03	0.8999E-01
6	5.335	13.107	0.642	-0.065	0.110	0.1848E-03	0.8368E-01
5	4.216	13.180	0.754	-0.062	0.117	0.1621E-03	0.6130E-01
4	3.089	13.352	0.861	-0.053	0.105	0.1419E-03	0.5627E-01
3	1.946	13.409	0.958	-0.035	0.094	0.1260E-03	0.5254E-01
2	0.902	11.177	1.036	0.002	0.083	0.8264E-04	0.3616E-01
1	0.000	9.738	1.097	0.057	0.074	0.0000E+00	0.0000E+00

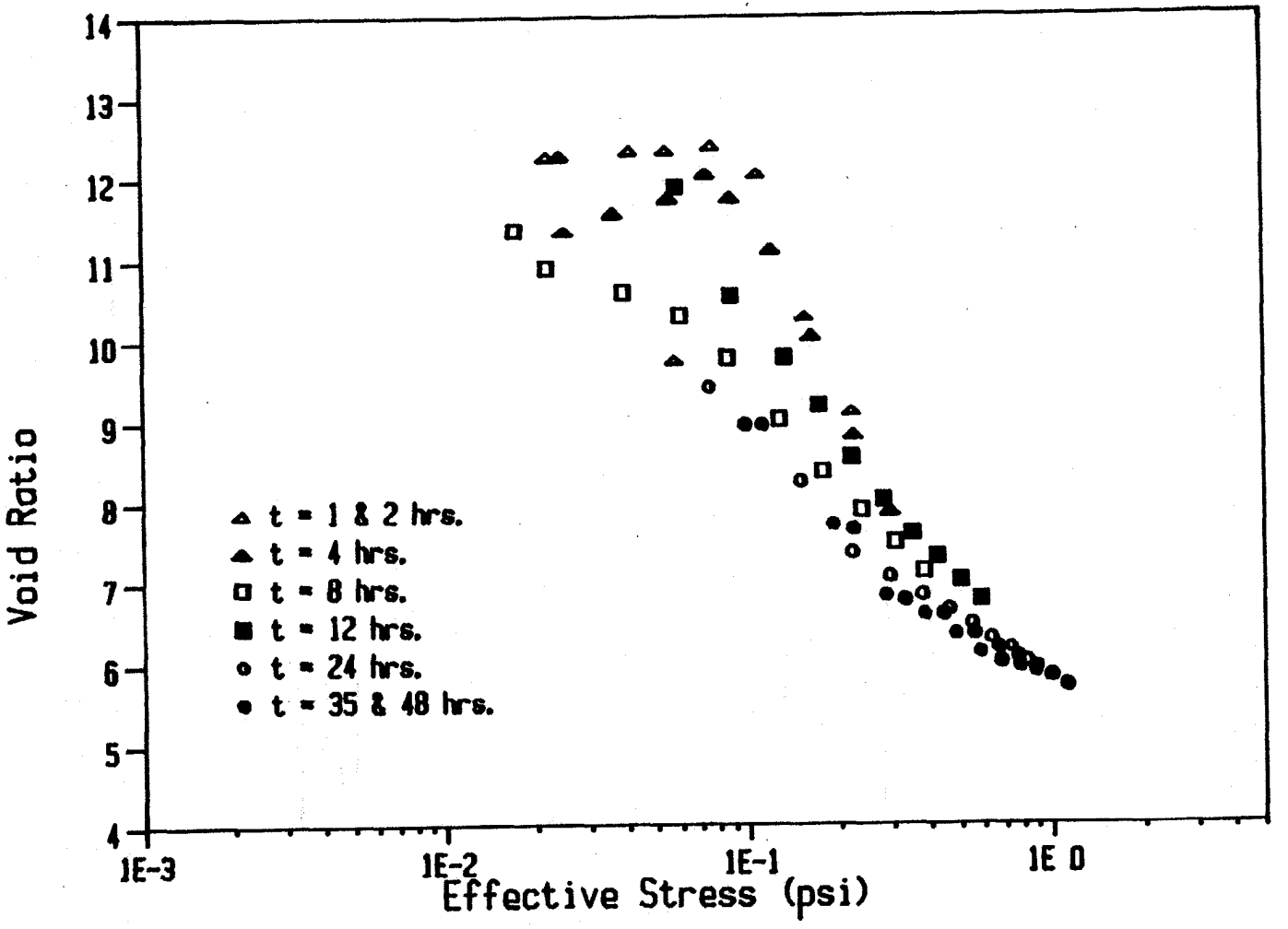

(a)

Figure 7.14 - Constitutive Relationships from Centrifuge Test CT-2.
a) Compressibility; b) Permeability

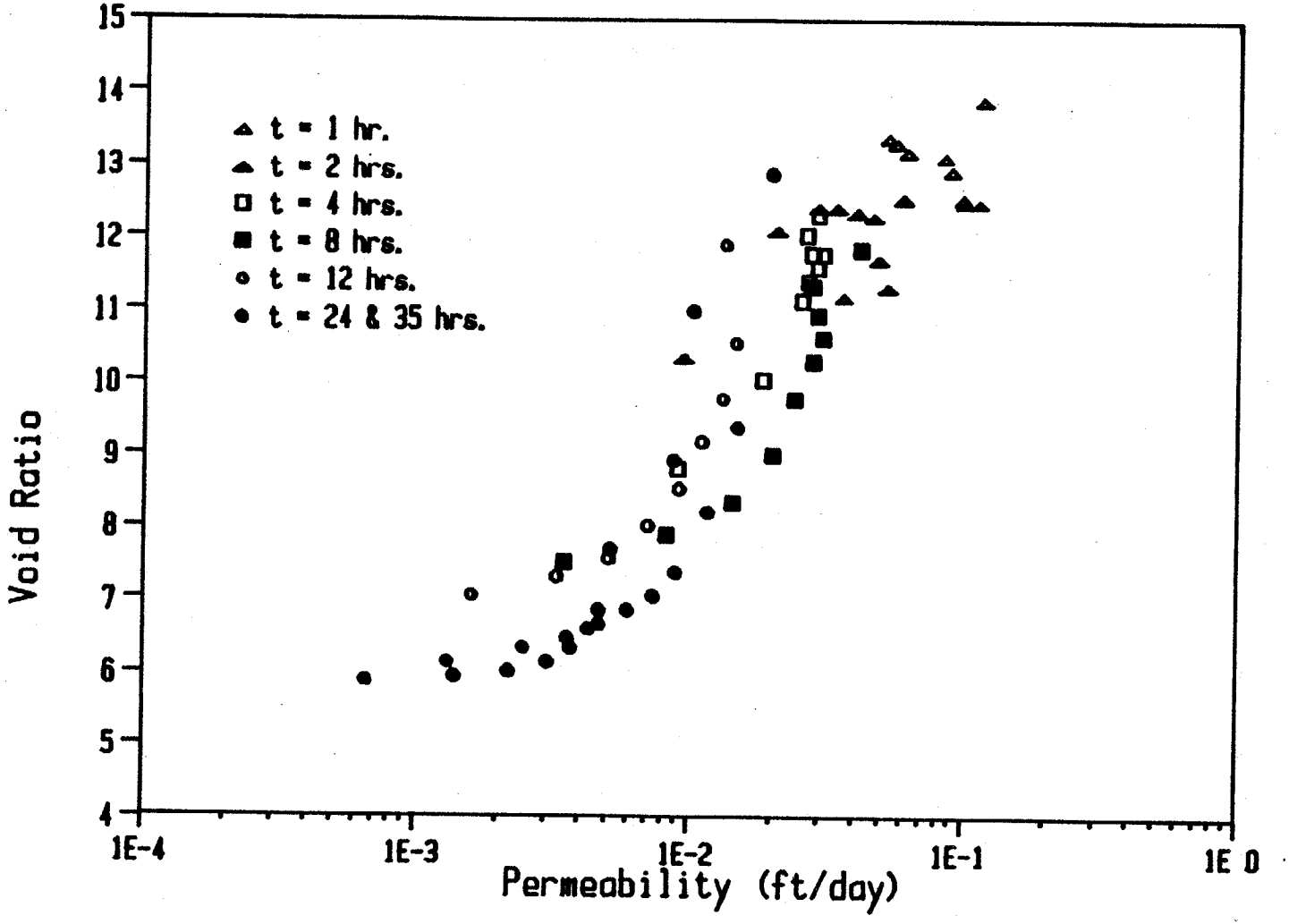

(b)

Figure 7.14--continued

excluded because very small gradients and solids velocities exist at this moment, which results in erroneous computation of the coefficient of permeability.

A comparison of the constitutive relationships obtained from centrifuge tests CT-1 and CT-2 is presented in Figure 7.15. The agreement between the results of both tests is very good. These constitutive relationships can be represented fairly well by power curves of the form of equations 4.31 and 4.32. A regression analysis with the data of Figure 7.15 was performed to obtain the corresponding parameters, with the following results

Compressibility Parameters from tests CT-1 and CT-2:

A = 16.359 B = -0.204 r = -0.940

Permeability Parameters from tests CT-1 and CT-2:

C = 1.029E-06 D = 4.297 r = 0.926

These parameters are for the effective stress in psf, and the coefficient of permeability in ft/day. The correlation coefficients obtained indicate a fairly good correlation. The power functions are also shown in Figure 7.15.

In order to quantify the agreement between the results of the two tests, the power function parameters of the data of test CT-2 only were determined. The results of the regression analysis were

Compressibility Parameters from test CT-2 only:

A = 16.956 B = -0.214 r = -0.933

Permeability Parameters from test CT-2 only:

C = 1.862E-06 D = 3.958 r = 0.903

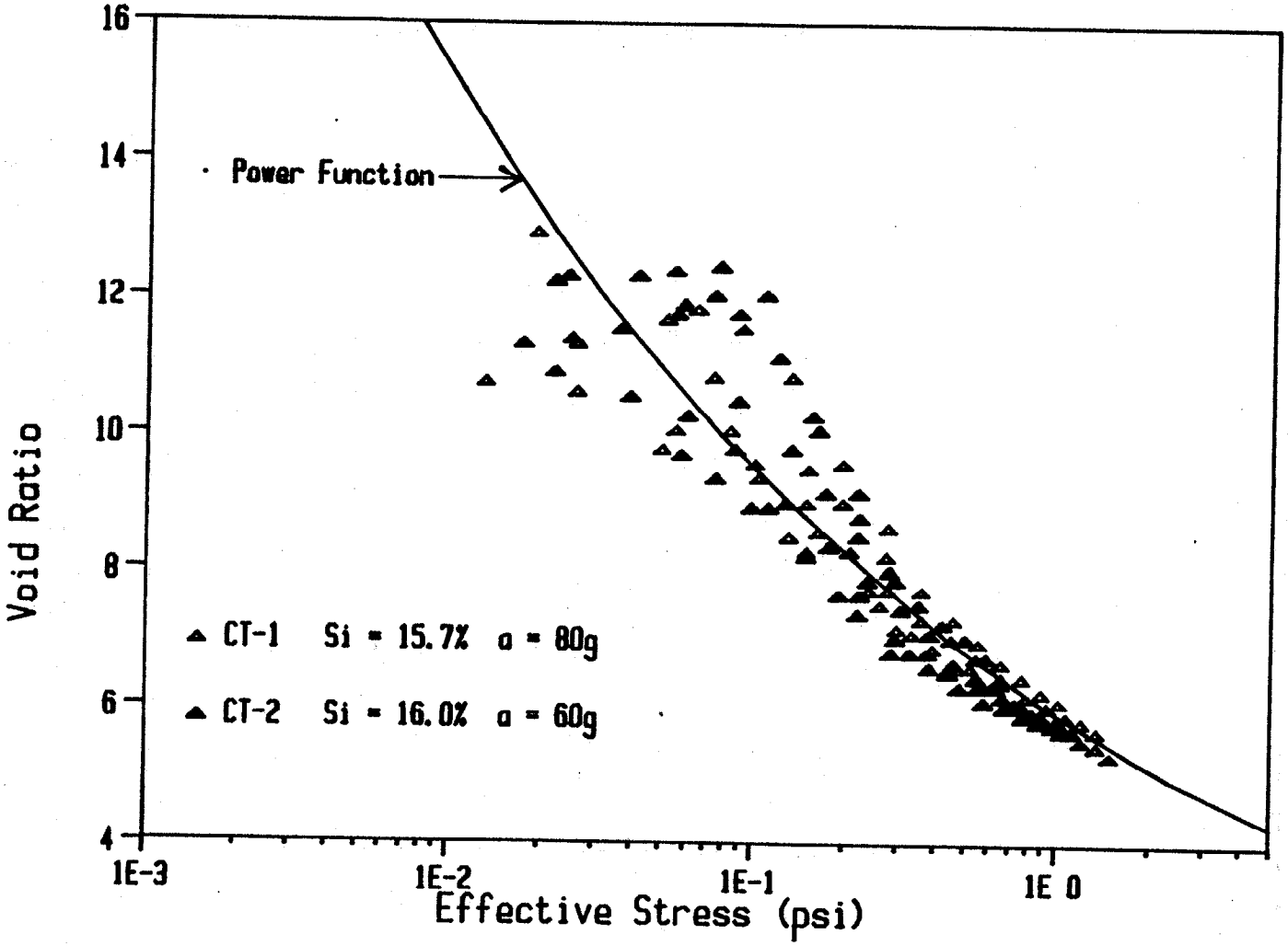

(a)

Figure 7.15 - Comparison of CT-1 and CT-2 Results. a) Compressibility Relationship; b) Permeability Relationship

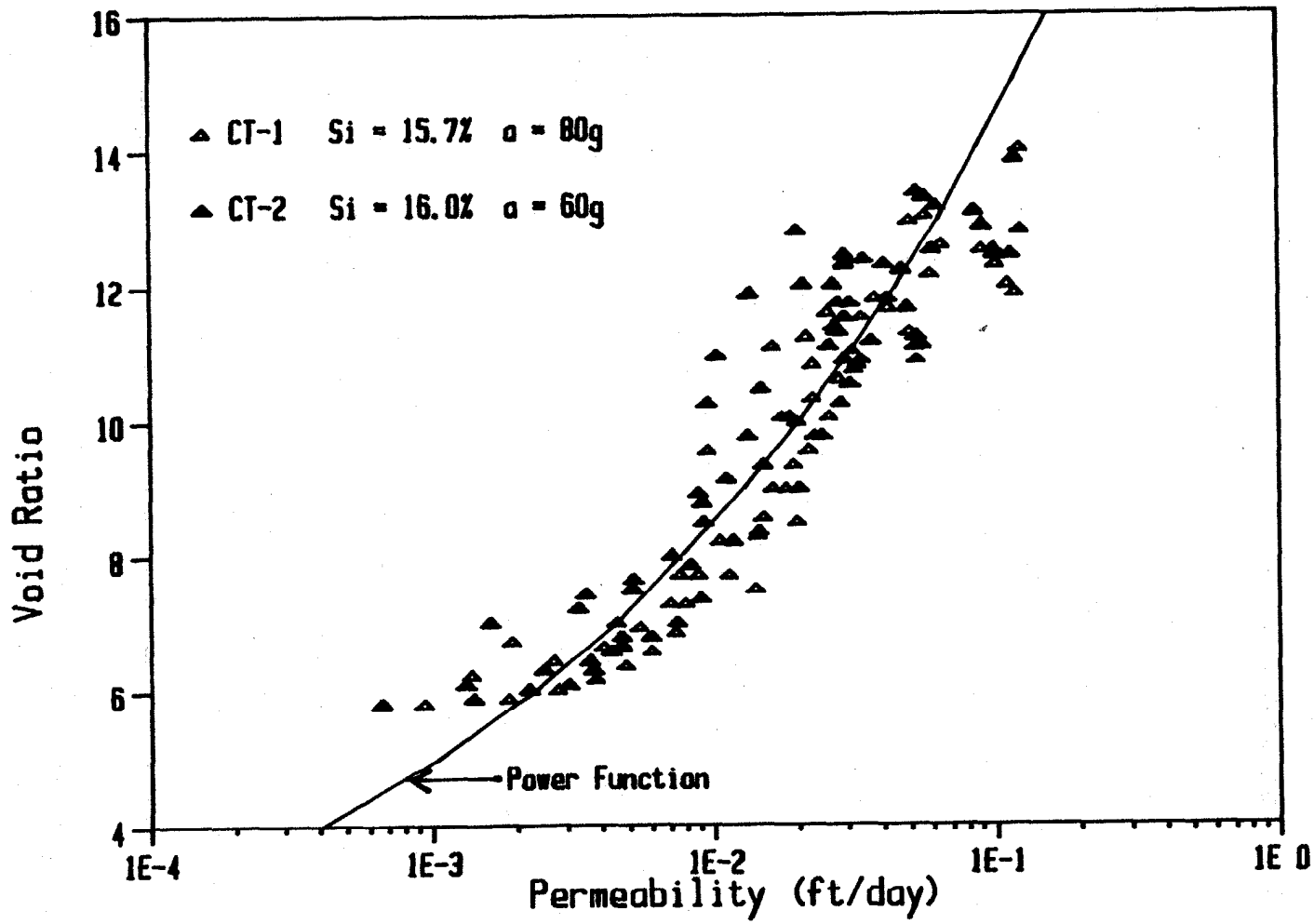

(b)

Figure 7.15--continued

These parameters compare very well with those obtained with the data of both tests. This result clearly shows the agreement between the constitutive relationships obtained from the two tests.

Comparison of CRD and Centrifuge Test Results

During the course of this research two completely different techniques for the determination of consolidation properties of slurries were developed, namely the automated slurry consolidometer and fully monitored centrifugal model tests. Accordingly, an excellent opportunity is presented to compare the results of the two techniques and evaluate their effectiveness.

For the purpose of comparison, two CRD tests were selected. They are CRD-1 and CRD-3, the two constant rate of deformation tests with initial solids contents similar to those of centrifuge tests CT-1 and CT-2. Figure 7.16 shows the constitutive relationships obtained with all four tests. The graphs also show the power function curves obtained with the centrifuge data.

The compressibility plots of Figure 7.16a show a very good agreement between the centrifuge data and the virgin zone of the curve of test CRD-3. The latter is the constant rate of deformation test performed at the slow deformation rate. This result tends to corroborate a conclusion of Chapter V, specifically that CRD tests performed at very slow rates describe better the actual soil behavior because

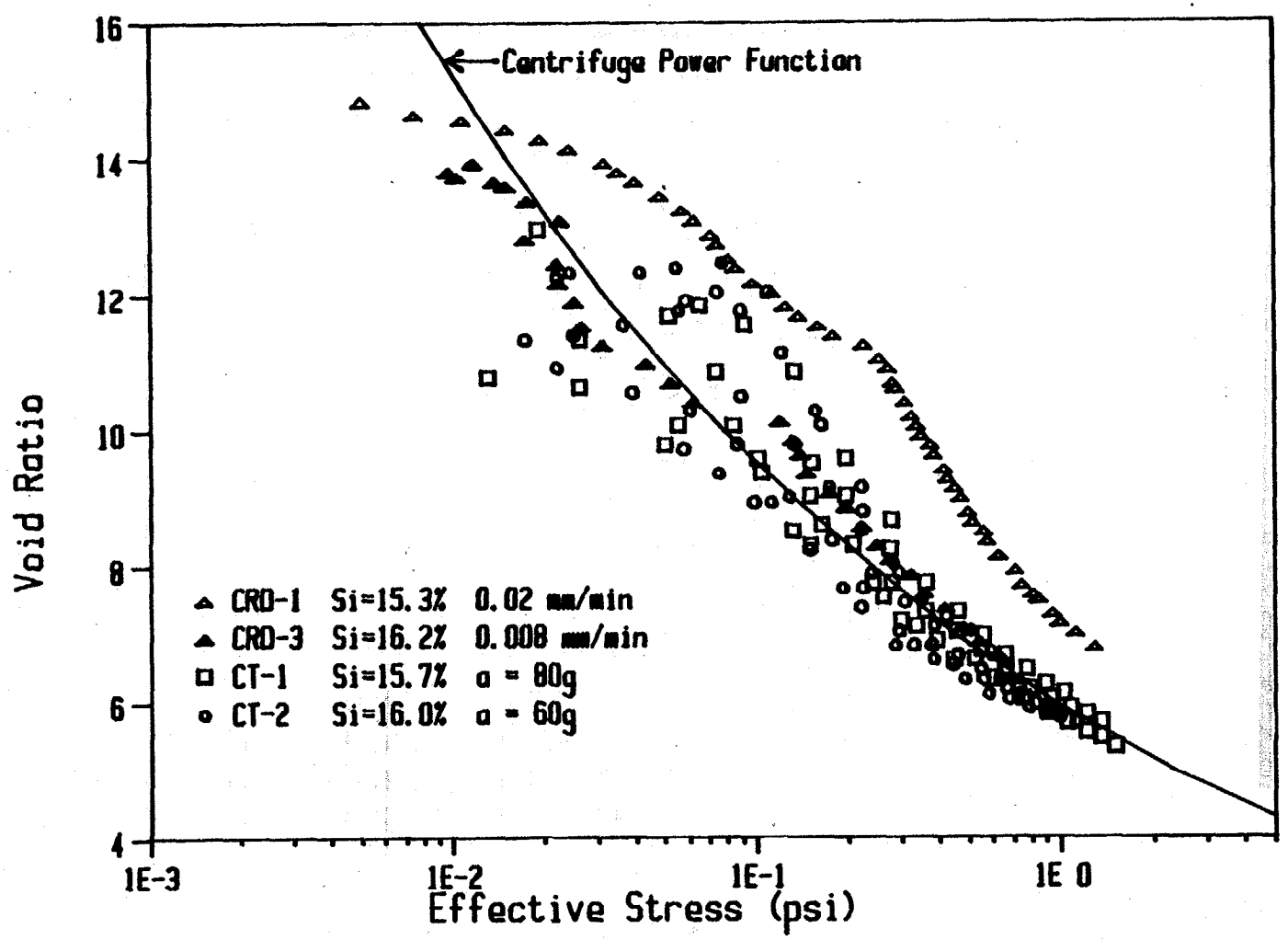

(a)

Figure 7.16 - Comparison of CRD and Centrifuge Test Results.
a) Compressibility Relationship; b) Permeability Relationship

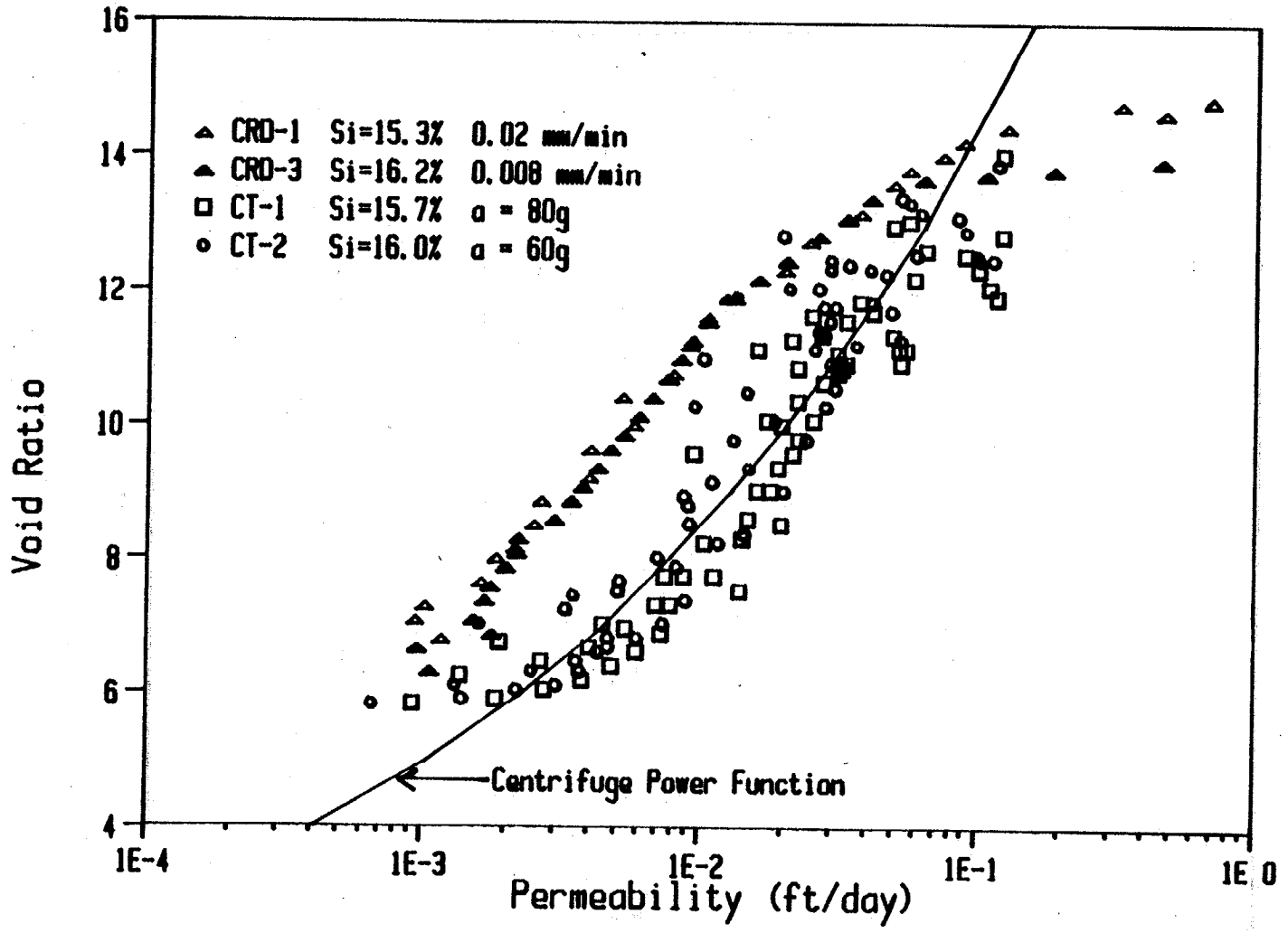

(b)

Figure 7.16--continued

they conform better to the analysis assumptions. As pointed out before in this chapter, the centrifuge curves do not show the preconsolidation effect observed in the CRD tests.

The permeability plots of Figure 7.16b, on the other hand, do not show the same good agreement between CRD and centrifuge tests. The latter, however, plot parallel to the virgin zone of the CRD tests. The centrifuge permeabilities are approximately a half order of magnitude higher than the CRD permeabilities. It is worth recalling at this point that the centrifuge permeabilities plotted in Figure 7.16b represent the "prototype" values. The "model" permeabilities would be even higher, 80 times in test CT-1 and 60 times in test CT-2; thus, the difference between CRD and "model" permeabilities would be about two orders of magnitude. Although the results of Figure 7.16b do not show a total agreement, these results at least demonstrate that the "model" permeability can not be equal to the permeability of the "prototype", which agrees with other studies (Goforth, 1986).

An explanation for the apparent disagreement between CRD and centrifuge test results with regard to the permeability relationship has not been found. However, it is important to recall that the process occurring in the centrifuge showed evidence of radial drainage and that an approximation was made in order to simulate a one-dimensional consolidation problem. Nevertheless, a more detailed study is necessary before a definite explanation can be

found. The following sections of this chapter further address the problem of radial drainage in the centrifuge and some of its implications.

Effect of Surcharge on Pore Pressure Response

It is believed that one of the factors that may be promoting radial drainage in the centrifuge tests reported is the absence of large horizontal confining stresses near the top of the specimen. The pore pressure profiles measured in the tests performed in the automated slurry consolidometer did not show any evidence of possible radial drainage; in these tests, a large horizontal effective stress surely existed as a result of the large surcharge being applied by the loading piston.

With this hypothesis in mind, it was decided to perform a centrifuge test with a sufficient surcharge to prevent the fast radial dissipation of excess pore pressure taking place near the top of the specimen. The shape of the excess pore pressure profiles would readily indicate whether radial drainage was being prevented. The test was not designed to obtain solids content profiles, and therefore could not be used to obtain the soil's constitutive properties.

To apply the surcharge load, a perforated aluminum plate with a vertical rod in the center was constructed. Underneath the plate and on top of the slurry, filter paper is placed to allow free drainage while preventing soil particle migration. The edge of the plate is wrapped with

teflon tape to reduce friction and at the same time prevent the slurry from being squeezed out around the plate. The submerged weight of the plate is 257.2 grams (0.5665 lb).

Two surcharge tests were performed as described in Table 7-l. The first one, test CT-4, was performed at 60 g's, while the second, CT-5, was at 80 g's. To start the test with the piston already submerged, the initial slurry height was 11.0 cm, while the water height was kept at 12.0 cm; in this way the zero readings of the transducers will not be changed. The initial solids content of test CT-4 was 16.04%.

Although it is clear that the "centrifuge weight" of the plate will change as it displaces away from the center of rotation, it is assumed that a constant acceleration of 60 g's applies. Using this value, the surcharge load applied by the plate was computed as 1.445 psi, a value somewhat larger than the self-weight buoyant stress at the bottom of the specimen.

The test ran successfully for less than four hours, when the photograph revealed that the plate had tilted and sunk. Nevertheless, some useful information could be obtained from the test results. Figure 7.17 shows the excess pore pressure profiles obtained from the transducer readings, along with the theoretical initial buoyant stress distribution. The curves show the expected behavior under a surcharge loading. Transducers No. 3 (elevation 9 cm) and

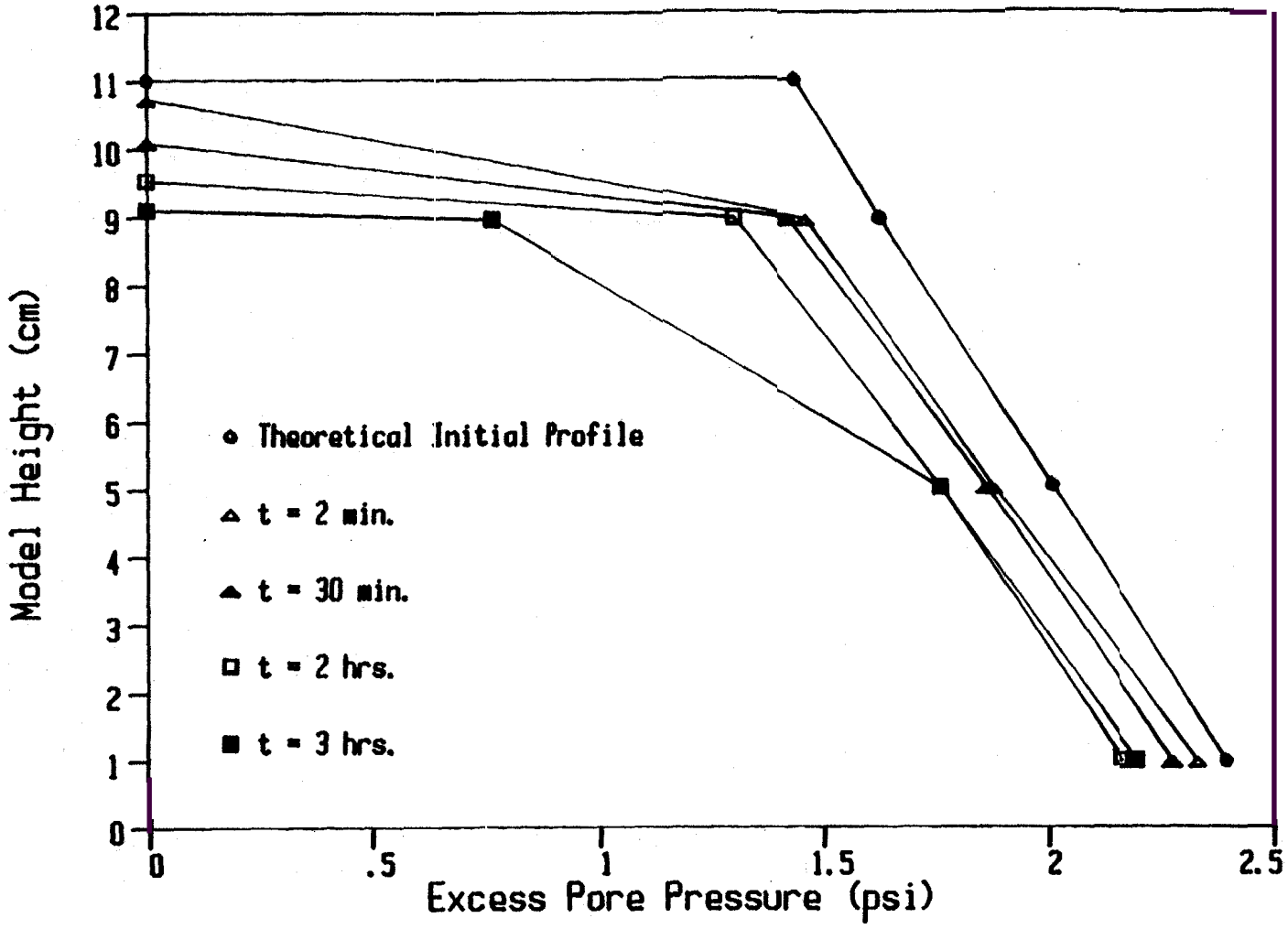

Figure 7.17 Pore Pressure Profiles for Test CT-4

No. 2 (elevation 5 cm) record relatively high excess pore pressures, without exhibiting the fast dissipation attributed to radial drainage in tests CT-1 and CT-2. It is not until t = 3 hours, when the specimen height is slightly higher than 9 cm, that u_3 begins to drop.

Due to the partial failure of test CT-4, the surcharge system had to be modified to prevent tilting of the loading plate. This was easily accomplished by constructing an acrylic cover for the bucket, with a hole in the center to allow only vertical displacement of the vertical rod connected to the plate. Figure 7.18 shows a photograph of the test container with the cover and loading piston assembled as for an actual test.

Test CT-5 was performed at 80 g's with the modified surcharge loading system. The specimen initial height was 11.0 cm (12 cm of water), and the initial solids content was 15.95%. With a normal acceleration of 80 g's, the surcharge load applied to the specimen by the loading plate was estimated to be 1.927 psi; this value is somewhat larger than the self-weight buoyant stress at the bottom of the specimen.

Unfortunately, this test could not be completed successfully either. Although the plate fitting in the bucket was initially snug, some slurry started escaping from the specimen and depositing on top of the plate. After 8 hours of test, there was about 4 mm of sediment on top of the plate, and the test was stopped.

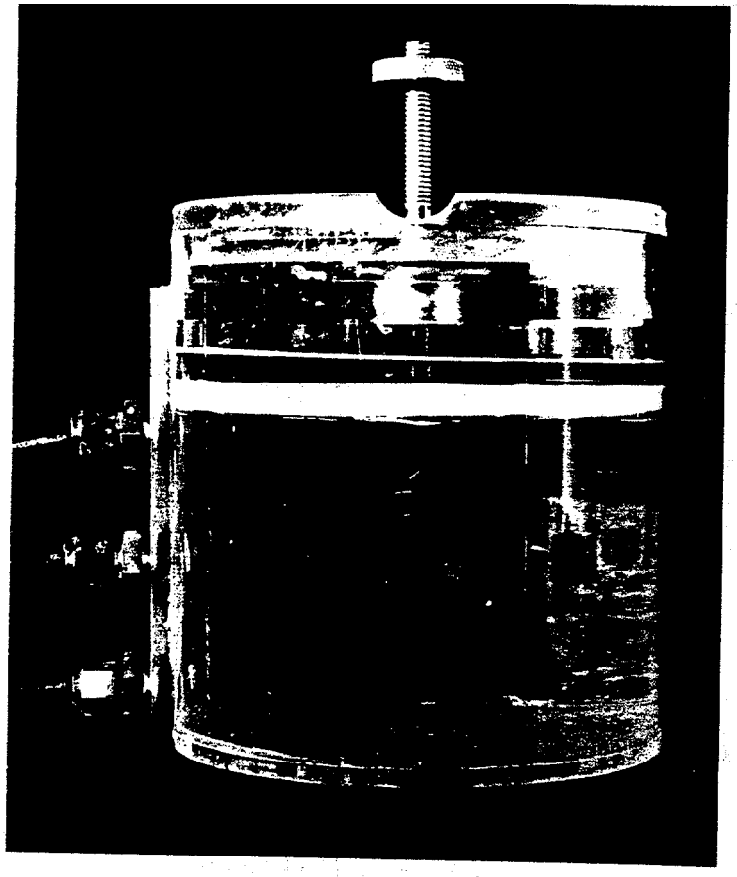

Figure 7.18 - Bucket Used in Centrifuge Surcharge Tests

Although test CT-5 was not completed, the results led to important conclusions and the main objective of the test was fulfilled. Figure 7.19 presents the height-time curve obtained for the test. The excess pore pressure profiles obtained from the transducer readings are shown in Figure 7.20, along with the theoretical buoyant stress distribution. Some apparent abnormalities are observed in the figure. The first two profiles (2 and 15 min) show relatively low excess pore pressures, which increase substantially at t = 1 hour. An explanation for this inconsistent trend can be found by comparing the 2 min profile with the initial buoyant stress distribution. It seems impossible that in such a short period of time so much excess pore pressure had been dissipated. Consequently, it is believed that the first two profiles only reflect part of the plate surcharge, due to the presence of side friction. As the piston displaces, some of the friction is released (most probably the container is not perfectly round), and the excess pore pressures suddenly increase.

Figure 7.21 shows the curves of excess pore pressure versus time at all three transducer locations. The curves clearly show how after some dissipation the excess pore pressures suddenly increase, most probably as a result of some friction release. It is very likely that during these periods of time that the friction was substantially reduced, some slurry had the chance to escape from the specimen.

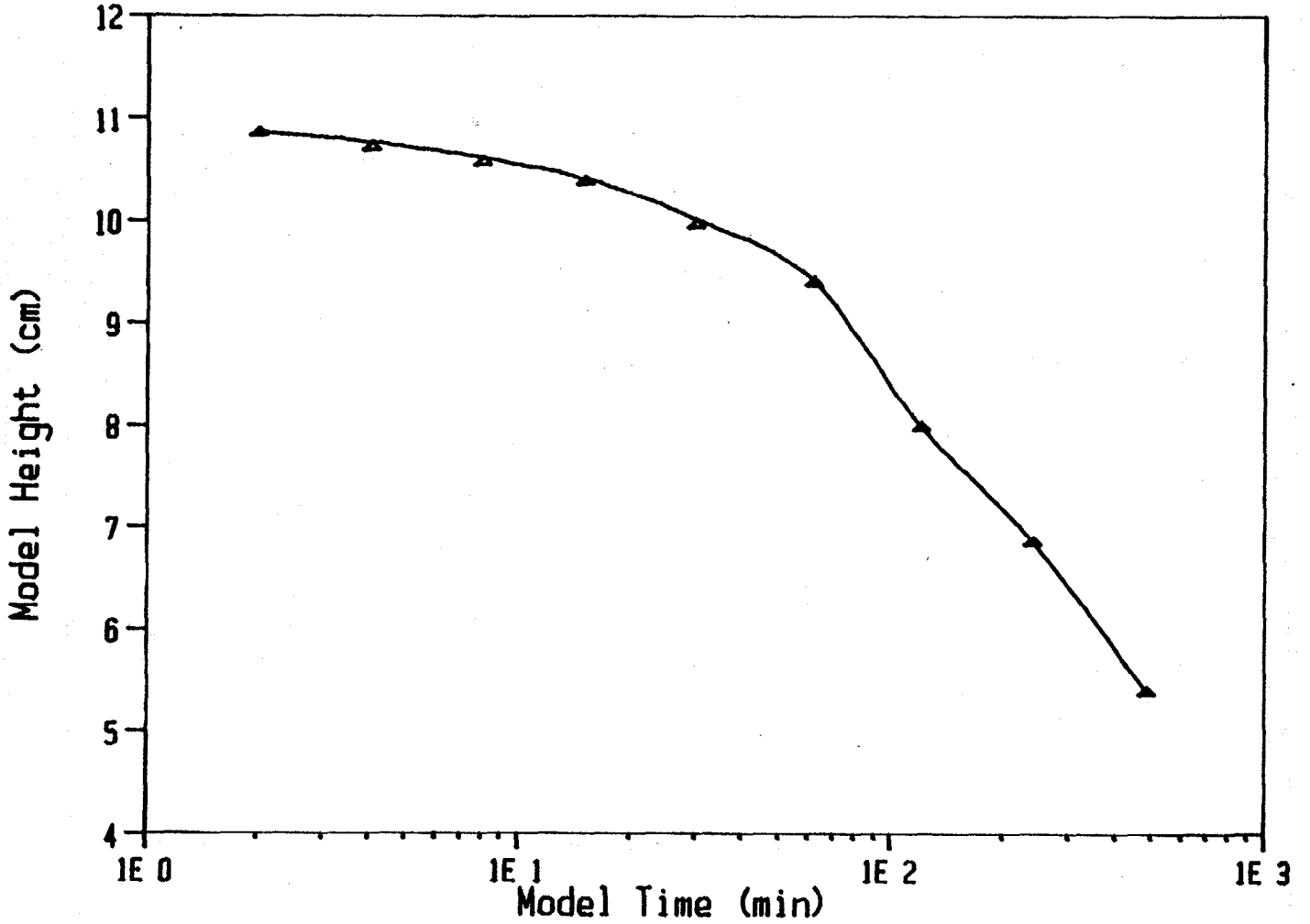

Figure 7.19 - Height-Time Relationship for Test CT-5

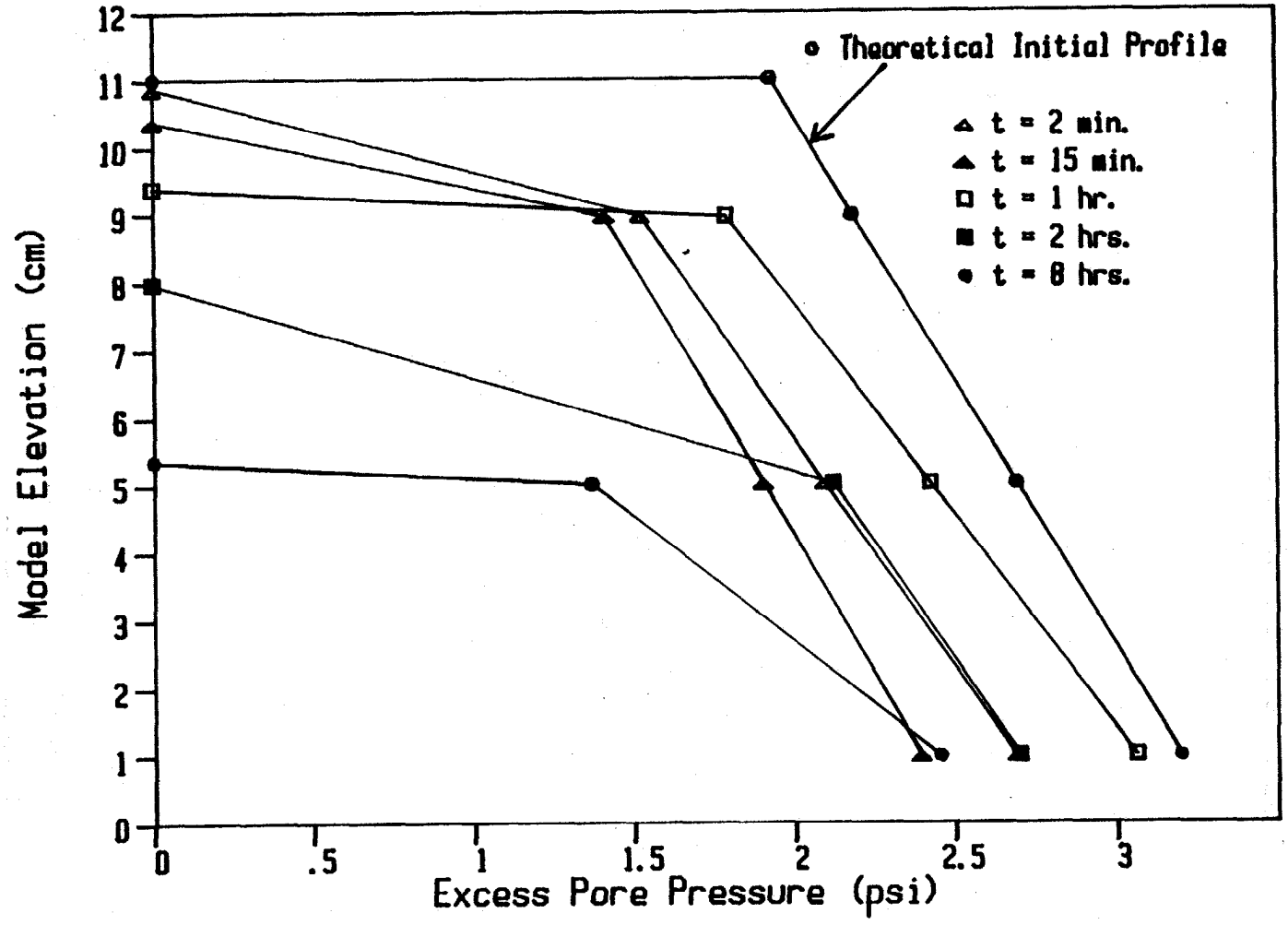

Figure 7.20 - Pore Pressure Profiles for Test CT-5

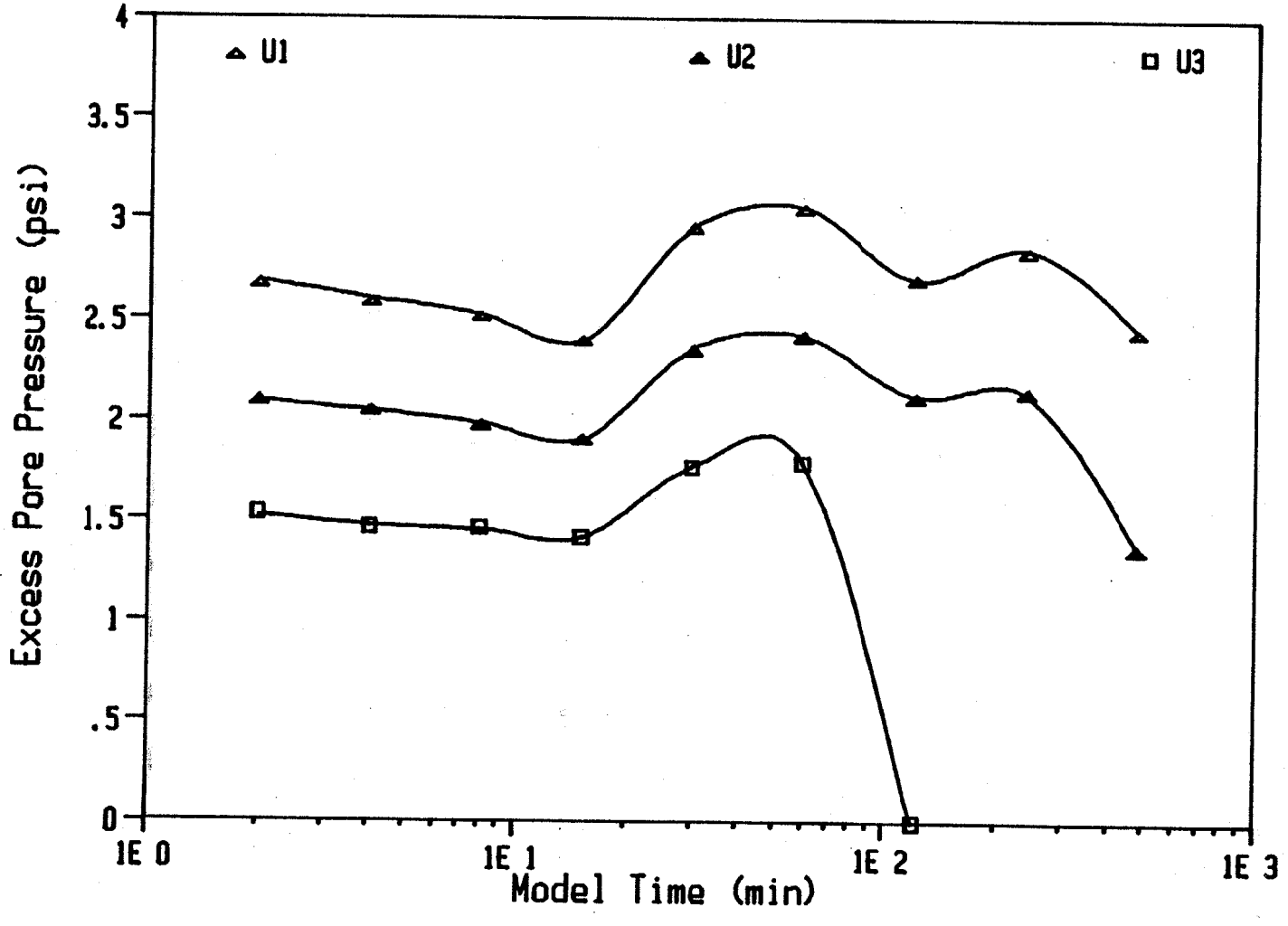

Figure 7.21 - Pore Pressure with Time for Test CT-5

Regardless of the friction problem, the excess pore pressure profiles obtained in test CT-5 (Figure 7.20) indicate that radial drainage was not occurring in the test. Similar to the results of test CT-5, and unlike those of tests CT-1 and CT-2, the excess pore pressures at transducers No. 2 and 3 do not dissipate too fast. The curves behave much as expected in a one-dimensiional problem with surcharge.

Some Comments on the Time Scaling Exponent

The purpose of this section is to present a somewhat speculative, but definitely valid, analysis about the effect of radial drainage upon the time scaling exponent and modelling of models. Although most of the analysis is theoretical, some experimental results will be presented as evidence of the points being considered.

First, let us review the basic equations used in modelling of models theory. If two centrifugal models are used to model the same prototype, the prototype time corresponding to a given average solids content can be expressed as

$$t_p = (t_{m1})n_1^x = (t_{m2})n_2^x \qquad (7.4)$$

where t_P is the prototype time,

t_{ml} is the time in model 1,

n_l is the acceleration (g's) in model 1,

t_{m2} is the time in model 2,

n_2 is the acceleration (g's) in model 2, and

x is the time scaling exponent.

The right hand side of Equation 7.4 can be rearranged in the form

$$(n_1/n_2)^x = t_{m2}/t_{m1} \tag{7.5}$$

from which the time scaling exponent is obtained as

$$x = \log(t_{m2}/t_{m1})/\log(n_1/n_2) \tag{7.6}$$

It is demonstrated in Appendix A and elsewhere (Croce et al., 1984) that for one-dimensional consolidation the time scaling exponent is 2. However, an experimental study presented by Bloomquist and Townsend (1984) found for Kingsford waste clay an exponent of 1.6 for solids content up to about 19%, and then increasing to the value of 2 at a solids content around 21%. These low values of x were attributed to the existence of hindered settling during most of the test, becoming pure consolidation only at the very end of the test.

If unnoticed radial drainage occurs during a centrifugal model test, the model time required to achieve a given degree of consolidation would obviously be reduced, as a result of a faster dissipation process. If the time scaling exponent were to be evaluated from the knowledge of the corresponding prototype time, and using the relationship

$$t_p = t_m \cdot n^x \tag{7.7a}$$

or

$$x = \log(t_p/t_m)/\log(n) \tag{7.7b}$$

the computed exponent x would be higher than the value it takes without radial drainage. In other words, if the "true" exponent is 2, a model with radial drainage would

deceivingly lead to a exponent higher than 2, in order to obtain the actual prototype time. Bloomquist (1982) used a prototype-size test to obtain the time scaling exponent. The IMC tank test consisted of a steel tank 9' x 14' x 22' deep, in which 20.75 ft of Kingsford clay were deposited at 12.6% solids content and allow to self-weight consolidate for 403 days. The test was modelled in the centrifuge at 80 g's, obtaining a constant exponent of 1.6. This result seems to invalidate the above statement concerning the value of x when this is obtained from the prototype time. However, the tank test itself, though representing the prototype, may have been affected by radial drainage considering its large depth/width ratio.

However, the exponent x is very rarely obtained from the prototype time (which is the unknown in the problem), but from the times in two models as expressed in equation 7.6. In this case, the effect of radial drainage upon x will be different.

During the process of modelling of models, the two models representing the prototype at different accelerations will have different heights. Consequently, it is reasonably valid to believe that they will be affected differently by radial drainage. Let us assume for a moment that a "perfect" modelling of models led to an exponent of 2, based on two model times, t_1 and t_2. Using these values in Equation 7.5, results that

$$(n_1/n_2)^2 = t_2/t_1 \qquad (7.8)$$

If modelling of model tests with radial drainage are performed, both times would be reduced, but in a different amount. Let t_1' and t_2' be the new model times influenced by radial drainage and expressed as

$$t_1' = C_1 \cdot t_1 \tag{7.9a}$$

and

$$t_2' = C_2 \cdot t_2 \tag{7.9b}$$

where C_1 and C_2 aredifferent reduction coefficients. Substituting t_1' and t_2' into equation 7.5 leads to

$$(n_1/n_2)x = t_2'/t_1'$$

and using equations 7.8 and 7.9,

$$(n_1/n_2)^x = (C_2 t_2)/(C_1 t_1) = (C_2/C_1)(n_1/n_2)^2 \tag{7.11}$$

Taking the logarithm of equation 7.11, the following equation results,

$$x \cdot \log(n_1/n_2) = \log(C_2/C_1) + 2 \cdot \log(n_1/n_2) \tag{7.12}$$

and solving for x,

$$x = 2 + \log(C_2/C_1)/\log(n_1/n_2) \tag{7.13a}$$

or

$$x = 2 - \log(C_1/C_2)/\log(n_1/n_2) \tag{7.13a}$$

Equation 7.13 shows that if the models were affected in the same amount by radial drainage ($C_1 = C_2$), the exponent would remain equal to 2. However, it seems logical to suppose that the shorter model will be affected less by radial drainage. If, for instance, model 1 is the higher acceleration model, and therefore the shorter model, then the coefficient C_1 would be closer to 1 than the coefficient C_2. Thus, with the ratios n_1/n_2 and C_1/C_2 both larger than one, according with Equation 7,13b, the time scaling exponent would be less than 2.

Certainly, equation 7.13 does not have any practical application. However, it serves the purpose of helping to visualize how the effect of radial drainage upon the model times may explain an exponent less than 2. Such an exponent will not lead to the correct time in the prototype; it only represents the value of x that satisfies equation 7.10.

Another important consequence of radial drainage upon modelling of model results can be found in the following reasoning. If the effect of radial drainage upon a centrifugal model depends on its height, then, two modelling of models supposedly equivalent (i.e.same acceleration ratio) may lead to different exponents. For example, a modelling of models performed with models at 100g and 50g is expected to produce an exponent higher than another modelling of models with accelerations of 50g and 25g but the same acceleration ratio of 2. This is so because the models in the first case are relatively shorter and therefore affected less by radial drainage.

The hypothesis that modelling of models conducted at different acceleration levels would lead to different exponents was investigated using the test results reported by Bloomquist and Townsend (1984). In this study, a modelling of models wasdone using three models, specifically a 6 cm model at 80 g's, an 8 cm model at 60 g's, and a 12 cm model at 40 g's. From their data, the model times corresponding to three different solids content were carefully obtained as reported in Table 7-4.

Table 7-4. Modelling of Model Results (Bloomquist and Townsend, 1984)

	a = 80 g's	a = 60 g's	a = 40 g's
S = 16%	91	151	289
S = 18%	189	330	628
S = 20%	382	713	1382

Two modelling of model analyses were done with these values. First, the values at 80 g's and 60 g's were used in one analysis, and secondly, the values at 60 g's and 40 g's. The exponent obtained from the analyses are reported in Table 7-5.

Table 7-5. Time Scaling Exponent Obtained from Data in Table 7-4

	80-60 Models	60-40 Models
Si = 16%	1.76	1.60
Si = 18%	1.94	1.59
Si = 20%	2.17	1.63

Several conclusions can be drawn from these results. First, the exponent is always higher in the 80-60 modelling of models (shorter models). Secondly, this increases with solids content at a much faster rate in the case of the 80-60 models, approaching a value close to 2 much earlier than reported by Bloomquist and Townsend (1984).

The results of a three-model modelling of models can be interpreted graphically. If the logarithm of equation 7.7a

is taken, the following expression is obtained,

$$\log(t_p) = \log(t_m) + x \cdot \log(n) \qquad (7.14)$$

Since the prototype time is a constant, say C, equation 7.14 can be rewritten as

$$\log(t_m) = -C + x \cdot \log(n) \qquad (7.15)$$

Thus, according to equation 7.15, if different model times are plotted versus the centrifuge accelerations in log-log scales, the resulting plot is a straight line whose slope is the exponent x.

Using above interpretation, the values shown in Table 7-5 are plotted in Figure 7.22. For each solids content, a unique straight line can be easily fit through the data. However, Figure 7.22 shows the graphical equivalent to doing two modelling of models with the data. The 80g and 60g points are joined by one straight line, and the 60g and 40g points are joined by another. An apparently minor but consistent change in slope is clearly noticed. The 8O-60 line has a larger slope in all three cases, indicating a higher time scaling exponent.

Finally, and to complement the results of previous studies with Kingsford waste clay, two of the tests of the present research were designed to conduct a modelling of model analysis (Table 7-l). They were test CT-2, performed at 60 g's with and model height of 12 cm, and test CT-3, run at 80 g's with an initial height of 9 cm. Their initial solids content were 16.05% and 16.02%, respectively. Test CT-2 lasted for 2880 minutes and the final model height was

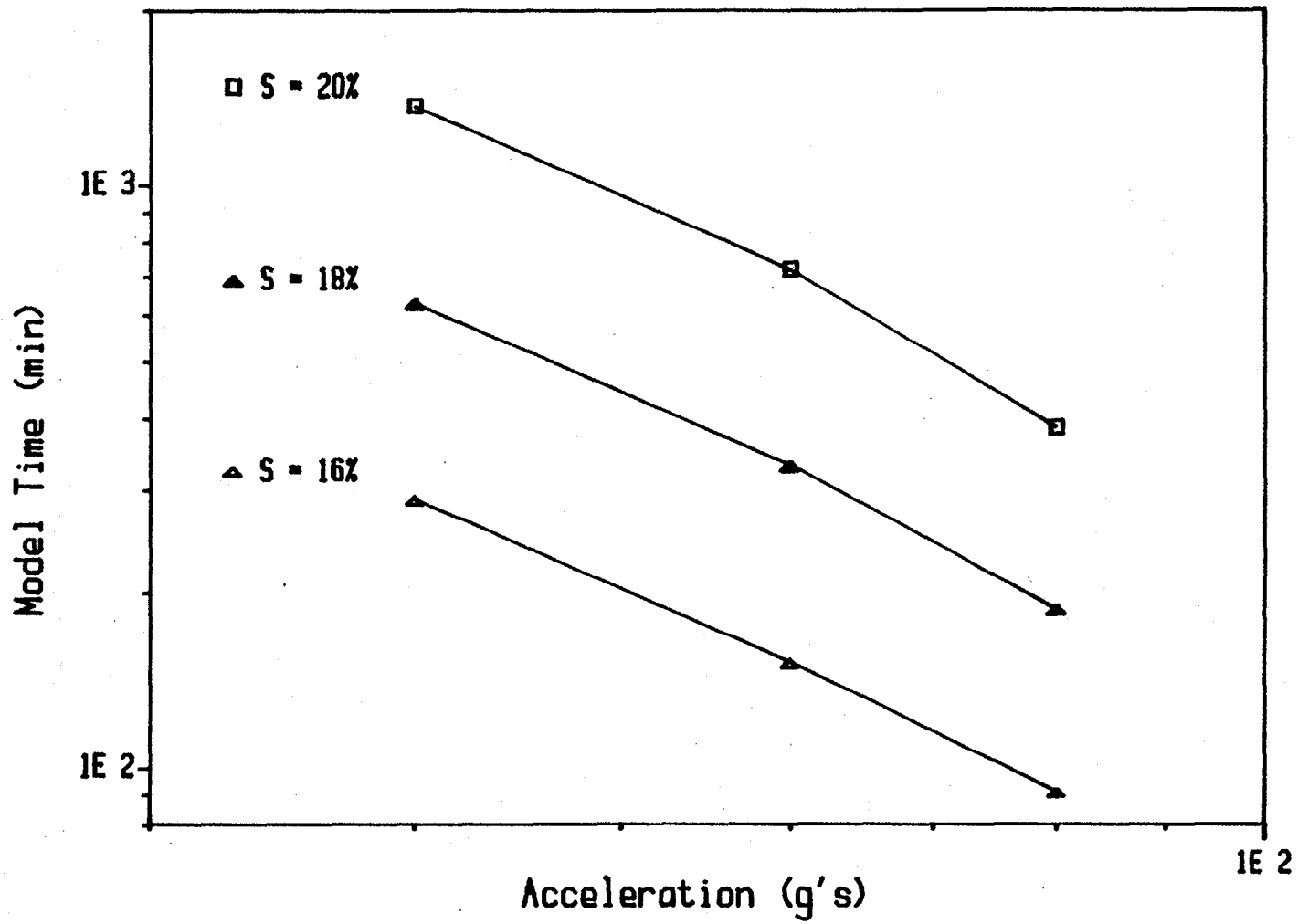

Figure 7.22 - Modelling of Models using Bloomquist and Townsend (1984) Data

6 cm. The duration of test CT-3 was 2115 minutes, with a final model height of 4.55 cm.

Figure 7.23 presents the plots of average void ratio versus log time for tests CT-2 and CT-3. The graph shows the expected behavior, and the final void ratio of the two models is reasonably close. The time scaling exponent was obtained for different void ratios, as presented in Table 7-6.

A very surprising result is obtained from the analysis. The exponents obtained are extremely low, regardless of the relatively high solids contents. Except for the values near the beginning and end of the tests, when it is more likely to obtain erroneous model times, the exponent increases with the solids content, as expected.

These modelling of model results appear to be consistent with the reasoning presented earlier about the effect of radial drainage on modelling of models. Bloomquist and Townsend (1984) data contains two tests with models at 80 g's and 60 g's, with heights of 6 cm and 8 cm, respectively. Their analysis produced exponents of 1.6 and above. The present modelling of models, on the other hand, was done with models at the same acceleration levels, but with larger specimens, specifically 9 cm for the 80g model and 12 cm for the 60g model. Therefore, it is expected that radial drainage would be more significant in the latter, thus, resulting in smaller time scaling exponent.

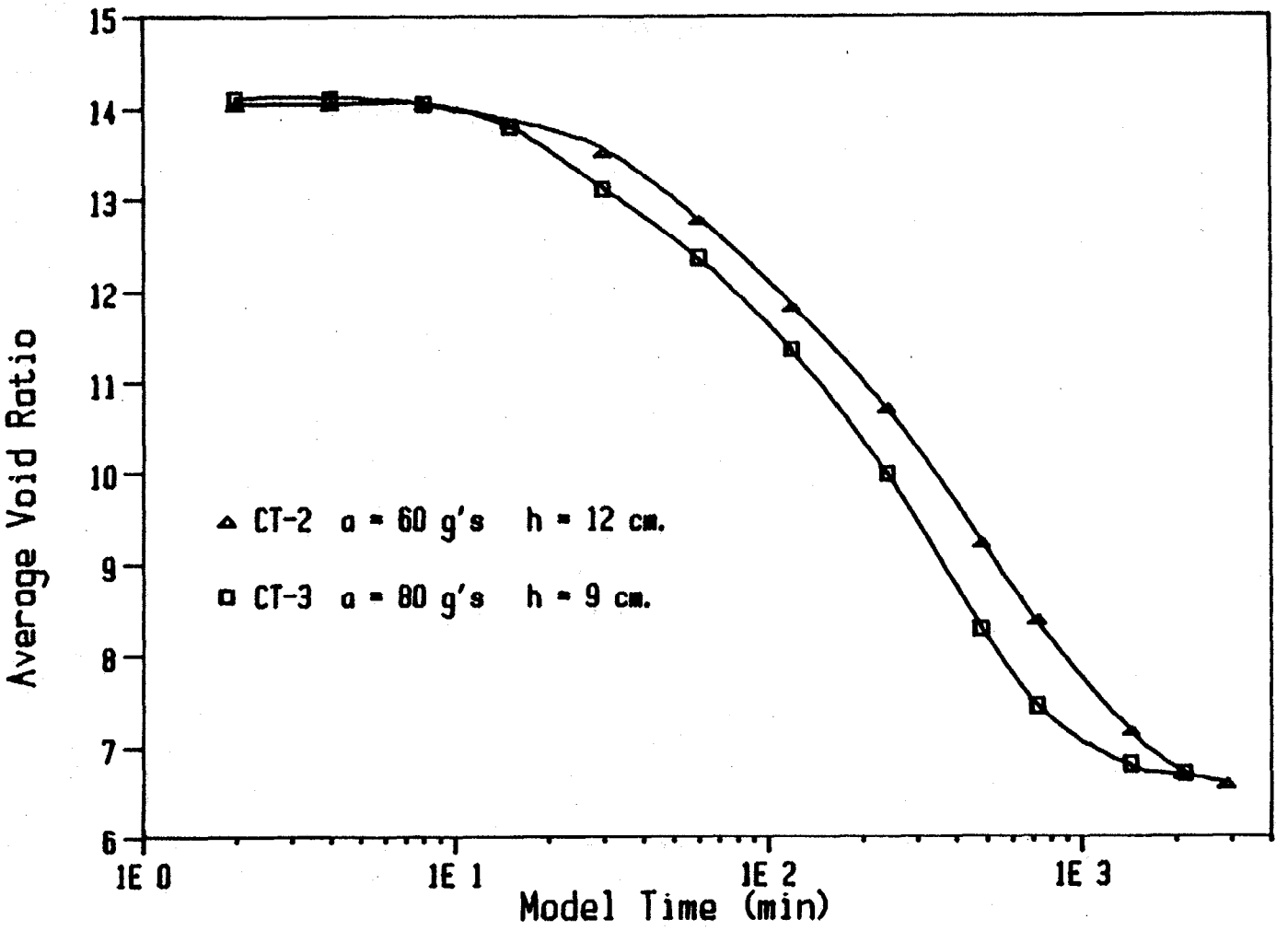

Figure 7.23 - Modelling of Models using Tests CT-2 and CT-3

Table 7-6. Modelling of Models on Tests CT-2 and CT-3

Void Ratio	Solids Content (%)	Time (min) CT-2	Time (min) CT-3	Exponent
13	17.25	51.7	33.8	1.48
12	18.42	105.3	77.0	1.09
11	19.77	202.1	144.1	1.18
10	21.32	332.7	235.4	1.20
9	23.14	536.1	359.6	1.39
8	25.30	859.3	542.7	1.60
7	27.91	1588.4	1042.6	1.46

In summary, there appears to be enough evidence in the test results reported in this research to believe that some degree of radial drainage takes place near the top of centrifugal model specimens. This radial drainage would definitely reduce the model times, but quantification of the magnitude of the effect is not possible. The degree of significance of radial drainage is probably a function of the specimen height, centrifuge acceleration, and elapsed time of test. All this introduces some uncertainty about the validity of the time scaling exponent obtained from modelling of models. It appears that a deceivingly low value of x would be obtained from tests with radial drainage. However, some of the evidence presented here is mostly circumstantial, and further studies are needed to verify above conclusions.

CHAPTER VIII
COMPARISON OF NUMERICAL AND CENTRIFUGAL PREDICTIONS

Introduction

An important aspect of this research is to use the obtained constitutive properties of slurries as input information into large deformation consolidation numerical analyses. The results of such numerical predictions can then be validated with the results of centrifugal model tests.

Several formulations of large strain consolidation theory have been derived. Among the most popular ones, for which computer codes have been written, are those by Somogyi (1979), Cargill (1982), and Yong et al. (1983). McVay et al. (1986) derived a general large-strain one-dimensional consolidation equation, based on continuity of the separate phases and balance of momentum of the fluid phase, in terms of excess pore pressure in combination with the spatial and material coordinates. They proved that the other forms of the governing equation can be obtained by simply adopting a different dependent variable (e.g. void ratio vs. excess pore pressure) and the appropriate coordinate system (e.g. reduced vs. spatial coordinates). Several studies (Hernandez, 1985; Zuloaga, 1986; McVay et al., 1986) have shown

that good agreement exists between the various approaches, as long as the same soil properties are used.

For the numerical predictions reported here, the piecewise linear approach developed by Yong and coworkers (1983) and later expanded by Zuloaga (1986) was used. An important advantage of this program is that it allows the input of the constitutive relationships in the form of data points, as an alternative to the traditional power curve parameters.

Many of the features of the program developed by Zuloaga (1986) UF-McGS, such as continuous filling, sand/clay mixes, etc., were not necessary for the analyses of the ponds to be considered here. Therefore, a simplified and more efficient version of the program, analyzing only quiescent conditions, was written in Turbo Pascal. The program is called YONG-TP. This program, which allows a surcharge, was found to run faster than the original program. A listing of this is included in Appendix I.

A total of five hypothetical ponds were analyzed. All of the ponds have been modeled in the centrifuge under quiescent conditions using Kingsford clay. Two of them were modeled by McClimans (1984). The first one, pond KC80-6/0 in McClimans notation, is a 16-ft high prototype, self-weight consolidating from a solids content of 16%. The second one, pond KC80-10.5/0, is a 27.6-ft high prototype with initial solids content of 16.3%. Hernandez (1985) used McClimans centrifuge data to obtain the prototype elapsed

time of consolidation. Hernandez reported using an incremental time scaling exponent as reported by Townsend and Bloomquist (1983). The settlement-time curves as presented by Hernandez were used for comparison with numerical predictions.

The other three ponds analyzed correspond to the centrifuge tests CT-1, CT-2/3, and CT-5 as described in Table 7-1. Pond CT-2/3 denotes a prototype modeled in the centrifuge by tests CT-2 and CT-3, used in the modelling of models. After the results obtained in Chapter VII concerning the influence of radial drainage on the time scaling exponent, it was decided to use the theoretical value of 2 to obtain the prototype time for these tests. Test CT-5 offers an specially interesting opportunity of comparing numerical and centrifugal predictions in a pond where a surcharge loading is applied. The initial solids content of all five ponds to be analyzed was around 16%.

The Constitutive Relationships

Through the readily availability of computer programs, several of which have been adapted to run on personal computers, the task of predicting the consolidation behavior of slurry ponds has been greatly simplified. However, without reliable soil properties the results of these numerical tools are meaningless. Hernandez (1985) and McVay et al. (1986) found tremendous disagreement among

predictions using different constitutive relationships reported for Kingsford clay.

It has been found during the development of this research that the constitutive relationships of remolded slurries are not unique. Instead, they show a zone similar to a preconsolidation effect, which is dependent upon the initial solids content. Therefore, material characterization of the ponds to beanalyzed should be based on laboratory tests with initial solids contents compatible to that of the pond.

Unfortunately, the centrifugal model tests reported in Chapter VII did not show this preconsolidation effect for the reasons already given. Consequently, the results of the automated slurry consolidometer tests were the first choice to characterize the slurry properties. Because of the irregular behavior found on the CHG compressibility curves, these tests were not even considered, leaving the CRD as the best option. Of the four CRD tests performed, only two of them had an initial solids content around 16% (Table 5-1). In addition, test CRD-3 started at a solids content of 16.2% and the first reading was taken after 2 hours, when the solids content was about 16.3%. Since the ponds' initial solids contents are below this value, the results of test CRD-3 could not be used because the computer program needs to determine the initial effective stress of the pond interpolating from the effective stress-void ratio data points. Thus, the results of test CRD-1, with an initial

solids content of 15.3%, were used to characterize Kingsford waste clay. Ten evenly spaced points were selected from Figure 5.1 to generate the input constitutive curves for the program. As an alternative to the data points, the power curves fit to the experimental data of test CRD-1 will also be used in the predictions. The corresponding parameters were given in Chapter V.

Prediction of Ponds KC80-6/0 and KC80-10.5/0

These two ponds are the ones modeled in the centrifuge by McClimans (1984), and whose prototype behavior was analyzed and reported by Hernandez (1985). Appendix I includes, as an example, the output of the program YONG-TP predicting the behavior of pond KC80-6/0, with the constitutive relationships (data points) obtained from test CRD-1.

Figure 8.1 presents the settlement predictions of pond KC80-6/0 obtained using the constitutive relationships obtained from test CRD-1, as well as the centrifugal model. One numerical prediction was based on the use of the direct experimental data points, while the other was obtained using the corresponding power curve parameters. The agreement between the prediction using direct data points and the centrifugal model is very good. In both cases, however, the total settlement predicted was about 0.5 ft less than that predicted with the centrifuge. The time needed to produce the total settlement, as well as the rate of settlement, are predicted better with the data points. The prediction based

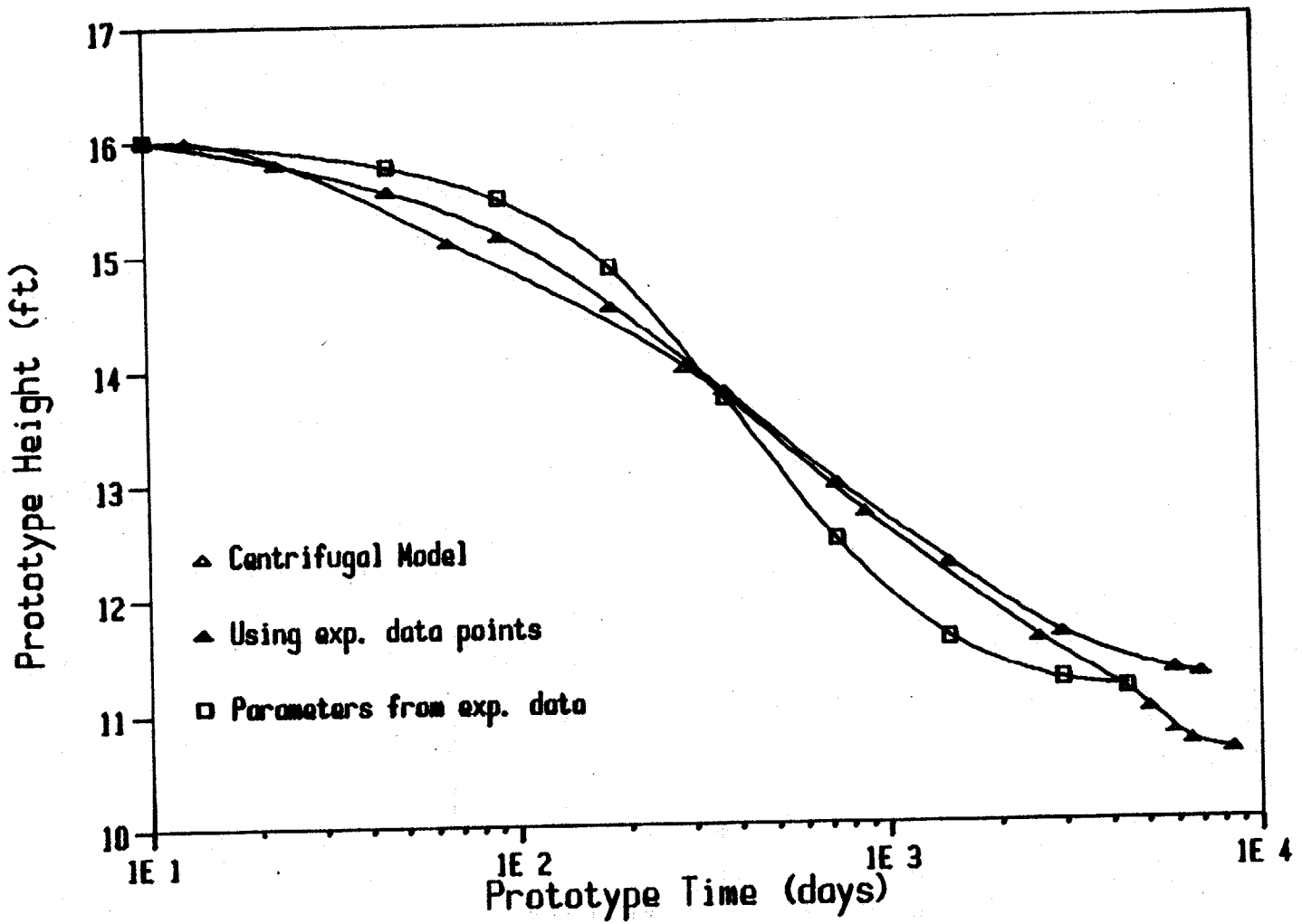

Figure 8.1 - Prediction of Pond KC80-6/0 using Constitutive Relationships obtained from Test CRD-1

on the parameters obtained from test CRD-1 bisects the centrifugal model prediction, initially underpredicting and later overpredicting the settlement rate.

To verify the output of the Turbo Pascal program used in the analyses reported in this research, YONG-TP, and to comparethe results of the piecewise linear approach with Somogyi's implicit scheme (1979), pond KC80-6/0 was analyzed using the computer programs UF-McGS (Zuloaga, 1986) and QSUS (Somogyi, 1979). Because of limitations of the latter, the constitutive relationships of the slurry were represented by the power curve parameters obtained from test CRD-1. Figure 8.2 presents the results of the three programs. The agreement among them is excellent.

The settlement predictions of pond KC80-10.5/0 are presented in Figure 8.3. The agreement between centrifugal and numerical predictions is good. Again, the use of the power curve parameters, instead of the experimental data points, results in the numerical prediction curve bisecting the centrifugal model results.

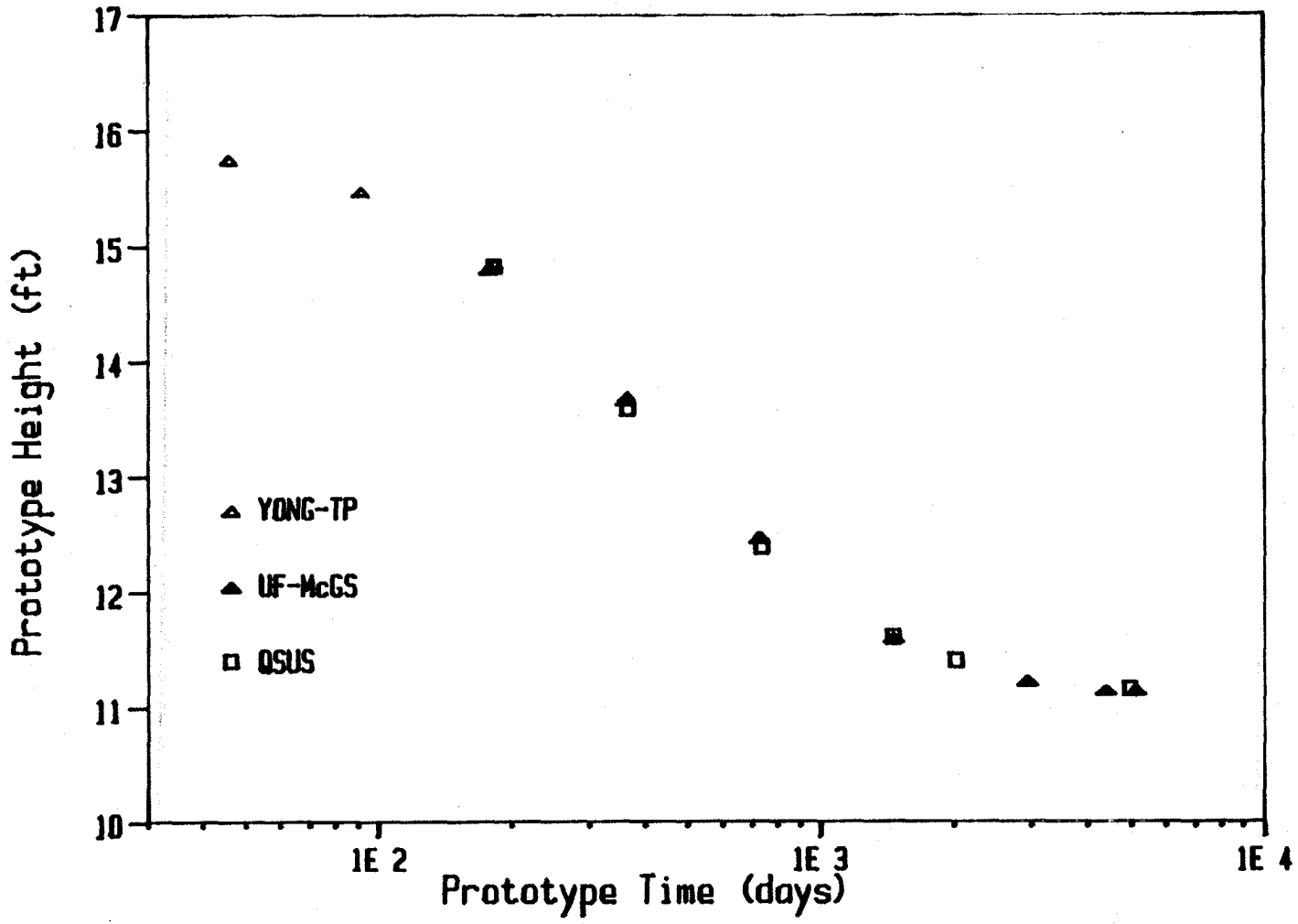

Figure 8.2 - Comparison of YONG-TP, UF-McGS, and QSUS Outputs

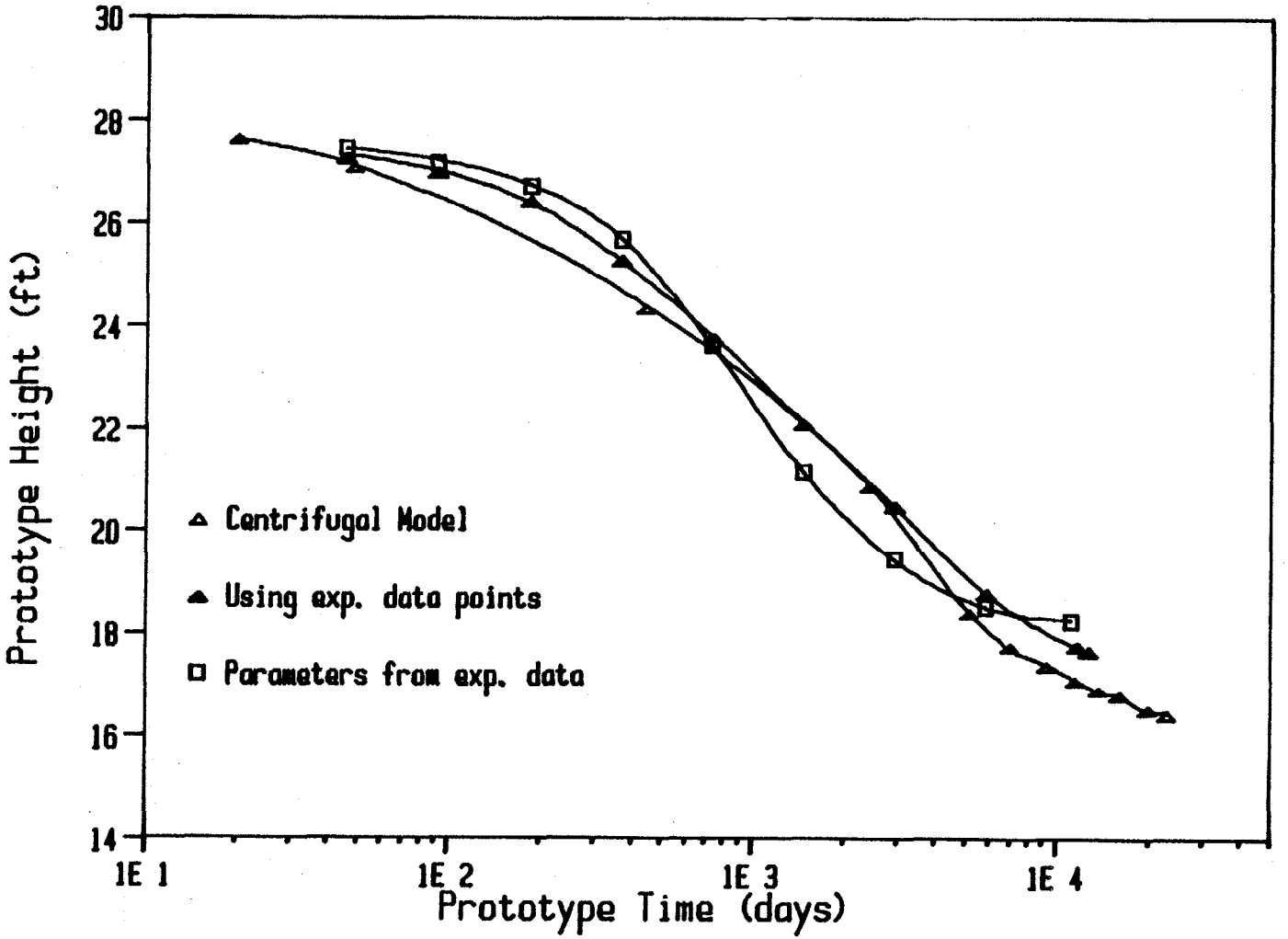

Figure 8.3 - Prediction of Pond KC80-10.5/0 using Constitutive Relationships obtained from Test CRD-1

Prediction of Ponds CT-1, CT-2/3, and CT-5

Pond CT-l, a 31.5-ft prototype, was modeled in the centrifuge by the test with the same name, as reported in Chapter VII. A numerical prediction was obtained using the results of test CRD-1 (data points). The results of the centrifugal model and the computer prediction are presented in Figure 8.4.

Surprisingly, the agreement between centrifugal and numerical predictions is very poor. The computer prediction underestimates both the total magnitude and rate of settlement. Similar results were obtained in the prediction of pond CT-2/3 presented in Figure 8.5. In this case, two centrifugal models were obtained from tests CT-2 and CT-3. The agreement of the two centrifugal models is very good. However, the numerical prediction suffers the same shortcomings found for pond CT-l.

The results of these two predictions led to the believe that somehow the material used in the centrifuge tests reported in Chapter VII was different from the one characterized by the constitutive relationships used in the predictions. In order to investigate this hypothesis, one of McClimans centrifuge tests, specifically KC80-10.5/0, was approximately reproduced using the material tested in Chapter VII. McClimans test KC80-10.5/0 was performed at 80 g's, with a specimen initial height of 10.5 cm. and initial solids content of 16.3%. The new test, denoted by CT-6, was

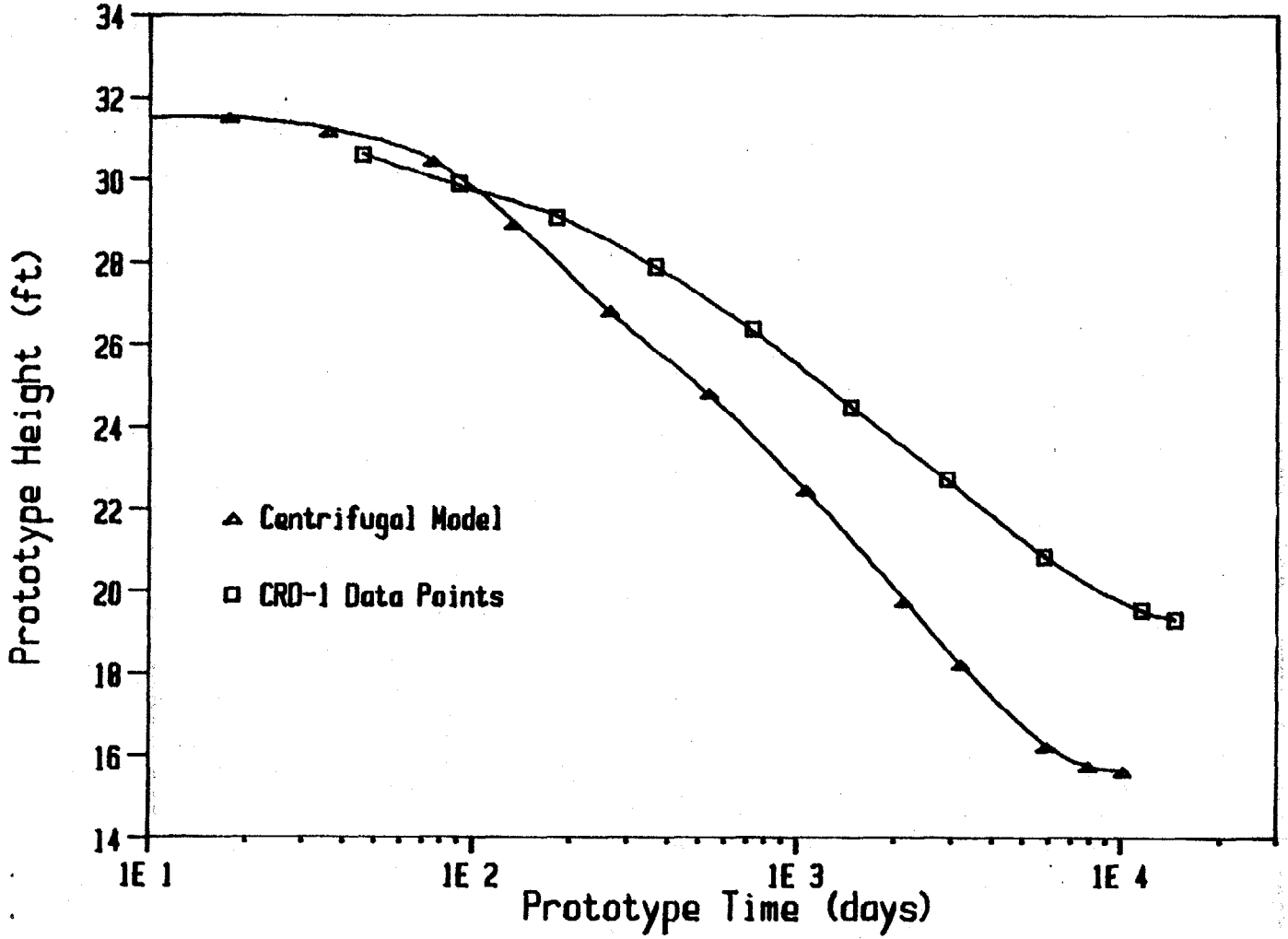

Figure 8.4 - Prediction of Pond CT-1 using Constitutive Relationships obtained from Test CRD-1

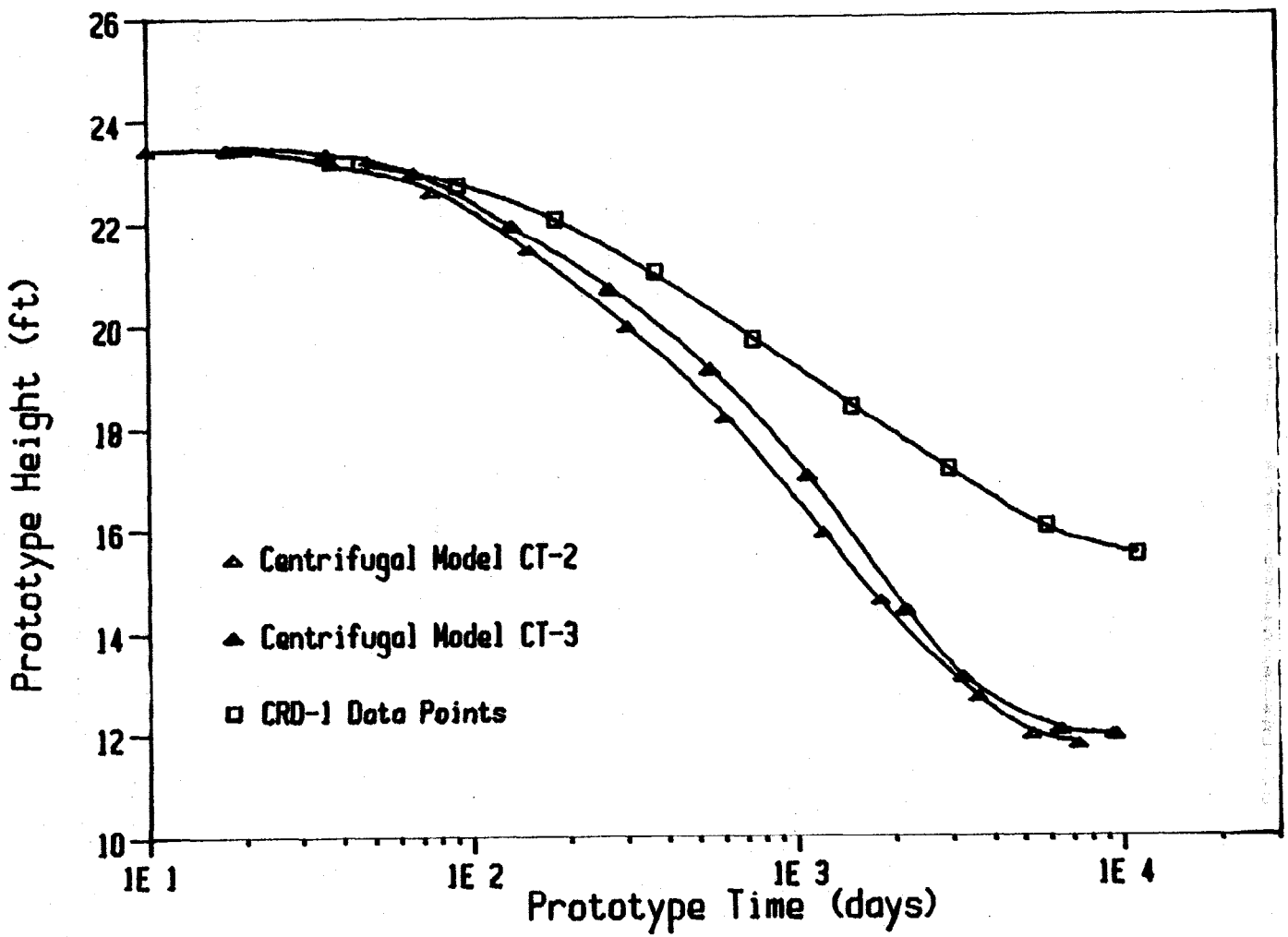

Figure 8.5 - Prediction of Pond CT-2/3 using Constitutive Relationships obtained from Test CRD-1

also performed at 80 g's, with an initial height of 10.7 cm and solids content of 15.95%.

The settlement plots for both tests are presented in Figure 8.6. These plots show, leaving no room for doubts, that the two materials do not behave similarly. The slurry of test CT-6 has both larger compressibility and larger permeability.

Given the results of Figure 8.6, the most reasonable step to follow was to re-analyze ponds CT-1 and CT-2/3 using the power curve parameters obtained from the same centrifuge tests. These parameters were given in Chapter VII and are repeated here for convenience.

A = 16.359 B = -0.204 C = 1.029E-06 D = 4.297

The resulting numerical prediction of pond CT-1 is compared with the centrifugal model in Figure 8.7. The numerical model predicts very well both the total settlement and the time required to achieve this value. With regard to the rate of settlement, the computer prediction bisects the centrifugal model curve. This peculiar result is attributed, at least in part, to the fact that the permeability relationship does not include the preconsolidation zone. Because of this, the permeability is initially too low, and toward the end of the test it is too high. It is also very likely that radial drainage effects, which are only being approximated, are partially responsible for the initial disagreement between numerical and centrifugal results.

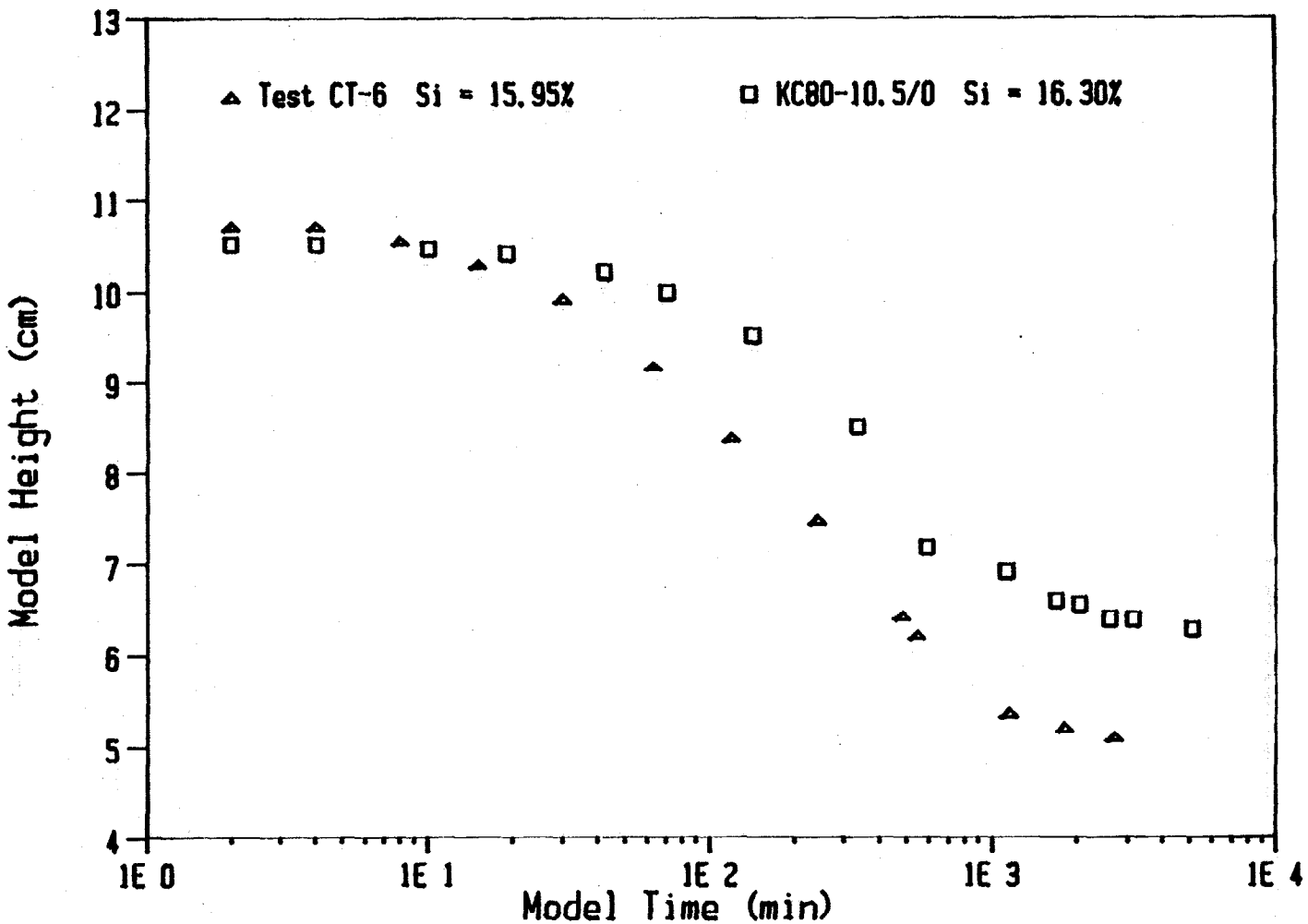

Figure 8.6 - Comparison of Centrifuge Tests KC80-10.5/0 and CT-6

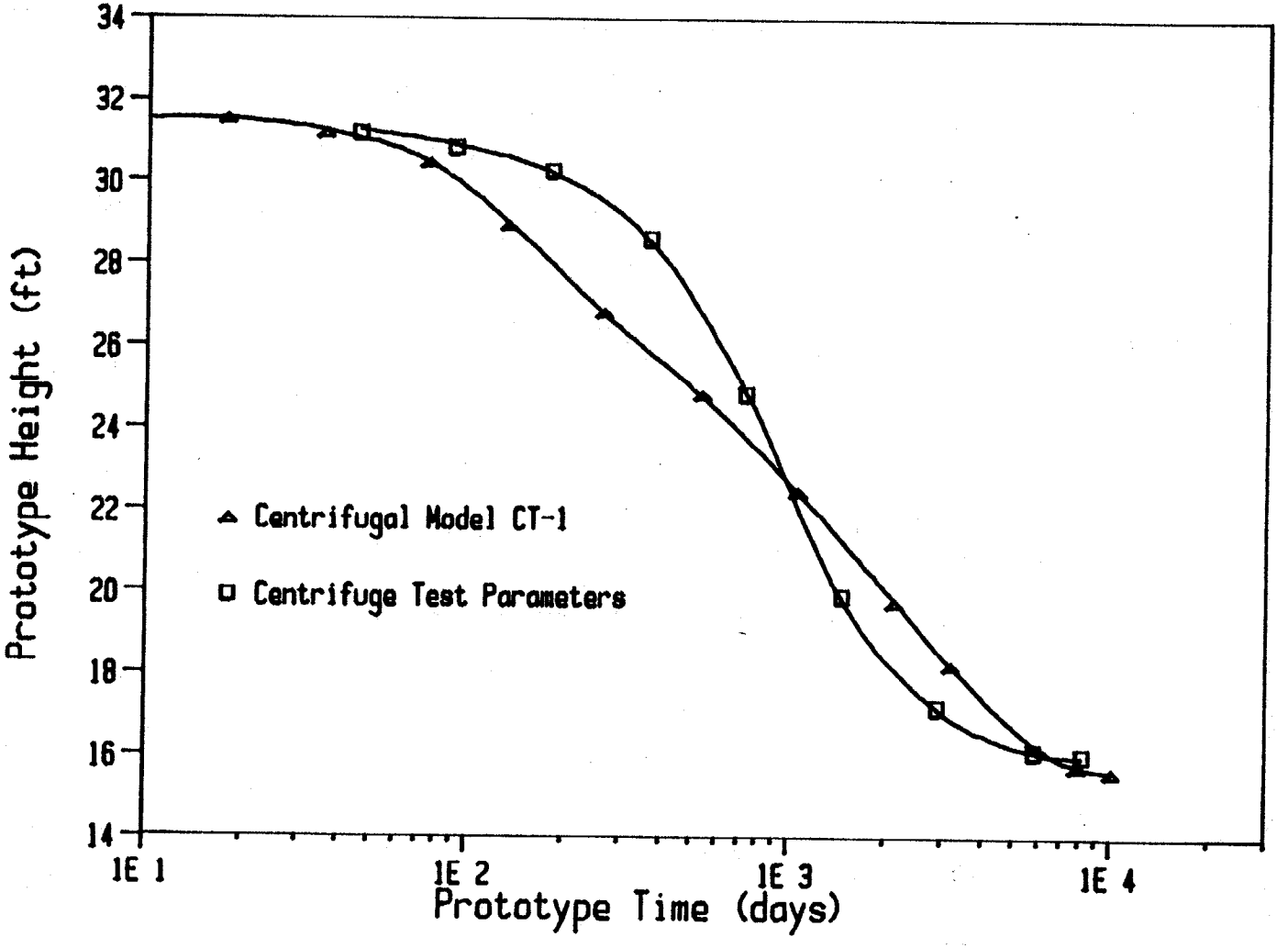

Figure 8.7 - Prediction of Pond CT-1 using Centrifuge Test Parameters

A comparison between measured and predicted void ratio profiles for pond CT-l, using the centrifuge parameters, is presented in Figure 8.8. At the end of the test, the agreement between the measured void ratios and the values predicted by the computer program is very good, except near the top of the pond. Theoretically, the void ratio at the surface of pond should not change. However, the results of this and other studies (Been and Sills, 1981; Lin and Lohnes, 1984) reveal that, without a known reason, the void ratio at the surface decreases as the pond consolidates.

The measured void ratio profile at a prototype time of 2.9 years is in good agreement with the prediction obtained at 2 years, only for the bottom half of the pond. In the upper portion of the pond, the two curves depart from each other, since the predicted curve must reach the initial void ratio of 14.53 at the-surface.

Figure 8.9 presents the pore pressure profiles predicted at four different times for pond CT-1 and using the centrifuge power curve parameters. In Chapter VII, Figure 7.7 showed the measured excess pore pressure at a time of 2 hours (model time), along with the parabolic distribution assumed to exist at the center of the specimen. At 80 g's with a time scaling exponent of 2, two hours in the model represent about 1.5 years in the prototype.

Using the results of Figure 8.9, the excess pore pressure distribution at 1.5 years (2 hours in the model) was obtained. A comparison of the latter with the results

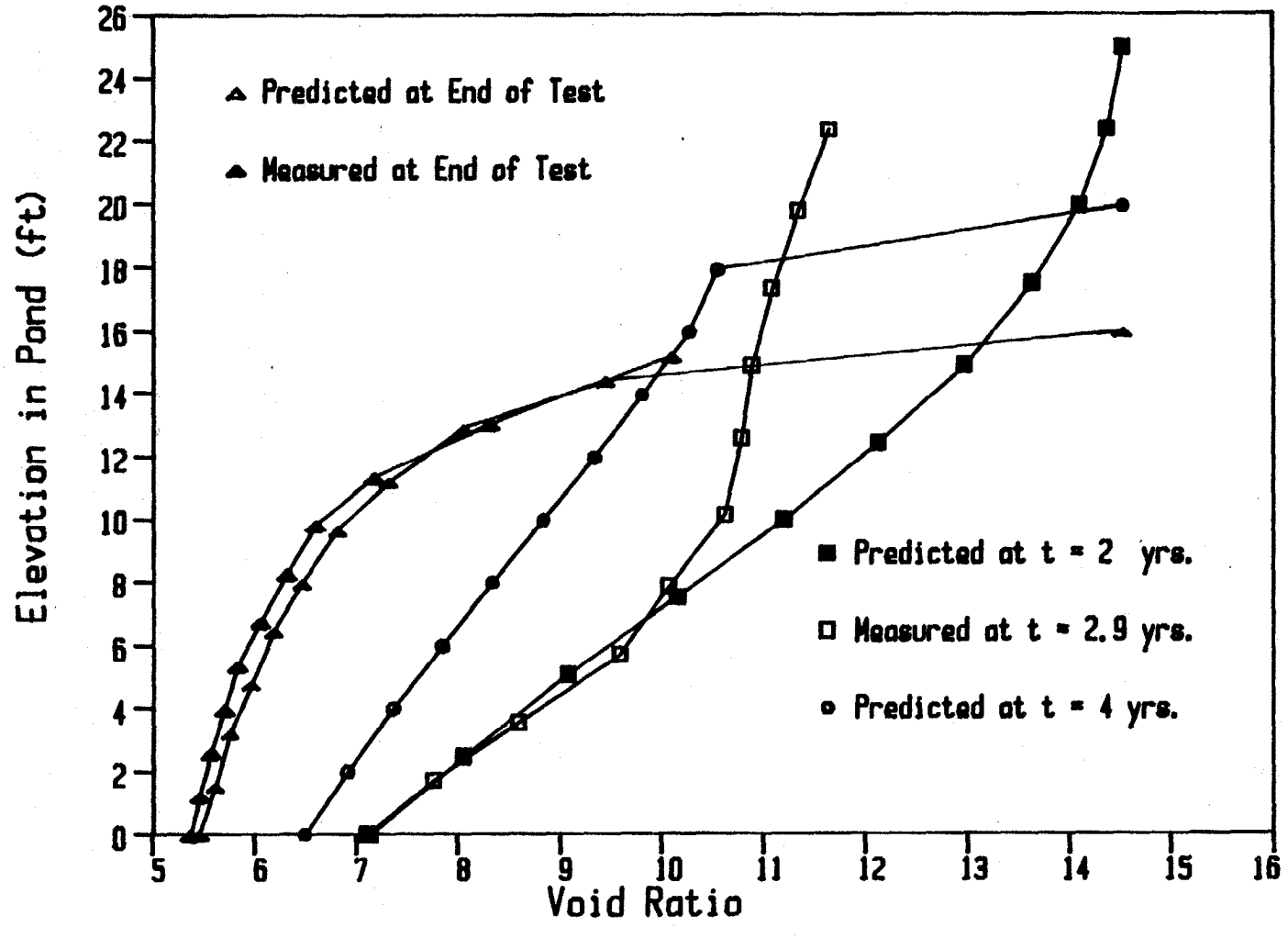

Figure 8.8 - Measured and Predicted Void Ratio Profiles for Pond CT-1

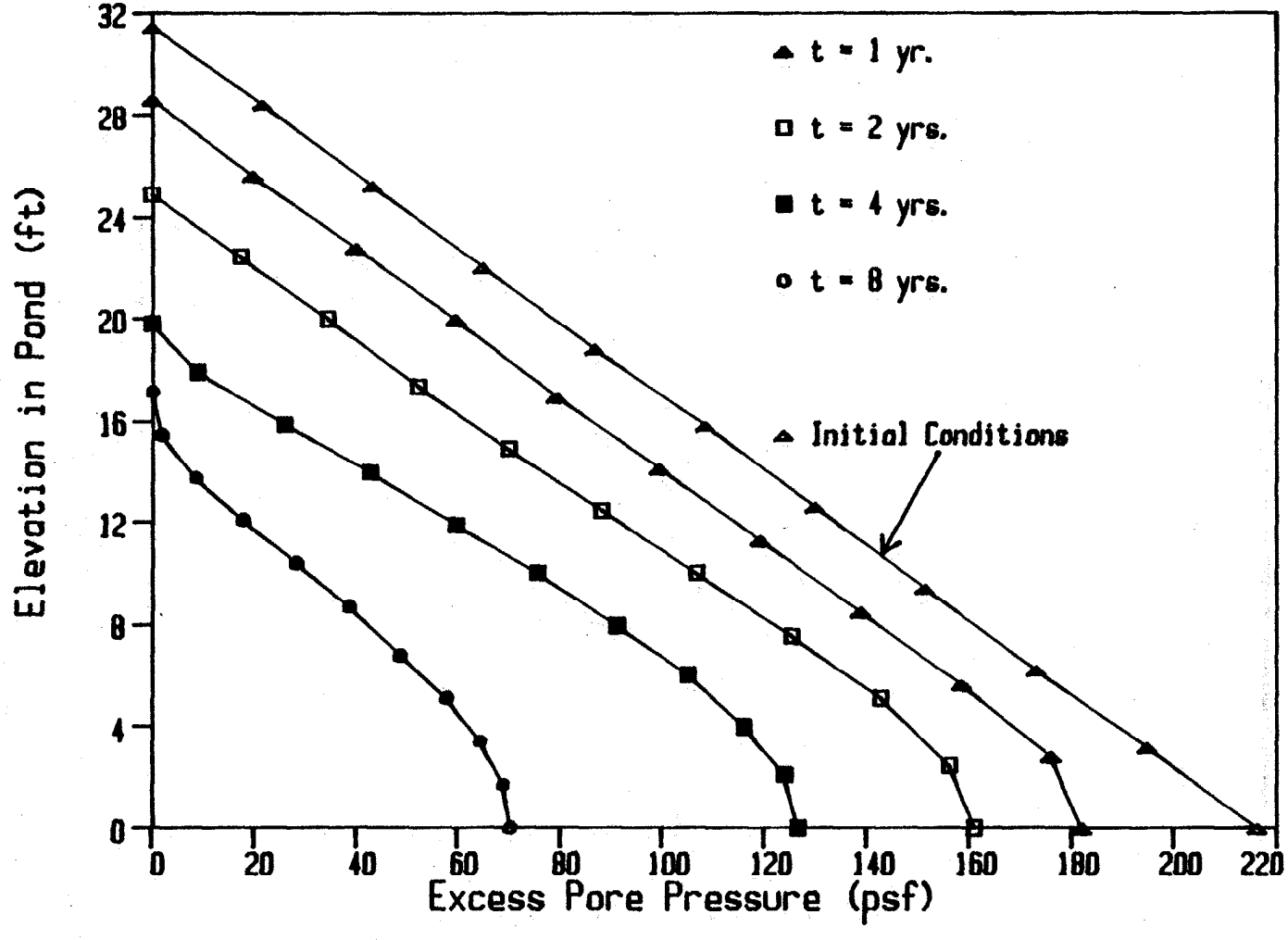

Figure 8.9 - Predicted Excess Pore Pressure Profiles for Pond CT-1

of Figure 7.7 is shown in Figure 8.10. The predicted distribution falls right in the middle between the measured values and the parabolic distribution, except near the top of the model. This local departure from the general trend is simply due to the difference between the measured model height of 9.5 cm and the predicted value of 10.18 cm. Figure 8.7 showed that the numerical model initially overpredicts the pond height.

The result of Figure 8.10 is consistent with the assumption made in Chapter VII to obtain the constitutive relationships from the centrifuge test data. Specifically, the assumption was that the excess pore pressure profile was the average of the measured distribution at the boundary and the parabolic distribution assumed at the center. In this way, a problem where radial drainage exists is approximated by a one-dimensional situation.

The next pond to be analyzed, CT-2/3, is a 23.6-ft prototype. Figure 8.11 presents the numerical prediction of this pond using the centrifuge test parameters, along with the two centrifugal models, CT-2 and CT-3. The prediction of the total settlement and time for consolidation is clearly much better than those obtained with the results of test CRD-1 or the other constitutive relationships proposed for Kingsford clay. Similar to pond CT-1, the computer prediction bisects the centrifuge curves.

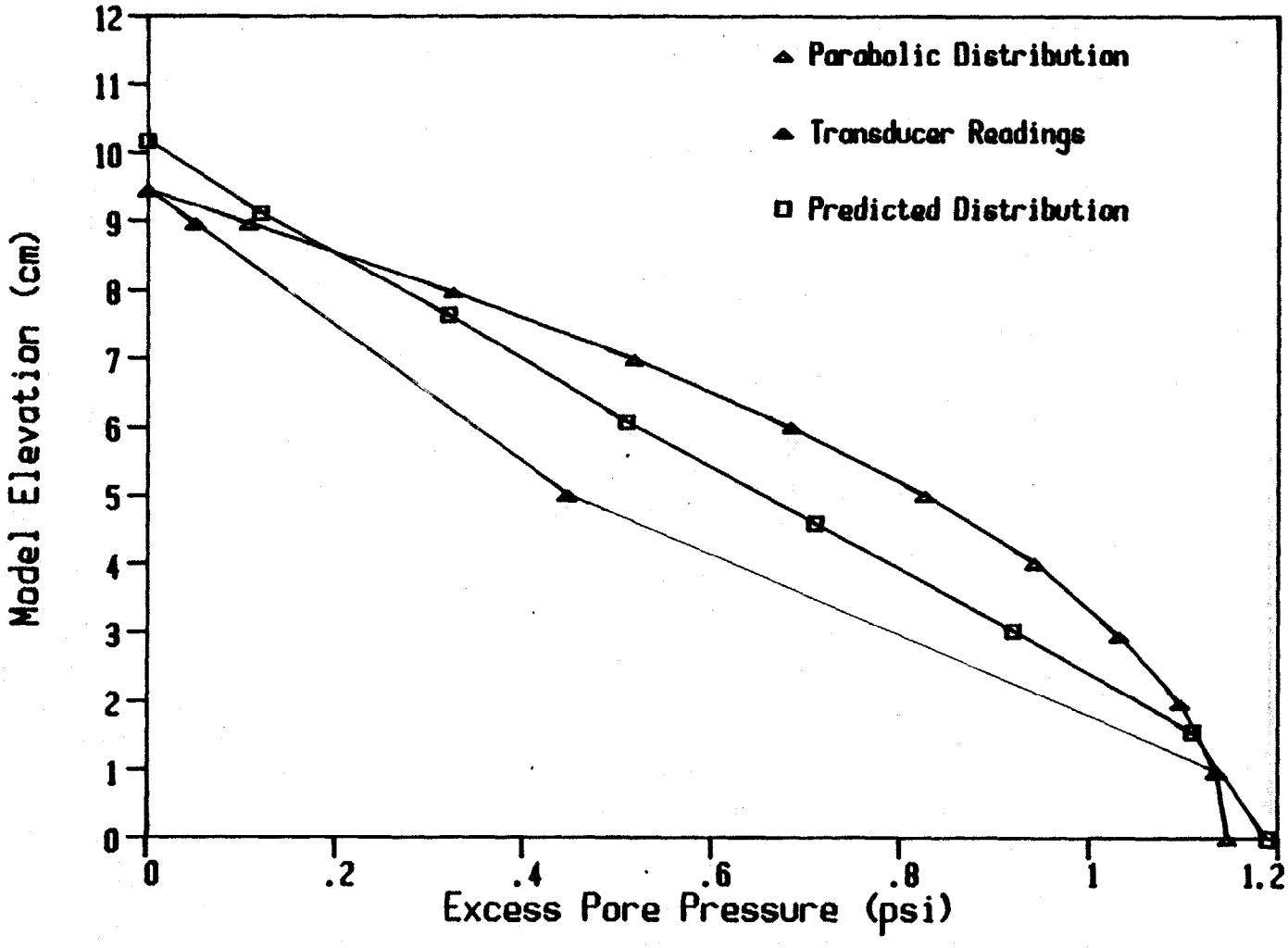

Figure 8.10 - Measured and Predicted Excess Pore Pressure Profiles at a Model Time of 2 hours for Pond CT-1

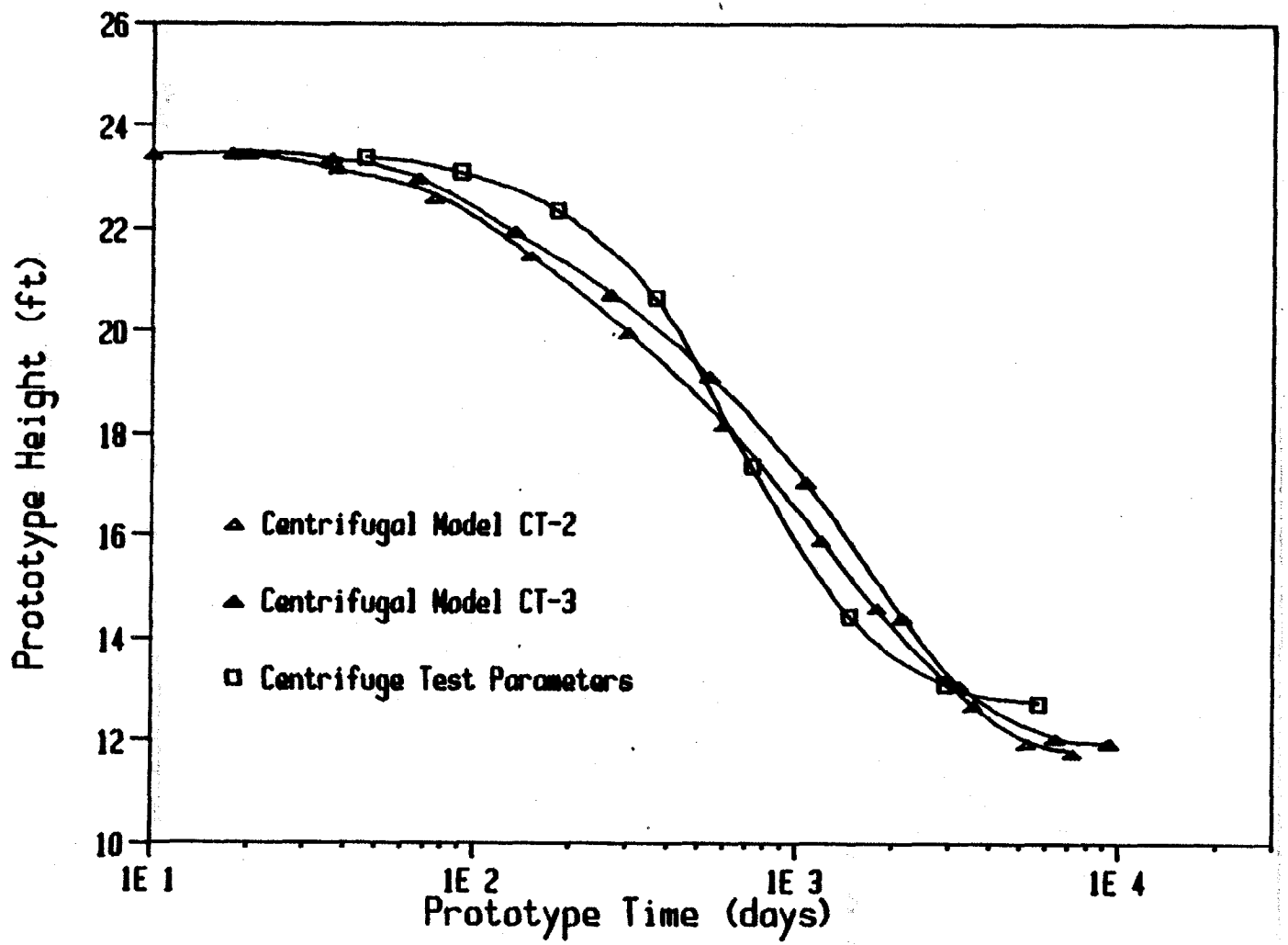

Figure 8.11 - Prediction of Pond CT-2/3 using Centrifuge Test Parameters

A comparison of measured and predicted void ratio profiles for pond CT-2/3 is presented in Figure 8.12. Again, the agreementat the end of the test is very good, except near the top of the pond. The profile measured at a prototype time of 3.3 years compares better with the one predicted at 2 years than with that at 4 years. Notice, however, that the corresponding measured height at 3.3 years is closer to the height predicted at 2 years. Thus at these two times the pond is under more similar conditions, which explains why the void ratio profiles at 2 and 3.3 years are in better agreement.

The results of the numerical prediction of ponds CT-1 and CT-2/3, using the centrifuge power curve parameters, are very good. Because these, parameters were obtained from the data collected from tests CT-1 and CT-2, these results were expected. Nevertheless, they demonstrate the validity of the numerical approach proposed in Chapter VI to obtain the constitutive properties of slurries from centrifugal model tests. However, it is necessary to evaluate the reasonable-ness of these constitutive relationships by predicting other ponds. The remaining of this chapter will analyze the predictions of ponds CT-5 and CT-6.

Pond CT-5 represents a hypothetical prototype corre-sponding to test CT-5, used for comparison with McClimans test KC80-10.5/0 in Figure 8.6. The prototype height is 28.08 ft and the initial solids content is 15.95%. A computer prediction of this pond was obtained using the

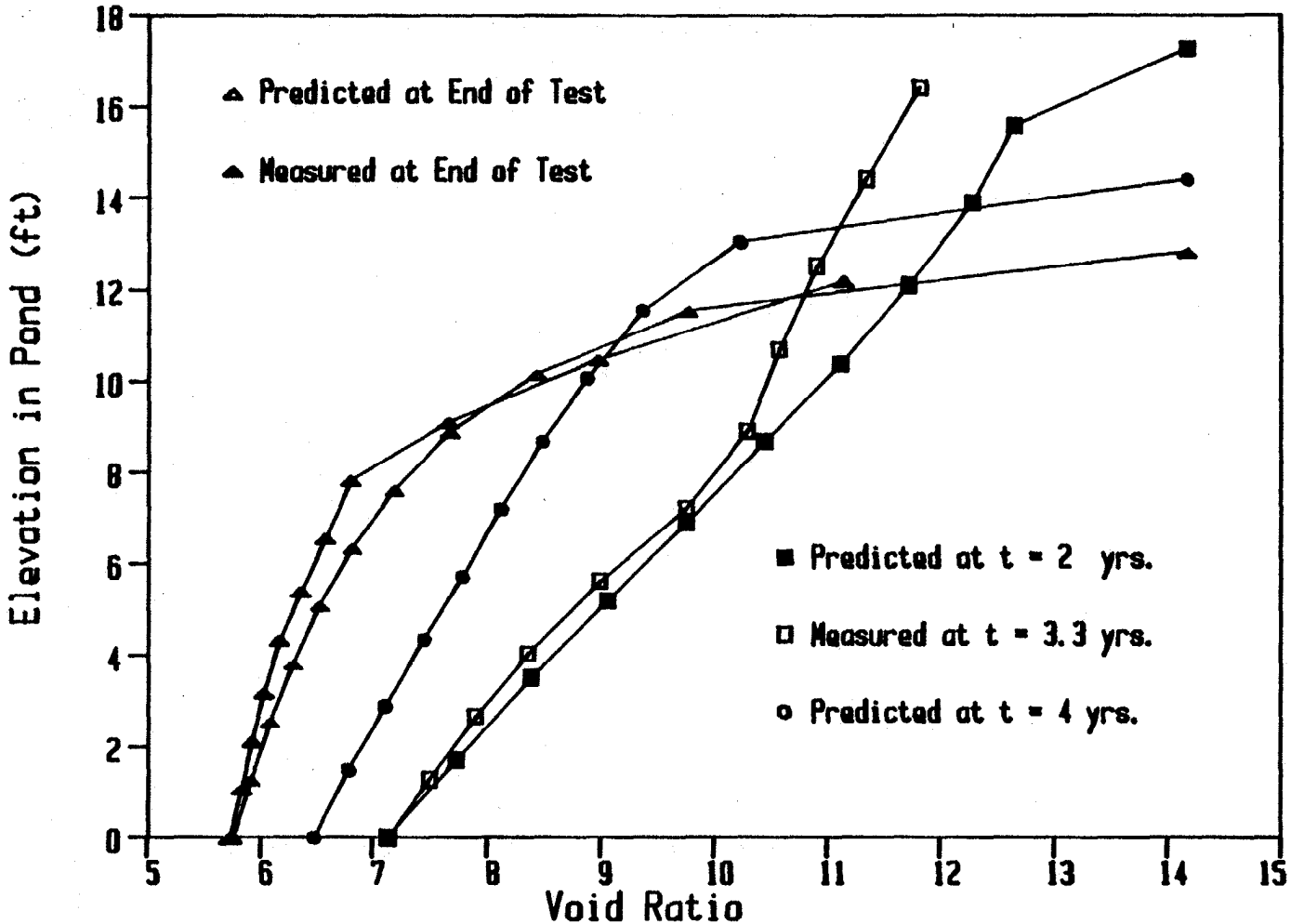

Figure 8.12 - Measured and Predicted Void Ratio Profiles for Pond CT-2/3

centrifuge power curve parameters. The centrifugal prediction was obtained using the time scaling exponent of 2 with the acceleration level of 80 g's. The results of the numerical and centrifugal predictions are shown in Figure 8.13. The computer analysis predicts quite well the final height of the pond and thetotal time required to achieve this height. The predicted rate of settlement is also in quite good agreement with the centrifugal model. Similar to previous predictions where power curve parameters were used, the numerical prediction bisects the centrifuge curve.

The last pond to be analyzed is pond CT-5, a 28.9-ft prototype with a surcharge of 263 psf. The centrifugal model test of this pond was only performed for 8 hours for the reasons given in Chapter VII. Nevertheless, this pond offers an excellent opportunity to validate the numerical prediction of a slurry pond with a surcharge load.

The pore pressure response observed in test CT-5 (Chapter VII) provides the basis for a more confident use of a time scaling exponent of 2 to obtain the prototype times of the centrifugal model. For the numerical prediction, the centrifuge test parameters were used, based on the analyses of the previous ponds CT-l, CT-2/3 and CT-6.

Figure 8.14 compares the numerical and centrifugal settlement predictions of pond CT-5. The agreement between the two curves is remarkably good. The predicted excess pore pressure profiles at various times is compared in Figure 8.15 with the values measured at the transducers at

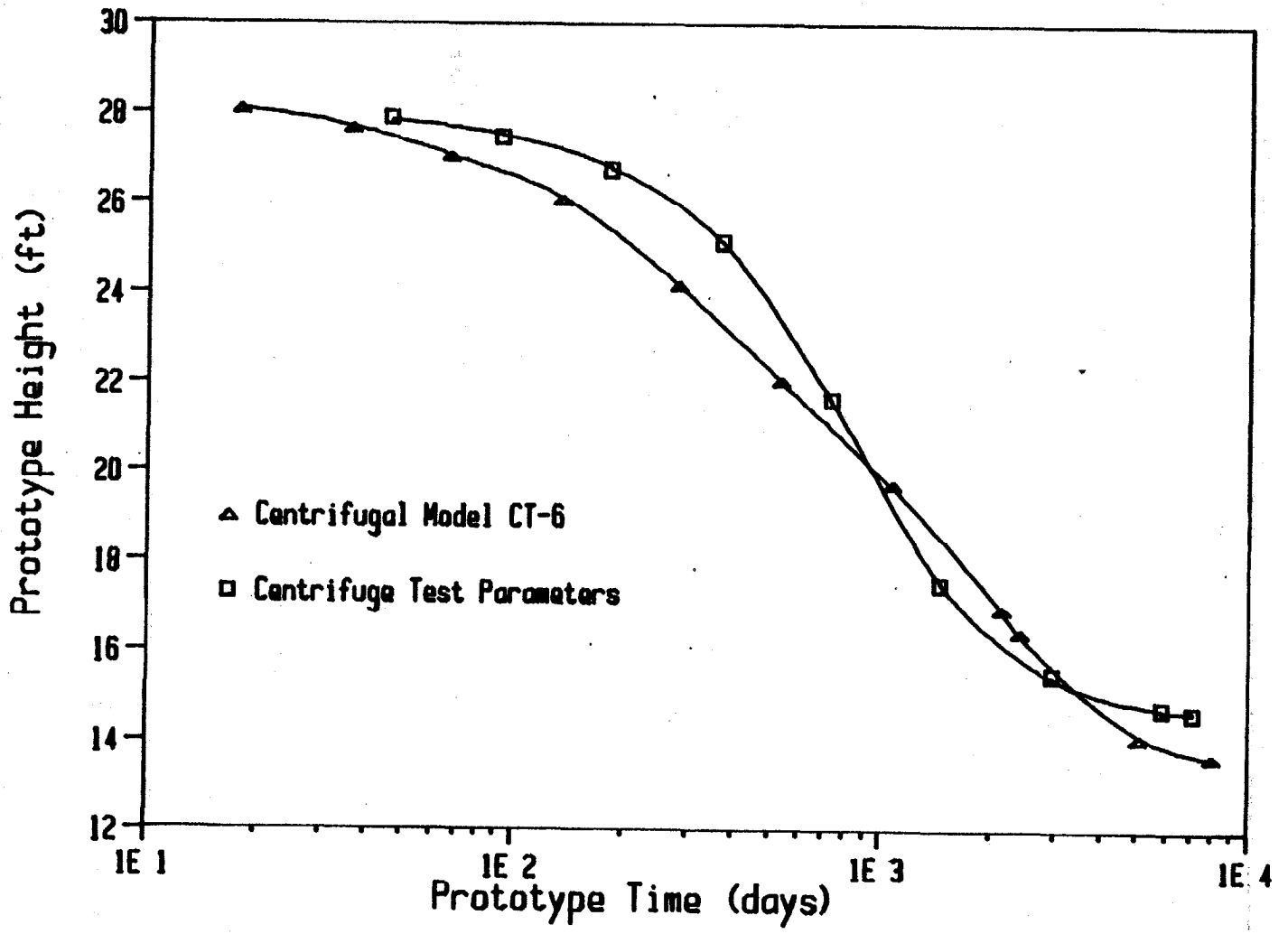

Figure 8.13 - Prediction of Pond CT-6 using Centrifuge Test Parameters

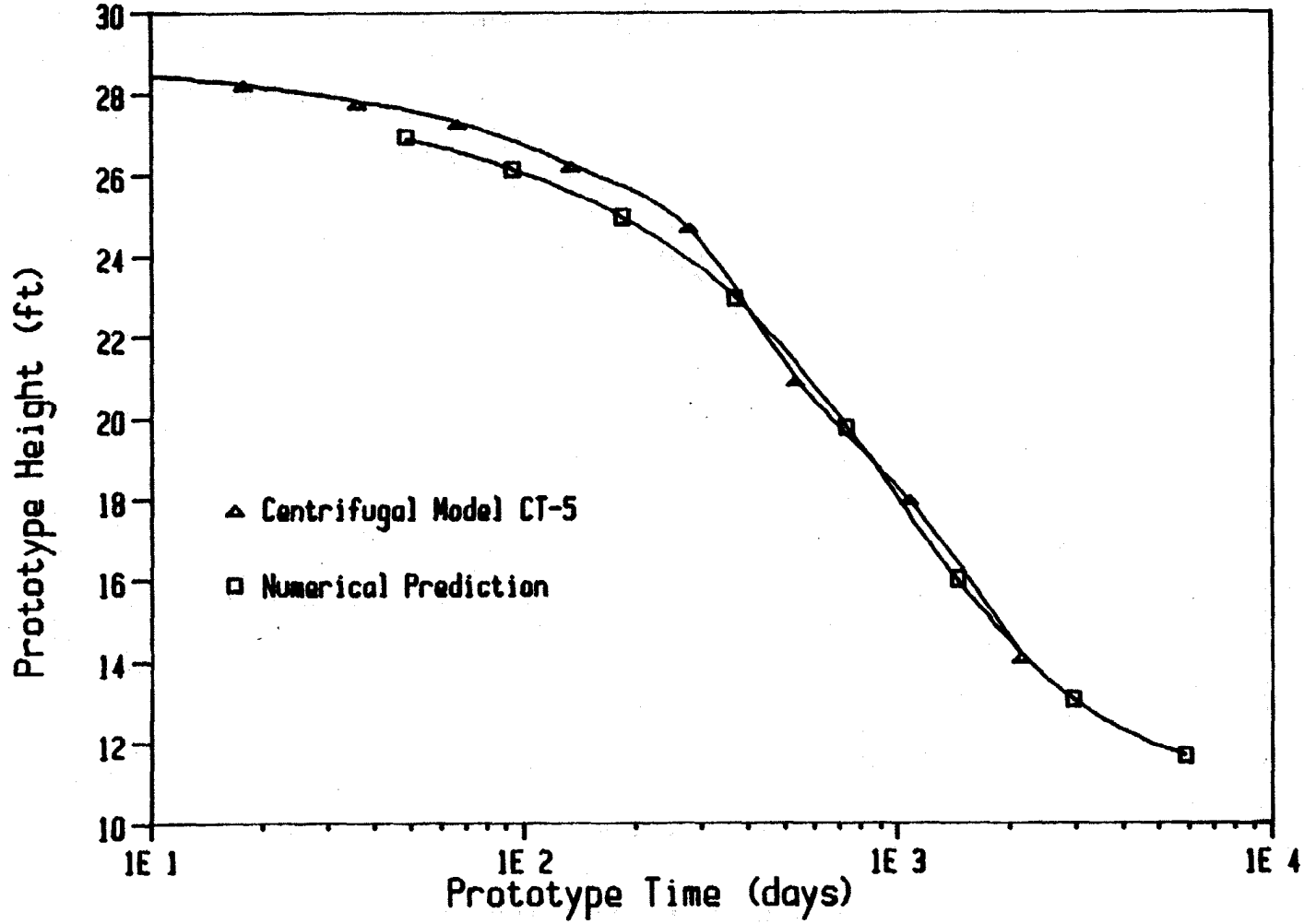

Figure 8.14 - Prediction of Pond CT-5 using Centrifuge Test Parameters

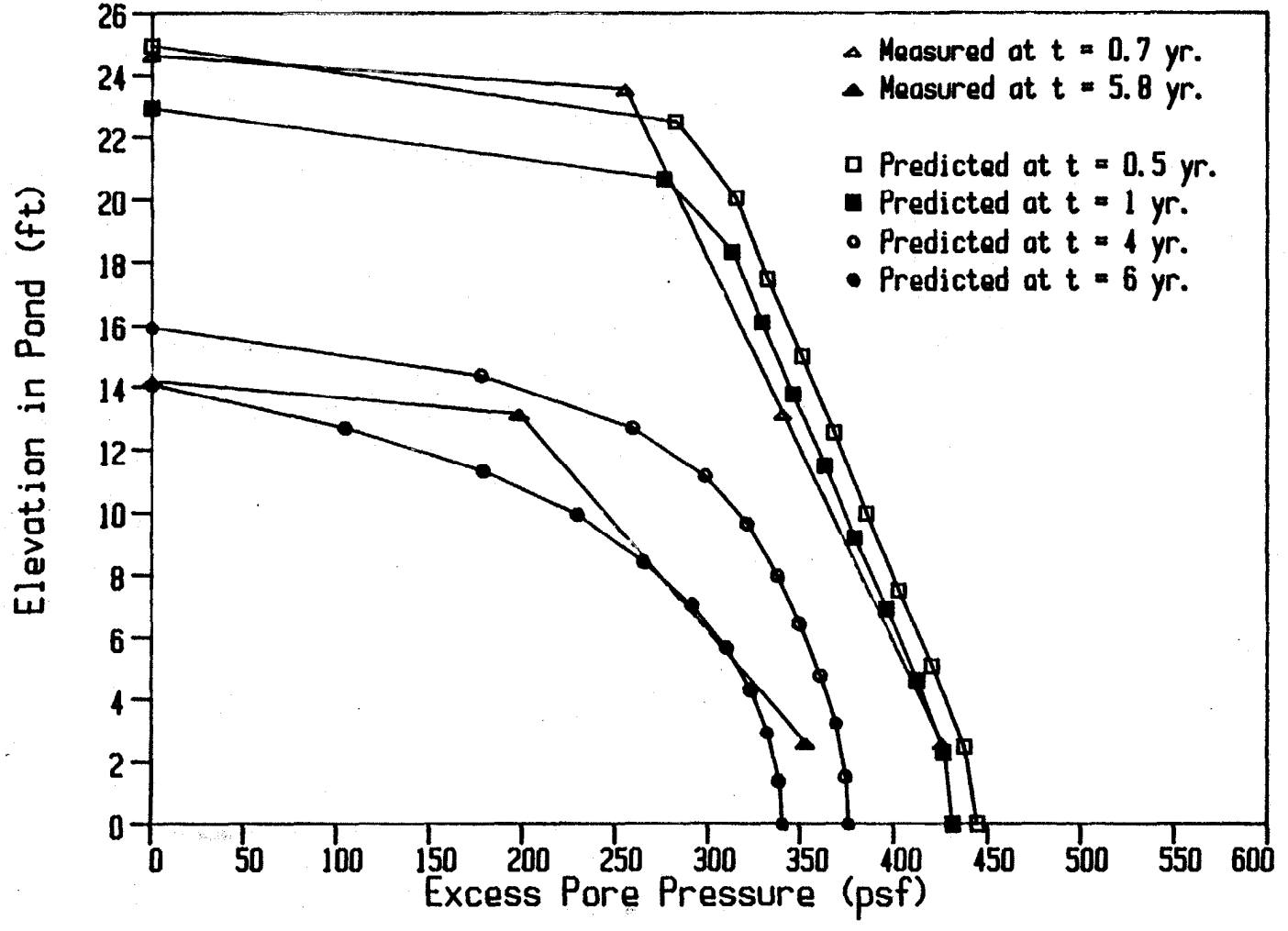

Figure 8.15 - Measured and Predicted Excess Pore Pressure Profiles for Test CT-5

prototype times of 0.7 and 5.8 years. Within the limitations of the data, the agreement between predicted and measured pore pressureis quite good.

After stopping test CT-5, two samples were cored and sliced to determine the void ratio-depth profile. The centrifuge was stopped shortly after 8 hours of test, corresponding to a prototype time of about 5.9 years. Figure 8.16 shows the two profiles obtained, along with the predicted curves at 4 and 6 years. Considering the difficulty of the sampling technique, it can be concluded that the measured profiles exhibit the right behavior and that their agreement with the predicted results is good. It is worth mentioning here that, because there was no initial intention of using this information, the samples for the determination of the void ratio profile were not obtained until four days after the end of the test. Thus, some swelling definitely had occurred in the specimen.

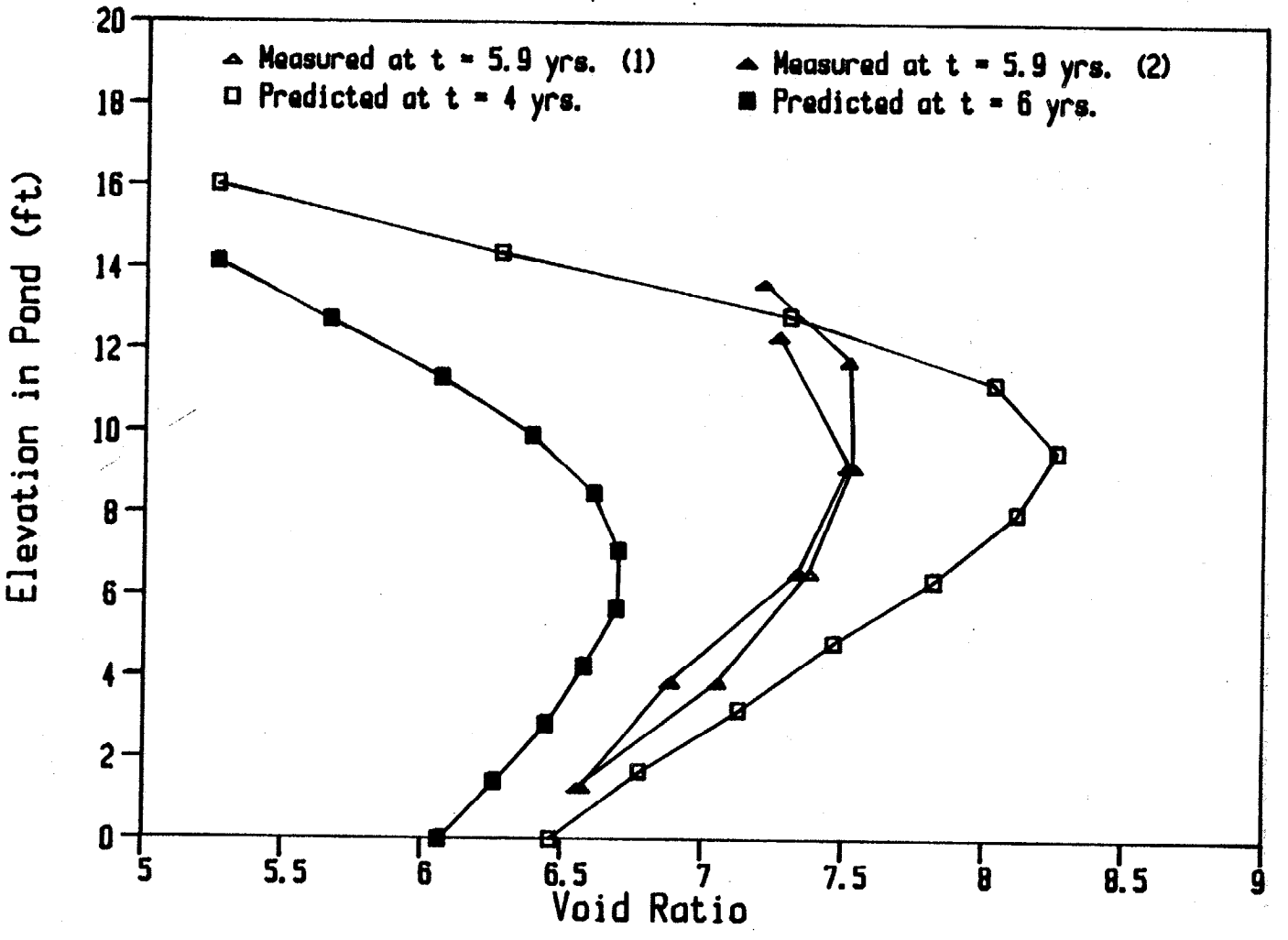

Figure 8.16 - Measured and Predicted Void Ratio Profiles for Pond CT-5

CHAPTER IX
CONCLUSIONS AND SUGGESTIONS FOR FUTURE RESEARCH

Summary and Conclusions

1. The main objective of this research was to develop techniques to obtain the consolidation properties of slurries, specifically the effective stress-void ratio relationship and the permeability-void ratio relationship. Two techniques were developed. The first one involved the design and construction of an automated slurry consolidometer, while the second used centrifugal model tests.

2. The automated slurry consolidometer proved to be an effective technique for determining the constitutive properties of slurries. The equipment is fully automated, requiring human intervention only during setting up and dismantling of the test.

3. The test chamber is an 8-inch (0.20 m) diameter cast acrylic cylinder. The specimen height can vary between 4 inches (0.10 m) and 8 inches (0.20 m). The test monitors the specimen height, pore pressure distribution across the specimen, load, and total stress at the bottom of the specimen. A stepping motor is used to produce the load,

which is transmitted to the specimen through a gear system and loading piston.

4. A Hewlett-Packard computer and control/data acquisition system is used to control and monitor the test. The controlling computer program was written in BASIC. A second program is used to reduce the data and plot the constitutive curves at the end of the test. The data reduction analysis uses well-accepted soil mechanics principles.

5. Two different loading conditions were investigated in the research, specifically Constant Rate of Deformation (CRD) and Controlled Hydraulic Gradient (CHG). The CRD test produced much better results and is recommended as the standard testing procedure. A typical CRD test lasts between 3 days and 1 week, depending on the rate of deformation and the initial and final conditions of the specimen,

6. The constitutive relationships obtained from the CRD tests show a "pseudo-preconsolidation" effect, which is a function of the initial solids content of the slurry. Thus, it is concluded that the constitutive relationships are not unique. This particular behavior is attributed to the initial highly remolded initial structure of the material.

7. In the case of the permeability relationship, the curves with different initial solids content approach a unique

virgin zone for the range of deformation rates investigated. The compressibility relationship, on the other hand, was found to be dependent upon the rate of deformation as well as initial solids content. Therefore, it is recommended that the test be performed at a slow rate, and values around 0.008 mm/min appear to be appropriate.

8. The results of this research indicate that the constitutive relationships of slurries can not be represented by the traditional power curve parameters. Instead, the actual experimental data points should be used, as input data for computer analysis.

9. The technique proposed to obtain the constitutive properties from centrifugal model tests has the advantage of better simulating the stress conditions of an actual pond. Additionally, the approach is not based on average values as is the case with the automated slurry consolidation tests. Instead, actual measurements of excess pore pressure and void ratio profiles with time are used to obtain the relationships using the effective stress principle, Darcy's law, and continuity. A numerical approach, based on updated Lagrangian coordinates and a material representation of the specimen, is used to analyze the data. A FORTRAN program was written for this purpose. However, the approach has several disadvantages. First, the obtaining of the samples for solids content measurements is not very accurate.

Second, the test does not provide information on the preconsolidation zone because it is not possible, with the technique used, to obtain the solids content profile early in the test. Nevertheless, the existence of the preconsolidation zone, at least in the compressibility curve, is clearly demonstrated by the fact that a condition of zero initial effective stresses was observed in the tests.

10. The series of centrifuge tests conducted revealed a problem with radial drainage in the acrylic bucket. Because of this, an approximation was necessary in order to simulate a pseudo one-dimensional situation and to be able to use the numerical approach proposed. The radial drainage evidences disappeared when a surcharge load was applied to the model.

11. It was demonstrated that the effect of radial drainage upon the models may explain the obtaining of a time scaling exponent of less than 2 from a modelling of models analysis. It is recommended that a value of 2 be used for initial solids content above 14%-16%.

12. The constitutive relationships of the slurry were obtained from two centrifuge tests performed at 60 g's and 80 g's. The permeability obtained from the analysis corresponds to the prototype value, which is n (the acceleration level) times smaller than the permeability in the model. The

agreement between the results of the two tests was very good.

13. The compressibility relationship obtained from the centrifuge tests was in good agreement with the results of the CRD tests performed at a rate of deformation of 0.008 mm/min. This result reaffirms the need to perform the CRD tests at low deformation rates. On the other hand, the permeability relationship obtained from the centrifuge tests plotted parallel to the virgin zone of the CRD curves. However, the centrifuge permeabilities are about a half order of magnitude higher. A full explanation of this apparent discrepancy requires further investigation.

14. Two groups of hypothetical ponds were predicted using a piecewise linear solution of the governing equation. One group corresponds to centrifuge tests reported by McClimans (1984), and the other corresponds to centrifuge tests conducted as part of this research. The two ponds modeled by McClimans were predicted using the constitutive relationships obtained from CRD tests, both in the form of data points and as power curve parameters. The agreement between centrifugal and numerical models was good for both ponds. The rate of settlement was predicted better using the constitutive relationships in the form of data points.

15. When the CRD constitutive relationships were used to predict the behavior of the recently conducted centrifuge tests, the predictions were not good. After some additional testing, it was concluded that the material used in the centrifuge tests was different from the more virgin slurry used in the early CRD tests (certainly different from the material used by McClimans). This was attributed to several factors, including aging of the slurry, the continuing addition of tap water, and the re-use of the same material. Accordingly, the prediction of the hypothetical ponds modeled in this research was repeated, this time using the parameters obtained from the centrifuge tests themselves. The agreement between centrifugal and numerical models was quite good, not only for those model ponds used to obtain the constitutive properties, but also for two different model ponds, including one with a surcharge. Not only were the settlement predictions good, but also the predictions of excess pore pressure and void ratio were reasonably good.

16. In summary, the use of numerical models is an excellent tool for predicting the consolidation behavior of slurry ponds. The constitutive input properties needed in the analysis can be obtained from either of the techniques developed in this research. However, the CRD automated slurry consolidation tests are recommended over the centri-fugal model tests. The latter technique is more appropriate for validation of computer results.

Suggestions for Future Research

1. A major aspect of the automated slurry consolidation apparatus requiring improvement is reducing piston friction. It is recommended that the present acrylic chamber be replaced by a metal chamber which will maintain a true bore and piston diameter capability. The chamber should be teflon coated and the piston edge should be sealed using a teflon O-Ring to minimize piston friction and, at the same time, prevent edge leakage of slurry.

2. The range of the total stress transducer at the bottom of the specimen needs to be reduced from 3 bars to 1 bar, and the transducer diaphragm should be flush with the bottom of the specimen. An accurate reading of this transducer is crucial to estimating the side friction on the specimen.

3. The range of the pore pressure transducers should also be improved. On the moving piston, a 1-psi (75 mbar) transducer is recommended. The rest of the transducers on the chamber side should be of 5-psi (350 mbar) to 14.5-psi (1 bar) range. This improvement of the transducer sensitivity is particularly important if CRD tests are to be performed at low deformation rates. By the same token, the range of the load cell should be limited to 100-200 pounds.

4. The significance of using average values to obtain the slurry properties is an aspect of the automated slurry

consolidometer that deserves further investigation. This study can be accomplished by performing several tests with similar initial conditions. The tests should be stopped at different times to obtain the solids content profiles. These and the excess pore pressure profiles with time would allow the obtaining of constitutive relationships in a way similar to that used in the centrifuge tests.

5. A more detailed study of the effect of the deformation rate is needed in order to make a better recommendation concerning the appropriate values for the CRD test.

6. The effect of the initial specimen height upon the constitutive properties needs to be investigated; the use of a smaller specimen (5-10 cm) may be advisable.

7. With respect to centrifugal modelling, the main shortcoming of the proposed approach to obtain the constitutive relationships is the determination of the void ratio profile. The technique used in this research yielded reasonable values, but it is not applicable during early stages of the test when the slurry is still very dilute. Therefore, if the centrifuge approach is to be developed further, this is the aspect of the test that requires improvement.

8. The results of the centrifuge tests conducted as part of this research suggest the existence of radial drainage in the specimen. However, additional testing is necessary to evaluate this effect and its influence on the time scaling exponent. Since the evidences of radial drainage were not observed in the tests with surcharge, it is recommended that a modelling of models analysis using surcharge be carried out. Such an analysis would allow a better evaluation of the time scaling exponent.

9. Finally, it is necessary to test other slurries in order to corroborate the findings of this research. Such study should concentrate on the CRD test using the automated slurry consolidometer. However, the centrifuge approach-could be used as a verification tool.